AD-A267 592

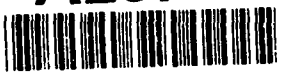

ION PAGE

Form Approved
OMB No. 0704 0188

1. AGENCY USE ONLY (Leave blank)	2. REPORT DATE	3. REPORT TYPE AND DATES COVERED
	MAY 1993	XXXXX/DISSERTATION

4. TITLE AND SUBTITLE
Synthesis, Reactivity, and Characterization of (- Hexacarbocyclic) Manganese Dicarbonyl Complexes with Sulfur and Phosphorus Ligands

5. FUNDING NUMBERS

6. AUTHOR(S)
Jeffrey Lynn Moler

7. PERFORMING ORGANIZATION NAME(S) AND ADDRESS(ES)
AFIT Student Attending: Univ of Iowa

8. PERFORMING ORGANIZATION REPORT NUMBER
AFIT/CI/CIA- 93-012D

9. SPONSORING/MONITORING AGENCY NAME(S) AND ADDRESS(ES)
DEPARTMENT OF THE AIR FORCE
AFIT/CI
2950 P STREET
WRIGHT-PATTERSON AFB OH 45433-7765

10. SPONSORING/MONITORING AGENCY REPORT NUMBER

11. SUPPLEMENTARY NOTES

12a. DISTRIBUTION/AVAILABILITY STATEMENT
Approved for Public Release IAW 190-1
Distribution Unlimited
MICHAEL M. BRICKER, SMSgt, USAF
Chief Administration

12b. DISTRIBUTION CODE

13. ABSTRACT *(Maximum 200 words)*

93 8 05 121

93-18054

14. SUBJECT TERMS	15. NUMBER OF PAGES 244
	16. PRICE CODE

17. SECURITY CLASSIFICATION OF REPORT	18. SECURITY CLASSIFICATION OF THIS PAGE	19. SECURITY CLASSIFICATION OF ABSTRACT	20. LIMITATION OF ABSTRACT

93-020

SYNTHESIS, REACTIVITY, AND CHARACTERIZATION OF (π-HEXACARBOCYCLIC)MANGANESE DICARBONYL COMPLEXES WITH SULFUR AND PHOSPHORUS LIGANDS

by

Jeffrey Lynn Moler

An Abstract

Of a thesis submitted in partial fulfillment
of the requirements for the Doctor of
Philosophy degree in Chemistry
in the Graduate College of
The University of Iowa

May 1993

Thesis supervisor: Associate Professor Darrell P. Eyman

ABSTRACT

A series of (η^5-pentamethylbenzyl)$Mn(CO)_2PR_3$ complexes has been synthesized. Phosphine ligand substitution increases the electron density on the manganese, enhancing the nucleophilicity of the exocyclic methylene of the η^5-benzyl complexes. The exocyclic methylene reacts with electrophiles to form C-C bonds with CH_3I and PhC(O)Cl and C-I bonds with I_2. (η^5-$C_6Me_5CH_2$)$Mn(CO)_2PMe_3$ (**2b**) reacts with $Mn(CO)_5Br$ to form [(η^6-$C_6Me_5CH_2Mn(CO)_5$)$Mn(CO)_2PMe_3$][PF_6], after metathesis with [NH_4][PF_6], and with (η^5-C_5H_5)$Fe(CO)_2I$ to form [(η^6-$C_6Me_5CH_2FeCp(CO)_2$)$Mn(CO)_2PMe_3$]I. The η^5-benzyl complexes react by a radical pathway with the halocarbons CCl_4, $CDCl_3$, and $CHBr_3$ to form new C-C bonds at the exocyclic methylene. ESR studies support a proposed radical mechanism in these reactions. The solid-state structure of **2b** is reported.

A series of (η^5-pentamethylbenzyl)manganese dicarbonyl phosphite complexes have been synthesized. Manganese-coordinated phosphites react with the exocyclic methylene of the coordinated pentamethylbenzyl ligand generating either benzyne or a carbene, an η^6-hexaalkylbenzene, and dialkyl- or diaryl phosphonate complexes. Their decomposition to phosphonates was observed under reduced pressure or in the presence of olefins. Benzyne, from the triphenylphosphite complexes was observed indirectly through the formation of diphenylene. The production of methylene carbenes was observed by the formation of ethene and cyclopropanes. The generation of olefins or cyclopropanes indicated that ethylidene was produced.

The solid-state structure of **11d** is reported.

The reaction of $(\eta^6\text{-}C_6Me_6)Mn(CO)_2SC(S)H$ with $[Ph_3C][BF_4]$ affords the adduct $[(\eta^6\text{-}C_6Me_6)Mn(CO)_2SCHSCPh_3][BF_4]$ (**52**). Reaction of **52** with aniline, diethylamine, and *tert*-butylamine produces $[(\eta^6\text{-}C_6Me_6)Mn(CO)_2SCHNEt_2][BF_4]$ (**53**), $[(\eta^6\text{-}C_6Me_6)Mn(CO)_2SCHNHPh][BF_4]$, and $[(\eta^6\text{-}C_6Me_6)Mn(CO)_2SCHNH\text{-}t\text{-}Bu][BF_4]$, respectively, which were characterized by FTIR, FAB-MS, and ^1H and ^{13}C NMR spectroscopies. The mass spectra of these complexes and $[((\eta^6\text{-}C_6Me_6)Mn(CO)_2)_2(\mu^2\text{-}\eta^2\text{-}SC(S)H)]^+$ have been investigated using FAB-MS/MS. The solid state structure of **53** is reported.

Abstract approved: Darrell P. Eyman
Thesis supervisor
Chair, Dept. of Chemistry
Title and department
4-26-93
Date

SYNTHESIS, REACTIVITY, AND CHARACTERIZATION OF (π-HEXACARBOCYCLIC)MANGANESE DICARBONYL COMPLEXES WITH SULFUR AND PHOSPHORUS LIGANDS

by

Jeffrey Lynn Moler

A thesis submitted in partial fulfillment
of the requirements for the Doctor of
Philosophy degree in Chemistry
in the Graduate College of
The University of Iowa

May 1993

Thesis supervisor: Associate Professor Darrell P. Eyman

Graduate College
The University of Iowa
Iowa City, Iowa

CERTIFICATE OF APPROVAL

PH.D. THESIS

This is to certify that the Ph.D. thesis of

Jeffrey Lynn Moler

has been approved by the Examining Committee for the thesis requirement for the Doctor of Philosophy degree in Chemistry at the May 1993 graduation.

Thesis committee: Darrell P. Eyman
Thesis supervisor

Richard F. Jordan
Member

Norman C. Baenziger
Member

David G. Bothwisch
Member

Louis Messerle
Member

To Jeanette, Alexandria, and Cassiopeia

I have seen all things that are done under the sun, and behold, all is vanity and a chase after wind.

What is crooked cannot be made straight, and what is missing cannot be supplied.

Though I said to myself, "Behold, I have become great and stored up wisdom beyond all who were before me in Jerusalem, and my mind has broad experience of wisdom and knowledge"; yet when I applied my mind to know wisdom and knowledge, madness and folly, I learned that this also is a chase after wind.

Qoheleth 1:14–1:17

ACKNOWLEDGMENTS

The United States Air Force and the Air Force Institute of Technology, Civilian Institutions Program for the opportunity and as the principal source of funding. Darrell P. Eyman for support and guidance. The members of the Eyman group and many others for the interesting discussions and enjoyable conversations. Steven J. Schauer for his initial contributions to this area of research. Norman C. Baenziger for his assistance in learning X-ray diffraction analysis. The Office of Research and Educational Development at the University of Iowa for partial support of research performed at the High-Field NMR Spectrometer Facility and High-Resolution Mass Spectrometry Center at the University of Iowa (HRMSCUI). Diane J. Lamb for obtaining accurate mass and peak matching spectral results at HRMSCUI. Larry Mallis for obtaining FAB-MS/MS spectra at HRMSCUI. The Bruker WM-360 NMR spectrometer and the Enraf-Nonius CAD-4 diffractometer were purchased in part with funds from the National Science Foundation (CHE82-01836 and CHE85-07623, respectively). Accurate mass spectral results from the Midwest Center for Mass Spectrometry were partially supported by the National Science Foundation, Biology Division (Grant No. DIR9017262).

TABLE OF CONTENTS

LIST OF TABLES

LIST OF FIGURES

LIST OF SCHEMES

LIST OF SYMBOLS

amu	Atomic Mass Units
Å	Ångström
δ	Chemical Shift
°	Degree of Angle
°C	Degrees Celsius, Centigrade
K	Degrees Kelvin
$\mathscr{F}$	Faraday
g	Grams
L	Liters
μg	Micrograms
μL	Microliters
μmol	Micromoles
mg	Milligrams
mL	Milliliters
mmu	Milli Mass Units
mmol	Millimoles
M	Molar, Moles per Liter
ppm	Parts per Million
cm^{-1}	Wavenumbers

LIST OF ABBREVIATIONS

n-Bu	$-(CH_2)_3CH_3$
t-Bu	$-C(CH_3)_3$
Cp	$\eta^5-C_5H_5$
Cp*	$\eta^5-C_5(CH_3)_5$
CV	Cyclic Voltammogram
DPPE	$(C_6H_5)_2PCH_2CH_2P(C_6H_5)_2$
DEPE	$(CH_3CH_2)_2PCH_2CH_2P(CH_2CH_3)_2$
EI-MS	Electron Impact Mass Spectrometry
Et	$-CH_2CH_3$
FAB-MS	Fast Atom Bombardment Mass Spectrometry
FTIR	Fourier Transform Infrared
Mc(*n*)	$(\eta^5-C_6(CH_3)_nH_{7-n})Mn(CO)_2$
Me	$-CH_3$
Mr(*n*)	$[(\eta^6-C_6(CH_3)_n)Mn(CO)_2]^+$
MS/MS	Tandem Mass Spectrometry
Mz(*n*)	$[\eta^5-C_6(CH_3)_n(CH_2)]Mn(CO)_2$
NMR	Nuclear Magnetic Resonance
Ph	$-C_6H_5$
i-Pr	$-CH_2(CH_3)_2$
THF	Tetrahydrofuran
UV-Vis	Ultraviolet-Visible

LIST OF NOMENCLATURE AND ENUMERATIONS

Compd No.	Compd Name, Formula
1	(η^6-hexamethylbenzene)manganese tricarbonyl hexafluorophosphate, $[(\eta^6\text{-}C_6Me_6)Mn(CO)_2PMe_3][PF_6]$
1a	(η^6-hexamethylbenzene)manganese dicarbonyl tri-*n*-butylphosphine hexafluorophosphate, $[(\eta^6\text{-}C_6Me_6)Mn(CO)_2P(n\text{-}Bu)_3][PF_6]$
1b	(η^6-hexamethylbenzene)manganese dicarbonyl trimethylphosphine hexafluorophosphate, $[(\eta^6\text{-}C_6Me_6)Mn(CO)_2PMe_3][PF_6]$
1c	(η^6-hexamethylbenzene)manganese dicarbonyl triphenylphosphine hexafluorophosphate, $[(\eta^6\text{-}C_6Me_6)Mn(CO)_2PPh_3][PF_6]$
1d	(η^6-hexamethylbenzene)manganese dicarbonyl trimethylphosphite hexafluorophosphate, $[(\eta^6\text{-}C_6Me_6)Mn(CO)_2P(OMe)_3][PF_6]$
1e	(η^6-hexamethylbenzene)manganese dicarbonyl triphenylphosphite hexafluorophosphate, $[(\eta^6\text{-}C_6Me_6)Mn(CO)_2P(OPh)_3][PF_6]$
2	(η^5-pentamethylcyclohexadienyl-*exo*-ene)manganese tricarbonyl, $(\eta^5\text{-}C_6Me_5CH_2)Mn(CO)_3$
2a	(η^5-pentamethylcyclohexadienyl-*exo*-ene)manganese dicarbonyl tri-*n*-butylphosphine, $(\eta^5\text{-}C_6Me_5CH_2)Mn(CO)_2P(n\text{-}Bu)_3$
2b	(η^5-pentamethylcyclohexadienyl-*exo*-ene)manganese dicarbonyl trimethylphosphine, $(\eta^5\text{-}C_6Me_5CH_2)Mn(CO)_2PMe_3$
2c	(η^5-pentamethylcyclohexadienyl-*exo*-ene)manganese dicarbonyl triphenylphosphine, $(\eta^5\text{-}C_6Me_5CH_2)Mn(CO)_2PPh_3$
2d	(η^5-pentamethylcyclohexadienyl-*exo*-ene)manganese dicarbonyl trimethylphosphite, $(\eta^5\text{-}C_6Me_5CH_2)Mn(CO)_2P(OMe)_3$
2e	(η^5-pentamethylcyclohexadienyl-*exo*-ene)manganese dicarbonyl triphenylphosphite, $(\eta^5\text{-}C_6Me_5CH_2)Mn(CO)_2P(OPh)_3$
4a	(η^6-methyl phenyl ketone pentamethylbenzene)manganese dicarbonyl tri-*n*-butylphosphine hexafluorophosphate, $[(\eta^6\text{-}C_6Me_5CH_2C(O)Ph)Mn(CO)_2P(n\text{-}Bu)_3][PF_6]$

4b (η^6–methyl phenyl ketone pentamethylbenzene)manganese dicarbonyl trimethylphosphine hexafluorophosphate, $[(\eta^6\text{–}C_6Me_5CH_2C(O)Ph)Mn(CO)_2PMe_3][PF_6]$

4c (η^6–methyl phenyl ketone pentamethylbenzene)manganese dicarbonyl triphenylphosphine hexafluorophosphate, $[(\eta^6\text{–}C_6Me_5CH_2C(O)Ph)Mn(CO)_2PPh_3][PF_6]$

4d (η^6–methyl phenyl ketone pentamethylbenzene)manganese dicarbonyl trimethylphosphite chloride, $[(\eta^6\text{–}C_6Me_5CH_2C(O)Ph)Mn(CO)_2P(OMe)_3]Cl$

4e (η^6–methyl phenyl ketone pentamethylbenzene)manganese dicarbonyl triphenylphosphite chloride, $[(\eta^6\text{–}C_6Me_5CH_2C(O)Ph)Mn(CO)_2P(OPh)_3]Cl$

5a (η^6–ethylpentamethylbenzene)manganese dicarbonyl tri–*n*–butylphosphine hexafluorophosphate, $[(\eta^6\text{–}C_6Me_5Et)Mn(CO)_2P(n\text{–}Bu)_3][PF_6]$

5b (η^6–ethylpentamethylbenzene)manganese dicarbonyl trimethylphosphine hexafluorophosphate, $[(\eta^6\text{–}C_6Me_5Et)Mn(CO)_2PMe_3][PF_6]$

5c (η^6–ethylpentamethylbenzene)manganese dicarbonyl triphenylphosphine hexafluorophosphate, $[(\eta^6\text{–}C_6Me_5Et)Mn(CO)_2PPh_3][PF_6]$

5e (η^6–ethylpentamethylbenzene)manganese dicarbonyl triphenylphosphite hexafluorophosphate, $[(\eta^6\text{–}C_6Me_5Et)Mn(CO)_2P(OPh)_3][PF_6]$

6 (η^6–ethylpentamethylbenzene)manganese dicarbonyl dimethyl phosphonate, $(\eta^6\text{–}C_6Me_5Et)Mn(CO)_2P(O)(OMe)_2$

7a (η^6–iodomethylpentamethylbenzene)manganese dicarbonyl tri–*n*–butylphosphine hexafluorophosphate, $[(\eta^6\text{–}C_6Me_5CH_2CH_2I)Mn(CO)_2P(n\text{–}Bu)_3][PF_6]$

7b (η^6–iodomethylpentamethylbenzene)manganese dicarbonyl trimethylphosphine hexafluorophosphate, $[(\eta^6\text{–}C_6Me_5CH_2CH_2I)Mn(CO)_2PMe_3][PF_6]$

7c (η^6–iodomethylpentamethylbenzene)manganese dicarbonyl triphenylphosphine iodide, $[(\eta^6\text{–}C_6Me_5CH_2CH_2I)Mn(CO)_2PPh_3]I$

7d (η^6-iodomethylpentamethylbenzene)manganese dicarbonyl trimethylphosphite hexafluorophosphate, $[(\eta^6\text{-}C_6Me_5CH_2CH_2I)Mn(CO)_2P(OMe)_3][PF_6]$

7e (η^6-iodomethylpentamethylbenzene)manganese dicarbonyl triphenylphosphite iodide, $[(\eta^6\text{-}C_6Me_5CH_2CH_2I)Mn(CO)_2P(OPh)_3]I$

8 (η^6-iodomethylpentamethylbenzene)manganese dicarbonyl dimethyl phosphonate, $(\eta^6\text{-}C_6Me_5CH_2CH_2I)Mn(CO)_2P(O)(OMe)_2$

9 (η^6-(methyl)iron(η^5-cyclopentadienyl) dicarbonyl pentamethylbenzene)manganese dicarbonyl trimethylphosphine iodide, $[(\eta^6\text{-}C_6Me_5CH_2FeCp(CO)_2)Mn(CO)_2PMe_3]I$

10 (η^6-(methyl)manganese pentacarbonyl pentamethylbenzene)manganese dicarbonyl trimethylphosphine hexafluorophosphate, $[(\eta^6\text{-}C_6Me_5CH_2Mn(CO)_5)Mn(CO)_2PMe_3][PF_6]$

11 *endo*-(η^5-hexamethylcyclohexadienyl)manganese tricarbonyl, *endo*-$(\eta^5\text{-}C_6Me_6H)Mn(CO)_3$

11a *endo*-(η^5-hexamethylcyclohexadienyl)manganese dicarbonyl tri-*n*-butylphosphine, *endo*-$(\eta^5\text{-}C_6Me_6H)Mn(CO)_2P(n\text{-}Bu)_3$

11b *endo*-(η^5-hexamethylcyclohexadienyl)manganese dicarbonyl trimethylphosphine, *endo*-$(\eta^5\text{-}C_6Me_6H)Mn(CO)_2PMe_3$

11c *endo*-(η^5-hexamethylcyclohexadienyl)manganese dicarbonyl triphenylphosphine, *endo*-$(\eta^5\text{-}C_6Me_6H)Mn(CO)_2PPh_3$

11d *endo*-(η^5-hexamethylcyclohexadienyl)manganese dicarbonyl trimethylphosphite, *endo*-$(\eta^5\text{-}C_6Me_6H)Mn(CO)_2P(OMe)_3$

11e *endo*-(η^5-hexamethylcyclohexadienyl)manganese dicarbonyl triphenylphosphite, *endo*-$(\eta^5\text{-}C_6Me_6H)Mn(CO)_2P(OPh)_3$

12 (η^6-2,2-dibromoethylpentamethylbenzene)manganese dicarbonyl bromide, $(\eta^6\text{-}C_6Me_5CH_2CHBr_2)Mn(CO)_2Br$

13 (η^6-2,2,2-trichloroethylpentamethylbenzene)manganese dicarbonyl chloride, $(\eta^6\text{-}C_6Me_5CH_2CCl_3)Mn(CO)_2Cl$

14 (η^6-2,2-dichloro-2-deuteroethylpentamethylbenzene)manganese dicarbonyl chloride, $(\eta^6\text{-}C_6Me_5CH_2CDCl_2)Mn(CO)_2Cl$

21a (η^6-hexamethylbenzene)manganese dicarbonyl triethylphosphite hexafluorophosphate, $[(\eta^6\text{-}C_6Me_6)Mn(CO)_2P(OEt)_3][PF_6]$

21b (η^6-hexamethylbenzene)manganese dicarbonyl d_9-trimethylphosphite hexafluorophosphate, $[(\eta^6\text{-}C_6Me_6)Mn(CO)_2P(OCD_3)_3][PF_6]$

21c (η^6-hexamethylbenzene)manganese dicarbonyl d_{15}-triphenylphosphite hexafluorophosphate, $[(\eta^6\text{-}C_6Me_6)Mn(CO)_2P(OC_6D_5)_3][PF_6]$

22a (η^6-toluene)manganese tricarbonyl hexafluorophosphate, $[(\eta^6\text{-}C_6H_5Me)Mn(CO)_3][PF_6]$

22b (η^6-d_8-toluene)manganese tricarbonyl hexafluorophosphate, $[(\eta^6\text{-}C_6D_5CD_3)Mn(CO)_3][PF_6]$

23a (η^6-toluene)manganese dicarbonyl triphenylphosphite hexafluorophosphate, $[(\eta^6\text{-}C_6H_5Me)Mn(CO)_2P(OPh)_3][PF_6]$

23b (η^6-d_8-toluene)manganese dicarbonyl d_{15}-triphenylphosphite hexafluorophosphate, $[(\eta^6\text{-}C_6D_5CD_3)Mn(CO)_2P(OC_6D_5)_3][PF_6]$

24a (η^5-pentamethylcyclohexadienyl-*exo*-ene)manganese dicarbonyl triethylphosphite, $(\eta^5\text{-}C_6Me_5CH_2)Mn(CO)_2P(OEt)_3$

24b (η^5-pentamethylcyclohexadienyl-*exo*-ene)manganese dicarbonyl d_9-trimethylphosphite, $(\eta^5\text{-}C_6Me_5CH_2)Mn(CO)_2P(OCD_3)_3$

24c (η^5-pentamethylcyclohexadienyl-*exo*-ene)manganese dicarbonyl d_{15}-triphenylphosphite, $(\eta^5\text{-}C_6Me_5CH_2)Mn(CO)_2P(OC_6D_5)_3$

25a (η^5-cyclohexadienyl-*exo*-ene)manganese dicarbonyl triphenylphosphite, $(\eta^5\text{-}C_6H_5CH_2)Mn(CO)_2P(OPh)_3$

25b (η^5-cyclohexadienyl-*exo*-ene)manganese dicarbonyl d_{15}-triphenylphosphite, $(\eta^5\text{-}C_6D_5CD_2)Mn(CO)_2P(OC_6D_5)_3$

26a (η^6-hexamethylbenzene)manganese dicarbonyl diethyl phosphonate, $(\eta^6\text{-}C_6Me_5Et)Mn(CO)_2P(O)(OEt)_2$

26b (η^6-hexamethylbenzene)manganese dicarbonyl dimethyl phosphonate, $(\eta^6\text{-}C_6Me_6)Mn(CO)_2P(O)(OMe)_3$

26c (η^6-1-deuteromethylpentamethylbenzene)manganese dicarbonyl d_6-dimethyl phosphonate, $(\eta^6\text{-}C_6Me_5CH_2D)Mn(CO)_2P(O)(OCD_3)_2$

26d (η^6-hexamethylbenzene)manganese dicarbonyl diphenyl phosphonate, $(\eta^6\text{-}C_6Me_6)Mn(CO)_2P(O)(OPh)_3$

26e (η^6-1-deuteromethylpentamethylbenzene)manganese dicarbonyl d_{10}-diphenyl phosphonate, $(\eta^6\text{-}C_6Me_5CH_2D)Mn(CO)_2P(O)(OC_6D_5)_2$

51 (η^6-hexamethylbenzene)manganese dicarbonyl dithioformate, $(\eta^6\text{-}C_6Me_6)Mn(CO)_2SC(S)H$

52 (η^6-hexamethylbenzene)manganese dicarbonyl triphenylmethyl dithioformate ester tetrafluoroborate, $[(\eta^6\text{-}C_6Me_6)Mn(CO)_2(SCHSCPh_3)][BF_4]$

53 (η^6-hexamethylbenzene)manganese dicarbonyl *N,N*-diethylthioformamide tetrafluoroborate, $[(\eta^6\text{-}C_6Me_6)Mn(CO)_2(SCHNEt_2)][BF_4]$

54 (η^6-hexamethylbenzene)manganese dicarbonyl *N*-phenylthioformamide tetrafluoroborate, $[(\eta^6\text{-}C_6Me_6)Mn(CO)_2(SCHNHPh)][BF_4]$

55 (η^6-hexamethylbenzene)manganese dicarbonyl *N-tert*-butylthioformamide tetrafluoroborate, $[(\eta^6\text{-}C_6Me_6)Mn(CO)_2(SCHNH(t\text{-}Bu))][BF_4]$

57 (η^6-hexamethylbenzene)manganese dicarbonyl triphenylisonitrile tetrafluoroborate, $[(\eta^6\text{-}C_6Me_6)Mn(CO)_2CNCPh_3][BF_4]$

58 manganese pentacarbonyl dithioformate, $Mn(CO)_5SCH(S)$

59 (η^5-pentamethylcyclopentadienyl)iron dicarbonyl dithioformate, $Cp^*Fe(CO)_2SCH(S)$

— Manganese Pentacarbonyl Bromide, $Mn(CO)_5Br$

INTRODUCTION

Historical

The chemistry of (arene)manganese carbonyl complexes has been studied since 1960, when Wilkinson and co-workers first reported the preparation of $[(\eta^6\text{-}C_6H_6)Mn(CO)_3]X$ complexes, structure I.[1] Derivatives of the cationic

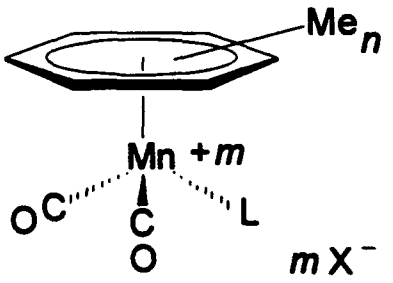

(L = CO, CN, C(O)NHR, $CONHNH_2$, C(O)OMe, NCO, Me, Ph, C(O)Me, C(O)Ph, halide, PR_3; $n = 0, 1, 3, 5, 6$; $m = 0, 1$)

I

(η^6-arene)manganese tricarbonyl complexes have been formed by substitution of one carbonyl by nucleophilic anions such as cyanide,[2] alkyls,[3] aryls,[3] acyls,[3] *N*-alkyl carboxyamides,[4] carboxyhydrazide,[4] isocyanate,[4] and carboalkyloxides.[5] These complexes, (η^6-arene)$Mn(CO)_2L$, are isoelectronic with the analogous iron complexes, $CpFe(CO)_2L$. The syntheses of (η^6-arene)manganese dicarbonyl halides, hydride, and alkyls were reported by Eyman and co-workers.[6] These complexes can be used as the starting materials for synthesizing a wide range of derivatives in nucleophilic substitution reactions paralleling those observed for the iron analogues. Phosphines can be substituted for one of the carbonyls in the (η^6-arene)manganese tricarbonyl

complexes by first oxidizing the carbonyl.[7,8]

Numerous studies of the reactivity of cationic (η^6–arene)manganese tricarbonyl complexes have been reported.[1,2,3,7,8,9] Nucleophilic attack at the arene ring which results in the formation of neutral (η^5–cyclohexadienyl)manganese tricarbonyl complexes, structure II, has been an important theme in these papers. The chemistry of mono-substituted phosphine (η^5–cyclohexadienyl)manganese dicarbonyl complexes has also been studied.[8] One consequence of the manganese tricarbonyl research was the identification of (η^5–$C_6Me_5CH_2$)$Mn(CO)_3$, structure III, formed in a deprotonation side-reaction in the synthesis of the cyclohexadienyl complexes by Eyman and co-workers.[10]

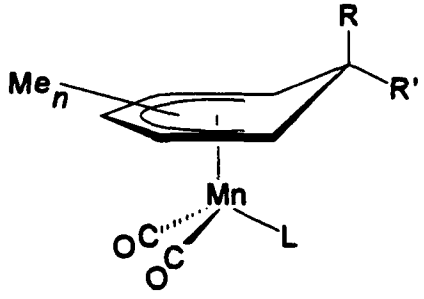

II

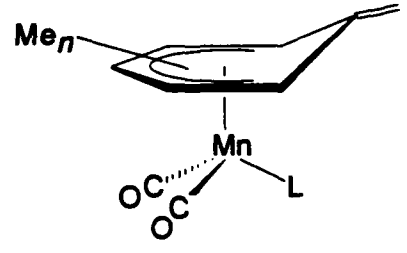

III

The deprotonation of coordinated arenes to form a reactive exocyclic methylene, which can be subsequently alkylated using a wide variety of reagents, provides a useful synthetic tool. Early work on chromium carbonyl complexes of toluene and ethylbenzene revealed an area of chemistry with great potential for the derivatization of coordinated arenes.[11] The deprotonation of CpFe(arene) complexes by strong bases was reported concurrently.[12,13] Conjugation with strained ring systems, fluorene [12,13c] or carbazole,[13c] or heteroatoms (O, S, or N) [13c] was found to stabilize the deprotonated CpFe(arene) complexes. However, it was not until the synthesis and

characterization of $CpFe^{II}(\eta^5\text{-}C_6Me_5CH_2)$,[14] structure IV, by an X-ray crystal structure that the exocyclic methylene was observed by Astruc and co-workers. These complexes were made by O_2 oxidation of the Fe(I) complexes or deprotonation of the Fe(II) complexes.[14a]

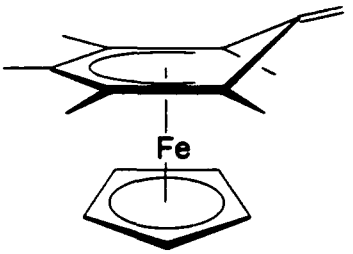

IV

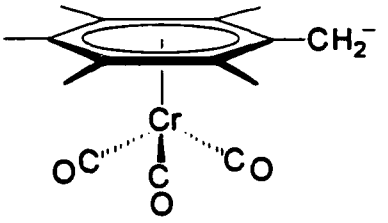

V

The configurations of the η^5-benzyl complexes, resulting from the deprotonation of coordinated arenes, provide part of the explanation for the observed reactivity of these complexes. Alternatively, the crystal structure reported for the deprotonated $CpFe^+$(fluorene) reveals that the arene, after removing a proton, remains nearly planar.[12] The planarity was explained by proposing a zwitterionic structure. The $K^+[(\eta^6\text{-}C_6Me_5CH_2^-)Cr(CO)_3]$ complex, structure V, was proposed to have a localized charge on the exocyclic methylene by Yaouanc et al.[15] However, a stable exocyclic double bond was formed by the deprotonation of $CpFe(\eta^6$-triphenylmethane).[13c] The exocyclic methylene found by Astruc was kinetically stabilized by the permethylation of the arene.[14a] Permethylation, for the same reason, allows many of the precursors and products to be thermally stable. The exocyclic methylene acts as a neutral nucleophile rather than a carbanion in most reactions. Although it is not a zwitterion, it can form zwitterions after reacting with CO_2, CS_2, and metal carbonyls.

The chemistry of the η^5-pentamethylcyclohexadienyl-*exo*-ene ligand, or more commonly the "η^5-pentamethylbenzyl" ligand, was extended using manganese as the metal ion by LaBrush et al.[10] LaBrush found that $[(\eta^6\text{-}C_6Me_6)Mn(CO)_3][PF_6]$ could be deprotonated using KH or other strong bases to form an η^5-benzyl complex, $(\eta^5\text{-}C_6Me_5CH_2)Mn(CO)_3$, structure III, similar to that observed by Astruc. And indeed, this complex underwent many of the nucleophilic reactions that had been observed by Astruc. Its reactivity was not as great as that observed for the iron complexes, evidenced by the lack of reaction with other organometallic complexes such as $Mn(CO)_5Br$ and $CpFe(CO)_2Cl$. However, it did apparently undergo radical reactions with halocarbons. The goal of the work reported in Chapter II was to increase the nucleophilic reactivity of the exocyclic methylene. This led to the syntheses of the (η^5-pentamethylbenzyl)manganese mono-substituted phosphine complexes.

The $(\eta^5\text{-}C_6Me_5CH_2)Mn(CO)_2PR_3$ (R = *n*-Bu, Me, Ph, OMe, OPh) complexes, structure III, exhibit greater reactivity than the manganese tricarbonyl complex.[16] The mono-phosphine substituted complexes form in solution in the presence of KH or other strong bases. The greater reactivity derived from phosphine substitution is demonstrated by the $(\eta^6\text{-}C_6Me_5CH_2)Mn(CO)_2PMe_3$ complex, which forms bimetallic complexes in reactions with $Mn(CO)_5Br$ and $CpFe(CO)_2I$. In addition, these mono-phosphine-substituted η^5-benzyls undergo all of the reactions displayed by the manganese tricarbonyl η^5-benzyl complex.

Carbenes and benzyne were found to be generated from the phosphite ester substituted (η^5-pentamethylbenzyl)manganese complexes. These phosphite ester complexes were observed to undergo a chemical reaction under reduced pressure ($\sim 10^{-3}$ torr) to form (η^6-hexamethylbenzene)manganese dicarbonyl dialkyl- and diaryl phosphonates, structure VI. This reaction was shown to involve the abstraction of

hydrogen from the alkyl or aryl substituent of the coordinated phosphite ligand resulting in the formation of carbenes or benzyne and a coordinated dialkyl- or diaryl-substituted phosphonate ligand. The results of these studies are reported in Chapter III.

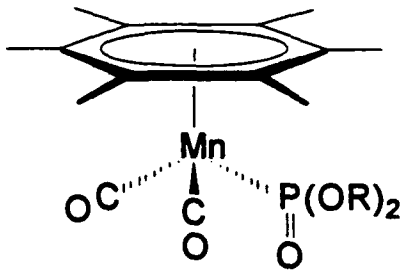

VI

Manganese dithioformates and thioformamides have been utilized in industrial metal treatments [17] and as additives in natural gas fuels,[18] and reported as potential lubricants.[19] The synthesis and reactivity of (η^6-arene)manganese dicarbonyl η^1-dithioformate compounds, structure VIII, was reported by Schauer et al.[20] One of

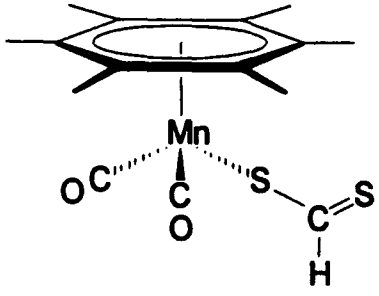

VIII

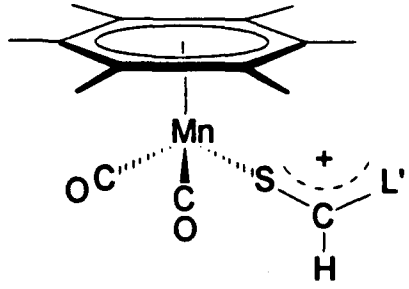

IX

the goals of our research was to study the reactions of the (η^6-arene)manganese

dicarbonyl η^1–triphenylmethyl dithioformate ester complex with nucleophiles. Subsequently, we reported the metal-mediated conversion of an η^1–dithioformate into thio–C_1 ligands, including thioformamides and alkanethiolates, structures IX.[21] These reactions have potentially useful synthetic applications in thioderivatization. Previously, potassium dithioformate has been used to form thioformamide derivatives of proteins to better understand their chemical and physical properties.[22]

CHAPTER I

GENERAL PROCEDURES

Introduction

A variety of spectroscopic and spectrometric techniques are available to aid in the identification of organometallic and coordination compounds. The techniques used in our studies are described. The laboratory preparations that have been changed or improved are reported. Tables are provided that list the various solvents, reagents, and compounds used and their sources.

Experimental

General Methods

Reactions and recrystallizations were performed under dinitrogen or argon using either standard Schlenk or glovebox techniques.[23] The glovebox, manufactured by Vacuum Atmospheres Corporation, provided a dry, inert atmosphere of dinitrogen or argon for the transfer and manipulation of air- and water-sensitive complexes. Solvents were dried over suitable reagents and freshly distilled under nitrogen.[24] Tetrahydrofuran was distilled from potassium/benzophenone or molten potassium. Tetrachloromethane and dichloromethane were distilled from phosphorus pentaoxide. Hexane was distilled from calcium hydride. Solvents were further deoxygenated prior to use by multiple freeze-pump-thaw cycles or by bubbling dinitrogen or argon through the solution. Glassware was heated to a minimum of 130 °C and vacuum-purged prior to use. Solid compounds were deoxygenated by multiple vacuum-purge cycles before

use. Untreated silica gel (60–200 mesh) was used for liquid chromatography purification of products.

Dimanganese decacarbonyl was typically sublimed at 47 °C (1.33×10^{-1} Pa) and stored in an inert atmosphere at −15 °C prior to use; however, the purity of $Mn(CO)_5Br$ produced from the sublimed material was the same as obtained using the unsublimed $Mn_2(CO)_{10}$ reagent. Trimethylamine-*N*-oxide was prepared by azeotropic distillation with benzene to remove waters of hydration, followed by vacuum pumping, and storage in a desiccator. Immediately prior to use, potassium hydride was washed three times with a minimum of 30 mL of dry hexane to remove mineral oil, then hexane was removed under reduced pressure.

Instrumentation

Infrared Spectroscopy. Infrared spectroscopy was used for the characterization and identification of compounds and monitoring of reactions, where the intensities of the carbonyl bands indicated the progress of the reaction. Infrared spectra were obtained on a Mattson Cygnus 25 FTIR spectrometer. The spectrometer was computer controlled and purged with dry, carbon dioxide-free air. The solution spectra were obtained using 0.5 mm potassium bromide cells, and solid state spectra, using KBr mull and press techniques. The solution cell was purged with inert gas prior to injection of the sample.

Nuclear Magnetic Resonance Spectroscopy. ^{1}H, ^{2}H, ^{13}C, $^{13}C\{^{1}H\}$, and ^{31}P NMR spectra were recorded on either a Bruker AC-300 or WM-360 spectrometer. ^{1}H, ^{2}H, ^{13}C, and $^{13}C\{^{1}H\}$ NMR shifts are reported with respect to Me_4Si (δ 0.0 ppm). ^{31}P NMR shifts are reported with respect to an external standard, H_3PO_4 (85 %) (δ 0.0 ppm). All downfield chemical shifts are positive. Spectra were obtained from samples

dissolved in an appropriate solvent, in 5 mm glass NMR tubes.

Mass Spectrometry. High resolution accurate mass measurements were obtained using a VG ZAB-HF mass spectrometer in the FAB ionization mode. A VG Trio-3 tandem mass spectrometer was used to obtain FAB-MS/MS spectra.[25] The Mn complexes were dissolved in neat 3-nitrobenzyl alcohol (NBA) and placed on a standard stainless-steel FAB probe tip. The VG ZAB-HF ion source was the standard VG Analytical, Inc., design using a saddle field fast atom gun. In either case, samples were sputtered using an ~8-keV beam of xenon atoms with neutral beam currents equivalent to 2.0 mA supplied by an ION TECH (Model B 50) current and voltage regulator/meter. The molecular ions generated were mass selected by the first quadrupole mass analyzer, collisionally activated in the hexapole collision cell using Xe gas with a collision energy of 7 eV. Collision gas was introduced until the analyzer gas pressure was 1.0×10^{-4} Pa (normal pressure: 1.0×10^{-6} Pa). The product fragment ions formed were then mass analyzed in the second quadrupole mass analyzer. Signal adding of eight scans (3 s per scan) was performed using the multichannel analysis (MCA) software of the VG II 250 J data system.

X-ray Crystallography. Crystallographic studies were performed using a Eraf-Nonius diffractometer and SDP software on a MicroVAX 2 computer. Details of specific experiments are discussed in subsequent chapters.

UV-Visible Spectroscopy. The UV-visible spectra were recorded on a Hewlett-Packard 8452A Diode Array Spectrophotometer.

Electrochemistry. Cyclic voltammograms were obtained, under inert-atmospheric conditions, using a three-electrode system consisting of a 6.28 mm^2 Pt disk working electrode, a coiled Pt wire counter electrode, and a Ag | AgCl reference

electrode. The supporting electrolyte for the reference electrode was a LiCl saturated, 0.1 M $[(n\text{-Bu})_4N][BF_4]$ THF solution. The reference electrode was suspended within a Luggin capillary to minimize the *IR* drop across the electrodes. Electrochemistry was carried out with a PAR 173 Potentiostat in conjunction with a PAR 175 Programmer. Cyclic voltammograms, recorded using a HP 7040A X-Y recorder, were corrected using ferrocene versus the Ag | AgCl reference electrode (E_p = +0.342 V) and a standard calomel electrode (SCE) (E_p = +0.630 V).

Organometallic Reagents

The reagents and solvents used in the preparation and reactions with these compounds are listed in Tables 2-5, and were used as supplied unless otherwise noted. The general synthesis of (hexamethylbenzene)manganese tricarbonyl hexafluorophosphate, $[(\eta^6\text{-}C_6Me_6)Mn(CO)_3][PF_6]$ (1), is outlined in Scheme I.[1a,9a,26] The published procedure for the synthesis of $Mn(CO)_5Br$ was modified to decrease reaction times and increase yields.[27]

$Mn(CO)_5Br$. $Mn_2(CO)_{10}$ (6.071 g, 15.56 mmol) was placed in a 250 mL Schlenk flask and deoxygenated by first evacuating, then purging the flask with dinitrogen. The compound was then dissolved in 100 mL of CS_2 which had been evacuated and purged with nitrogen one time. Final deoxygenation was accomplished by bubbling dinitrogen through the orange-yellow solution for 15 min, which also served to cool the solution. A positive pressure of nitrogen was maintained over the solution. Bromine (1.80 mL, 34.94 mmol) was then injected into the solution over a period of 10-15 s. The solution color turned very dark red. The solution was carefully heated to reflux. The heat was then removed, and the solution was stirred for 2 hours. The solvent and excess bromine were removed under reduced pressure using a liquid-nitrogen-cooled solvent trap.

Scheme I. Synthesis of $[(\eta^6\text{-}C_6Me_6)Mn(CO)_3][PF_6]$

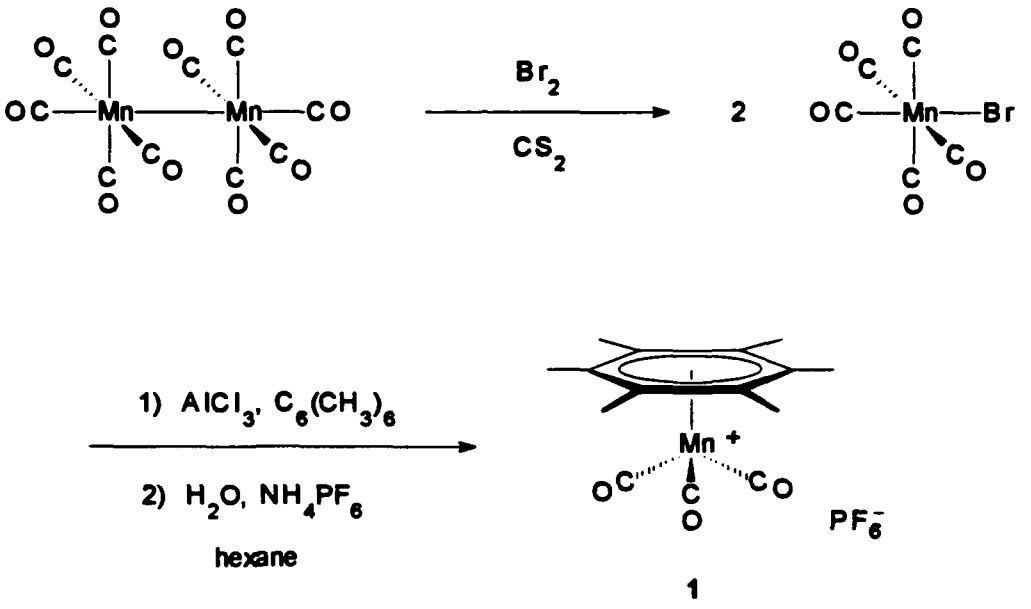

The $Mn(CO)_5Br$ was isolated as an orange powder. Product formation was confirmed by comparison to the IR spectral data in Table 1. Yield: 97-99%.

$[(\eta^6\text{-}C_6Me_6)Mn(CO)_3][PF_6]$ (1). $Mn(CO)_5Br$ (8.425 g, 30.65 mmol) and hexamethylbenzene (10.114 g, 62.33 mmol) were dissolved in 250 mL of dry hexane in a 500 mL Schlenk flask and deoxygenated by bubbling nitrogen through the solution for 15 min. The orange solution was carefully heated to reflux. $AlCl_3$ (10.2 g, 76.5 mmol) was added to the stirred, hot solution. The flask was then connected to a reflux condenser, then nitrogen was used to flush the flask and column for 3 min. The solution was refluxed with stirring for 0.5 h past the time required for the solution to turn colorless and a dark orange solid to form on the sides of the flask—usually about 2.5 hours. The hot hexane was decanted, and the solids were washed two times with

200 mL portions of dry hexane. The hexane solution was collected to recover unreacted hexamethylbenzene. The solid product was hydrolyzed by the rapid addition of 200 mL of ice. The mixture was stirred until all orange solid dissolves—usually 2-3 hours. The mixture was filtered until a clear yellow solution was obtained. A solution of $[NH_4][PF_6]$ (6.278 g, 76.50 mmol) in 20 mL of H_2O was added to the stirred yellow filtrate, immediately precipitating compound **1**. The resulting very pale yellow powder was filtered, washed with 200 mL of diethyl ether, and then dried in a desiccator overnight. Product formation was confirmed by IR and NMR spectral results, listed in Table 1. Yield: 75-85%.

$[(\eta^6\text{-}C_6Me_6)Mn(CO)_2(PR_3)][PF_6]$ (R = P(n-Bu)$_3$ (1a), PMe_3 (1b), PPh_3 (1c), $P(OMe)_3$ (1d), $P(OPh)_3$ (1e)). Compound **1** and the appropriate phosphines were used to prepare **1a–e** by slightly modified published procedures.[1a,9a,26,8] The chemical reaction is depicted in eq 1. The synthesis of **1c** required meticulously dried Me_3NO (the azeotropic distillation with benzene was repeated) for high yields.

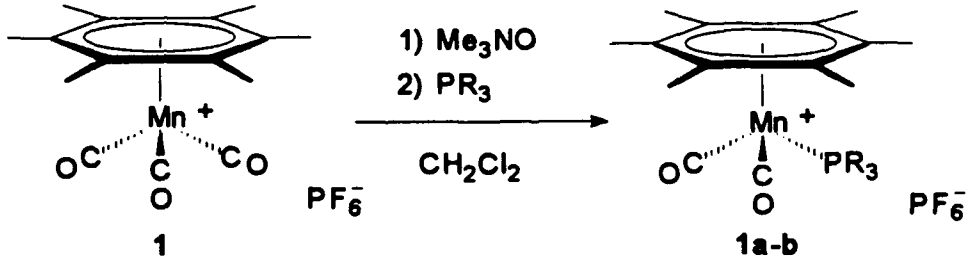

(1)

Typical isolation was accomplished by adsorbing the product on silica (~50 mL) in solution, removing the solvent on a rotary-evaporator, placing the resulting silica on a prepared silica column (~50 mL), adding additional silica (~10 mL) on top, and eluting the products with increasingly polar solvent mixtures.

Table 1. IR and ^{1}H NMR Spectral Data for $Mn(CO)_5Br$ and 1

Compound	ν_{CO}, cm^{-1} [a]	δ, ppm [b]
$Mn(CO)_5Br$	2136, 2083, 2046, 2005	
	2301, 2138, 2052, 2009, 1975 [c]	
1	2056, 1993	2.26 (s, 18 H, CH_3)
	2060, 2001 [c]	

[a] Solution spectra obtained in THF.

[b] ^{1}H NMR spectra obtained in d_6–acetone.

[c] Solution spectra obtained in dichloromethane.

The solvent mixture polarity was increased by first using hexane (600 mL, 100%), then hexane:acetone mixtures (400 mL; 11:2, 5:1, 1:1 mL ratios). A yellow areneless product was eluted with the first hexane:acetone mixture (11:2). The second mixture washed the column of impurities. Finally, the product, a yellow band, was eluted with the 1:1 hexane:acetone mixture. Subsequently, the solvent was removed from the product using a rotary-evaporator until approximately 3-5 mL remained. The oil was washed, first with diethyl ether, then with petroleum ether, during which the compounds **1a–1d** crystallized out. Compound **1e** was recrystallized by dissolving the oil in diethyl ether (~50 mL) and adding petroleum ether (~20 mL) until the solution became cloudy, then placing the mixture in the freezer (−20 °C) for 2 hours. IR and NMR spectroscopic characterization data are listed in Appendix A.

(η^5-$C_6Me_5CH_2$)Mn(CO)$_3$ (2). (η^5-Pentamethylbenzyl)manganese tricarbonyl (2) was prepared by combining 1 and a 50:1 excess of dry KH in deaerated hexane and heating for 24 h, eq 2. Although longer than the published procedure which uses a hexane/THF mixture, this method produced exclusively 2, which does not require

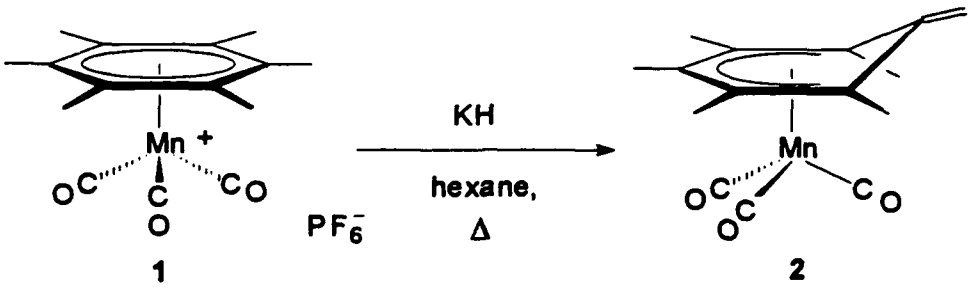

(2)

further purification. Continuous production of 2 was be accomplished by decanting product, then adding solvent in a cycle until the starting materials were depleted.

(η^6-C_6Me_6)Mn(CO)$_2$SC(S)H (21). (η^6-Hexamethylbenzene)manganese dicarbonyl dithioformate (51) was prepared by published procedures, shown in Eq 3.[20]

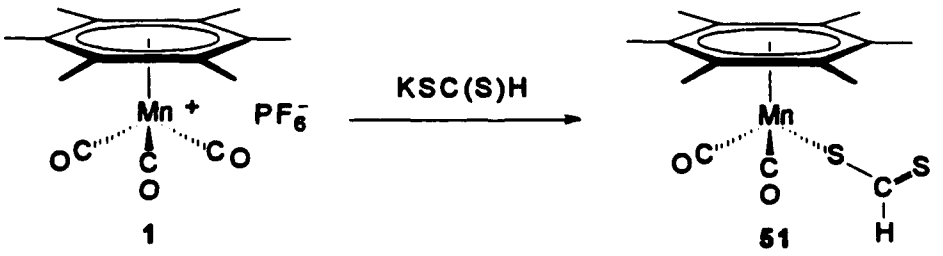

(3)

The reagents and solvents used in the syntheses and in reactions with these compounds are listed in Tables 2-5, and were used as supplied unless otherwise noted. Aniline, obtained from Matheson Coleman and Bell, was distilled under dinitrogen immediately

prior to use.

Inorganic and Organic Reagents

General inorganic and organic reagents used in syntheses and reactions reported here are listed in Table 2.

K[SC(S)H]. Carbon disulfide (5.00 mL, 83.1 mmol) was added via syringe to 100 mL of a freshly prepared 0.80 M solution of K[B(*i*-OPr)$_3$H].[28] The colorless solution turned orange and precipitation of an orange-yellow solid followed. The mixture was stirred for 1 hour, then concentrated and filtered. The product was recrystallized from ethanol. Yield: 35%.

$(C_6D_5O)_3P$. d_{15}-Triphenylphosphite was prepared by substituting d_6-phenol for phenol in the synthesis reported by Gottlieb.[29]

$(CD_3O)_3P$. d_9-Trimethylphosphite was prepared by substituting d_4-methanol in the literature synthesis.[30]

Solvents

Deuterated Solvents. The deuterated solvents used in NMR studies are listed in Table 4.

General Solvents. The solvent used in syntheses, reactions, liquid-chromatographic separations, and crystallizations are listed in Table 5.

Table 2. Inorganic and Organic Reagents

Compound	Notation	Source
acetic acid	AcOH	Fischer
aluminumtrichloride	$AlCl_3$	Fischer, ASAR Baker, ECB
ammonium hexafluorophosphate	$[NH_4][PF_6]$	Aldrich
aniline	$H_2NC_6H_5/H_2NPh$	MCB
benzoyl chloride	$C_6H_5C(O)Cl/PhC(O)Cl$	Aldrich
bromine	Br_2	Fischer
t-butylamine	$H_2NC(CH_3)_3/H_2N$-*t*-Bu	Aldrich
t-butyllithium	$(CH_3)_3CLi$	Aldrich
carbon disulfide	CS_2	Fischer
diethylamine	$HN(CH_2CH_3)_2/HNEt_2$	Aldrich
9,10-dihydroanthracene	9,10-DHA	Aldrich
diphenylphosphine	$PH(C_6H_5)_2/PHPh_2$	Aldrich
ethanol	CH_3CH_2OH/EtOH	Fischer
hexamethylbenzene	$C_6(CH_3)_6$/HMB	Lancaster, Aldrich
iodine	I_2	MCB
iodomethane	CH_3I/MeI	Aldrich
methanol	CH_3OH/MeOH	EM
methyllithium	$(CH_3)Li$/MeLi	Aldrich
phenol	PhOH	Baker
potassium hydride (35 wt %)	KH	Aldrich
potassium hydroxide	KOH	EM
sodium cyanide	NaCN	Allied

Table 2 — continued

Compound	Notation	Source
sodium hydroxide	NaOH	EM
tetrachloromethane	CCl_4	Fischer
tribromomethane (96%)	$CHBr_3$	Aldrich
tri-*n*-butylphosphine	$P[(CH_2)_3CH_3]/P(n\text{-}Bu)_3$	Aldrich
tributyltin hydride	$[CH_3(CH_2)_3]SnH/Bu_3SnH$	Aldrich
trichloromethane	$CHCl_3$	EM
triethylaluminum	$Al(CH_2CH_3)_3/AlEt_3$	Aldrich
trimethylalumium	$Al(CH_3)_3/AlMe_3$	Aldrich
trimethylamine-*N*-oxide	$(CH_3)_3NO/Me_3NO$	Eastman
trimethylphosphine	$P(CH_3)_3/PMe_3$	Aldrich
trimethylphosphite	$P(OCH_3)_3/P(OMe)_3$	Aldrich
triphenylcarbenium tetrafluoroborate	$(C_6H_5)_3CBF_4/Ph_3CBF_4$	Aldrich
triphenylphosphine	$P(C_6H_5)_3/PPh_3$	Aldrich, Baker Eastman
triphenylphosphite	$P(OC_6H_5)_3/P(OPh)_3$	Aldrich

[a] Source abbreviations: Aldrich (*Aldrich Chemical Co.*), Allied (*Allied Chemical Co.*), ASAR (), Baker (*Baker Chemical Co.*), Eastman (*Eastman Organic Chemicals*), EM (*EM*), Fischer (*Fischer Scientific*), Lancaster (*Lancaster Synthesis, Inc.*), MCB (*Matheson Coleman and Bell*), Pressure (*Pressure Chemicals*), and Strem (*Strem Chemical*).

Table 3. Organometallic Reagents

Compound	Notation	Source [a]
(cyclopentadienyl)iron dicarbonyl iodide	FpI	Schlom, P.
endo-(η^5-hexamethylcyclohexadienyl) manganese dicarbonyl trimethyl-phosphite	**11d**	Synder, D. B.
(η^6-hexamethylbenzene)manganese dicarbonyl chloride	Mr(6)Cl	Morken, A. M.
(pentamethylcyclopentadienyl)iron dicarbonyl chloride	Fp*I	Schlom, P.
manganese decacarbonyl	$Mn_2(CO)_{10}$	Pressure

[a] Source abbreviation: Pressure (*Pressure Chemical Co.*).

Table 4. Deuterated Solvents

Compound	Notation	Source [a]
d_6-acetone (99.8 atom % D)	$(CD_3)_2CO$	Cambridge
d_6-benzene (99.5 atom % D)	C_6D_6	Aldrich, Cambridge
d_4-methanol (99.95 atom % D)	CD_3OD	Aldrich
d_6-phenol (98+ atom % D)	C_6D_5OD	Cambridge
d_8-tetrahydrofuran (99.5 atom % D)	$(CD_2)_4O$	Aldrich
d_8-toluene (99+ atom % D)	$C_6D_5CD_3$	Aldrich
d-trichloromethane (99.8 atom % D)	$CDCl_3$	Aldrich
tetramethylsilane [b]	tms	Aldrich

[a] Source abbreviations: Aldrich (*Aldrich Chemical Co.*) and Cambridge (*Cambridge Isotope Lab.*).
[b] NMR standard reference.

Table 5. General Solvents

Compound	Notation	Source [a]
acetone		EM
benzene		EM
dichloromethane	CH_2Cl_2	EM
diethyl ether		Fischer
hexane		EM
tetrahydrofuran	THF	Fischer
		EM

[a] Source abbreviations: Eastman (*Eastman Organic Chemicals*), EM (*EM*), Fischer (*Fischer Scientific*), and MCB (*Matheson Coleman and Bell*).

CHAPTER II

PREPARATION, CHARACTERIZATION, AND REACTIVITY OF $(\eta^5\text{-}C_6Me_5CH_2)Mn(CO)_2PR_3$ (R = *n*-Bu, Me, Ph, OMe, OPh). CRYSTAL STRUCTURE OF $(\eta^5\text{-}C_6Me_5CH_2)Mn(CO)_2PMe_3$.[16]

Introduction

The activation of hydrocarbon C–H bonds with subsequent formation of new C–C and C–H has been accomplished using four systematic approaches. The C–H bond can be oxidized by a radical mechanism,[31] eq 4, or reduced by oxidative addition

$$R\cdot + O_2 \longrightarrow ROO\cdot \xrightarrow{RH} ROOH + R\cdot \qquad (4)$$

to transition metals, eq 5.[32] Bercaw introduced the term "σ-bond metathesis" for the

$$R\text{–}H + M \longrightarrow R\text{–}M\text{–}H \qquad (5)$$

"heterolytic" cleavage of C–H bond by electrophilic metal that are coordinatively unsaturated and electron deficient, eq 6.[33] Astruc has developed a third route in which

$$L_nM\text{–}R + R'\text{–}H \longrightarrow L_nM\text{–}R' + R\text{–}H \qquad (6)$$

(R, R′ = H, alkyl, alkenyl, aryl, alkynyl)

initiation occurs by a single electron transfer to O_2 from an organoiron complex, eq 7.[34] A methyl group of the coordinated hexamethylbenzene ligand in the intermediary

$$MRH + O_2 \longrightarrow MRH^{+}O_2^{-} \xrightarrow{-HO_2} MR \qquad (7)$$

$CpFe(\eta^6\text{-}C_6Me_6)^{+}O_2^{\cdot-}$ complex is subsequently deprotonated by $O_2^{\cdot-}$. Astruc also has formed the complex, $CpFe(\eta^5\text{-}C_6Me_5CH_2)$, by deprotonation of methyl substituents of the arene in $[CpFe(\eta^6\text{-}C_6Me_6)]^{+}$ using KO_2 and *t*-BuOK.[14c] We have reported similar observations for the (arene)manganese complex, $[(\eta^6\text{-}C_6Me_6)Mn(CO)_3][PF_6]$ (**1**).[10] In our experiments, a methyl of the hexamethylbenzene ligand of **1** is deprotonated using KH, or other strong bases, to form $(\eta^5\text{-}C_6Me_5CH_2)Mn(CO)_3$ (**2**), eq 8. Gladfelter

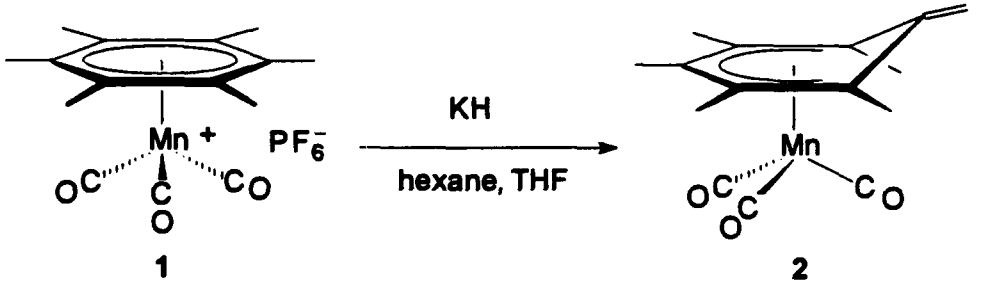

1 **2** (8)

confirmed and extended this chemistry to other (η^6-arene)manganese tricarbonyl complexes.[35] The complexes generated by each of these methods can undergo a variety of reactions at the exocyclic methylene leading to the formation of new C–C bonds and carbon bonds to other elements.

The exocyclic methylene on the metal-coordinated pentahapto–cyclohexadienyl–*exo*–ene ligand, (η^5–pentamethylbenzyl), can undergo nucleophilic, radical, and other reactions to form C–C, C–I, C–Mn, C–Fe, and C–H bonds. Astruc et al. extensively

investigated the reactivity of the CpFe(η^5-pentamethylbenzyl) (**3**) complex with a variety of electrophiles.[14,36] Reactivity of the exocyclic methylene provided an efficient means of alkylating and functionalizing the methyl groups in the CpFe(arene) complex.[37] Similar reactions for **2** have been reported by our laboratory.[10]

Although **2** undergoes many of the same nucleophilic and radical substitution reactions as **3** at the exocyclic methylene, it is less nucleophilic.[10] Apparently, the carbonyl ligands in **2** contribute less electron density to the metal, and therefore decrease reactivity at the exocyclic methylene. Astruc reported the formation of several stable bimetallic complexes resulting from the reaction of **3** with transition metal halides.[14c] Complex **2** is not sufficiently nucleophilic to displace halide from organotransition metal halide complexes, including $Mn(CO)_5Br$ and $(\eta^5\text{-}C_5H_5)Fe(CO)_2Cl$.[10] The reactivity of **2** might be anticipated to be enhanced by increasing the electron density on the metal. This can be accomplished by selective ligand substitution, for example, replacement of one carbonyl on the manganese with a stronger σ-donor ligand such as alkyl- and aryl-substituted phosphines and phosphites.[38] Alkyl- and aryl-substituted phosphites are good σ-donors, but have greater π back-bonding capability than alkyl- and aryl phosphines. This places the electron-donor ability of the phosphite ligand between that of the phosphines and carbonyl ligands. Increased σ-donation to the manganese should increase the electron density at the exocyclic methylene, thus enhancing its reactivity. Hydride transfer from *endo*-$(\eta^5\text{-}C_6Me_6H)Mn(CO)_2PR_3$ is directly affected by the σ-donor ability of the phosphine substituent.[8] Substitution of cyanide, a strong σ-donor, for carbonyl allows the formation of $[(\eta^5\text{-}C_6Me_5CH_2)Mn(CO)_2CN]^-$, which is strongly nucleophilic at the exocyclic methylene.[39]

The preparation and reactivity of $(\eta^5\text{-}C_6Me_5CH_2)Mn(CO)_2PR_3$ (R = *n*-Bu (**2a**), Me (**2b**), Ph (**2c**), OMe (**2d**), OPh (**2e**)) is reported in this chapter. Phosphine ligand

substitution for a carbonyl increases the nucleophilic reactivity of the exocyclic methylene in **2a–e** over that observed for **2**. The solid state structure of **2b** demonstrates that phosphine substitution for a carbonyl in **2** does not significantly alter the π-carbocyclic system of the η^5–pentamethylbenzyl ligand. The effect of enhanced nucleophilicity at the exocyclic methylene may arise through an electronic transmission other than through the π-carbocyclic system.

Experimental

Deprotonation of Mono-substituted Phosphine Complexes

(η^5–$C_6Me_5CH_2$)Mn(CO)$_2$PMe$_3$ (2b). *Procedure a.* A tetrahydrofuran solution (30 mL) of **1b** (172 mg, 348 μmol) was added to an excess of dry KH (>50 equiv) with stirring. Immediately, the color of the solution turned from pale to golden yellow. After 15 min, the solution was decanted and the solvent removed under reduced pressure. Hexane was used to extract the product. The procedure was repeated producing yellow–orange crystals of **2b** in nearly quantitative yield. Compound **2b** was purified by sublimation at 65–70 °C, providing orange crystals in a yield of 118 mg (97%). IR carbonyl stretching frequencies and $^{31}P\{^1H\}$ NMR spectroscopic results for **2a–e** are listed in Table 6. ^1H NMR spectral results for **2a–e** are listed in Table 7. $^{13}C\{^1H\}$ NMR spectral results for **2a–e** are listed in Table 8. Results from the HREI-MS analyses of **2a–e** are listed in Table 9.

Procedure b. A tetrahydrofuran solution (100 mL) of **1b** (250 mg, 505 μmol), when injected with 1.1 equiv of either methyllithium or *tert*-butyllithium turned from a light yellow to golden–yellow color. Carbonyl stretching frequencies indicate that an equilibrium prevails between **1b** and **2b**. IR (THF): 1970, 1924, 1858 cm^{-1}.

Table 6. $^{31}P\{^1H\}$ NMR and IR Spectral Data for $(\eta^5\text{-}C_6Me_5CH_2)Mn(CO)_2L$ (**2a–e**)

		$^{31}P\{^1H\}$ NMR	IR
compd no.	L	δ, ppm [a]	ν_{CO}, cm^{-1}
2a	$P(n\text{-}Bu)_3$	57.2	1920, 1859 [c] 1928, 1867 [d]
2b	PMe_3	21.3	1924, 1858 [c] 1932, 1870 [d]
2c	PPh_3	83.0	1927, 1864 [c] 1934, 1878 [d]
2d	$P(OMe)_3$	196.4	1939, 1877 [c] 1948, 1886 [d]
2e	$P(OPh)_3$	170.0	1955, 1893 [c] 1964, 1899 [d]

[a] Spectra were obtained in d_6–benzene at 298 K and externally referenced to H_3PO_4 (85%). All peaks appeared as singlets.

[c] Solution spectra were obtained in THF.

[d] Solution spectra were obtained in hexane.

Procedure c. A slurry of NaOH in tetrahydrofuran added to **1b** (125 mg, 252 μmol) produced a golden-yellow mixture of **1b** and **2b**. Here again, the carbonyl stretching frequencies indicate that an equilibrium prevails between **1b** and **2b**. IR (THF): 1970, 1924, 1858 cm^{-1}.

$(\eta^5\text{-}C_6Me_5CH_2)Mn(CO)_2P(n\text{-}Bu)_3$ (2a). Using *procedure a* (*vide supra*) and substituting **1a** (154 mg, 248 μmol), **2a** yielded 114 mg (97%) of orange crystals.

$(\eta^5\text{-}C_6Me_5CH_2)Mn(CO)_2PPh_3$ (2c). Using *procedure a* (*vide supra*) and substituting **1c** (156 mg, 229 μmol), **2c** yielded 113 mg (92%) of orange crystals.

Table 7. ^{1}H NMR Spectral Data for (η^5-$C_6Me_5CH_2$)Mn(CO)$_2$L (2a–e)

compd no.	L	^{1}H NMR [a] δ, ppm [b]	
2a	P(*n*-Bu)$_3$	3.63	(d, 2 H, =CH_2, $^2J_{P-H}$ = 1.2 Hz)
		2.07	(s, 3 H, -CH_3)
		1.91	(s, 6 H, -CH_3)
		1.69	(s, 6 H, -CH_3)
		1.43	(m, 12 H, P(-CH_2-))
		1.31	(m, 6 H, P(CH_2-))
		0.89	(t, 9 H, P(-CH_3), $^3J_{H-H}$ = 7.2 Hz)
2b	PMe_3	3.60	(s, 2 H, =CH_2, $^2J_{P-H}$ = 1.4 Hz)
		2.02	(s, 3 H, -CH_3)
		1.87	(s, 6 H, -CH_3)
		1.56	(s, 6 H, -CH_3)
		1.15	(d, 9 H, P(CH_3), $^2J_{P-H}$ = 10.1 Hz)
2c	PPh_3	7.73–7.38	(m, 15 H, P(C_6H_5))
		3.61	(s, 2 H, =CH_2)
		1.98	(s, 3 H, -CH_3)
		1.70	(s, 6 H, -CH_3)
		1.32	(s, 6 H, -CH_3)
2d	P(OMe)$_3$	3.95	(s, 2 H, =CH_2)
		3.26	(d, 9 H, P(OCH_3), $^3J_{P-H}$ = 10.8 Hz)
		2.01	(s, 3 H, -CH_3)
		1.87	(s, 6 H, -CH_3)
		1.83	(s, 6 H, -CH_3)
2e	P(OPh)$_3$	7.63–7.39	(m, 15 H, P(OC_6H_5))
		3.28	(s, 2 H, =CH_2)
		2.00	(s, 3 H, -CH_3)
		1.86	(s, 6 H, -CH_3)
		1.82	(s, 6 H, -CH_3)

[a] Obtained in d_6-benzene at 298 K.

[b] (multiplicity, no. of protons, assignment, coupling).

Table 8. $^{13}C\{^1H\}$ NMR Spectral Data for $(\eta^5\text{-}C_6Me_5CH_2)Mn(CO)_2L$ (**2a–e**)

		$^{13}C\{^1H\}$ NMR [a]	
compd no.	L	δ, ppm [b]	
2a	$P(n\text{-}Bu)_3$	228.7	(d, CO, $^2J_{P\text{-}C}$ = 21.8 Hz)
		145.5	(s, $\underline{C}=CH_2$)
		108.0, 87.3	(s, ring–C)
		79.6	(s, $=CH_2$)
		27.3–24.3, 19.9–18.5, 14.8–12.0	(s, $P(CH_2)_3CH_3$)
		17.9–15.7	(s, $-CH_3$)
2b	PMe_3	233.0	(br s, CO)
		146.4	(s, $\underline{C}=CH_2$)
		108.4, 77.2	(s, ring–C)
		77.2	(s, $=CH_2$)
		19.2	(s, $P(CH_3)$)
		18.0, 17.7–17.1, 16.2	(s, $-CH_3$)
2c	PPh_3	228.8	(br s, CO)
		145.0	(s, $\underline{C}=CH_2$)
		134.1–129.3	(s, $P(C_6H_5)$)
		106.4, 81.8	(s, ring–C)
		79.6	(s, $=CH_2$)
		17.2–16.3	(s, $-CH_3$)
2d	$P(OMe)_3$	230.3	(br s, CO)
		148.0	(s, $\underline{C}=CH_2$)
		107.9, 86.6, 80.3	(s, ring–C)
		76.9	(s, $=CH_2$, $J_{C\text{-}H}$ = 156.5 Hz) [c]
		51.9	(d, $P(OCH_3)$, $J_{P\text{-}C}$ = 5.1 Hz)
		17.9, 16.8, 15.8	(s, $-CH_3$)

Table 8 — continued

compd no.	L	^{13}C NMR [a] δ, ppm [b]	
2e	$P(OPh)_3$	227.9	(d, CO, $^2J_{P-C}$ = 27 Hz)
		152.5	($\underline{C}=CH_2$
		147.1, 129.8–121.4	($P(\underline{O}C_6H_5)$)
		107.5, 86.6, 84.9, 82.7	(ring–C)
		77.4	($=CH_2$)
		17.7, 16.7, 15.3	($-CH_3$)

[a] Obtained in d_6-benzene at 298 K.

[b] (mult., assignment, coupling).

[c] Undecoupled ^{13}C NMR results.

Table 9. HREI-MS Data for $(\eta^5$-$C_6Me_5CH_2)Mn(CO)_2L$ (**2a–e**)

compd no.	chemical formula	MW_{calc}	M^+_{exp}, *m/z*	Δ*m*, mmu
2a	$C_{26}H_{44}O_2P_1Mn_1$	474.2459	474.2456	−0.4
2b	$C_{17}H_{26}O_2P_1Mn_1$	348.1051	348.1062	+1.1
2c	$C_{32}H_{32}O_2P_1Mn_1$	(*a*)	—	—
	$[PPh_3]$	262.0911	262.0912	+0.1
	$[(C_6Me_5CH_2)Mn]$	216.0711	216.0682	−2.8
	$[C_6Me_5CH_2]$	161.1330	161.1334	+0.4
2d	$C_{17}H_{26}O_5P_1Mn_1$	396.0898	396.0922	+2.4
2e	$C_{32}H_{32}O_5P_1Mn_1$	582.1368	582.1345	−2.3

[a] Not observed.

(η^5-$C_6Me_5CH_2$)Mn(CO)$_2$P(OMe)$_3$ (2d). Using *procedure a* (*vide supra*) and substituting **1d** (303 mg, 559 μmol), **2d** was isolated as orange-yellow crystals in a yield of 217 mg (98%).

(η^5-$C_6Me_5CH_2$)Mn(CO)$_2$P(OPh)$_3$ (2e). Using *procedure a* (*vide supra*) and substituting **1e** (301 mg, 413 μmol), **2e** was isolated as yellow-orange crystals in a yield of 231 mg (96%).

Reactions of [NH_4][PF_6] with Complexes 2a–e

The η^5-benzyl (**2a–e**, ~250 μmol) was mixed with 1.1 equiv of [NH_4][PF_6] in ~15 mL dry THF. An immediate color change from the orange-yellow of the η^5-benzyl (**2a–e**) to yellow of the cationic species (**1a–e**) was observed. Complete conversion was verified by the presence of only the ν_{CO} of complexes **1a–e** in the IR spectra, listed in Table 10.[8] Recoverable yields were greater than 85%.

Reactions of PhC(O)Cl with Complexes 2a–e

A 50 mL THF solution of a η^5-benzyl (**2a–e**, 150–300 μmol) was injected with 3 equiv of benzoyl chloride and stirred for ~5 min. An immediate color change from yellow-orange to yellow was observed. Verification of complete reaction was obtained by observing the IR ν_{CO} shift to the higher frequencies of cationic species. The Cl^- anion was metathesized with 1.1 equiv of [NH_4][PF_6] for **4a–c**. The product was purified by LC on SiO_2 (hexanes-acetone). Spectroscopic characterizations for the previously unreported compounds follow.

[(η^6-$C_6Me_5CH_2C(O)Ph$)Mn(CO)$_2$P(n-Bu)$_3$][PF_6] (4a). Compound **4a** was isolated as a yellow powder with a yield of 136 mg (99%). IR carbonyl stretching frequencies for **4a–e** are listed in Table 11. ^{1}H NMR spectral results for **4a–e** are listed in Table 12. $^{31}P\{^1H\}$ NMR spectral results for **4a–e** are listed in Table 13.

Table 10. IR Spectral Data for $[(\eta^6\text{-}C_6Me_6)Mn(CO)_2L][PF_6]$ (1a–e)

compd no.	L	IR ν_{CO}, cm^{-1}	Yield, %
1a	$P(n\text{-}Bu)_3$	1969, 1920	92
1b	PMe_3	1972, 1923	95
1c	PPh_3	1978, 1926	87
1d	$P(OMe)_3$	1990, 1941	93
1e	$P(OPh)_3$	1996, 1947	85

[a] Solution spectra were obtained in THF.

Table 11. IR Spectral Data for $[(\eta^6\text{-}C_6Me_5CH_2C(O)Ph)Mn(CO)_2L]X$

compd no.	L	IR ν_{CO}, cm^{-1}	IR $\nu_{C=O}$, cm^{-1}
4a	$P(n\text{-}Bu)_3$	1979, 1932 [a]	1689
4b	PMe_3	1975, 1926 [b]	1688
4c	PPh_3	1981, 1933 [b]	1685
4d	$P(OMe)_3$	1984, 1935 [b]	1686
4e	$P(OPh)_3$	1998, 1953 [b]	1706

[a] Solution spectra were obtained in CH_2Cl_2.

[b] Solution spectra were obtained in THF.

Table 12. ^{1}H NMR Spectral Data for [(η^6-$C_6Me_5CH_2C(O)Ph$)$Mn(CO)_2L$]X

		^{1}H NMR [a]	
compd no.	L	δ, ppm [b]	
4a	$P(n\text{-}Bu)_3$	8.17–7.49	(m, 5 H, $-C_6H_5$)
		4.88	(s, 2 H, $-CH_2$)
		2.61	(s, 3 H, $-CH_3$)
		2.50	(s, 6 H, $-CH_3$)
		2.42	(s, 6 H, $-CH_3$)
		1.9	(d-t, 6 H, $P(CH_2-)$)
		1.47	(m, 12 H, $P(-CH_2-)$)
		0.96	(t, 9 H, $P(-CH_3)$, $^3J_{H-H}$ = 6.28 Hz)
4b	PMe_3	8.19–7.61	(m, 5 H, $-C_6H_5$)
		4.89	(s, 2 H, $-CH_2-$)
		2.60	(s, 6 H, $-CH_3$)
		2.40	(s, 9 H, $-CH_3$)
		1.69	(d, 9 H, $P(CH_3)$, $^2J_{P-H}$ = 8.33 Hz)
4c	PPh_3	8.17–7.58	(m, 20 H, $-C_6H_5$ and $P(C_6H_5)$)
		4.30	(s, 2 H, $-CH_2-$)
		2.34	(s, 3 H, $-CH_3$)
		2.32	(s, 6 H, $-CH_3$)
		2.12	(s, 6 H, $-CH_3$)
4d	$P(OMe)_3$	8.19–7.51	(m, 5 H, $-C_6H_5$)
		4.77	(s, 2 H, $-CH_2-$)
		3.40	(br s, 9 H, $P(OCH_3)$)
		2.51–2.24	(m, 15 H, $-CH_3$)
4e	$P(OPh)_3$	8.19–7.59	(m, 5 H, $-C_6H_5$)
		7.39–7.23	(m, 15 H, $P(OC_6H_5)$)
		4.63	(s, 2 H, $-CH_2-$)
		2.21	(s, 3 H, $-CH_3$)
		2.19	(s, 6 H, $-CH_3$)
		2.09	(s, 6 H, $-CH_3$)

[a] Obtained in d_6-acetone at 298 K.

[b] (mult., no. protons, assignment, coupling).

Table 13. $^{31}P\{^{1}H\}$ NMR Data for $[(\eta^6\text{-}C_6Me_5CH_2C(O)Ph)Mn(CO)_2L]X$

		^{31}P NMR [a]	
compd no.	L	δ, ppm [b]	
4a	$P(n\text{-}Bu)_3$	56.7	(s, PBu_3)
		−142.6	(sp, PF_6^-, $J_{P\text{-}F}$ = 706.4 Hz)
4b	PMe_3	36.99	(s, PMe_3)
		−141.92	(sp, PF_6^-, $J_{P\text{-}F}$ = 706.7 Hz)
4c	PPh_3	76.16	(s, PPh_3)
		−142.01	(sp, PF_6^-, $J_{P\text{-}F}$ = 707.2 Hz)
4d	$P(OMe)_3$	196.0	(s, $P(OMe)_3$)
4e	$P(OPh)_3$	159.73	(s, $P(OPh)_3$)

[a] Spectra were obtained in d_6-acetone at 298 K.

[b] (mult., assignment, coupling).

The results of HRFAB–MS analyses of **4a–e** are listed in Table 14.

$[(\eta^6\text{-}C_6Me_5CH_2C(O)Ph)Mn(CO)_2PMe_3][PF_6]$ (4b). Compound **4b** was isolated as a light yellow powder with a yield of 198 mg (68%). Anal. Found (Calcd) for $C_{24}H_{31}O_3P_2F_6Mn_1$ (**4b**) C, 48.24 (48.17); H, 5.12 (5.22).

$[(\eta^6\text{-}C_6Me_5CH_2C(O)Ph)Mn(CO)_2PPh_3][PF_6]$ (4c). Compound **4c** was isolated as a yellow powder with a yield of 142 mg (82%).

$[(\eta^6\text{-}C_6Me_5CH_2C(O)Ph)Mn(CO)_2P(OMe)_3]Cl$ (4d). Compound **4d** was isolated as a pale yellow powder with a yield of 167 mg (89%).

Table 14. HRFAB-MS Data for $[(\eta^6\text{-}C_6Me_5CH_2C(O)Ph)Mn(CO)_2L]X$

compd no.	chemical formula	MW_{calc}	M^+_{exp}, *m/z*	Δm, mmu
4a	$C_{33}H_{49}O_3P_1Mn_1$	579.2800	579.2799	−0.1
4b	$C_{24}H_{31}O_3P_1Mn_1$	453.1391	453.1394	+0.3
4c	$C_{39}H_{37}O_3P_1Mn_1$	639.1861	639.1853	−0.8
4d	$C_{24}H_{31}O_6P_1Mn_1$	501.1239	501.1248	+0.9
4e	$C_{39}H_{37}O_6P_1Mn_1$	687.1708	687.1698	−1.0

$[(\eta^6\text{-}C_6Me_5CH_2C(O)Ph)Mn(CO)_2P(OPh)_3]Cl$ (4e). Compound **4e** was isolated as a pale yellow powder with a yield of 215 mg (75%). $^{13}C\{^1H\}$ NMR spectral results for **4e** are listed in Table 15.

$C_6Me_5CH_2C(O)Ph$. One attempt of synthesizing **4d**, using hexane as the solvent, resulted in decomposition of the yellow product. Evaporation of the hexane solution resulted in the formation of white needle crystals of pentamethylbenzyl phenyl ketone in a yield of 72 mg (56%, based on the moles of starting material, **2d**). Spectral characterizations of $C_6Me_5CH_2C(O)Ph$ are listed in Table 16.

Reactions of CH_3I with Complexes 2a–e

A 100 mL THF solution of a η^5-benzyl (**2a–c**, **2e**, 0.3–1 mmol) was injected with 40 equiv of iodomethane to provide pseudo-first-order rate conditions, and stirred for ~5 min. The solution color immediately changed from yellow-orange to yellow. A shift of ν_{CO} in the IR spectra to the higher frequencies of cationic species indicated reaction completion. The I^- anion was metathesized with 1.1 equiv of $[NH_4][PF_6]$. The products **5a–c** and **5e** were purified by LC on SiO_2 (hexanes–acetone). Spectroscopic characterizations for the previously unreported compounds follow.

Table 15. $^{13}C\{^1H\}$ NMR Data for $[(\eta^6\text{-}C_6Me_5CH_2C(O)Ph)Mn(CO)_2P(OPh)_3]Cl$

		$^{13}C\{^1H\}$ NMR [a]	
compd no.	L	δ, ppm [b]	
4e	$P(OPh)_3$	221.27	(br s, CO)
		206.25	(s, C=O)
		151.17, 131.33, 130.62	(s, $-OC_6H_5$)
		127.05, 121.96	(s, ring-C)
		65.94	(s, $-CH_2-$)
		17.21, 16.81, 15.51	(s, $-CH_3$)

[a] Obtained in d_6-acetone at 298 K.

[b] (mult., assignment).

Table 16. Spectral Characterization of $C_6Me_5CH_2C(O)Ph$

	^1H NMR [a]		IR [b]
compd	δ, ppm [c]		$\nu_{C=O}$, cm^{-1}
$C_6Me_5CH_2C(O)Ph$	8.16–7.55	(m, 5 H, $-C_6H_5$)	1680
	4.54	(s, 2 H, $-CH_2-$)	
	2.22	(s, 3 H, $-CH_3$)	
	2.20	(s, 6 H, $-CH_3$)	
	2.10	(s, 6 H, $-CH_3$)	

[a] Obtained in d_6-acetone at 298 K.

[b] Solution spectra obtained in THF.

[c] (mult., no. protons, assignment).

Table 17. IR Spectral Data for $[(\eta^6\text{-}C_6Me_5Et)Mn(CO)_2L]X$

compd no.	L	IR [a] ν_{CO}, cm^{-1}
5a	$P(n\text{-}Bu)_3$	1967, 1918
5b	PMe_3	1971, 1921
5c	PPh_3	1976, 1927
6	$P(O)(OMe)_2$	1964, 1915
5e	$P(OPh)_3$	1995, 1955

[a] Solution spectra were obtained in CH_2Cl_2.

[b] Solution spectra were obtained in THF.

$[(\eta^6\text{-}C_6Me_5Et)Mn(CO)_2P(n\text{-}Bu)_3][PF_6]$ (5a). Compound **5a** was isolated as a yellow powder with a yield of 256 mg (53%). IR carbonyl bands for **5a–c**, **5e**, and **6** are listed in Table 17. ^1H NMR spectral results for **5a–c**, **5e**, and **6** are listed in Table 18. $^{31}P\{^1H\}$ NMR spectral results for **5a–c**, **5e**, and **6** are listed in Table 19. The results of HRFAB–MS analyses for **5a–c**, **5e**, and **6** are listed in Table 20. Anal. Found (Calcd) for $C_{27}H_{47}O_2P_2F_6Mn_1$ (**5a**) C, 51.18 (51.11); H, 7.32 (7.47).

$[(\eta^6\text{-}C_6Me_5Et)Mn(CO)_2PMe_3][PF_6]$ (5b). Compound **5b** was isolated as a yellow powder with a yield of 502 mg (89%). $^{13}C\{^1H\}$ NMR spectral results for **5b** and **6** are listed in Table 21.

$[(\eta^6\text{-}C_6Me_5Et)Mn(CO)_2PPh_3][PF_6]$ (5c). Compound **5c** was isolated as a yellow powder with a yield of 379 mg (55%).

Table 18. ^{1}H NMR Spectral Data for $[(\eta^6\text{-}C_6Me_5Et)Mn(CO)_2L]X$

compd no.	L	^{1}H NMR [a] δ, ppm [b]	
5a	$P(n\text{-}Bu)_3$	2.89	(q, 2 H, $-CH_2-$, $^3J_{H-H}$ = 7.49 Hz)
		2.50	(s, 3 H, $-CH_3$)
		2.47–2.46	(m, 12 H, $-CH_3$)
		1.88	(d-t, 6 H, $P(CH_2-)$, $^3J_{H-H}$ = 7.0 Hz, $^2J_{P-H}$ = 9.08 Hz)
		1.47	(m, 12 H, $P(-CH_2-)$)
		1.11	(m, 3 H, $-CH_3$)
		0.96	(m, 9 H, $P(-CH_3)$)
5b	PMe_3	2.89	(q, 2 H, $-CH_2-$, $^3J_{H-H}$ = 6.28 Hz)
		2.49, 2.46	(br s, 15 H, $-CH_3$)
		1.63	(d, 2 H, $P(CH_3)$, $^2J_{P-H}$ = 10.01 Hz)
		1.22	(t, 3 H, $-CH_3$, $^3J_{H-H}$ = 6.98 Hz)
5c	PPh_3	7.96–7.49	(m, 15 H, $P(C_6H_5)$)
		2.64	(q, 2 H, $-CH_2-$, $^3J_{H-H}$ = 7.56 Hz)
		2.23	(s, 6 H, $-CH_3$)
		2.22	(s, 3 H, $-CH_3$)
		2.18	(s, 6 H, $-CH_3$)
		1.12	(t, 3 H, $-CH_3$, $^3J_{H-H}$ = 7.56 Hz)
6	$P(O)(OMe)_2$	3.45	(d, 6 H, $P(OCH_3)$, $^3J_{P-H}$ = 10.73 Hz)
		2.75	(q, 2 H, $-CH_2-$, $^3J_{H-H}$ = 7.66 Hz)
		2.34, 2.33, 2.30	(br s, 15 H, $-CH_3$)
		1.16	(t, 3 H, $-CH_3$, $^3J_{H-H}$ = 7.55 Hz)

Table 18 — continued

compd no.	L	^{1}H NMR [a] δ, ppm [b]	
5e	$P(OPh)_3$	7.54–7.18	(m, 15 H, $P(OC_6H_5)$)
		2.85	(br s, 2 H, $-CH_2-$)
		2.47 2.39	(br s, 15 H, $-CH_3$)
		1.29	(br s, 3 H, $-CH_3$)

[a] Obtained in d_6–acetone at 298 K.

[b] (mult., no. protons, assignment, coupling).

$[(\eta^6\text{-}C_6Me_5Et)Mn(CO)_2P(OPh)_3][PF_6]$ (5e). Compound **5e** was isolated as a yellow powder with a yield of 45 mg (65%).

CH_3I and 2b in the Presence of KH. Iodomethane (200 μL, 3.21 mmol) was added to a THF solution of **2b** (388 mg, 1.114 mmol) and KH (~1 mmol). The progress of the reaction was monitored by IR spectroscopy for 5.5 h. The two products were isolated by column chromatography. The red band eluted first, and was identified as $(\eta^6\text{-}C_6Me_5Et)Mn(CO)_2I$ by IR and ^{1}H and $^{31}P\{^1H\}$ NMR spectroscopies. The final yellow band, $[(\eta^6\text{-}C_6Me_{6-n}Et_n)Mn(CO)_2PMe_3]I$ (n = 1, 2, 3), was isolated as yellow cubic crystals. A 4:3:1 ratio of the three products (n = 1–3) was determined by MS. Spectral Characterizations are reported in Table 22.

Table 19. $^{31}P\{^{1}H\}$ NMR Data for $[(\eta^6\text{-}C_6Me_5Et)Mn(CO)_2L]X$

compd no.	L	^{31}P NMR [a] δ, ppm [b]	
5a	$P(n\text{-}Bu)_3$	57.4	(s, PBu_3)
		−142.2	(sp, PF_6^-, $J_{P\text{-}F}$ = 706.3 Hz)
5b	PMe_3	36.40	(s, PMe_3)
		−141.59	(sp, PF_6^-, $J_{P\text{-}F}$ = 707.1 Hz)
5c	PPh_3	77.26	(s, PPh_3)
		−142.00	(sp, PF_6^-, $J_{P\text{-}F}$ = 707.2 Hz)
6	$P(O)(OMe)_3$	137.43	(s, $P(O)(OMe)_2$)
5e	$P(OPh)_3$	172.23	(s, $P(OPh)_3$)
		−142.65	(sp, PF_6^-, $J_{P\text{-}F}$ = 707.0 Hz)

[a] Spectra were obtained in d_6–acetone at 298 K.

[b] (mult., assignment, coupling).

Table 20. HRFAB–MS Data for $[(\eta^6\text{-}C_6Me_5Et)Mn(CO)_2L]X$

compd no.	chemical formula	MW_{calc}	M^+_{exp}, *m/z*	Δm, mmu
5a	$C_{27}H_{47}O_2P_1Mn_1$	489.2694	489.2685	−1.0
5b	$C_{18}H_{29}O_2P_1Mn_1$	363.1286	363.1287	+0.1
5c	$C_{21}H_{35}O_2P_1Mn_1$	549.1755	549.1766	+1.1
6	$C_{17}H_{26}O_5P_1Mn_1$	396.0898	396.0904	+0.6
5e	$C_{21}H_{35}O_5P_1Mn_1$	597.1603	597.1589	−1.4

Table 21. $^{13}C\{^1H\}$ NMR Spectral Data for $[(\eta^6\text{-}C_6Me_5Et)Mn(CO)_2L]X$

		$^{13}C\{^1H\}$ NMR [a]	
compd no.	L	δ, ppm [b]	
5b	PMe_3	225.52	(d, CO, $^3J_{P\text{-}C}$ = 25 Hz)
		114.81, 114.43, 111.02, 110.68, 110.39, 110.22	(s, ring–C)
		24.74	(s, $-CH_2-$)
		19.27	(d, $P(CH_3)$, $^3J_{P\text{-}C}$ = 30.8 Hz)
		17.33, 16.45, 13.50	(s, $-CH_3$)
6	$P(O)(OMe)_2$	226.7	(d, CO, $^3J_{P\text{-}C}$ = 60 Hz)
		112.71, 109.90, 108.98, 108.62	(s, ring–C)
		50.27	(d, $P(OCH_3)$, $^3J_{P\text{-}C}$ = 7.7 Hz)
		24.42	(s, $-CH_2-$)
		16.90, 16.10, 13.82	(s, $-CH_3$)

[a] Obtained in d_6–acetone at 298 K.

[b] (mult., assignment, coupling).

CH_3I and 2d. *(a) In THF.* Iodomethane (320 μL, 2.73 mmol) was injected into a THF solution of **2d** (142 mg, 358 μmol). The reaction mixture was maintained at 23 °C and monitored by IR spectroscopy for 7.33 h. The only product isolated from the reaction was $(\eta^6\text{-}C_6Me_5Et)Mn(CO)_2P(O)(OMe)_2$ (**6**) using LC on SiO_2 (hexanes-acetone-methanol).

Table 22. Spectral Data for $[(\eta^6\text{-}C_6Me_{6-n}Et_n)Mn(CO)_2L][PF_6]$

n		
	IR [a]	
	ν_{CO}, cm^{-1}	
1–3	1972, 1924	
	^1H NMR [b]	
	δ, ppm [c]	
1–3	2.89	(m, 3 H, $-CH_2-$)
	2.53–2.46	(m, 12 H, $-CH_3$)
	1.63	(d, 9 H, $P(CH_3)$, J_{P-H} = 10.01 Hz)
	1.22	(m, 10 H, $-CH_3$)
	$^{31}P\{^1H\}$ NMR [b]	
	δ, ppm [c]	
1–3	33.8	(s, PMe_3)
	HRFAB-MS	
	MW_{calc} $[M^+]$	M^+_{exp} m/z Δm
1	363.1286	363.1287 +0.1
2	377.1442	377.1428 −1.4
3	391.1599	391.1593 −0.6

[a] Solution spectrum obtained in THF.

[b] Obtained in d_6-acetone at 298 K.

[b] (mult., assignment, coupling).

(b) In Hexane. The reaction of **2d** (141 mg, 365 μmol) with CH_3I (2.05 mL, 32.9 mmol) produced a 2:3 ratio of **6** to $(\eta^6\text{-}C_6Me_5Et)Mn(CO)_2I$ by both IR and ^1H NMR spectroscopies. The products were purified as above.

(c) Catalytic — 0.05% CH_3I. A 0.05% CH_3I solution (1.33 μL, 21.4 μmol) in hexane reacted catalytically with **2d** (169 mg, 426 μmol), producing **6** in a 35% recoverable yield. Compound **6** was purified as above.

$(\eta^6\text{-}C_6Me_5Et)Mn(CO)_2P(O)(OMe)_2$ (6). Compound **6** was isolated as a yellow powder with a yield of 98 mg (51%).

Kinetic Measurements of Reactions of CH_3I with 2a–e. The kinetics were measured over 3–4 half-lives using the intensities of IR carbonyl stretching bands. The reaction solutions were maintained at 25 (3) °C in a mineral oil bath. A ratio of 40:1 iodomethane to "η^5-benzyl" complex was used to provide pseudo-first-order conditions. Pseudo-first-order rate constants were calculated from the slope of time versus the $\log([A]/[A_o])$ plots using the SlideWrite*Plus* program. The plot for the reaction involving **2b** is illustrated in Figure 1. The reaction with **2b** was repeated to demonstrate reproducibility. Complex **2b** was also studied with initial concentration ratios close to 1:1 using iodomethane. A second order rate constant of 1.5 (2) $\times 10^{-2}$ $L \cdot mole^{-1} \cdot s^{-1}$ was obtained for **2b** from a plot of $([2b]^{-1} - [2b_o]^{-1})$ versus time, illustrated in Figure 2. In each reaction the order for iodomethane and **2b** were both found to be one.

Reactions of I_2 with Complexes 2a–e

Solutions of 50 mL THF and η^5-benzyl (**2a–e**, 250–300 μmol) were injected with 3 equiv of iodine and stirred for ~5 min. The solution immediately changed color from yellow-orange to orange.

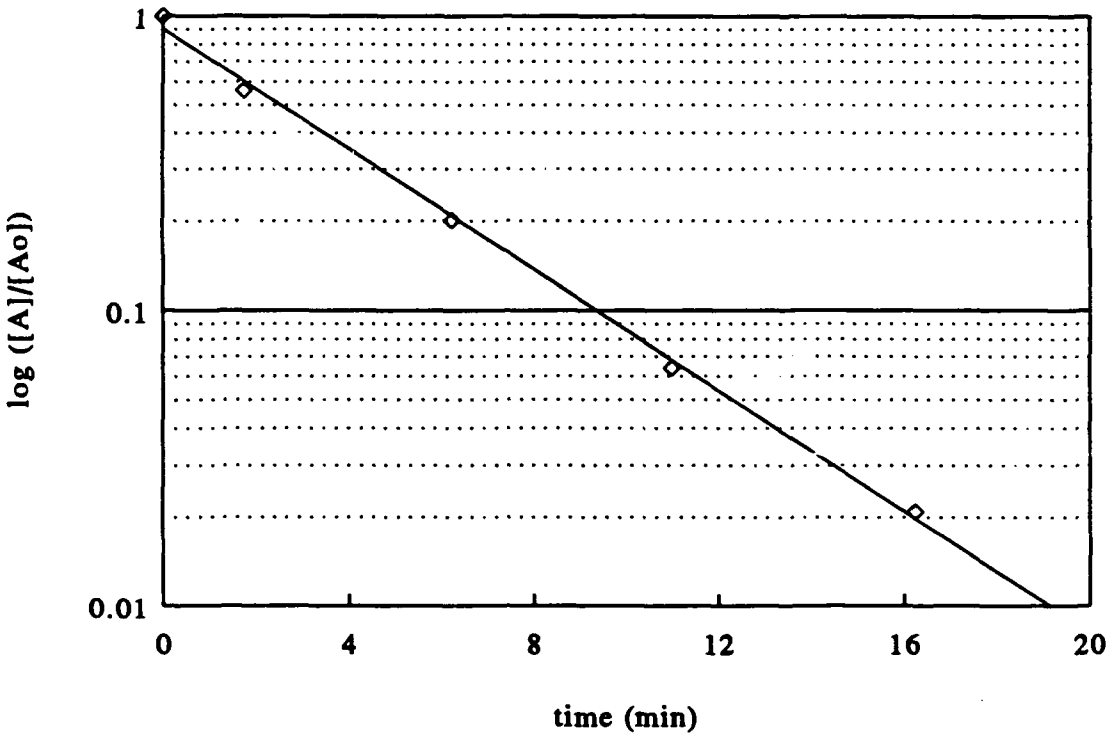

Figure 1. Plot of log([**2b**]/[**2b**$_o$]) vs. time to calculate the pseudo-first-order rate constant for the reaction of **2b** and CH_3I at 25 °C.

Monitoring of the IR ν_{CO} shifts to the higher frequencies of the cationic species indicated that the reaction was complete. The I^- anion was metathesized with $[NH_4][PF_6]$ for **2a**, **2b**, and **2d**. The products were purified by LC on SiO_2 (hexanes-acetone). Spectroscopic characterizations for the previously unreported compounds follow.

[(η^6-$C_6Me_5CH_2I$)Mn(CO)$_2$P(*n*-Bu)$_3$][PF_6] (7a). Compound **7a** was isolated as a yellow powder with a yield of 182 mg (98%). IR carbonyl bands for **7a–e** and **8** are listed in Table 23. ^{1}H NMR spectral results for **7a–e** and **8** are listed in Table 24. Anal. Found (Calcd) for $C_{26}H_{44}O_2P_2F_6I_1Mn_1$ (**7a**) C, 41.53 (41.84); H, 5.81 (5.94).

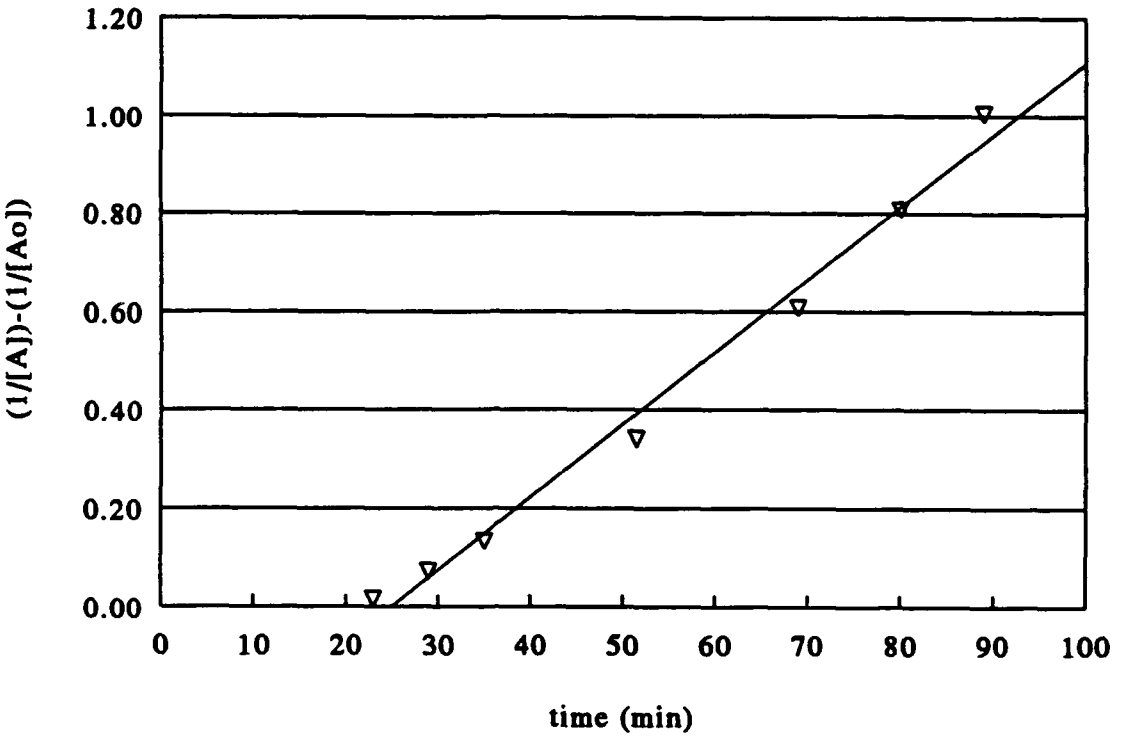

Figure 2. Plot of $([\mathbf{2b}]^{-1} - [\mathbf{2b}_o]^{-1})$ vs. time to calculate the second-order rate constant for the reaction of **2b** and CH_3I at 25 °C.

$^{31}P\{^1H\}$ NMR spectral results for **7a–e** and **8** are listed in Table 25. The results of HRFAB–MS analyses of **7a–e** and **8** are listed in Table 26.

$[(\eta^6\text{–}C_6Me_5CH_2I)Mn(CO)_2PMe_3][PF_6]$ (7b). Compound **7b** was isolated as a yellow powder with a yield of 207 mg (97%). $^{13}C\{^1H\}$ NMR spectral results are listed in Table 27.

$[(\eta^6\text{–}C_6Me_5CH_2I)Mn(CO)_2PPh_3]I$ (7c). Compound **7c** was isolated as a yellow powder with a yield of 223 mg (84%).

Table 23. IR Spectral Data for $[(\eta^6\text{-}C_6Me_5CH_2I)Mn(CO)_2L]X$

compd no.	L	IR ν_{CO}, cm^{-1}
7a	$P(n\text{-}Bu)_3$	1975, 1927 [a]
7b	PMe_3	1978, 1930 [b]
7c	PPh_3	1982, 1935 [b]
7d	$P(OMe)_3$	1996, 1948 [b]
7e	$P(OPh)_3$	2001, 1957 [b]
8	$P(O)(OMe)_2$	1964, 1918 [b]

[a] Solution spectra were obtained in CH_2Cl_2.

[b] Solution spectra were obtained in THF.

$[(\eta^6\text{-}C_6Me_5CH_2I)Mn(CO)_2P(OMe)_3][PF_6]$ (7d). Compound **7d** was isolated as a yellow powder with a yield of 460 mg (75%).

$[(\eta^6\text{-}C_6Me_5CH_2I)Mn(CO)_2P(OPh)_3]I$ (7e). Compound **7e** was isolated as a yellow powder with a yield of 85 mg (21%).

$(\eta^6\text{-}C_6Me_5CH_2I)Mn(CO)_2P(O)(OMe)_2$ (8). Compound **8** was isolated as a yellow powder with a yield of 40 mg (9%).

Reactions of $Mn(CO)_5Br$ and $(C_5H_5)Fe(CO)_2I$ with Complex **2b**

$[(\eta^6\text{-}C_6Me_5CH_2FeCp(CO)_2)Mn(CO)_2PMe_3]I$ (9). $CpFe(CO)_2I$ (103 mg, 339 μmol) and **2b** (129 mg, 370 μmol) were combined and solvated with THF. The carbonyl stretching frequencies and ^1H, $^{13}C\{^1H\}$, and $^{31}P\{^1H\}$ NMR data are listed in Table 28.

Table 24. ^{1}H NMR Spectral Data for [(η^6-$C_6Me_5CH_2I$)$Mn(CO)_2L$]X

		^{1}H NMR [a]	
compd no.	L	δ, ppm [b]	
7a	$P(n\text{-}Bu)_3$	4.70	(s, 2 H, $-CH_2-$)
		2.55	(s, 3 H, $-CH_3$)
		2.50	(s, 12 H, $-CH_3$)
		1.92	(d-t, 6 H, $P(CH_2-$), $^3J_{H-H}$ = 7.12 Hz, $^2J_{P-H}$ = 9.01 Hz)
		1.49	(m, 12 H, $P(-(CH_2)_2-)$)
		0.96	(t, 9 H, $P(-CH_3)$, $^3J_{H-H}$ = 6.28 Hz)
7b	PMe_3	4.71	(s, 2 H, $-CH_2I$)
		2.56	(s, 3 H, $-CH_3$)
		2.51	(s, 6 H, $-CH_3$)
		2.49	(s, 6 H, $-CH_3$)
		1.65	(d, 9 H, $P(CH_3)$, $^2J_{P-H}$ = 10.16 Hz)
7c	PPh_3	7.67–7.64, 7.57–7.50	(m, 15 H, $P(C_6H_5)$)
		4.18	(s, 2 H, $-CH_2I$)
		2.30	(s, 9 H, $-CH_3$)
		2.21	(s, 6 H, $-CH_3$)
7d	$P(OMe)_3$	4.62	(s, 2 H, $-CH_2I$)
		3.90	(d, 9 H, $P(OCH_3)$, $^3J_{P-H}$ = 9.22 Hz)
		2.82	(s, 3 H, $-CH_3$)
		2.47	(s, 12 H, $-CH_3$)
7e	$P(OPh)_3$	7.43–7.18	(m, 15 H, $P(OC_6H_5)$)
		4.62	(s, 2 H, $-CH_2I$)
		2.58	(s, 3 H, $-CH_3$)
		2.53	(s, 6 H, $-CH_3$)
		2.48	(s, 6 H, $-CH_3$)

Table 24 — continued

		^{1}H NMR [a]	
compd no.	L	δ, ppm [b]	
8	$P(O)(OMe)_2$	3.84	(d, 6 H, $P(OCH_3)$, $^3J_{P-H}$ = 11.90 Hz)
		3.62	(vt, 4 H, $-CH_2CH_2I$)
		2.79	(s, 6 H, $-CH_3$)
		2.57	(s, 3 H, $-CH_3$)
		2.53	(s, 6 H, $-CH_3$)

[a] Obtained in d_6-acetone at 298 K.

[b] (mult., no. protons, assignment, coupling).

Table 25. $^{31}P\{^1H\}$ NMR Data for $[(\eta^6\text{-}C_6Me_5CH_2I)Mn(CO)_2L]X$

		^{31}P NMR [a]	
compd no.	L	δ, ppm [b]	
7a	$P(n\text{-}Bu)_3$	56.12	(s, PBu_3)
		−142.64	(sp, PF_6^-, J_{P-F} = 707.2 Hz)
7b	PMe_3	36.37	(s, PMe_3)
		−142.00	(sp, PF_6^-, J_{P-F} = 708.0 Hz)
7c	PPh_3	74.81	(s, PPh_3)
7d	$P(OMe)_3$	161.74	(s, $P(OMe)_3$)
		−142.00	(sp, PF_6^-, J_{P-F} = 707.2 Hz)
7e	$P(OPh)_3$	170.9	(s, $P(OPh)_3$)
8	$P(O)(OMe)_2$	132.2	(s, $P(O)(OMe)_2$)

[a] Spectra were obtained in d_6-acetone at 298 K.

[b] (mult., assignment, coupling).

Table 26. HRFAB-MS Data for $[(\eta^6\text{-}C_6Me_5CH_2I)Mn(CO)_2L]X$

compd no.	chemical formula	MW_{calc}	M^+_{exp}, *m/z*	Δm, mmu
7a	$C_{26}H_{44}O_2P_1Mn_1I_1$	601.1504	601.1492	−1.6
7b	$C_{17}H_{26}O_2P_1Mn_1I_1$	475.0096	475.0106	+1.0
7c	$C_{32}H_{32}O_2P_1Mn_1I_1$	661.0565	661.0569	+0.4
7d	$C_{17}H_{26}O_5P_1Mn_1I_1$	522.9943	522.9953	+1.0
7e	$C_{32}H_{32}O_5P_1Mn_1I_1$	709.0413	709.0433	+2.0
8 [a]	$C_{16}H_{23}O_5P_1Mn_1I_1$	508.9824	508.9805	−1.9

[a] $[M + H^+]$

Table 27. $^{13}C\{^1H\}$ NMR Spectral Data for $[(\eta^6\text{-}C_6Me_5CH_2I)Mn(CO)_2PMe_3][PF_6]$ (**7b**)

		$^{13}C\{^1H\}$ NMR [a]	
compd no.	L	δ, ppm [b]	
7b	PMe_3	224.8	(br s, CO)
		111.70, 109.12	(s, ring–C)
		19.14	(d, PCH_3, $J_{P\text{-}C}$ = 31.2 Hz)
		17.64, 17.34, 16.39	(s, $-CH_3$)
		1.24	(s, $-CH_2I$)

[a] Obtained in d_6–acetone at 298 K.

[b] (mult., assignment).

Table 28. Spectral Data for $[(\eta^6\text{-}C_6Me_5CH_2FeCp(CO)_2)Mn(CO)_2PMe_3]I$

IR [a]	^1H NMR [b]	
ν_{CO}, cm^{-1}	δ, ppm [c]	
2001, 1961, 1950, 1910	5.29	(s, 5 H, Cp–H)
	2.45	(s, 2 H, $-CH_2-$)
	2.31, 2.09, 1.68	(s, 17 H, $-CH_3$)
	1.44	(d, 9 H, $P(CH_3)_3$, $^2J_{P-H}$ = 8.34 Hz)

$^{31}P\{^1H\}$ NMR [b]		$^{13}C\{^1H\}$ NMR [b]	
δ, ppm [c]		δ, ppm [c]	
28.2	(s, PMe_3)	226.4	(br s, CO)
		110.31, 108.69	(s, ring–C)
		86.05	(s, Cp)
		18.39	(s, $P(CH_3)$)
		17.58–16.51	(s, ring–CH_3)

[a] Solution spectra obtained in d_8–THF.

[b] Obtained in d_8–THF at 213 K.

[c] (mult., assignment, coupling).

$[(\eta^6\text{-}C_6Me_5CH_2Mn(CO)_5)Mn(CO)_2PMe_3][PF_6]$ (10). $Mn(CO)_5Br$ (124 mg, 451 μmol) in ~40 mL of THF was combined with **2b** (149 mg, 428 μmol) in ~50 mL of THF at −55 °C. The reaction mixture was warmed to −45 °C and stirred for 1 h. The resulting bromide salt was metathesized with 1.1 equiv of $[NH_4][PF_6]$ to give a yellow–orange solid. The carbonyl stretching frequencies and the observed peaks from ^1H, $^{13}C\{^1H\}$, and $^{31}P\{^1H\}$ NMR spectra are listed in Table 29.

Table 29. Spectral Data for $[(\eta^6\text{-}C_6Me_5CH_2Mn(CO)_5)Mn(CO)_2PMe_3][PF_6]$

IR [a]	^{1}H NMR [b]	
ν_{CO}, cm^{-1}	δ, ppm [c]	
2082, 2045, 2006, 1973, 1928	2.35	(br s, 5 H, $-CH_2-$, $-CH_3$)
	1.98	(br s, 12 H, $-CH_3$)
	1.65	(d, 9 H, $P(CH_3)$, $^2J_{P-H}$ = 10.24 Hz)

$^{31}P\{^1H\}$ NMR [b]		$^{13}C\{^1H\}$ NMR [b]	
δ, ppm [c]		δ, ppm [c]	
37.6	(s, PMe_3)	226.1	
−141.9	(sp, PF_6^-, J_{P-F} = 706.9 Hz)	222.0, 220.0, 218.4, 212.5	(s, CO)
		131.92	(s, ring-C-CH_2-)
		110.73	(s, ring-C)
		17.07, 16.81, 16.06, 15.79	(s, ring-CH_3)
		−8.0	(s, $-CH_2-$)

[a] Solution spectra obtained in d_8-THF.

[b] Obtained in d_8-THF at 253 K.

[c] (mult., assignment, coupling).

General Procedure for the Reactions of Bu_3SnH with Complexes 2a–e

The η^5-benzyl (**2a–e**, 150–200 μmol) was mixed with 2.2 equiv of Bu_3SnH in 15–25 mL dry THF. Immediate color changes from the orange-yellow of the η^5-benzyls (**2a–e**) to the pale yellow of the *endo*-$(\eta^5\text{-}C_6Me_6H)Mn(CO)_2PR_3$ complexes (R = *n*-Bu (**11a**), Me (**11b**), Ph (**11c**), OMe (**11d**), and OPh (**11e**)) were observed.

Complete conversion was verified by the presence of only the ν_{CO} of complexes **11a–e** in the IR spectra, Table 30.[8]

Reactions of $CHBr_3$ with Complexes **2a–e**

A 1.1 equiv sample of bromoform was injected into a stirred solution of 50 mL hexane and η^5–benzyl (**2a–e**, 200–370 μmol). For each of the phosphine derivatives, a lavender colored precipitate, $(\eta^6\text{–}C_6Me_5CH_2CHBr_2)Mn(CO)_2Br$ (**12**), quantitatively formed leaving the solution clear and colorless. Chromatography of the product removed the eliminated phosphine, detected by odor, and excess bromoform, leaving only **12** as the product for each of the reactions.

$(\eta^6\text{–}C_6Me_5CH_2CHBr_2)Mn(CO)_2Br$ (12). Compound **12** was isolated as a shiny lavender powder with a yield of 182 mg (98%). IR carbonyl stretching frequencies are listed in Table 31. ^1H NMR spectral results are listed in Table 32. The results of HRFAB–MS analysis are listed in Table 33. The isotopic abundances of ^{79}Br (50.7%) and ^{81}Br (49.3%) in the $C_6Me_5CH_2CHBr_2$ result in the formation of three peaks in its mass spectrum that are 2 amu apart in an approximately 1:2:1 ratio.

Reactions of CCl_4 or $CDCl_3$ with Complexes **2a** and **2b**

The chlorocarbon (40 equiv, R'X = CCl_4 or $CDCl_3$), distilled and deaerated with Ar, was added to the η^5–benzyl (**2a–b**, 250 μmol), forming a red solution. The red solution of $(\eta^6\text{–}C_6Me_5CH_2CCl_3)Mn(CO)_2Cl$ (**13**), obtained from reaction of **2b** with CCl_4, typically decomposed within 2–4 h. $(\eta^6\text{–}C_6Me_5CH_2CDCl_2)Mn(CO)_2Cl$ (**14**) was obtained as a red solid from the reaction of the η^5–benzyls with $CDCl_3$. When exposed to laboratory light, **14** decomposed within 4 h; but in the dark under vacuum or inert atmosphere, it was stable for over 24 h. Spectroscopic characterization of the reaction mixtures and products follow.

Table 30. IR Spectral Data for *endo*-(η^5-C_6Me_6H)$Mn(CO)_2L$ (11a–e)

compd no.	L	IR ν_{CO}, cm^{-1}	Yield, %
11a	$P(n\text{-}Bu)_3$	1908, 1846	99
11b	PMe_3	1910, 1847	98
11c	PPh_3	1913, 1865	95
11d	$P(OMe)_3$	1924, 1865	98
11e	$P(OPh)_3$	1941, 1882	96

[a] Solution spectra were obtained in THF.

Table 31. IR Spectral Data for (η^6-$C_6Me_5CH_2R'$)$Mn(CO)_2X$ (12–14)

compd no.	R'	X	IR [a] ν_{CO}, cm^{-1}
12	$CHBr_2$	Br	1975, 1930
13	CCl_3	Cl	1977, 1931
14	$CDCl_2$	Cl	1975, 1929

[a] Solution spectra were obtained in THF.

Table 32. ^{1}H NMR Spectral Data for (η^6-$C_6Me_5CH_2R'$)$Mn(CO)_2X$ (12–14)

			^{1}H NMR	
compd no.	R′	X	δ, ppm [a]	
12 [b]	$CHBr_2$	Br	6.24	(t, 1 H, $-CHBr_2$, $^3J_{H-H}$ = 7.22 Hz)
			3.83	(d, 2 H, $-CH_2-$, $^3J_{H-H}$ = 7.28 Hz)
			2.44	(s, 6 H, $-CH_3$)
			2.29	(s, 9 H, $-CH_3$)
13 [c]	CCl_3	Cl	4.10	(br s, 2 H, $-CH_2CCl_3$)
			2.19	(br s, 6 H, CH_3)
			2.00	(br s, 9 H, CH_3)
14 [d]	$CDCl_2$	Cl	3.54	(br s, 2 H, $-CH_2-$)
			2.30	(br s, 6 H, $-CH_3$)
			2.19	(br s, 9 H, $-CH_3$)
			4.21 [e]	(br s, $-CDCl_2$)

[a] (mult., no. protons, assignment, coupling).

[b] Obtained in d_6-acetone at 298 K.

[c] Obtained in d_6-benzene at 298 K.

[d] Obtained in $CDCl_3$ at 298 K.

[e] Obtained in THF at 298 K.

Table 33. HRFAB-MS Data for $(\eta^6\text{-}C_6Me_5CH_2CHBr_2)Mn(CO)_2Br$

chemical formula	MW_{calc}	M^+_{exp}, *m/z*	Δm, mmu	rel abund.
$C_{13}H_{18}{}^{79}Br_2$[a]	335.9739	335.9738	−0.1	2.7%
$C_{13}H_{18}{}^{79}Br_1{}^{81}Br_1$	333.9757	333.9751	−0.6	5.4%
$C_{13}H_{18}{}^{81}Br_2$	331.9775	331.9782	+0.7	2.9%

[a] $C_6Me_5CH_2CHBr_2$ results from loss of arene from the molecular ion.

$(\eta^6\text{-}C_6Me_5CH_2CCl_3)Mn(CO)_2Cl$ (13). Compound **13** was observed in a red solution of d_6-benzene and formed in >95% yield according to the IR spectrum. IR carbonyl stretching frequencies for **13** and **14** are listed in Table 31. ^1H NMR spectral results for **13** and **14** are listed in Table 32. $^{13}C\{^1H\}$ NMR spectral results for **13** and **14** are listed in Table 34.

Reaction mixture of 2a + $CDCl_3$. A solution of **2a** in $CDCl_3$ immediately turned from yellow to red upon exposure to light. After ~5 min. of exposure to light, the solution was protected from light and analyzed by $^{31}P\{^1H\}$ NMR spectroscopy. $^{31}P\{^1H\}$ NMR ($CDCl_3$): δ 54.09 (s, PBu_3 (**2a**)), 23.14 (s, PBu_3), −32.82 (s, free PBu_3).

Reaction mixture of 2b + $CDCl_3$. The yellow solution immediately turned red upon exposure to light. After the solution had been exposed to light for ~5 min., it was analyzed by $^{31}P\{^1H\}$ NMR spectroscopy. $^{31}P\{^1H\}$ NMR ($CDCl_3$): δ 36.88 (s, PMe_3 (**2b**)), 11.67 (s, PMe_3), −59.90 (s, free PMe_3).

$(\eta^6\text{-}C_6Me_5CH_2CDCl_2)Mn(CO)_2Cl$ (14). Compound **14** was observed as a red solution in $CDCl_3$ and formed in >95% yield according to the IR spectrum.

Table 34. $^{13}C\{^1H\}$ NMR Spectral Data for $(\eta^6\text{-}C_6Me_5CH_2R')Mn(CO)_2X$ (13, 14)

			$^{13}C\{^1H\}$ NMR	
compd no.	R′	X	δ, ppm [a]	
13 [b]	CCl_3	Cl	135.1, 134.3, 133.1, 102.1	(s, ring–C)
			53.1	(s, $-CCl_3$)
			17.8, 17.6, 17.1, 14.4	(s, ring–CH_3)
14 [c]	$CDCl_2$	Cl	228.7	(s, CO)
			131.9, 106.1, 104.2, 102.0	(s, ring–C)
			42.2	(s, $-CDCl_2$)
			16.5, 16.1, 15.8	(s, ring–CH_3)

[a] (mult., assignment, coupling).

[b] Obtained in d_6–benzene at 298 K.

[c] Obtained in $CDCl_3$ at 298 K.

X-ray Data Collection, Solution, and Refinement of 2b.

Crystals of **2b** were obtained as orange prisms by sublimation under reduced pressure. A summary of the crystal data and refinement parameters are given in Table 35. A crystal, 0.39 × 0.15 × 0.12 mm, sealed in a glass capillary tube under dinitrogen, was mounted on the diffractometer. Graphite monochromated Mo Kα radiation, average wavelength = 0.710 73 Å, was used to collect data at 295 K on an Enraf–Nonius CAD4 diffractometer, using an ω scan range, 0.80 + 0.35 tan θ, background at 25% below and above range; the horizontal aperture was varied from 2.5 to 3.0 mm depending on the angle; the scan speed ranged from 0.71 to 3.3 deg/min for a hemisphere with θ ranging from 1 to 25°. Lorentz, polarization, and empirical

absorption corrections were made (μ = 6.9 cm^{-1}, maximum and minimum corrections, 0.97–1.0 on F). Three standards, used to monitor crystal decay, indicated a maximum decline in F^2 of 10.7%; intensity corrections for decay were made. A total of 4163 reflections was measured for the full sphere ($\pm h, \pm k, \pm l$) in reciprocal space for 2θ ranging from 2–50°. Averaging 2047 independent reflections greater than 3σ above background gave 1163 reflections that were used in the least-squares refinement. The cell dimensions for the monoclinic crystal, space group $P2_1/c$, a = 11.967 (4) Å, b = 10.093 (6) Å, c = 15.232 (4) Å, $\alpha = \gamma = 90°$, β = 102.70 (5)°, were obtained by a least squares fit to 19 orientation reflections in the angular range of 10–45° for 2θ.

The positions of the manganese and phosphorus atoms were located by Patterson methods. Positional parameters are reported in Appendix B. Subsequent cycles of least-squares refinement and difference Fourier calculations were used to locate all other non-hydrogen atoms and half the hydrogen atoms, including H12A and H12B on the exocyclic methylene. During the final stages of refinement, the remaining hydrogen atom positions were calculated by assigning C–H distances of 0.95 Å and normalizing their positions with respect to located hydrogen atoms. No solvent molecules were found. Anisotropic refinement on all non-hydrogen atoms, except C14, (185 variables, including scale and extinction) gave R values of R_1 = 0.059 and R_2 = 0.078; the standard deviation of an observation of unit weight = 1.28; the maximum parameter shift/estimated error was less than 0.03; the maximum peak height on the final electron density difference map was 0.56 $e^-/Å^3$. Weights used in refinement are $1/s^2(F)$, where $s^2(F) = s^2(F)' + [(0.07)F]^2$, and $s^2(F)'$ is the larger of the estimate of the propagated error due to counting error or the estimated error based on agreement of equivalent reflections in the averaging step. The data were processed using scattering factor tables provided in the Enraf–Nonius SDP software package.[40]

Table 35. Crystallographic Data and Refinement Parameters for **2b** [a]

fw	348.11	space group	$P2_1/c$
a, Å	11.967 (4)	T, °C	23
b, Å	10.093 (6)	λ, Å	0.710 73
c, Å	15.232 (4)	ρ_{calc}, g cm^{-3}	1.556
β, deg	74.69 (5)	linear abs coeff, cm^{-1}	7.7
V, Å^3	1794.4 (8)	transm coeff	1.00–0.97
Z	4	reflections measured	4163
R_1 [b]	0.059	independent reflections	2047
R_2 [c]	0.078	after averaging ($> 3\sigma$)	1163
		parameters refined	185

[a] In this and subsequent tables esd's are given in parentheses.

[b] $R_1 = \sum \| F_o | - | F_c \| / \sum | F_o |$.

[c] $R_2 = [\sum w(| F_o | - | F_c |)^2 / \sum w | F_o |^2]^{1/2}$, $w = 1/\sigma^2(F)$, where $\sigma^2(F) = \sigma^2(F) + [(\mathrm{PWT})F]^2$, PWT = 0.07.

Results and Discussion

Synthesis and Characterization of 2a–e

The weak nucleophilic reactivity of **2** at the exocyclic methylene suggests that similar compounds in which a carbonyl is replaced by a stronger σ-donor ligand such as a phosphine ligand could show increased reactivity. The syntheses of **2a–e** were carried out in a 4:1 solution of hexane and THF, which by solubilizing the starting materials, optimizes the formation of the η^5-benzyl complexes.[10] In hexane, a nonpolar solvent, KH acts to deprotonate **1a–e**, rather than acting as a hydride nucleophile. Alternate syntheses, using alkyllithium or sodium hydroxide in THF, form the η^5-benzyl, but experimental conditions make isolation of the product difficult. Compounds **2b** and **2d** can be purified by sublimation, while **2a**, **2c**, and **2e** decompose

at sustained elevated temperatures under reduced pressure. Typically, all the η^5-benzyls formed were purified by repeated extraction with hexane to remove them from excess KH. Purity of the products, **2a–e**, was checked by observing the carbonyl bands in the IR spectra, which are distinct from those of the cationic starting materials, **1a–e**, and the cyclohexadienyls, **11a–e**.[8] In the ^{1}H NMR spectra, **2a–e** each have three characteristic singlets for the inequivalent methyl groups in a 3:6:6 ratio. The exocyclic methylene protons occur as doublets or broad singlets (δ 3.63–3.26). The exocyclic methylene doublets (1.2–1.4 Hz) becomes a singlet upon decoupling using the frequency of the ^{31}P resonance. The methyl protons of the phosphine in **2b** and **2d** appear as doublets, split by phosphorus, at δ 1.15 and 3.26, respectively. The phenyl protons of both **2c** and **2e** occur between δ 7.73–7.38. The butyl groups in **2a** display three proton resonances at δ 1.43, 1.31, and 0.89 for the methylenes adjacent to the phosphorus atom, intervening methylenes, and the terminal methyls, respectively. In the ^{31}P{^{1}H} NMR spectra, only the trimethylphosphine derivative, **2b**, deviates substantially from its cationic precursor, **1b**, by shifting upfield by 15 ppm. In each case, only one phosphorus resonance is observed. In the ^{13}C{^{1}H} NMR spectra, a peak between δ 233.0–228.0 is observed for the CO carbon atoms. Appropriate resonances are observed for the coordinated ring carbon atoms (δ 108.4–76.9) and ring methyl carbon atoms (δ 18.0–15.3). The carbon atoms of the phosphine ligands occur at δ 27.3–12.0 (**2a**), 19.2 (**2b**), 134.1–129.3 (**2c**), 51.9 (**2d**), and 147.1–121.4 (**2e**). The uncoordinated ring carbon atoms appear at δ 145.5 (**2a**), 146.4 (**2b**), 145.0 (**2c**), 148.0 (**2d**), and 152.5 (**2e**) and the exocyclic methylene carbon atom occurs at δ 79.6 (**2a**), 78.8 (**2b**), 79.6 (**2c**), 80.3 (**2d**), and 82.7 (**2e**); based on similar assignments for **2** [10] and **3**.[14a] The ^{13}C–^{1}H coupling constant of 156.5 Hz for the exocyclic methylene of **2d** matches those observed for **2** [10] (158 Hz) and **3** [14a] (156.5 Hz). Because these couplings are virtually the same, they could not provide a suitable measure for potential

reactivity of the exocyclic methylene. High resolution EI-MS provided the molecular formulas for compounds **2a–e**, which agree with their proposed structures.

Crystallographic Study of **2b**

The crystallographic study was performed to establish the molecular structure of **2b** and to compare it to the published structures of (η^5-$C_6Me_5CH_2$)$Mn(CO)_3$[10] (**2**) and $CpFe(\eta^5$-$C_6Me_5CH_2)$ [14] (**3**). The solid state structure of **2b** is illustrated in the ORTEP plot in Figures 3 and 4. Selected bond distances and angles are given in Table 36. Supplemental Figures and Tables are found in Appendix B. In this "piano stool" structure, the three ligands underneath the (η^5-pentamethylbenzyl)Mn fragment represent the "legs" that are positioned in an eclipsed configuration with respect to the ring carbon atoms. The trimethylphosphine ligand is found positioned beneath the exocyclic double bond; where apparently, it experiences the smallest van der Waals repulsion, Figure 3b. The phosphite ligand in *endo*-(η^5-C_6Me_6H)$Mn(CO)_2P(OMe)_3$ was found eclipsing the C4 carbon atom rather than beneath the saturated ring carbon atom and is discussed in more detail in Chapter V.[8] In **2b**, the near random positioning of the methyl groups on the phosphine is consistent with free rotation about the Mn–P bond. This causes the anisotropic thermal factors for the phosphine methyl carbon atoms to be twice as large as normal, resulting in increased R values and uncertainties.

The C–C bond distance, 1.33 (2) Å, between the unbound ring carbon atom (C6) and the exocyclic methylene carbon atom (C12) is consistent with typical C–C double bonds, matches the bond length found in **2** [10] (1.332 (6) Å), and is slightly shorter than in **3** [14] (1.376 (9) Å). The C6 atom is 0.4 Å above the plane formed by the five bound ring carbon atoms, Figure 4,[41] indicating that the η^5-benzyl ligand is bound pentahapto rather than hexahapto. The folding dihedral angle, C5/C6/C1 to

C1/C2/C3/C4/C5, of the η^5–pentamethylbenzyl ligand is 29 (1)°, which is less than that found in **2** (32°) and **3** (32.6°).[14c-e] This angle is best illustrated in Figure 4a. The folding angles for the η^5–pentamethylbenzyl ligands are well below the typical range for metal-coordinated η^5–cyclohexadienyl ligands (39–50°) which have a saturated uncoordinated ring carbon atom.[8,42,43] Based on MO treatments developed by Hoffmann,[43b] Connelly,[44] and Astruc,[45] shown in Figure 5, the folding dihedral angle is dependent upon secondary molecular orbital interactions between the filled metal $d_{xy}(1e_s)$ orbital and the substituent on the uncoordinated ring carbon atom of the cyclohexadienyl. For an *endo*–η^5–hexamethylcyclohexadienyl, there is significant repulsion between the $d_{xy}(1e_s)$ orbital and the *endo*–methyl. However, for an η^5–pentamethylcyclohexadienyl–*exo*–ene, there is less steric repulsion and the possibility of symmetry allowed overlap between the $d_{xy}(1e_s)$ orbital and exocyclic π-antibonding orbital (π_a). Thus, it should be anticipated that a smaller dihedral angle is observed with an exocyclic methylene, Figure 6a, compared to an endo alkyl substituent. Furthermore, in the η^5–pentamethylbenzyl ligands, the exocyclic double bond tilts down toward the metal atom. The tilt angle of the C6–C12 bond, relative to the C5/C6/C1 plane, is calculated to be 4.0 (2)°, using the displacement of C12 from the C5/C6/C1 plane, −0.092 (3) Å, and the C6–C12 bond length. This 4° tilt is about half the tilt angle found in **2** [10] (9°) and **3** [14] (10°). The smaller tilt angle may be attributable to steric interaction with the trimethylphosphine ligand, which has a cone angle of 118°, whereas a carbonyl has a cone angle of 46°.[38] The exocyclic methylene is calculated to be twisted 30° with respect to the C5/C6/C1 plane, using the hydrogen atom positions for H12a and H12b from the Fourier synthesis. Because the calculation of the twist angle depends on the H12A and H12B positions, the error in the twist angle is uncertain. Theoretical calculation of a 30° twist of a double bond decreases the orbital overlap in the π-bonding orbital (π_s) by only 4%.[46]

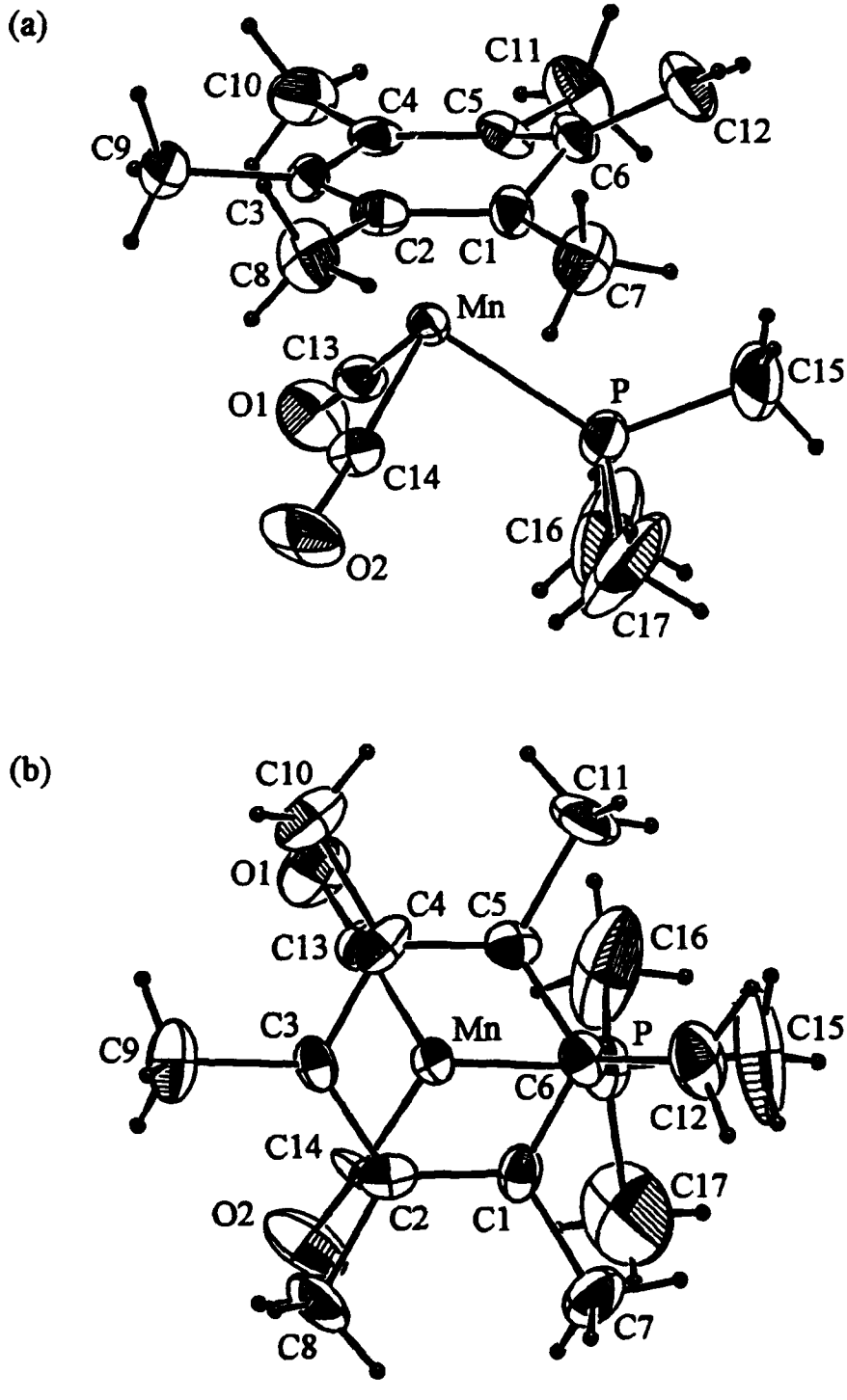

Figure 3. ORTEP drawing of **2b**: (a) canted side view and (b) bottom view

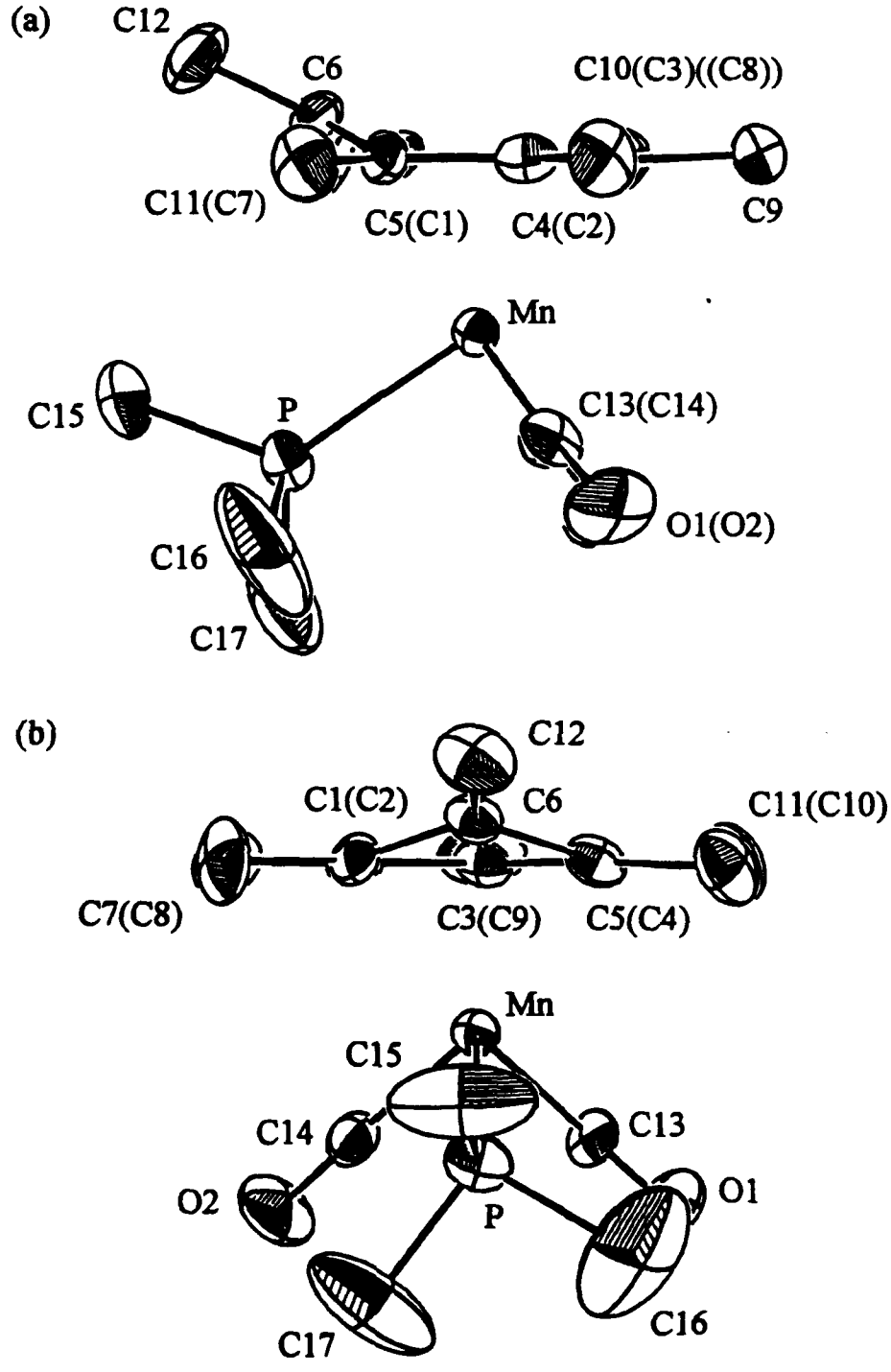

Figure 4. ORTEP drawing of 2b orthogonal side views

Table 36. Selected Bond Distances (Å) and Angles (°) for **2b**

		Distances	
Mn–C1	2.27 (1)	C1–C2	1.403 (16)
Mn–C2	2.16 (1)	C1–C7	1.516 (17)
Mn–C3	2.11 (1)	C2–C3	1.401 (15)
Mn–C4	2.15 (1)	C2–C8	1.534 (14)
Mn–C5	2.26 (1)	C3–C9	1.519 (16)
Mn–P	2.244 (3)	C3–C4	1.442 (15)
Mn–C13	1.764 (13)	C4–C5	1.377 (16)
Mn–C14	1.740 (11)	C4–C10	1.525 (17)
P–C15	1.737 (18)	C5–C6	1.453 (15)
P–C16	1.782 (22)	C5–C11	1.528 (14)
P–C17	1.732 (16)	C6–C1	1.444 (14)
O1–C13	1.157 (12)	C6–C12	1.332 (16)
O2–C14	1.153 (12)		
		Angles	
C13–Mn–C14	85.7 (5)	C1–C2–C8	121.0 (12)
P–Mn–C13	91.1 (4)	C3–C2–C8	117.8 (12)
P–Mn–C14	91.0 (4)	C2–C3–C4	117.3 (9)
Mn–C13–O1	178.1 (12)	C2–C3–C9	123.3 (12)
Mn–C14–O2	176.8 (12)	C4–C3–C9	119.1 (12)
Mn–P–C15	116.8 (7)	C3–C4–C5	120.2 (10)
Mn–P–C16	113.4 (7)	C3–C4–C10	119.6 (12)
Mn–P–C17	125.1 (6)	C5–C4–C10	120.1 (12)
C15–P–C17	101.9 (11)	C4–C5–C6	120.5 (10)
C15–P–C16	97.8 (14)	C4–C5–C11	120.6 (12)
C16–P–C17	97.1 (12)	C6–C5–C11	116.9 (11)
C2–C1–C6	119.4 (12)	C5–C6–C1	111.7 (9)
C6–C1–C7	119.5 (11)	C5–C6–C12	126.1 (12)
C2–C1–C7	119.1 (11)	C1–C6–C12	122.0 (12)
C1–C2–C3	121.2 (10)		

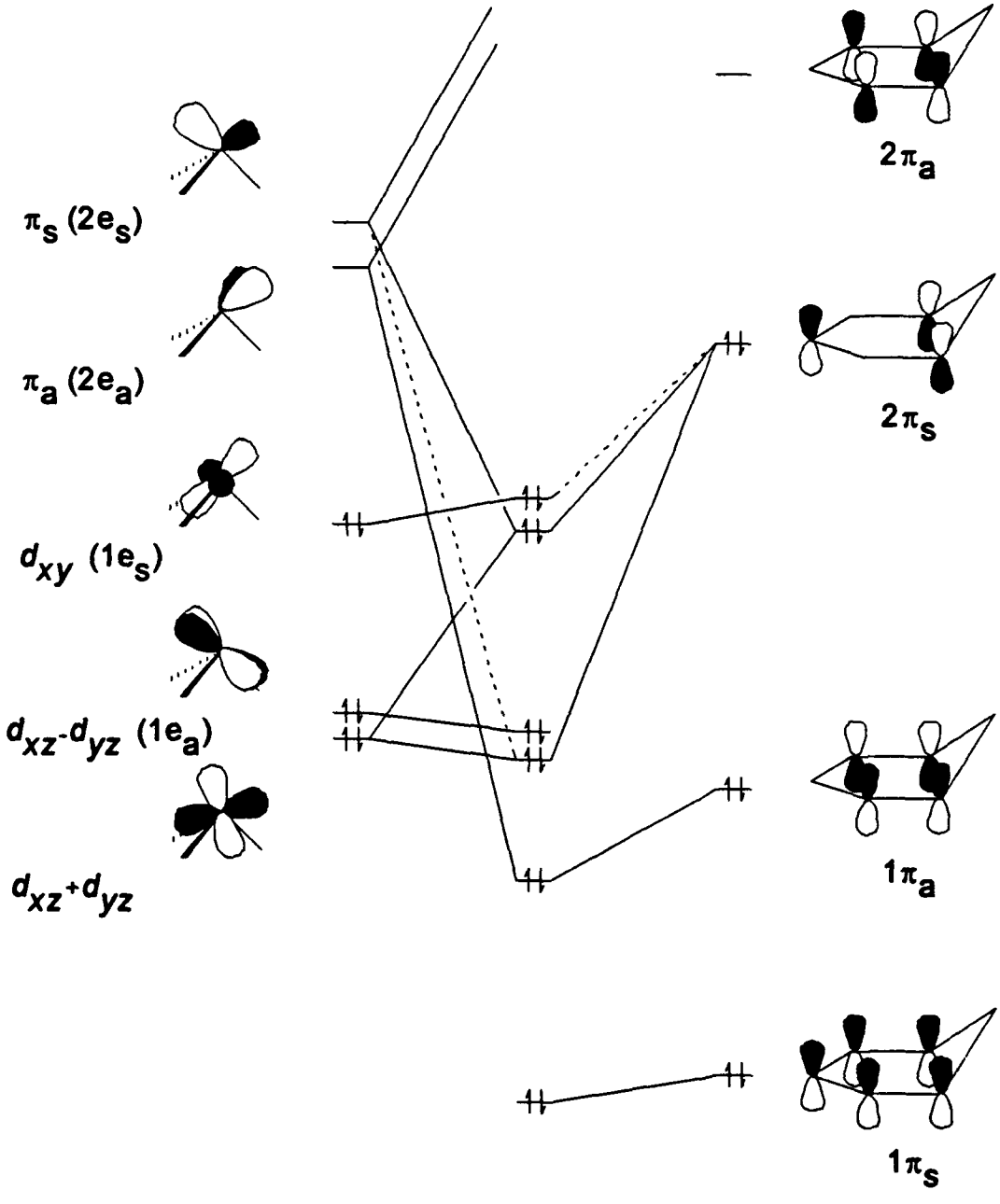

Figure 5. MO diagram for the interaction of transition metals and η^5-cyclohexadienyl ligands (ref 44 and 43)

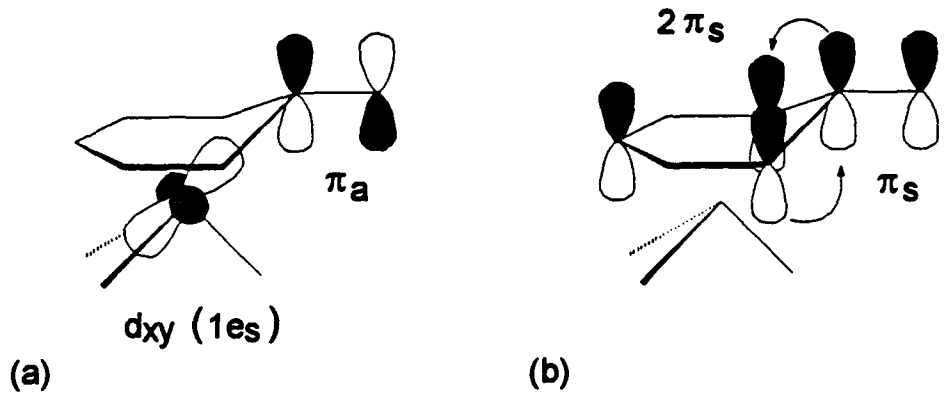

Figure 6. Molecular orbital interactions involving the manganese and η^5–cyclohexadienyl–*exo*–ene ligand

Haddon also notes that the σ-bond is unaffected by the twist of the double bond.[46] The smaller twist in **2b** compared to **2** may be attributed to greater secondary orbital interaction between the exocyclic π-antibonding orbital (π_a) and the filled metal $d_{xy}(1e_s)$ orbital, a smaller twist was found in **3** with a Cp ligand. The twist may be further stabilized by a symmetry-allowed interaction between the $2\pi_s$ orbital set for the η^5–cyclohexadienyl ring and the π_s orbital of the exocyclic double bond, Figure 6b. The steric demands of the adjacent methyl groups also may contribute to the twist as was suggested by Astruc for **3**.[14a,45b] The exocyclic CH_2 twist for **2b** lies between the values determined for **2** [10] (38°) and **3** [14] (11°), reflecting the differences in electron density on the metal d_{xy} orbital from the CO, PMe_3, and $C_5H_5^-$ ligands.

The manganese atom of **2b** may be viewed as occupying a pseudo–octahedral environment with the η^5–pentamethylbenzyl ligand occupying three facial coordination sites. The η^5–pentamethylbenzyl ring is shifted close to the centroid of the C1–C2–C3–C4–C5 crescent to maximize orbital overlap with the π-bonding basis set of the manganese.[43] The Mn–C3 bond length (2.11 (1) Å) is the shortest, whereas, the

Mn–C5 (2.26 (1) Å) and Mn–C1 (2.27 (1) Å) bonds are the longest. The constraints imposed by the σ-bonding orbital set require that the tripod of ligands eclipse the C2, C4, and C6 ring carbon atoms.[43] The C13–Mn–C14, P–Mn–C13, and P–Mn–C14 bond angles of 87.7 (5)°, 91.1 (4)°, and 91.0 (4)°, respectively, agree with a pseudo–octahedral symmetry for the manganese atom. The structural parameters we obtained here were used in a preliminary molecular modeling exercise; the details and results of which are presented in Appendix B.

General Reactivity of **2a–e**

η^5–Pentamethylbenzyl complexes, **2a–e**, have been shown to undergo a diversity of reactions, Schemes II and III. The coordinated η^5–pentamethylbenzyl ligand is the strong conjugate base of a relatively weak acid, the coordinated η^6–hexamethylbenzene. The exocyclic double bond can be protonated by Brønstead acids to reform the cationic (η^6–arene)manganese starting compound. This was verified for the title compounds by the addition of $[NH_4][PF_6]$ (1:1) in THF to protonate **2a–e**. The reaction was observed to proceed quantitatively by IR spectroscopy. The recoverable yield was greater than 95% for each complex. The exocyclic double bonds of the η^5–benzyl ligands of **2a–e** react with 2 equiv of Bu_3SnH to form *endo*–(η^5–C_6Me_6H)$Mn(CO)_2PR_3$, **11a–e**. Under catalytic hydrogenation reaction conditions (0.1 g Pd/C (3%), 30 mL THF, 22.4 mL H_2, 48 h), the π-carbocyclic ligand is lost and no **11a–e** is observed. The exocyclic double bond can act as a nucleophile or undergo radical reactions with halocarbons.[10]

Nucleophilic Reactions of **2a–e**

The nucleophilic properties of the exocyclic double bonds of **2a–e** are demonstrated by the formation of C–C, C–I, C–Fe, and C–Mn bonds, Scheme II. The absence of an ESR signal suggests that the oxidation state of the manganese is unchanged.

Scheme II. Nucleophilic reactions of **2a–e**

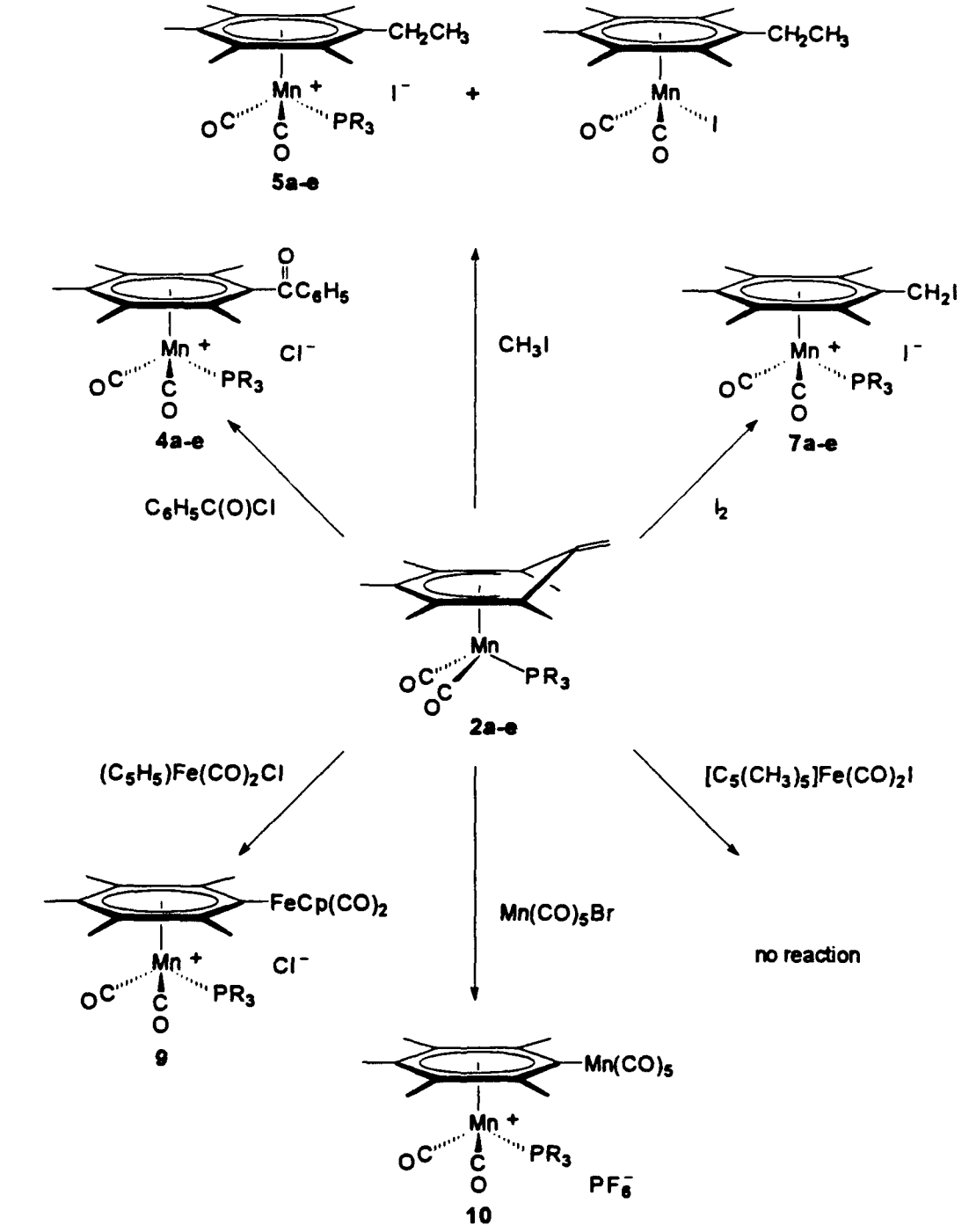

Scheme III. Radical and other reactions of **2a–e**

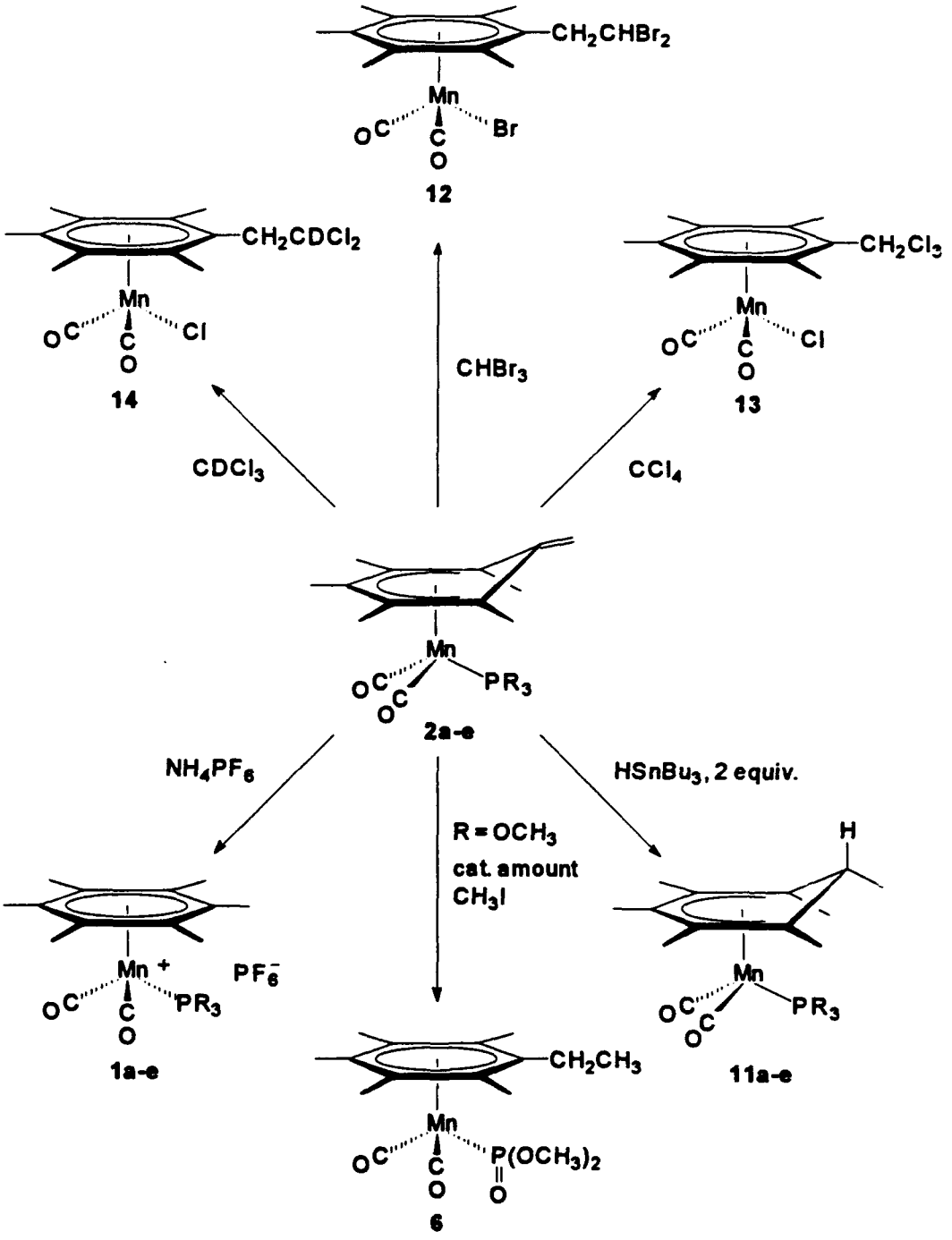

The η^5-benzyls, **2a–e**, attack iodomethane, benzoyl chloride, and iodine, in either hexane or THF, to yield new C–C and C–I bonds. The electrophilic portion, $E^{\delta+}$, of these polarizable reagents is added to the activated exocyclic double bond of the η^5-benzyl, eq 9. As illustrated in eq 9, this reaction probably proceeds as a simple S_N2 reaction. The proposed transition state, depicted without methyl groups in eq 9, shows the filled $d_{xy}(1e_s)$ orbital of the manganese overlapping with the empty p orbital of the C6 carbon atom to stabilize the transition state. The displaced $X^{\delta-}$ becomes the

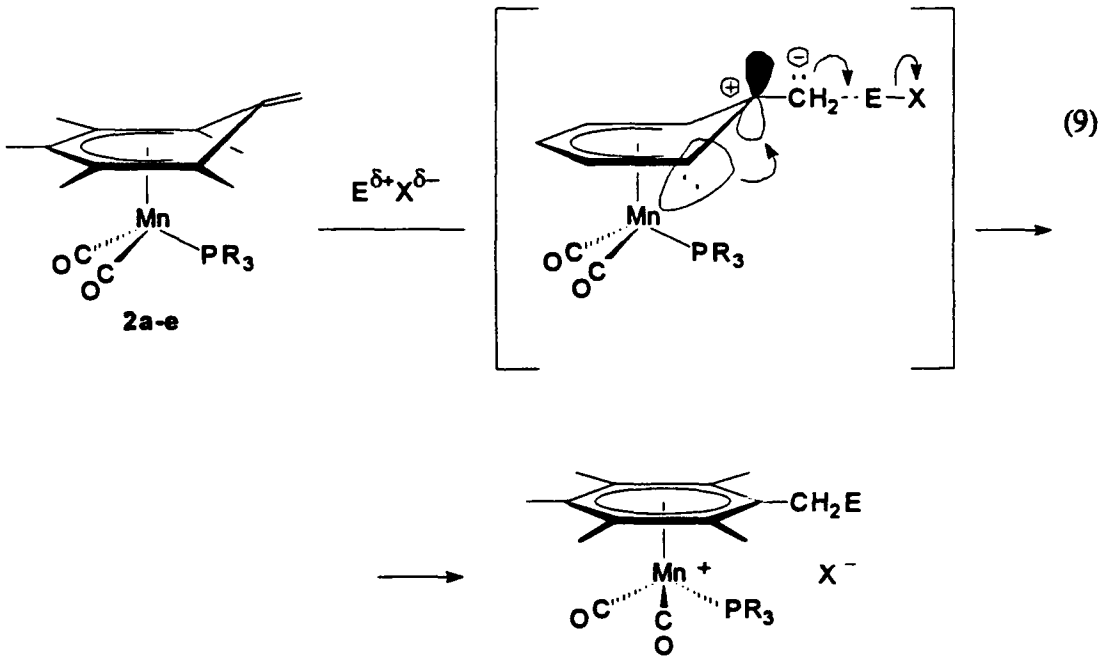

(9)

counter ion of the new cationic (η^6-arene)manganese complex. The enhanced reactivity of **2a–e** cannot be explained by the ground state alone, wherein the exocyclic double bond lengths in **2** and **2b** are equivalent, while the bond length in **3** is longer. Additionally, the twist angle of **3** is much smaller than found in **2** and **2b**. Therefore, it is likely that the enhanced reactivity arises during the formation of the transition state

rather than the ground state.

Compounds **2a–e** were observed to react with benzoyl chloride at rates which are much faster than the rate reported for the tricarbonyl complex, **2**, based on the time required for complete reaction.[10] The reaction time of **2c–2e** were longer than **2a** and **2b**. In all cases, the reactions went quantitatively to **4a–e** as determined by IR spectroscopy. The IR spectra of **4a–c** and **4e** displayed carbonyl stretches that are 2–3 cm^{-1} higher than the starting compounds **1a–1c** and **1e**, while **4d** was lower by 6 cm^{-1}; all of which are in the characteristic range observed for terminal carbonyls of cationic (η^6–arene)manganese complexes. The newly formed ketone C=O band for these products appears between 1706–1685 cm^{-1}. The products were purified by chromatography as the chloride or metathesized with $[NH_4][PF_6]$ in acetone. The products, **4a–e**, were characterized by ^1H and $^{31}P\{^1H\}$ NMR spectroscopy and high resolution FAB mass spectrometry using 3-NBA matrix. The $-CH_2C(O)-$ protons appear between δ 4.30–3.89. The retention of the phosphine ligands coordinated to the manganese was confirmed by observation of characteristic proton resonances for the respective phosphine ligands in the ^1H NMR spectra. The $^{31}P\{^1H\}$ NMR spectra each contained a single peak for the respective phosphine ligands. The cationic molecular ions of **4a–e** were observed in HR–FAB MS, verifying their molecular formulas.

The reactions of **2a–e** with both iodomethane and iodine further substantiate the nucleophilic character of the η^5–pentamethylbenzyl ligand. For CH_3I, the alkyl fragment is added to the exocyclic methylene and I^- becomes the counter ion. The pseudo–first–order rate constants, k, calculated for the reaction of **2a–e** with excess CH_3I are listed in Table 37. As the electronic contribution from the phosphine ligand increases, k for the methylation reaction increases. For **2b** in THF, a trace amount, less than 2%, of (η^6–C_6Me_5Et)$Mn(CO)_2I$ (**19**) forms by way of a competing radical mechanism (Scheme IV) that will be discussed later.

Table 37. Electrochemical and Rate Data for $(\eta^5\text{-}C_6Me_5CH_2)Mn(CO)_2PR_3$ (**2a–e**)

Compd	O_I[a], $E_{p,a}$	k (s^{-1})[b]	$\nu_{CO}(A_1)$[c]	χ[d]
2a	0.65	1.6 (5) × 10^{-3}	1921	1.4
2b	0.67	7.3 (4) × 10^{-3}	1924	2.6
2c	0.86	3.3 (4) × 10^{-4}	1927	4.3
2d	1.04	1.0 (3) × 10^{-4}	1939	7.7
2e	1.20	1.7 (3) × 10^{-4}	1955	9.7

[a] E_{pa} (anodic peak potential), V vs. SCE; 0.1 M $(n\text{-}Bu)_4NBF_4$/THF; sweep rate = 200 $mV{\cdot}s^{-1}$; error = ±10 mV; Pt working electrode.

[b] Pseudo-first-order rate constants for the reaction: **2a–e** + CH_3I → $[(\eta^6\text{-}C_6Me_5Et)Mn(CO)_2PR_3]I$. Reactions observed in THF at 22 °C.

[c] Infrared symmetric carbonyl stretching frequency observed in THF.

[d] Tolman electronic factors for PR_3 ligands (ref 38).

For **2d**, an Arbuzov-like product, **6**, is observed to form exclusively in THF and as a mixture with **19** in hexane. The possibility of the catalytic formation of **6** was verified by the observation that the addition of a catalytic amount of CH_3I (0.05%) to a hexane solution of **2d** yields over 35% of **6**. The remaining compounds, **2a–c** and **2e**, produced the expected nucleophilic reaction products, **5a–c** and **5e**, and only a trace of **19**, anticipated from a radical pathway, was observed during the chromatographic purification of the products. ^1H NMR spectra of **5a–e** displayed a characteristic ethyl group triplet for the methyl (δ 1.22–1.12) and quartet for the methylene (δ 2.89–2.64). In the reaction of I_2 with **2a–e**, I^+ adds to the exocyclic methylene and I^- becomes the counter ion. The reaction of **2d** and I_2 produces **8**, an Arbuzov-like product, in small amounts (9%). The ^1H NMR spectra of compounds **7a–e** show the distinctive downfield shift of the $-CH_2I$ protons (δ 4.71–4.18), which is anticipated from the

combined field effects of an η^6-arene and iodide substituted on a ring methyl. The $^{31}P\{^1H\}$ NMR spectra of **5a–e** and **7a–e** each contain a single peak for the respective phosphine ligands. HR-FAB MS identified the molecular ions of **5a–e** and **7a–e**, $[(\eta^6\text{-arene})Mn(CO)_2PR_3]^+$, that verify their corresponding molecular formulas.

In the presence of KH, multiple alkylations are observed in the products, $[(\eta^6\text{-}C_6Me_{6-n}Et_n)Mn(CO)_2PMe_3]I$ (n = 1–3), of the reaction of **2b** with excess CH_3I. Reactions of this type, using KH or other bases, have been used by Astruc to produce a variety of "tentacled" arene complexes of iron and cobalt.[47] In our reaction, a minimal amount of KH and only 24 h of reaction time resulted in a maximum of three alkylation attacks on the ring methyls and a product ratio of 4:3:1 (n = 1–3), determined by MS. HR-FAB MS identified the molecular ions of the three products, verifying their corresponding molecular formulas.

Reactions of 2b with $Mn(CO)_5Br$ and $CpFe(CO)_2I$. Compound **2b** reacted with $Mn(CO)_5Br$ at −45 °C to form **10**, an orange product. The carbonyl stretching frequencies observed for the coordinated -$Mn(CO)_5$ are like those obtained by Astruc for $[CpFe(\eta^6\text{-}C_6Me_5CH_2Mn(CO)_5)][PF_6]$.[14c] The ^1H and $^{13}C\{^1H\}$ NMR spectra of **10** display resonances similar to those observed by Astruc. Both IR and NMR spectra confirm the formation of the C–Mn bond at the exocyclic methylene carbon atom. Under similar reaction conditions, $CpFe(CO)_2I$ reacts with **2b** to form **9**. The ν_{CO} shift to higher frequencies suggests the return of the C_6 ring to hexahapto coordination and the addition of the $[CpFe(CO)_2]^+$ moiety to the exocyclic methylene. Corresponding changes in the resonances of the ^1H and $^{13}C\{^1H\}$ NMR spectra and comparison with the spectral results reported by Astruc for $[CpFe(\eta^6\text{-}C_6Me_5CH_2Mn(CO)_5)][PF_6]$ confirm the formation of **9**.[14c]

Radical Reactions of 2a–e

LaBrush et al. proposed a radical mechanism for the reaction of **2** with tetrachloromethane, deuterated chloroform, and bromoform to form complexes of the type $(\eta^6\text{-}C_6Me_5CH_2CH_nX_{3-n})Mn(CO)_2X$ (n = 0, 1), similar to that shown in Scheme IV using R'X (R' = CH_nX_{3-n}) as a typical halocarbon.[10] Addition of a radical inhibitor, 9,10–dihydroanthracene (9,10–DHA), slows the rates of these reactions in laboratory light and stops the reaction in the dark after photoinitiation. The phosphine derivatives **2a–e** produce similar products with halocarbon reagents in this process and are influenced in the same way by 9,10–DHA. The proposed initiation of the radical mechanism is the photoinduced dissociation of the phosphine followed by coordination of the halocarbon to the resulting 16-electron manganese species, shown proceeding to the right in Scheme IV. Halocarbons coordinated to second and third row transition metals are well documented in the literature.[48] Recent work has established that first row transition metals also coordinate halocarbons.[49] The anticipated weakening of the C–X bond upon coordination in $(\eta^5\text{-}C_6Me_5CH_2)Mn(CO)_2(XR')$ **(LD1)**, would facilitate homolytic cleavage of the C–X bond to generate $(\eta^5\text{-}C_6Me_5CH_2)Mn(CO)_2X\cdot$ **(LD2)** and R'· (n = 0, 1) radicals. The possible oxidative addition of R'X to the manganese followed by homolysis of the metal–carbon bond to form the radicals is unlikely due to steric considerations and formation of a 20–electron intermediate. However, an alternate initiation process involving electron transfer, shown proceeding to the left in Scheme IV, would produce a manganese(II) species **(ET1)** that could react with a R'· to form an (η^6–arene)manganese cation **(ET2)**. Formation of **ET1** would be accompanied by generation of R'·.

Formation of the R'· radical serves to initiate a chain mechanism that begins with an attack on a second molecule of **2a–e** at the exocyclic methylene to form the 19-electron $[(\eta^6\text{-arene})Mn(CO)_2L]\cdot$ **(PG1)** (L = PR_3) radical. The 17-electron species,

Scheme IV. Proposed radical pathways for 2a–e and halocarbons

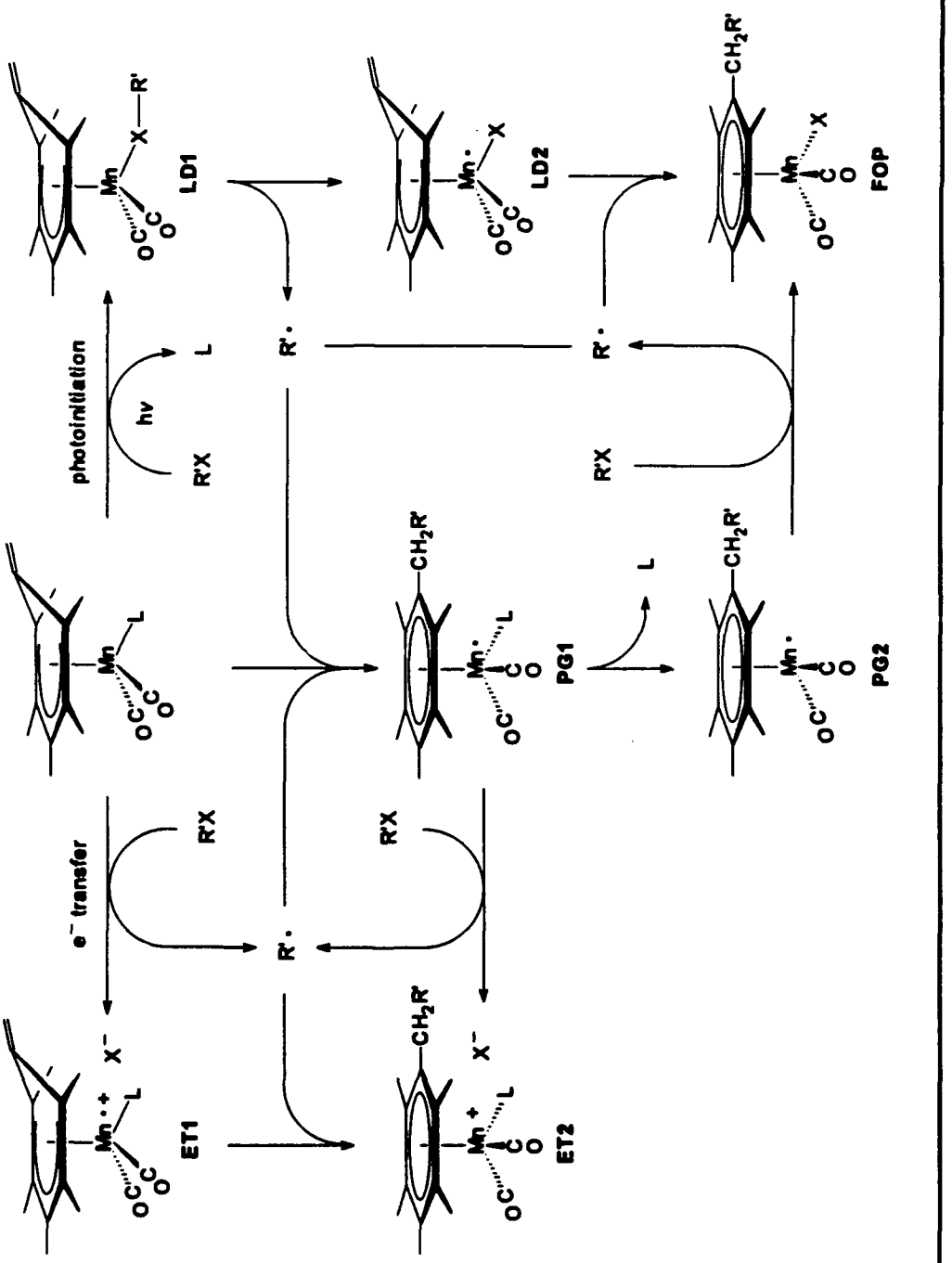

[(η^6-arene)Mn(CO)$_2$]$\cdot$ (**PG2**), formed by PR_3 dissociation from **PG1**, abstracts a halogen atom from another R'X, resulting in regeneration of R'$\cdot$. Reaction of R'$\cdot$ with the **LD2** or coupling with another R'$\cdot$ radical furnishes a termination step.

The rates of reaction between the (η^5-pentamethylbenzyl)manganese complexes and a halocarbon are greater when a phosphine is substituted for a carbonyl. This can be partially attributed to the increased lability of the phosphines over a carbonyl in **PG1**. The reaction of **2a–e** with CCl_4 is much faster than $CDCl_3$, while the reaction of $CHBr_3$ is instantaneous and quantitative in hexane, forming a lavender precipitate, (η^6-$C_6Me_5CH_2CHBr_2$)Mn(CO)$_2$Br.

ESR Studies of the Reactions of **2**, **2a**, and **2b** with CCl_4

ESR spectra of the reactions of **2**, **2a**, and **2b** with CCl_4 provide support of the mechanism proposed in Scheme IV. No evidence was found for radicals in the ESR spectra of each of the starting compounds observed as frozen THF glasses at 77 K. The featureless ESR spectrum of diamagnetic **2a** in the absence of halocarbon is shown in Figure 7(a). A g_{iso}-value of 2.192 (3) (10% pitch standard) was obtained from the ESR spectrum of **2a** after the addition of CCl_4 at room temperature, followed by transfer to the ESR tube, and immediately thereafter freezing the solution. Under the same conditions, the identical g_{iso}-values, within experimental error, for **2** and **2b** were obtained. This value is consistent with one unpaired electron on the manganese. The appearance of the ESR spectrum of the reaction mixture of **2a** and CCl_4, Figure 7(b), is typical of all three reaction mixtures— overlaying spectra verified that they were identical. The manganese (I = 5/2) hyperfine splitting constants, A, for the six-line spectra indicate that the radical species is metal-centered with an A-value of 8.6 (3) mT (**2**, **2a**, **2b**). The g_{iso}- and A-values are consistent with reported cases of one unpaired electron on manganese(II) complexes in an octahedral environment.[50]

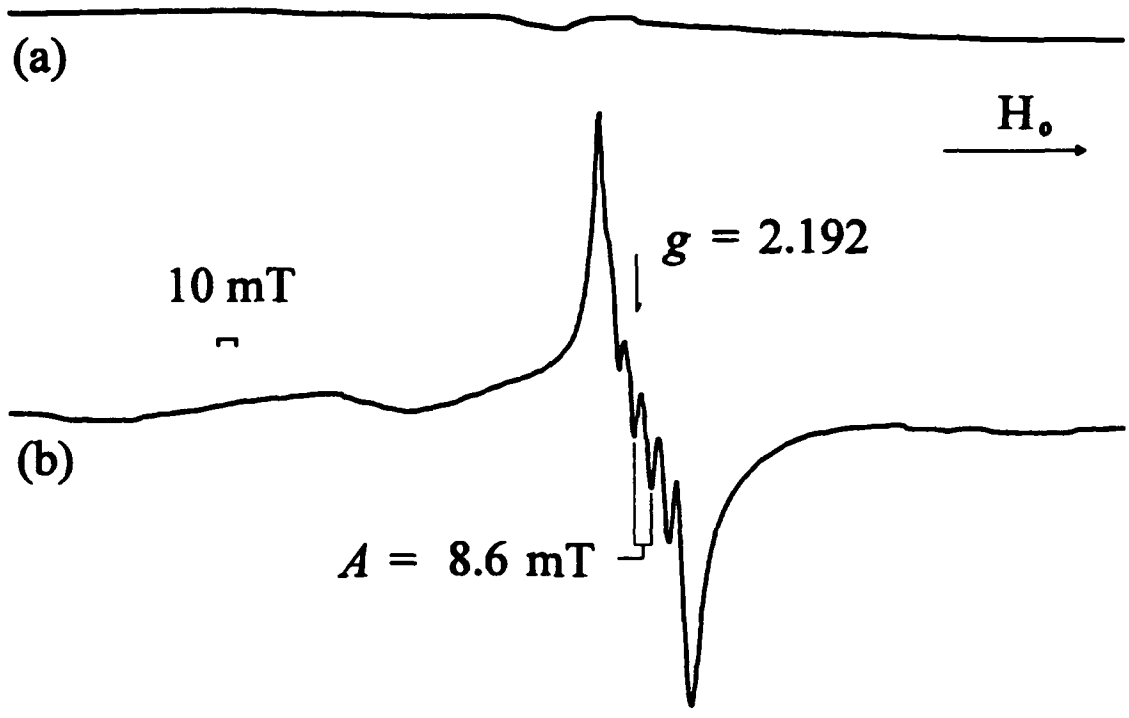

Figure 7. ESR spectra for (a) **2a** in THF and (b) **2a** + CCl_4 in THF, both at 77 K

Typical *A*-values have a reported range of 9.5-5.7 mT. These results suggest that the ESR signal results from **LD2** rather than **PG2**, a manganese(0) species. Hyperfine splitting constants for manganese(0) species have a reported range of 16.7-12.7 mT.[51] The absence of phosphorus hyperfine splitting suggests that the ESR-active species does not have a coordinated phosphorus ligand, and therefore must be **LD2** rather than **PG1** or **ET1**. Furthermore, the lack of phosphorus hyperfine splitting precludes manganese decomposition products containing the phosphine. Loss of an η^6-arene or η^5-benzyl ligand, in addition to the phosphine, from the manganese would require coordination of six THF molecules to recover an octahedral environment that would be consistent with the experimental data. A plot of ESR signal intensity versus time, illustrated in Figure 8, shows that the signal reaches a maximum then decrease to zero on time scale

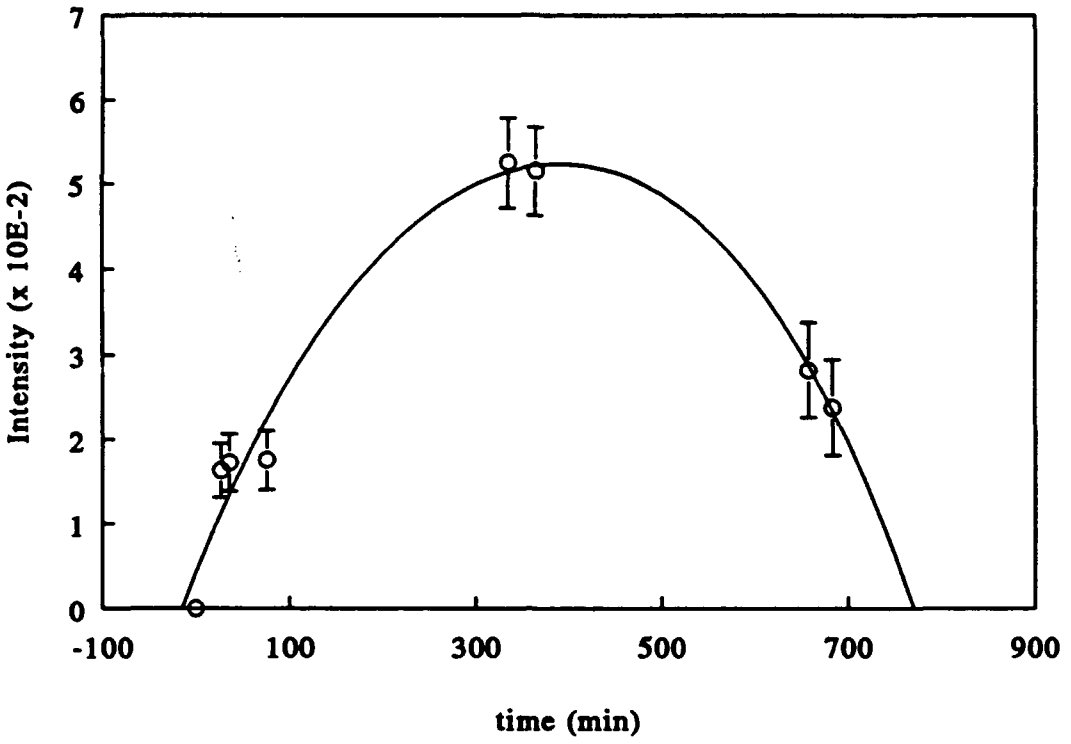

Figure 8. Plot of ESR signal intensity of **2a** + CCl_4 in THF vs. time

consistent with NMR experimental conditions.

The $^{31}P\{^1H\}$ NMR spectrum of the (**2a** or **2b**) + CCl_4 reaction mixtures each contain three resonances. The first is assigned to the uncoordinated PMe_3 (δ −59.9) or $P(n\text{-Bu})_3$ (δ −32.8) released during the reaction. The second arises from the coordinated PMe_3 (δ 11.7) or $P(n\text{-Bu})_3$ (δ 23.1) of a product in which arene is displaced by additional phosphine ligands. The third is assigned to $[(\eta^6\text{-}C_6Me_5CH_2CDCl_2)Mn(CO)_2PR_3]Cl$ (R = Me (δ 36.9), *n*-Bu (δ 54.1)), which results from the displacement of Cl^- from the inner-coordination sphere of manganese by phosphine liberated in the formation of **LD1** and **PG2** in Scheme IV. In an independent experiment, the reaction mixture of $(\eta^6\text{-}C_6Me_6)Mn(CO)_2Cl$ and an excess

of P(*n*-Bu)$_3$ displayed two of the same ^{31}P resonances as found in the reaction of **2a** and $CDCl_3$, [(η^6-C_6Me_6)Mn(CO)$_2$PR$_3$]Cl (δ 55.0) produced from the chloride displacement and the free P(*n*-Bu)$_3$ (δ −32.8).

Preliminary UV-Visible studies of **2b** and **2d** in hexane displayed little change, upon addition of CCl_4, in the charge transfer bands observed between 240–190 nm. The absence of new charge transfer bands supports ligand dissociation rather than electron transfer as the initiation process in the reactions of **2a–e** with CCl_4.

Electrochemical Studies of **2a–e** and **2**

In order to compare the donor-acceptor properties of the phosphine ligands on the manganese complexes, we have studied the electrochemical properties of **2a–e**. The cyclic voltammetry of **2a–e**, in 0.1 M [(*n*-Bu)$_4$N][BF_4] THF solution, was performed at a stationary-platinum-disk electrode at scan rates in the range of 200–500 mV·s^{-1} without positive feedback. At a scan rate of 200 mV·s^{-1}, **2a–e** exhibit two oxidation peaks, O_I ($E_{p,a}$ = 0.65–1.20 V vs SCE) (Table 37) and O_{II} ($E_{p,a}$ = 1.36–1.64 V vs SCE), with one reduction peak, R_I ($E_{p,c}$ = −0.81–−1.16 V vs SCE) being present on the reverse scan.

The first oxidation peak O_I is plotted versus the Tolman electronic factors (χ) for the phosphine and phosphite derivatives, **2a–e**, Figure 9.[38] The symmetric IR stretching frequency for the carbonyls (ν_{CO} (A_1)), another indicator of electron density on the manganese, varies monotonically with χ, Figure 9. Results from the electrochemistry of *endo*-(η^5-C_6Me_6H)Mn(CO)$_2$PR$_3$ complexes led us to expect a linear correlation between the O_I peak and Tolman electronic factors for the substituted phosphine and phosphite ligands.[8,52] Comparison of O_I for **2a–e** shows that **2a–c** are more easily oxidized than **2d** and **2e**, consistent with the fact that the phosphites are better π-acceptors or weaker σ-donors than the phosphines.

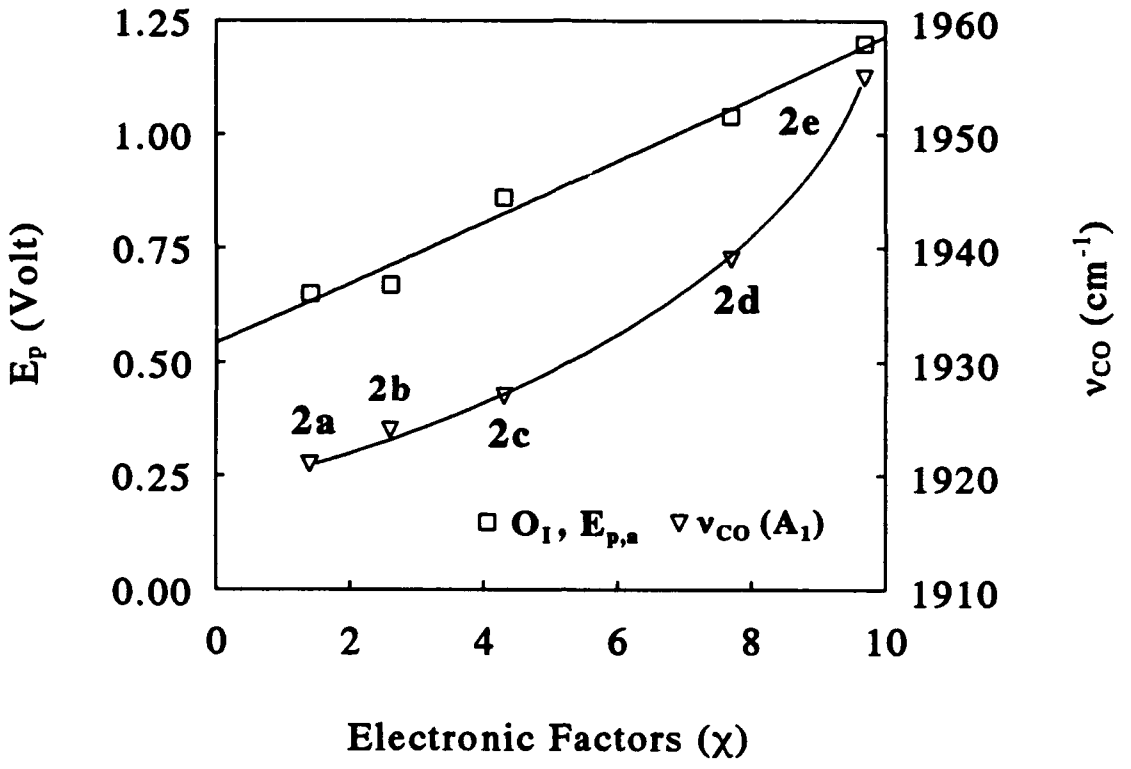

Figure 9. Oxidation potentials (O_I) and carbonyl stretching frequencies vs. Tolman electronic factors (χ) for (η^5-$C_6Me_5CH_2$)$Mn(CO)_2PR_3$ (**2a–e**)

Peak O_I is chemically irreversible at all scan rates observed, both at 292 and 223 K. The average absolute numbers of electrons, calculated from the peak areas, approximates a one electron transfer (n = 1.0–1.4) which supports the formation of monoradical cations of **2a–e**, eq 10. Peak R_I results from the reduction of the product

$$\mathbf{2x} \rightarrow \mathbf{2x^+} + \mathbf{e^-} \qquad E_{p,a} = 0.65\text{–}1.20\ \text{V} \qquad (10)$$

of the following chemical reaction from O_I. This was verified by reversing the scan

immediately after traversing O_I and scanning negative to obtain R_I. Peak R_I was not observed without first oxidizing **2a–e**.

Conclusions

A series of (η^5–pentamethylbenzyl)$Mn(CO)_2PR_3$ complexes has been synthesized from the cationic [(η^6–hexamethylbenzene)$Mn(CO)_2PR_3$]$^+$ complexes and characterized. The solid-state structure of **2b** confirms the pentahapticity and the uncoordinated exocyclic double bond in the η^5–cyclohexadienyl ligand. Comparison of the structure of **2b** with the published structures of **2** [10] and **3** [14c–d] reveals the electronic and steric effects which other ligands on the metal induce in the geometry of the η^5–benzyl ligand. Phosphine substitution for a carbonyl on the manganese increases the electron density at the exocyclic methylene, enhancing its nucleophilicity. This is illustrated by comparison of pseudo-first-order rate constants for the reaction of **2a–e** with CH_3I. The observed oxidation po..ntials also reflect both the reactivity of the exocyclic methylene and the electron density associated with the various phosphine ligands (alkyl > aryl > alkoxy > aryloxy). In the ^1H NMR spectra, coupling of the phosphorus atom to the methylene protons of **2a–b** is observed and the magnitude of this coupling supports arguments for direct interactions between the manganese d_{xy} orbital and the exocyclic methylene. The phosphine derivatives undergo similar nucleophilic and radical reactions to those observed for **2**. Nucleophilic reactions of the exocyclic methylene with electrophiles are observed which form C–C bonds with CH_3I and PhC(O)Cl and C–I bonds with I_2. [(η^6–$C_6Me_5CH_2Mn(CO)_5$)$Mn(CO)_2PMe_3$][PF_6] is formed from the reaction of **2b** with $Mn(CO)_5Br$. (η^5–C_5H_5)$Fe(CO)_2I$ and **2b** react to form [(η^6–$C_6Me_5CH_2FeCp(CO)_2$)$Mn(CO)_2PMe_3$]I. As well, the η^5–benzyls undergo conversion to *endo*–(η^5–C_6Me_6H)$Mn(CO)_2PR_3$ using two equiv of Bu_3SnH, but not by catalytic hydrogenation. The η^5–benzyls can also react by a radical pathway with the

halocarbons CCl_4, $CDCl_3$, and $CHBr_3$, to form new C–C bonds at the exocyclic methylene. Additional support for the radical mechanism in reactions with halocarbons was provided by the presence of a single manganese-centered radical species observed in ESR studies of **2**, **2a**, and **2b** with CCl_4 and $CDCl_3$.

A slightly different chemistry is observed for (η^5–pentamethylbenzyl)manganese dicarbonyl cyanide derivatives.[39] The absence of similar radical intermediates with the cyanide derivatives supports ligand dissociation as an integral part of the initiation process of reactions of **2a–e** with halocarbons.

CHAPTER III

THE FORMATION OF BENZYNE AND FREE CARBENES FROM COORDINATED PHOSPHITE ESTER LIGANDS IN $(\eta^5\text{-}C_6Me_5CH_2)Mn(CO)_2PR_3$ (R = OEt, OMe, OPh).

Introduction

We have found that benzyne and carbenes are formed spontaneously from (η^5-pentamethylcyclohexadienyl-*exo*-ene)manganese dicarbonyl phosphite complexes in solid-state reactions. These reactions are of interest because benzyne and carbenes can play an important role in organic syntheses.[53]

Free carbene ligands generated in solution usually have a singlet ground state.[54] However, gas phase generated carbenes can be a mixture of singlet and triplet states; some relative energies of these states for various free carbenes have been reported.[55] The methylene singlet and triplet state energy difference is ca. 0.5 eV[54b] and its heat of formation is ~385 kJ.[54a] Methylene reacts with olefins to form cyclopropanes.[53] The isomerization of cyclopropane to propene requires 276 kJ, and only 272 kJ is required for the geometrical isomerization of cyclopropanes.[54a] The energies of isomerization are low enough that reaction conditions can preclude an absolute assignment of a single or triplet state to a gas phase carbene.

The electronic state of carbene determines the geometry of products formed in their reaction with alkenes. A triplet state permits free rotation in the transition state, while a singlet state results in retention of configuration of the alkene. Free gas phase carbenes usually have a triplet ground state with a low-lying singlet excited state and

generally exhibit nucleophilic behavior.[56] The nucleophilicity can be increased by alkyl-substitution on the methylene to form alkylidenes, which are more likely to be nucleophilic. The excited triplet state is lowered in energy by alkyl substitution. Substitution of electron-deficient groups on the methylene can make the carbene electrophilic.

We have previously reported the synthesis, reactivity, and characterization of $(\eta^5\text{-}C_6Me_5CH_2)Mn(CO)_2PR_3$ (**2a–e**) complexes, eq 11.[16] These complexes are formed

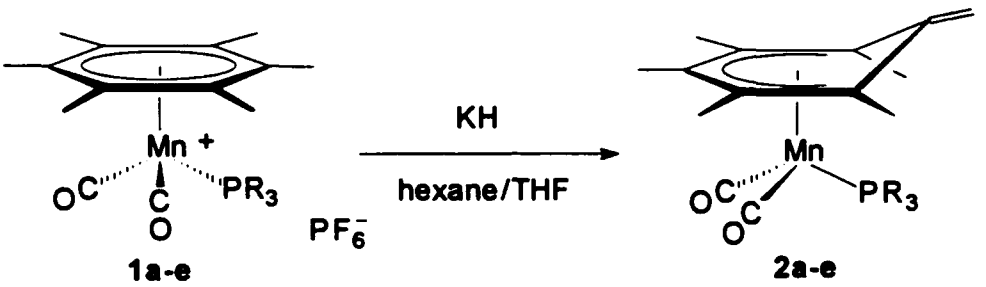

(11)

using KH as a base in a 9:1 hexane/THF solution to deprotonate a methyl group of the coordinated arene ligand of the cationic $[(\eta^6\text{-}C_6Me_6)Mn(CO)_2P(OR)_3][PF_6]$ (**1d**, **1e**) complexes. During the course of our experiments, a sample of $(\eta^5\text{-}C_6Me_5CH_2)Mn(CO)_2P(OPh)_3$ (**2e**) was found to decompose in a solid-state reaction, while stored under vacuum, to form $(\eta^6\text{-}C_6Me_6)Mn(CO)_2P(O)(OPh)_2$ (**26d**). Further investigation led to the discovery that benzyne was formed in this reaction.

The exocyclic methylene on the metal-coordinated pentahapto–cyclohexadienyl–*exo*–ene ligand, "η^5–pentamethylbenzyl", is thought to abstract a proton from a phenyl group on the coordinated phosphite producing a benzyne and the coordinated diphenyl phosphonate. We report here the studies on the coordinated triethyl-, trimethyl-, and triphenylphosphite complexes that proceeded from this observation.

The preparation and decompositions of $(\eta^5\text{-}C_6Me_5CH_2)Mn(CO)_2P(OR)_3$

(R = Et (**24a**), $-CD_3$ (**24b**), $-C_6D_5$ (**24c**)) complexes are reported in this chapter. It will be shown that the coordinated phosphite ligand forms an Arbuzov-like product, a coordinated disubstituted phosphonate ligand, and a proton is transferred from an alkyl or aryl group on the phosphite to the exocyclic methylene. This generates either a benzyne, methylene carbene, or alkylidene. In Chapter II, we argued that the enhanced nucleophilicity at the exocyclic methylene may arise by electronic transmission through the manganese d_{xy} orbital rather than through the π-carbocyclic system. This was supported by molecular orbital treatments developed by Hoffmann,[43b] Connelly,[44] and Astruc.[45] The manganese d_{xy} orbital could stabilize the transition state and allow greater negative potential to localize at the exocyclic methylene: thereby, increasing its nucleophilicity. Decreased reaction times and larger rate constants for the nucleophilic reactions for the (η^5-benzyl)manganese complexes with the stronger σ-donating phosphine ligands. Electronic transmission through the d_{xy} orbital is supported by the observed ^1H-^{31}P coupling for the exocyclic methylene in a number of ^1H NMR spectra of phosphine-substituted η^5-benzyl complexes (**2a-b**, **24a**) that cannot reasonably be attributed to transmission through five bonds, Figure 10.

Experimental

Preparation of Mono-substituted Phosphite Cationic Complexes

$[(\eta^6$-$C_6Me_6)Mn(CO)_2P(OEt)_3][PF_6]$ (21a). Compound **1** (850 mg, 1.90 mmol) and $P(OEt)_3$ (349 mg, 2.10 mmol) are used in the procedure outlined in Chapter I, p 13, to obtain the bright yellow product, **21a** in a yield of 494 mg (59%). Carbonyl stretching frequencies from the solution IR spectra of **21a-c** are listed in Table 38. The $^{31}P\{^1H\}$ NMR spectral results for **21a-c** are tabulated in Table 39. The ^1H and ^2H NMR spectra of **21a-c** are listed in Table 40.

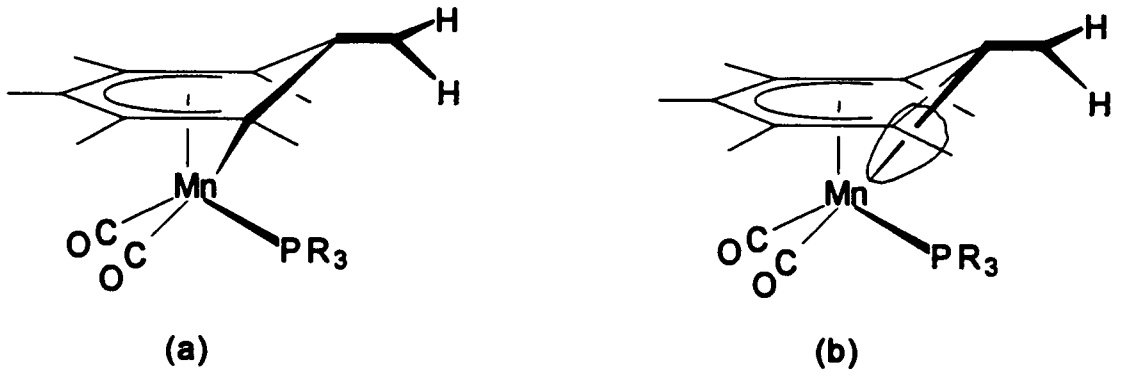

Figure 10. Proposed paths for ^{1}H–^{31}P coupling through (a) the π-carbocyclic system and (b) the manganese d_{xy} orbital to the exocyclic methylene protons

The $^{13}C\{^{1}H\}$ NMR spectral results of **21a–c** are provided in Table 41. Results from the HRFAB–MS analyses of **21a–c** are listed in Table 42.

$[(\eta^6\text{–}C_6Me_6)Mn(CO)_2P(OCD_3)_3][PF_6]$ (21b). Compound 1 (650 mg, 1.46 mmol) and $P(OCD_3)_3$ (286 mg, 2.15 mmol) are used in the procedure outlined in Chapter I, p 13, to obtain the bright yellow product, **21a**, in a yield of 302 mg (51%).

$[(\eta^6\text{–}C_6Me_6)Mn(CO)_2P(OC_6D_5)_3][PF_6]$ (21c). Compound 1 (700 mg, 1.57 mmol) and $P(OC_6D_5)_3$ (498 mg, 1.53 mmol) are used in the procedure outlined in Chapter I, p 13, to obtain the bright yellow product, **21a**, in a yield of 655 mg (58%).

Synthesis of Starting Materials for Cross-over Experiment

$[(\eta^6\text{–}C_6H_5Me)Mn(CO)_3][PF_6]$ (22a). Toluene (5 mL, 47 mmol) was substituted for hexamethylbenzene in the procedure outlined in Chapter I, p 12, to obtain **22a** as a pale yellow powder in a yield of 735 mg (43%). Carbonyl stretching frequencies from the solution IR spectra of **22a** and **22b** are listed in Table 38.

Table 38. IR Spectral Data for **21a–23b**

compd no.	arene	L	IR ν_{CO}, cm^{-1}
21a	HMB	$P(OEt)_3$	1988, 1938 [a]
21b	HMB	$P(OCD_3)_3$	1990, 1941 [a]
21c	HMB	$P(OC_6D_5)_3$	1996, 1947 [a]
22a	toluene	CO	2078, 2020 [b]
22b	d_8-toluene	CO	2078, 2020 [b]
23a	toluene	$P(OC_6H_5)_3$	2018, 1973 [a] 2021, 1977 [b]
23b	d_8-toluene	$P(OC_6D_5)_3$	2002, 1956 [b]

[a] Solution spectra obtained in THF.

[b] Solution spectra obtained in acetone.

The ^1H and ^2H NMR spectral results for **22a** and **22b** are listed in Table 40. The $^{13}C\{^1H\}$ NMR spectral results for **22a** and **22b** are listed in Table 41. The parent ion of **22a**, $C_{10}H_8O_3Mn$ (m/z = 231) was found in the low resolution FAB–MS analysis.

$[(\eta^6\text{–}C_6D_5CD_3)Mn(CO)_3][PF_6]$ (22b). d_8–Toluene (5 mL, 47 mmol) was substituted for hexamethylbenzene in the preparation described for **1** in Chapter I, p 12. A very pale yellow powder, **22b**, was obtained in a yield of 585 mg (43%). The result of the HRFAB–MS analysis of **22b** is listed in Table 42.

Table 39. $^{31}P\{^1H\}$ NMR Spectral Data for **21a–23b**

compd no.	arene	L	$^{31}P\{^1H\}$ NMR δ, ppm [a]	
21a	HMB	$P(OEt)_3$	174.4	(s, $P(OEt)_3$)
			−142.7	(sp, PF_6^-, J_{P-F} = 708.0 Hz)
21b	HMB	$P(OCD_3)_3$	181.8	(s, $P(OMe)_3$)
			−142.7	(sp, PF_6^-, J_{P-F} = 707.2 Hz)
21c	HMB	$P(OC_6D_5)_3$	172.8	(s, $P(OPh)_3$)
			−142.0	(sp, PF_6^-, J_{P-F} = 706.9 Hz)
23a	toluene	$P(OC_6H_5)_3$	172.8	(s, $P(OPh)_3$)
			−142.0	(sp, PF_6^-, J_{P-F} = 706.9 Hz)
23b	d_8-toluene	$P(OC_6D_5)_3$	172.3	(s, $P(OPh)_3$)
			−142.8	(sp, PF_6^-, J_{P-F} = 707.2 Hz)

[a] Spectra were obtained in d_6-acetone at 298 K and externally referenced to H_3PO_4 (85%).

[c] Solution spectra were obtained in THF.

[d] Solution spectra were obtained in hexane.

[(η^6-C_6H_5Me)Mn(CO)$_2$P(OPh)$_3$][PF_6] (23a). Using the procedure outlined in Chapter I, p 13, and substituting **22a** (500 mg, 2.16 mmol) and $P(OPh)_3$ (700 μL, 2.68 mmol) a yellow powder, **23a**, was obtained in a yield of 318 mg (28%). The solution carbonyl stretching frequencies of **23a** and **23b** are listed in Table 38. Results from the $^{31}P\{^1H\}$ NMR spectra of **23a** and **23b** are listed in Table 39. The ^1H and ^2H NMR spectral results for **23a** and **23b** are listed in Table 40. The $^{13}C\{^1H\}$ NMR spectral results for **23a** and **23b** are listed in Table 41. The parent ion of **23a**, $C_{27}H_{23}O_5PMn$ (m/z = 513) was found in the low resolution FAB–MS analysis.

Table 40. ^1H and ^2H NMR Spectral Data for **21a–23b**

compd no.	arene	L	^1H NMR [a]/^2H NMR δ, ppm [b]	
21a	HMB	$P(OEt)_3$	4.19	(d·q, 6 H, $P(OCH_2-)$, $^2J_{P-H} = {}^3J_{H-H}$ = 6.9 Hz, 6.9 Hz)
			2.44	(s, 18 H, ring–CH_3)
			1.37	(t, 9 H, $P(-CH_3)$, $^3J_{H-H}$ = 7.0 Hz)
21b	HMB	$P(OCD_3)_3$	2.44	(s, 18 H, ring–CH_3)
			4.09 [c]	(s, 9 D, $P(OCD_3)$, $^3J_{P-D}$ = 1.5 Hz)
21c	HMB	$P(OC_6D_5)_3$	2.47	(s, 18 H, ring–CH_3)
			7.78–7.24 [c]	(m, 15 D, $P(OC_6D_5)$)
22a	toluene	CO	6.98–6.64	(m, 5 H, ring–CH)
			2.47	(s, 3 H, ring–CH_3)
22b	d_8-toluene	CO	7.00–6.60 [d]	(m, 5 D, ring–CD)
			2.47 [d]	(s, 3 D, ring–CD_3)
23a	toluene	$P(OC_6H_5)_3$	7.55–7.19	(m, 15 D, $P(OC_6H_5)$)
			6.43–5.63	(m, 5 H, ring–CH)
			2.30	(s, 18 H, $-CH_3$)
23b	d_8-toluene	$P(OC_6D_5)_3$	7.78–7.24 [d]	(m, 15 D, $P(OC_6D_5)$)
			6.98–6.64 [d]	(m, 5 D, ring–CD)
			2.47 [d]	(s, 18 H, $-CD_3$)

[a] Obtained in d_6-acetone at 298 K.

[b] (multiplicity, no. of protons, assignment, coupling).

[c] Obtained in THF at 298 K.

[d] Obtained in acetone at 298 K.

Table 41. $^{13}C\{^1H\}$ NMR Spectral Data for **21a–23b**

	arene	$^{13}C\{^1H\}$ NMR [a]	
compd no.	L	δ, ppm [b]	
21a	HMB	224.21	(d, CO, $^2J_{P-C}$ = 45.6 Hz)
	$P(OEt)_3$	111.49	(s, ring–C)
		64.56	(d, $P(OCH_2-)$, J_{H-H} = 9.3 Hz)
		17.16	(s, ring–CH_3)
		16.15	(d, $P(-CH_3)$, J_{H-H} = 6.7 Hz)
21b	HMB	223.9	(d, CO, $^2J_{P-C}$ = 45.9 Hz)
	$P(OCD_3)_3$	111.62	(s, ring–C)
		54.10	(d·sp, $-CD_3$, $^2J_{P-C}$ = 14.5 Hz, J_{C-D} = 8.2 Hz)
		17.13	(s, ring–CH_3)
21c	HMB	228.6	(s, CO)
	$P(OC_6D_5)_3$	151.81, 130.69, 126.58, 120.94	(s, $P(OC_6H_5)$)
		112.59	(s, ring–C)
		17.40	(s, ring–CH_3)
22a	toluene	226.2	(s, CO)
	CO	121.72, 103.65, 101.07, 98.32	(s, ring–C)
		20.40	(s, ring–CH_3)
22b	d_8-toluene	228	(s, CO)
	CO	121, 103, 101, 98	(s, ring–C)
		17	(s, ring–CH_3)
23a	toluene	220.10	(d, CO, J_{C-P} = 41 Hz)
	$P(OC_6H_5)_3$	151.17	(d, $P(OC_6H_5)$, J_{C-P} = 9 Hz)
		131.21, 126.97 120.50	(s, $P(OC_6H_5)$)
		121.26, 101.20, 97.76	(s, ring–C)
		19.87	(s, ring–CH_3)

Table 41 — continued

compd no.	arene L	$^{13}C\{^1H\}$ NMR [a] δ, ppm [b]	
23b	d_8-toluene	221.8	(d, CO, J_{C-P} = 54 Hz)
	$P(OC_6D_5)_3$	157.88	(s, $P(OC_6D_5)$ and ring–C)
		129.55, 119.46, 115.45	(t, $P(OC_6D_5)$ and ring–C, J_{C-D} = 24 Hz)
		20.0	(m, ring–CD_3)

[a] Obtained in d_6–acetone at 298 K.

[b] (mult, assignment, coupling).

Table 42. HREI-MS Data for **21a–c** and **22b**

compd no.	chemical formula	MW_{calc}	M^+_{exp}, *m/z*	Δ*m*, mmu
21a	$C_{20}H_{33}O_5P_1Mn_1$	439.1446	439.1452	+1.4
21b	$C_{17}H_{18}D_9O_5P_1Mn_1$	406.1541	406.1555	+1.4
21c	$C_{32}H_{18}D_{15}O_5P_1Mn_1$	598.2388	598.2398	+1.0
22b	$C_{10}D_8O_3Mn_1$	239.0356	239.0372	+1.6

$[(\eta^6\text{-}C_6D_5CD_3)Mn(CO)_2P(OC_6D_5)_3][PF_6]$ (23b). Using the procedure outlined in Chapter I, p 13, and substituting **22b** (500 mg, 2.09 mmol) and $P(OC_6D_5)_3$ (700 mg, 2.15 μmol) a yellow solid, **23b**, was obtained in a yield of 255 mg (22%). The parent ion of **23b**, $C_{27}D_{23}O_5PMn$ (m/z = 536) was found in the low resolution FAB-MS analysis.

Deprotonation of Mono-substituted Phosphite Complexes

$(\eta^5\text{-}C_6Me_5CH_2)Mn(CO)_2P(OEt)_3$ (24a). Using procedure *a* for the synthesis of **2b** from Chapter II, p 24, **21a** (189 mg, 431 μmol) produced yellow-orange crystals of **24a**. After **24a** was purified by repeated extraction with hexane (3 times), a yield of 182 mg (97%) was obtained. IR carbonyl stretching frequencies and $^{31}P\{^1H\}$ NMR spectroscopic results from **24a-c** are listed in Table 43. ^1H NMR spectral results from **24a** are listed in Table 44. $^{13}C\{^1H\}$ NMR spectral results from **24a-c** are listed in Table 45. Results from the HREI-MS analyses of **24a-c** are listed in Table 46.

$(\eta^5\text{-}C_6Me_5CH_2)Mn(CO)_2P(OCD_3)_3$ (24b). Using the procedure for **24a** (*vide supra*) and substituting **21a** (150 mg, 369 μmol), **24b** was isolated as orange crystals in a yield of 145 mg (97%). ^1H and ^2H NMR spectral results for **24b** and **24c** are listed in Table 44.

$(\eta^5\text{-}C_6Me_5CH_2)Mn(CO)_2P(OC_6D_5)_3$ (24c). Using the procedure for **24a** (*vide supra*) and substituting **21c** (156 mg, 260 μmol), **24c** was isolated as orange crystals in a yield of 143 mg (92%).

Table 43. $^{31}P\{^{1}H\}$ NMR and IR Spectral Data for **24a–25b**

	benzyl	$^{31}P\{^{1}H\}$ NMR	IR
compd no.	L	δ, ppm [a]	ν_{CO}, cm^{-1}
24a	$C_6Me_5(CH_2)$	191.4	1946, 1883 [b]
	$P(OEt)_3$		1937, 1875 [c]
24b	$C_6Me_5(CH_2)$	197.1	1948, 1885 [b]
	$P(OCD_3)_3$		1939, 1877 [c]
24c	$C_6Me_5(CH_2)$	170.4	1955, 1893 [b]
	$P(OC_6D_5)_3$		1964, 1899 [c]

[a] Spectra were obtained in d_6-benzene at 298 K and externally referenced to H_3PO_4 (85%). All peaks appeared as singlets.

[b] Solution spectra obtained in THF.

[c] Solution spectra obtained in hexane.

Reactions of Phosphite Derivatives

Compounds **2d–e** and **24a–c** (~300 mg, 502–757 μmol) were kept at room temperature either under vacuum or under ~1 atm of an olefin for 4–42 days, after which IR and NMR spectroscopic analyses indicated an Arbuzov-like product, a dialkyl or diaryl phosphonate derivative, formed. Spectral characterization of the phosphonate complexes follow.

Table 44. ^1H and ^2H NMR Spectral Data for **24a–c**

compd no.	L	^1H NMR [a] / ^2H NMR [b] δ, ppm [c]	
24a	$P(OEt)_3$	3.97	(d, 2 H, $=CH_2$, $^2J_{P-H}$ = 1.1 Hz)
		3.79	(q, 6 H, $P(OCH_2-)$, $^3J_{H-H}$ = 6.9 Hz)
		2.06	(d, 6 H, $-CH_3$, $^2J_{H-H}$ = 0.8 Hz)
		1.90	(s, 6 H, $-CH_3$)
		1.88	(d, 6 H, $-CH_3$, $^2J_{H-H}$ = 1.1 Hz)
		1.02	(t, 9 H, $P(-CH_3)$, $^3J_{H-H}$ = 7.1 Hz)
24b	$P(OCD_3)_3$	3.96	(s, 2 H, $=CH_2$)
		3.30 [b]	(d, 9 D, $P(OCD_3)$, $^3J_{P-D}$ = 1.5 Hz)
		2.00	(s, 6 H, $-CH_3$)
		1.87	(s, 6 H, $-CH_3$)
		1.83	(s, 3 H, $-CH_3$)
24c	$P(OC_6D_3)_3$	7.9–7.2 [b]	(m, 15 D, $P(OC_6D_5)$)
		3.95	(s, 2 H, $=CH_2$)
		1.84	(s, 6 H, $-CH_3$)
		1.79	(s, 6 H, $-CH_3$)
		1.75	(s, 3 H, $-CH_3$)

[a] Obtained in d_6–benzene at 298 K.

[b] Obtained in THF at 298 K.

[c] (multiplicity, no. of protons, assignment, coupling).

Table 45. $^{13}C\{^1H\}$ NMR Spectral Data for **24a–c**

		$^{13}C\{^1H\}$ NMR [a]	
compd no.	L	δ, ppm [b]	
24a	$P(OEt)_3$	229.82	(d, CO, $^2J_{P-C}$ = 33.4 Hz)
		147.54	(s, $\underline{C}=CH_2$)
		106.89, 85.56, 81.11	(s, ring–C)
		76.54	(s, $=CH_2$)
		60.26	(d, $P(OCH_2-)$, $^2J_{P-C}$ = 6.0 Hz)
		17.73, 16.67, 15.46	(s, ring–CH_3)
		16.16	(d, $P(-CH_3)$, $^2J_{P-C}$ = 6.0 Hz)
24b	$P(OCD_3)_3$	229.5	(d, CO, $^2J_{P-C}$ = 35.8 Hz)
		147.43	(s, $\underline{C}=CH_2$)
		106.95, 85.61	(s, ring–C)
		81.25	(d, ring–C, J_{C-D} = 3.1 Hz)
		76.72	(s, $=CH_2$)
		50.40	(d-sp, $-OCD_3$, $^2J_{P-C}$ = 14.8 Hz, J_{D-C} = 4.8 Hz)
		17.81, 16.58, 15.48	(s, ring–CH_3)
24c	$P(OC_6D_5)_3$	227.7	(s, CO)
		147.12	(s, $\underline{C}=CH_2$)
		152.40, 129.60, 127.26, 124.31, 121.26	(s, $P(OC_6H_5)$)
		107.49, 82.75	(s, ring–C)
		77.35	(s, $=CH_2$)
		17.69, 16.76, 16.05, 15.28	(s, ring–CH_3)

[a] Obtained in d_6–benzene at 298 K.

[b] (mult, assignment, coupling).

Table 46. HREI-MS Data for **24a–c**

compd no.	chemical formula	MW_{calc}	M^+_{exp}, *m/z*	Δm, mmu
24a	$C_{20}H_{32}O_5P_1Mn_1$	438.1368	438.1356	−1.2
24b	$C_{17}H_{17}D_9O_5P_1Mn_1$	405.1463	405.1435	−1.8
24c	$C_{32}H_{17}D_{15}O_2P_1Mn_1$	597.2309	597.2289	−2.0

(η^6-C_6Me_5R)Mn(CO)$_2$P(O)(OR′)$_2$ (R = Me, R′ = Et (26a); R = R′ = Me (26b); R = CH_2D, R′ = CD_3 (26c); R = Me, R′= Ph (26d); R = CH_2D, R′ = C_6D_5 (26e)). IR carbonyl stretching frequencies and $^{31}P\{^1H\}$ NMR spectroscopic results for **26a–e** are listed in Table 47. ^1H and ^2H NMR spectral results for **26a–e** are listed in Table 48. $^{13}C\{^1H\}$ NMR spectral results for **26a–e** are listed in Table 49. Results from the HREI-MS analyses of **26a–e** are listed in Table 50.

(*a*) ***26a***. Compound **26a** was not isolated from **24a** held in vacuum for 28 days. An areneless decomposition product typical of manganese phosphine complexes was formed as determined by IR spectroscopy. The ^1H NMR spectrum revealed only free hexamethylbenzene and triethylphosphite. However, **26a** was isolated from the composition mixture of **24a** after heating to 70 °C for 96 h with 101 kPa of propene (~1 atm), by first extracting with hexane to remove the areneless decomposition product and free hexamethylbenzene, followed by extracting **26a** with diethyl ether. Although conversion to **26a**, using the carbonyl bands in the IR spectrum, was ~25%; however, only 15 mg (5%) of a yellow solid was isolated.

Table 47. $^{31}P\{^{1}H\}$ NMR and IR Spectral Data for **26a–e**

			$^{31}P\{^{1}H\}$ NMR	IR
compd no.	R	R′	δ, ppm [a]	ν_{CO}, cm^{-1}
26a	Et	Me	134.23	1965, 1917 [c]
26b	Me	Me	133.80	1963, 1914 [c]
26c	$-CD_3$	$-CH_2D$	134.1	1963, 1914 [c]
26d	Ph	Me	142.09 [d]	1970, 1923 [c]
26e	$-C_6D_5$	$-CH_2D$	144.2	1971, 1923 [c]

[a] Spectra were obtained in d_6-acetone at 298 K and externally referenced to H_3PO_4 (85%). Peaks are assigned to $P(O)(OR)_2$ and appear as singlets unless otherwise noted.

[c] Solution spectra obtained in THF.

[d] Peak observed as a doublet with J_{P-C} = 60 Hz.

(*b*) ***26b***. After 14 days in laboratory light under static vacuum, ~48% of **2b** was converted to **26b** as evidenced by the IR carbonyl bands. After 36 days, ~89% of **2b** was converted to **26b** and the experiment was terminated. Purification required multiple extractions with THF, diethyl ether, and hexane, 24 mg (8%) of yellow powder was recovered.

(*c*) ***26c***. After 45 days in laboratory light under static vacuum, ~63% of **24b** was converted to **26c** as evidenced by the IR carbonyl bands. Hexane was used to extract unreacted **24b** from the reaction mixture. Purification required multiple extractions with THF, diethyl ether, and hexane, 19 mg (10%) of yellow powder was isolated.

Table 48. ^1H and ^2H NMR Spectral Data for **26a–e**

			^1H and ^2H NMR	
compd no.	R	R′	δ, ppm [a,b]	
26a	Et	Me	3.79	(m, 4 H, $P(OCH_2-)$)
			2.26	(s, 18 H, $-CH_3$)
			1.02	(t, 6 H, $P(-CH_3)$, $^3J_{H-H}$ = 7 Hz)
26b	Me	Me	3.55	(s, 6 H, $P(OCH_3)$)
			1.60	(s, 18 H, $-CH_3$)
26c	$-CD_3$	$-CH_2D$	4.09 [c]	(s, 6 D, $P(OCD_3)$)
			2.35 [c]	(m, 1 D, $-CDH_2$)
			2.36	(m, 17 H, $-CDH_2$ and $-CH_3$)
26d	Ph	Me	7.20–6.76	(m, 10 H, $P(OC_6H_5)$)
			2.38	(s, 18 H, $-CH_3$)
26e	$-C_6D_5$	$-CH_2D$	7.26–6.75 [d]	(m, 10 D, $P(OC_6D_5)$)
			2.34 [d]	(m, 1 D, $-CDH_2$)
			2.38	(m, 17 H, $-CDH_2$ and $-CH_3$)

[a] (multiplicity, no. of protons, assignment, coupling).

[b] Obtained in d_6-acetone at 298 K unless otherwise noted.

[c] Obtained in acetone at 298 K.

[d] Obtained in THF at 298 K.

(*d*) ***26d***. After 4 days under dynamic vacuum, 100 mg (μmol) **2e** was completely converted to **26d**. Subsequently, after 30 days in laboratory light under static vacuum, ~65% of **2e** was converted to **26d** as evidenced by the IR carbonyl bands. The product was absorbed on SiO_2 and unreacted **2e** was eluted with hexane–acetone.

Table 49. $^{13}C\{^1H\}$ NMR Spectral Data for **26a–e**

			$^{13}C\{^1H\}$ NMR	
compd no.	R	R′	δ, ppm [a,b]	
26a	Et	Me	229.82	(d, CO, $^2J_{P-C}$ = 33.4 Hz)
			106.89	(s, ring–C)
			60.26	(d, $P(OCH_2-)$, $^2J_{P-C}$ = 6.0 Hz)
			17.73	(s, ring–CH_3)
			16.16	(d, $P(-CH_3)$, $^2J_{P-C}$ = 6.0 Hz)
26b	Me	Me	229.5 [c]	(d, CO, $^2J_{P-C}$ = 35.8 Hz)
			106.95 [c]	(s, ring–C)
			50.40	(m, $P(OCH_3)$)
			16.58 [c]	(s, ring–CH_3)
26c	$-CD_3$	$-CH_2D$	229.5	(s, CO)
			106.95	(s, ring–C)
			50.40	(m, $P(OCD_3)$)
			17.81, 16.58	(s, ring–CH_3)
26d	Ph	Me	226.06	(d, CO, $^2J_{P-C}$ = 47 Hz)
			153.82, 129.78, 123.32, 121.92	(s, $P(OC_6H_5)$)
			109.25	(s, ring–C)
			16.82	(s, ring–CH_3)
26e	$-C_6D_5$	$-CH_2D$	227.7	(s, CO)
			152.40, 129.60, 124.31, 121.26	(s, $P(OC_6D_5)$)
			107.49	(s, ring–C)
			17.69, 16.76	(s, ring–CH_3)

[a] $(\eta^5-C_6Me_5R')Mn(CO)_2P(O)(OR)_2$

[b] (mult, assignment, coupling).

[c] Obtained in d_6–acetone at 298 K unless otherwise noted.

Table 50. HREI-MS Data for **26a–e**

compd no.	chemical formula	MW_{calc}	M^+_{exp}, *m/z*	Δm, mmu
26a	$C_{18}H_{28}O_5P_1Mn_1$	410.1055	410.1043	−1.2
26b	$C_{16}H_{24}O_5P_1Mn_1$	382.0741	382.0730	−1.1
26c [a]	$C_{14}H_{17}D_7O_3P_1Mn_1$	333.1283	333.1241	−4.2
26d	$C_{26}H_{28}O_5P_1Mn_1$	506.1055	506.1087	+3.2
26e [a]	$C_{24}H_{17}D_{11}O_3P_1Mn_1$	461.1847	461.1802	−4.5

[a] Parent ion − 2 CO.

Compound **26d** was eluted with acetone and methanol and yielded 72 mg (33%) of yellow powder. Much of the phosphonate compound could not be desorbed from the silica support.

(*e*) ***26e***. After 30 days in laboratory light under static vacuum, ~63% of **24c** was converted to **26e** as evidenced by the IR carbonyl bands. The product was absorbed on SiO_2 and unreacted **2e** was eluted with hexane–acetone. Compound **26d** was eluted with acetone and methanol and yielded 30 mg (15%) of yellow powder. The much of the phosphonate compound could not be desorbed from the silica support.

(η^5-$C_6Me_5CH_2$)Mn(CO)$_2$P(OEt)$_3$ (24a). (*a*) *In vacuum*. Compound **24a** undergoes a small amount of decomposition to form ethylidene and the diethyl phosphonate complex. High resolution peak matching MS experiments found a peak (*m/z* = 28.03130 amu) that can be assigned to ethene (C_2H_4) and a peak (*m/z* = 56.06260 amu) that can be assigned to either 2-butene or methylcyclopropane. 2-Butene would result from two ethylidenes dimerizing, while methylcyclopropane could result from an ethylidene reacting with ethene which is a product of ethylidene

rearrangement. 1,1,1- trimethylcyclopropane, the product of ethylidene reacting with the 2-butene formed, was not observed.

(*b*) *With propene.* No peaks were observed that could be assigned as were in (*a*) and no peak for 1,2-dimethylcyclopropane was found.

(η^5-$C_6Me_5CH_2$)$Mn(CO)_2P(OMe)_3$ (2d/24b). (*a*) *In vacuum.* With **2d** and **24b**, the exocyclic methylene abstracts a proton from the methyl group of the trimethylphosphite ligand to form **26b** and **26c**, respectively.

(*b*) *With 2,3-dimethyl-2-butene.* 2,3-dimethyl-2-butene was added to **2d** and stored under laboratory light and nitrogen atmosphere and at room temperature (21-23 °C) for 4 weeks. High resolution peak matching MS analysis revealed a peak (*m/z* = 98.10955 amu) that can be assigned to 1,1,2,2-tetramethylcyclopropane. A GC/MS experiment confirms the cyclopropane formation by matching the fragmentation pattern with the standard spectrum.

(*c*) *With cis-2-butene.* Compound **24b** was combined with *cis*-2-butene and stored under laboratory light and at room temperature (21-23 °C) for 4 weeks. Peak matching MS analysis displayed a peak (*m/z* = 72.09080 amu) that can be assigned to 1,2-dimethyl-3,3-d_2-cyclopropane. The ^{1}H NMR spectrum was compared to the standard spectrum of 1,2-dimethylcyclopropane, confirming the cyclopropane formation with peaks at δ 1.29 (m, 6 H, $-CH_3$) and δ 0.88 (m, 2 H, >CH-).[57] The insufficient sample precluded ^{2}H NMR analysis. Compound **2d** was combined with *cis*-2-butene and stored under laboratory light and at room temperature (21-23 °C) for 7 days followed by 4 days at 78 °C. The reaction vessel after purging was heated to 90 °C to release trapped 1,2-dimethylcyclopropane from the decomposed **2d** and transferred to a J. Young NMR tube and dissolved in d_6-acetone for ^{1}H NMR analysis.

(η^5-$C_6Me_5CH_2$)Mn(CO)$_2$P(OPh)$_3$ (2e/24c). (*a*) *In vacuum.* Compounds **2e** and **24c** underwent an α-hydrogen elimination from a phenyl on the triphenylphosphite ligand to form **26d** and **26e**, respectively. HREI-MS analyses revealed a peak (*m/z* = 152.0656 amu, +3.0 mmu) assigned to diphenylene and a peak (*m/z* = 160.1126 amu, −0.2 mmu) assigned to d_8-diphenylene.

Calculation of Theoretical Intramolecular Distances in **2d** and **2e**

The distance between the hydrogen atom on the coordinated phosphite ligand and the exocyclic methylene carbon atom of the "benzyl" ligand may be a critical factor in the proposed decomposition of the coordinated phosphite ligand complexes. Using the bond distances and angles from the crystal structures of **2b** and **11d**, the distance between hydrogen atoms and the exocyclic methylene carbon atom was calculated. For the trimethylphosphite complex, **2d**, the C···H approach distance was calculated to be 1.1 (3) Å. For the triphenylphosphite complex, **2e**, the C···H approach distance was calculated to be 1.0 (4) Å. Both of these distances are within two atomic radii of a carbon atom which could increase the likelihood of the reaction being intramolecular.[58] These distances are based on the closest approach of the two atoms, and no calculations of the probability of the approach occurring is provided.

Results and Discussion

Synthesis and Characterization of **24a–c**

The deuterium labeled complexes, **23a–b** and **24a–b**, were synthesized to determine the source of the proton in the decomposition of the trimethyl- and triphenylphosphite complexes to dimethyl and diphenyl phosphonate complexes. Carbene formation with phenyl and methyl substituents on the phosphites suggests that

the formation of alkylidene from the decomposition of the triethylphosphite could occur. The syntheses of **24a–c** were carried out as described in Chapter 2.[16] Purity of the products, **24a–e**, was checked by observing the carbonyl bands in the IR solution spectra in hexane, which are distinct from those of the cationic starting materials and the η^5–cyclohexadienyls complexes. In the ^1H NMR spectra, **24a–c** each have three characteristic singlets for the inequivalent methyl groups in a 3:6:6 ratio between δ 1.75–2.06. The exocyclic methylene protons in **24b–c** occur as singlets (δ 3.96–3.95), and in **24a** occur as a doublet (δ 3.98) coupled to the phosphorus atom (J_{P-H} = 1.1 Hz). Compounds **24b** and **24c** have 99.95 and 98+ atom % deuterium incorporation in the phosphite ester ligands. In the ^2H NMR spectrum, the methyl deuteriums of the phosphite ester ligand on **24b** appear as doublets, split by phosphorus, at δ 3.24. ^2H NMR of **24c** produces a multiplet from δ 7.73–7.38 for the deuteriums on the triphenylphosphite ester ligand. In the ^1H NMR spectrum of **24a**, the triethylphosphite ester ligand produces a quartet at δ 3.79 for the methylenes adjacent to the phosphorus atom and a triplet at δ 0.89 for the terminal methyls. In each case, only one phosphorus resonance is observed in the $^{31}P\{^1H\}$ NMR spectra. In the $^{13}C\{^1H\}$ NMR spectra, a peak between δ 227.7–229.8 is observed for the CO carbon atoms. Appropriate resonances are observed for the coordinated ring carbon atoms (δ 107.5–81.1) and ring methyl carbon atoms (δ 17.8–15.3). The carbon atoms of the phosphine ligands occur at δ 60.3, 16.2 (**24a**), 50.4 (**24b**), and 152.4–127.3 (**24c**). The uncoordinated ring carbon atoms appear at δ 147.5 (**24a**), 147.4 (**24b**), and 147.1 (**24c**) and the exocyclic methylene carbon atom appears at δ 76.5 (**24a**), 76.7 (**24b**), and 77.4 (**24c**) and are based on assignments from known compounds with η^5–pentamethylbenzyl ligands. These ^1H and $^{13}C\{^1H\}$ NMR results agree with similar assignments for **2a–e**.[16] High resolution EI-MS provided the molecular formulas for compounds **24a–c**, which agree with their proposed structures and the incorporation of deuterium.

Conversion of Phosphites into Dialkyl- and Diaryl Phosphonates

The exocyclic methylene protons of the η^5–benzyl, are coupled to the phosphorus atom coordinated to the manganese. Transmission of the coupling through the filled d_{xy} orbital of the manganese overlapping with the empty p orbital of the uncoordinated ring-carbon atom provides a shorter path than the five bond path through the π-carbocyclic system, Figure 10. The shorter path is consistent with the electronic contribution to the exocyclic methylene apparent in nucleophilic reactions. Therefore, it is likely that the ^1H–^{31}P coupling is through the four-bond d_{xy} path rather than the five-bond-π-carbocyclic path in Figure 10.

Reactions of Triphenylphosphites. The decomposition of **24c** is depicted in Scheme V and is illustrative of the reaction of **2e**. In solution, the triphenylphosphite ligand is the least reactive of the phosphine ligands to an Arbuzov–like reaction that would form diphenyl phosphonate complexes under nucleophilic reaction conditions.[16,59] However, **2d** left under vacuum over a period of 4 days led to the serendipitous discovery of **26d**. Following the characterization of **26d**, **24c** was synthesized to confirm the suspected reaction mechanism.

The mechanism for **2e** converting to **26d** is thought to be by α-hydrogen abstraction from a phenyl on the triphenylphosphite. This could be explained by proton transfer to the exocyclic methylene, producing the diphenyl phosphonate ligand. The formation of **26d** is confirmed by characteristic resonances for η^6–coordinated hexamethylbenzene and the diphenyl phosphonate ligand in the ^1H and ^{31}P NMR spectra and HREI–MS analysis. Hydrogens on the phenyl groups that are α to the carbon bonded to the oxygen are acidic and undergo abstraction in many organic reactions.[60] To verify this, $P(OC_5D_6)_3$ was synthesized from PCl_3 and C_6D_5OD (98+ atom % D) and used to produce **24c**.[29,30]

Scheme V. Proposed decomposition pathway for $(\eta^5\text{-}C_6Me_5CH_2)Mn(CO)_2P(OC_6D_5)_3$

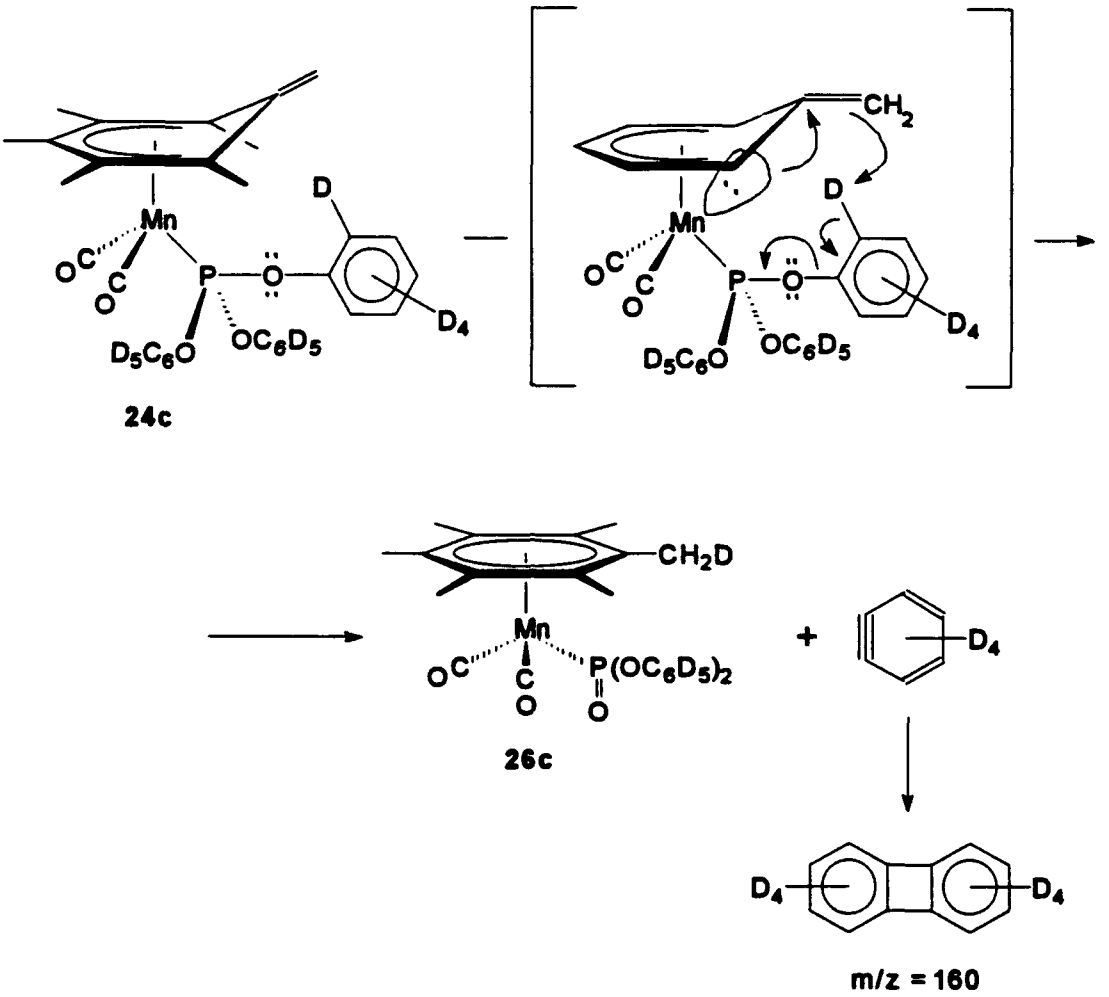

If the d_{15}–triphenylphosphite ester ligand of **24c** undergoes an α-deuterium abstraction to form the d_{10}–diphenyl phosphonate ligand in **26e**, the product easily can be identified by the ^1H, ^2H, and ^{31}P NMR spectra. In fact, after 4 weeks, **26e** has been formed and is identified by ^2H NMR resonances between δ 7.26–6.75 for the deuterated phenyls and a singlet at δ 2.34 in a 10:1 ratio indicative of the d_{10}–$P(O)(OPh)_2$ ligand and a $-CH_2D$ group on the arene. The ^1H NMR spectrum shows residual protons (< 1% H)

in the phenyl region and a broad multiplet at δ 2.38 for the two protons split by the deuterium with the singlet for the arene methyls superimposed on the multiplet. However, Brill and Landon point out that the most important diagnostic tool for the formation of the phosphonates is the chemical shift of the ^{31}P resonance.[59a] The chemical shift of the phosphonate ligands are 40–85 ppm more shielded than the phosphite ester ligands in analogous complexes. The ^{31}P resonances of both **26d** and **26e** are shifted ~28 ppm upfield from those of the triphenylphosphite ester ligands in **2e** and **24c**. The IR stretching frequency for P=O in the $(O)(OMe)_2^-$ ligand appears in the 1125–1200 cm^{-1} range. Brill and Landon state,[59a] "While this mode is diagnostic, its identity may be obscured by C–C and C–O modes." And indeed, examination of the IR spectrum in the 1125–1200 cm^{-1} region reveals several bands that could be attributed to any of these three modes. The molecular formulas of **26d** and **26e**, and the incorporation of eleven deuteriums in **26e**, are confirmed by the HREI-MS analyses. The byproducts of benzyne formation, diphenylene (*m/z* = 152) and d_8-diphenylene (*m/z* = 160), were also identified by the HREI-MS analyses.

Reactions of Trimethylphosphites. The decomposition of **24b** is depicted in Scheme VI and is illustrative of the reaction of **2d**. Trimethylphosphite in the presence of a nucleophile undergoes an Arbuzov-like reaction to form the dimethyl phosphonate.[38] We have reported several reactions of **2d** with electrophiles in solution that resulted in the formation of dimethyl phosphonate complexes.[16] However, in the solid state, under vacuum and exposed to laboratory light at 22 (3) °C, **2d** decomposed to **26b** over a period of 14–36 days. We are attributing this behavior to the nucleophilicity of the exocyclic methylene of the η^5-benzyl ligand. After **26b** was identified, **24b** was synthesized using $P(OCD_3)_3$ produced from PCl_3 and CD_3OD (99.95 atom % D) and used to produce **24c**.[30]

Scheme VI. Proposed decomposition pathway for $(\eta^5\text{-}C_6Me_5CH_2)Mn(CO)_2P(OCD_3)_3$

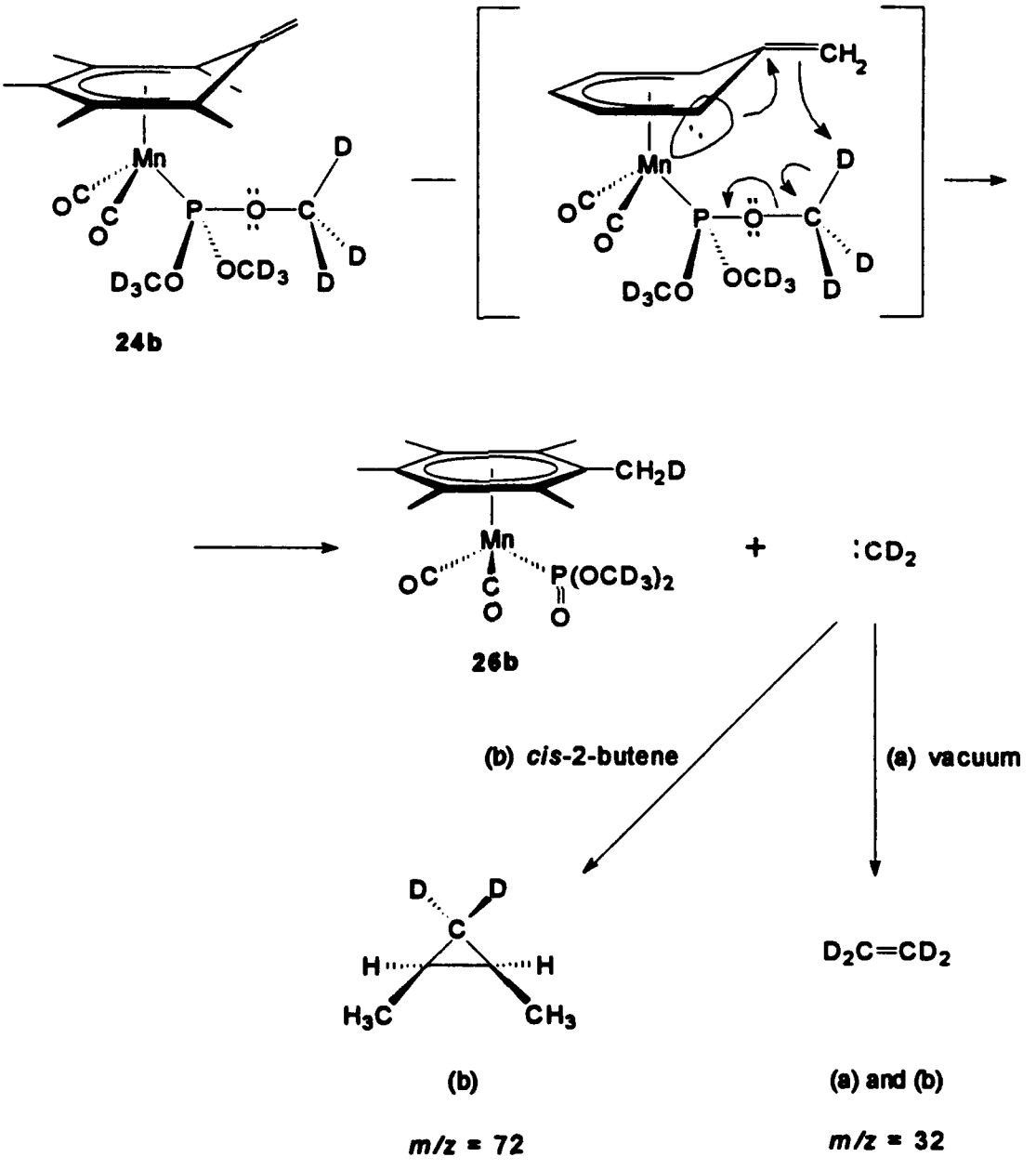

24b

26b

(b)

m/z = 72

(a) and (b)

m/z = 32

After 45 days, 63% of **24b** was converted to **26c**. The ^{1}H, ^{2}H, and ^{31}P NMR spectra provide the identification of the dimethyl phosphonate products, **26b** and **26c**, formed by the abstraction of hydrogen or deuterium from the phosphite ligand. The formation of **26b** is confirmed by characteristic resonances for η^6-coordinated hexamethylbenzene and the dimethyl phosphonate ligand in the ^{1}H and ^{31}P NMR spectra and HREI-MS analysis. The ^{2}H NMR spectrum of **26c** displays a singlet at δ 4.09 for the deuterated methyls and a singlet at δ 2.35 in a 6:1 ratio indicative of the d_6-P(O)(OMe)$_2$ ligand and a -CH_2D group on the arene. The ^{1}H NMR spectrum shows residual protons (< 0.1% H) in the dimethyl phosphonate region and a singlet superimposed on broad multiplet at δ 2.36 for the two protons split by the deuterium and the arene methyls. The ^{31}P resonances of both **26b** and **26c** are shifted 48-52 ppm upfield from the resonances of the corresponding trimethylphosphite ester ligands in **2d** and **24b**, which agree with the results of Brill and Landon.[59a] The IR spectrum in the 1125-1200 cm^{-1} region contains several bands that could be attributed to P=O, C-C, or C-O modes. The molecular formulas of **26b** and **26c** are confirmed by the HREI-MS analyses. As well, the MS analysis verifies the incorporation of seven deuteriums in **26c**.

After the (η^6-hexamethylbenzene)manganese dimethyl phosphonate complex was identified and methylene formation proposed as part of the mechanism, we attempted to trap the methylene with olefins. When 2,3-dimethyl-2-butene was added to **2d**, 1,1,2,2-tetramethylcyclopropane (*m/z* = 70.07825 amu) was formed and identified by MS analyses. Compound **24b** combined with *cis*-2-butene forms 1,2-dimethyl-3,3-d_2-cyclopropane (*m/z* = 72.0908 amu), which was identified by matching its mass peak to a standard. The ^{1}H NMR spectrum agrees with the formation of d_2-cyclopropane observed in the MS analysis with peaks at δ 1.29 and δ 0.88 assigned to the two methyl groups and the ring protons, respectively, based on the standard spectrum for

1,2-dimethylcyclopropane.[57]

Reactions of Triethylphosphite. The decomposition of **24a** is depicted in Scheme VII. The diethyl phosphonate complex, **26a**, was identified by the lower frequency carbonyl bands in the IR spectrum associated with increased electron density from a phosphonate, characteristic proton shifts for η^6-hexamethylbenzene and the diethyl phosphonate ligand in the ^{1}H NMR spectrum, and a diagnostic upfield shift of 40 ppm in the phosphonate resonance in the ^{31}P NMR spectrum. The molecular formula of **26a** is confirmed by the HRFAB-MS analysis. Compound **26a** forms in very small amounts, and therefore only traces of the carbenes and their decomposition products were observed. Ethene (m/z = 28.03130 amu) and methylcyclopropane or 2-butene (m/z = 56.06260 amu) were identified in experiments matching MS peaks to standards. 2-Butene could result from two ethylidenes dimerizing, while methylcyclopropane could result from an ethylidene reacting with ethene that has formed by rearrangement of ethylidene.

Conclusions

A series of ethyl, methyl, and phenyl phosphite complexes were synthesized and characterized. The nucleophilicity of the exocyclic methylene facilitates an α-hydrogen abstraction from the triphenylphosphite ligand to create the Arbuzov-like product, (η^6-hexamethylbenzene)manganese dicarbonyl diphenyl phosphonate. Their decomposition to phosphonates was observed under reduced pressure or in the presence of olefins. The production of benzyne in the decomposition of the triphenylphosphite complexes was observed indirectly through the formation of diphenylene. The production of methylene was observed by the formation of ethene and cyclopropanes. Carbene formation is verified by trapping the methylene with either 2,3-dimethyl-2-butene or *cis*-2-butene to form 2,2,3,3-tetramethylcyclopropane or

Scheme VII. Proposed decomposition pathway for $(\eta^5\text{-}C_6Me_5CH_2)Mn(CO)_2P(OEt)_3$

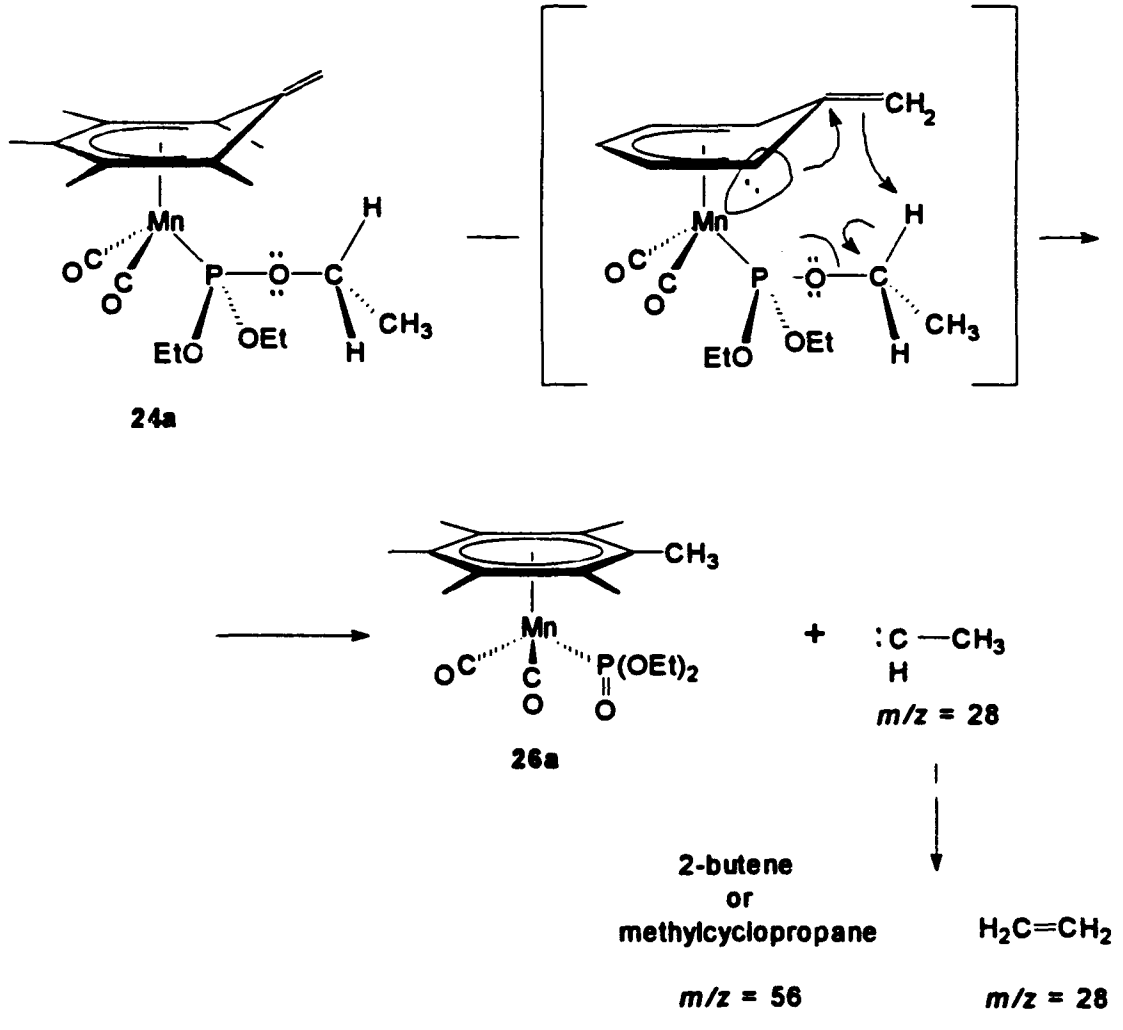

1,2-dimethylcyclopropane, respectively. The generation of olefins or cyclopropanes in very small amounts indicated that ethylidene was produced. The triethylphosphite complex, while forming ethylidene, did not react as fast or to the extent observed with the trimethyl- or triphenylphosphites complexes. The extent of reaction of the phosphites to form the phosphonates appeared to be adversely affected by the presence

of the trapping olefins or nitrogen. This may be attributable to adventitious oxygen. Lower concentrations of olefins and variations of radiation exposure and temperature may provide a more efficient process for carbene formation and trapping when using the (η^5–cyclohexadienyl–*exo*–ene)manganese trialkyl- and triarylphosphites.

CHAPTER IV

CRYSTAL STRUCTURE OF $(\eta^5\text{-}C_6Me_6H)Mn(CO)_2P(OMe)_3$[8]

Introduction

The formation of η^5-cyclohexadienyl complexes from the reaction of borohydride or aluminum hydride reagents with η^6-arene complexes is well known and is commonly used in the activation of arenes and their functionalization.[61] The $[(\eta^6\text{-}C_6Me_6)Mn(CO)_2PR_3][PF_6]$ complexes react with $[Bu_4N][BH_4]$ to yield the *endo*-$(\eta^5\text{-}C_6Me_6H)Mn(CO)_2PR_3$ complexes, eq 12. Neutral or anionic nucleophiles can

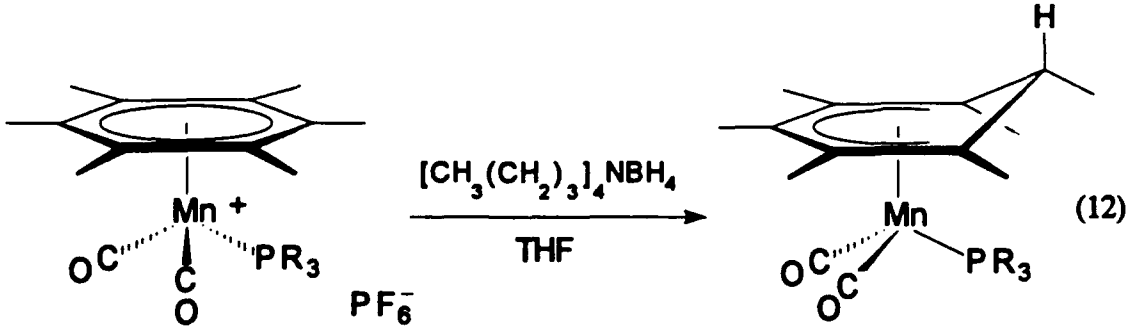

1x **11x** (12)

attack at the exo side of η^6-arene complexes of $[CoCp]^+$,[62] $[Cr(CO)_3]$,[60] $[Mn(CO)_3]^+$,[63] and $[FeCp]^+$[64] and result in the formation of exo-substituted η^5-cyclohexadienyl complexes. As well, the *endo*-$(\eta^5\text{-}C_6Me_6H)Mn(CO)_2PR_3$ (R = *n*-Bu, Me, Ph, OMe, OPh) complexes can be synthesized by reacting Bu_3SnH with the corresponding $(\eta^5\text{-}C_6Me_5CH_2)Mn(CO)_2PR_3$ complexes, eq 13.[16,65]

When the exo-substituent is a hydride, it can be removed by hydride abstracting

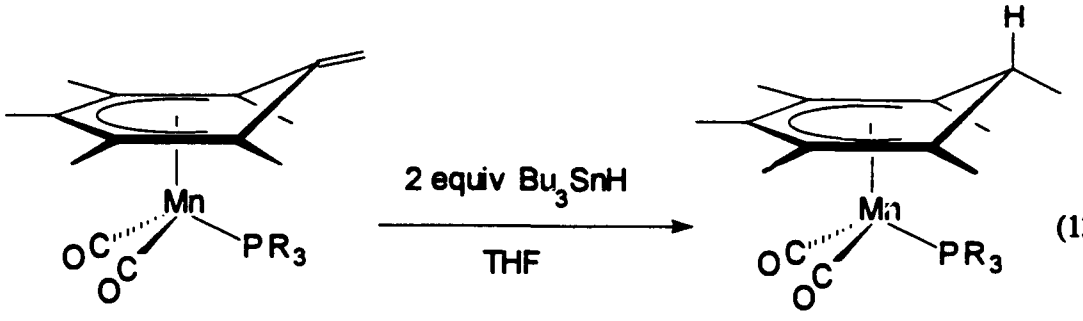

(13)

agents, e.g., $[Ph_3C]^+$ and $[C_7H_7]^+$, yielding the cationic η^6–arene complexes.[66] Astruc has proposed two mechanistic routes for this reaction.[67] The first is a one–step transfer of the hydride to the abstracting reagent, and the second is a two–step process where electron transfer is followed by a hydrogen atom transfer. The reactivity of the *exo*–hydride is due in part to an electronic contribution from the manganese, through the filled d_{xy} orbital, to the $2p$ orbital of the uncoordinated ring carbon.[8] A similar argument was used to explain the increased nucleophilicity of **2a–e** in Chapter 2. The filled d_{xy} orbital interacts with the π_a orbital of the exocyclic double bond in the (η^5–pentamethylcyclohexadienyl–*exo*–ene)manganese complexes to increase their nucleophilic reactivity.[16]

This chapter discusses the solid-state structure characteristics of *endo*–$(\eta^5$–$C_6Me_6H)Mn(CO)_2P(OMe)_3$.

Experimental

Synthesis of 11d

***endo*–$(\eta^5$–$C_6Me_6H)Mn(CO)_2P(OMe)_3$ (11d).** The yellow crystals used in the following crystallographic structure determination were synthesized by the addition of THF (40 mL) to a mixture of $[(n\text{–Bu})_4N][BH_4]$ (1 mmol) and $[(\eta^6$–$C_6Me_6)Mn(CO)_2P(OMe)_3][PF_6]$ (1 mmol), followed by LC purification on SiO_2

(hexanes–acetone) which resulted in a 78% yield.[8] The IR and NMR characteristics of **11d** are listed in Appendix A.

Solid State Structure of endo–(η^5–C_6Me_6H)$Mn(CO)_2P(OMe)_3$ (**11d**)

Collection and Reduction of X–ray Data. A suitable crystal of **11d** was grown by recrystallization from hexane solutions at −20 °C. Crystals on glass fibers were sealed in glass capillary tubes, mounted on a goniometer head, and optically centered on an Enraf–Nonius CAD4 diffractometer. The cell constants and an orientation matrix for data collection for **11d** were obtained from refinement of 22 randomly selected reflections in the range $2° < \theta < 25°$. A summary of the data collection for **11d** can be found in Table 51. A complete listing of data collection parameters is found in Appendix C. The choice of the space group was confirmed by determining the systematic absences in the observed reflections and subsequent least–squares refinement of the structure.

Data for **11d** was collected using the ω–θ scan technique using a peak counting time to background time of 2:1. Variable scan rates of θ and ω varied from 1 to 7 deg/min and variable scan ranges calculated by θ scan width = 0.80 + 0.35 tan θ. Several standard reflections were monitored periodically during data collection and were used to correct for the small loss in intensity. Lorentz and polarization corrections were made for the data set. A half sphere of reflections were collected and Freidel equivalents were not averaged in the 3380 final reflections. Only reflections with $F_o > 3\sigma(F_o)$ were used in the final least–squares refinements.

The position of the manganese and phosphorus atoms were located by Patterson methods. Subsequent cycles of least–squares refinement and difference Fourier calculations, and reference to the DIRDIF program output, were used to locate all other non–hydrogen atoms and the *exo*–cyclic hydrogen atoms in **11d**.

Table 51. Crystallographic Data and Refinement Parameters for **11d** [a]

fw, amu	398.32	space group	$P2_12_12_1$
a, Å	8.945 (6)	T, °C	23
b, Å	12.911 (4)	λ, Å (graphite)	0.710 73
c, Å	16.528 (6)	ρ_{calc}, $kg \cdot m^{-3}$	1.386
V, Å^3	1909 (5)	linear abs coeff, cm^{-1}	7.7
Z	4	transm coeff	1.00–0.97
systematic	$h00$, $h \neq 2n$	reflections collected	7547
absences	$0k0$, $k \neq 2n$	independent reflections	3861
	$00l$, $l \neq 2n$	after averaging ($> 3\sigma$)	3380
R_1 [b]	0.025	parameters refined	217
R_2 [c]	0.033		

[a] In this and subsequent tables esd's are given in parentheses.

[b] $R_1 = \sum \| F_o | - | F_c \| / \sum | F_o |$.

[c] $R_2 = [\sum w(| F_o | - | F_c |)^2 / \sum w | F_o |^2]^{1/2}$, $w = 1/\sigma^2(F)$, where $\sigma^2(F) = \sigma^2(F) + [(PWT)F]^2$, PWT = 0.07.

The positional parameters and isotropic parameters of non-hydrogen atoms are listed in Appendix C. During the final stages of refinement, the remaining hydrogen atom positions were calculated and idealized with assigned C–H distances of 0.95 Å. No solvent molecules were found. For **11d**, the space group $P2_12_12_1$ provides a single position for an enantiomorph. Refinement on the other enantiomorph for **11d** resulted in an increase in R_1 from 0.025 to 0.036. Final values for hydrogen atom atomic coordinates, anisotropic temperature factors, and F_{obs} and F_{calc} are provided in Tables found in Appendix C.

Results and Discussion

Crystallographic Study of 11d

The X-ray crystallographic study of **11d** was performed to establish the ground state structure of the mono-substituted phosphite complex for comparison with the bis-substituted phosphite complex, *endo*-(η^5-C_6Me_6H)Mn(CO)($P(OMe)_3$)$_2$.[8] The ORTEP structures of compound **11d** are shown in Figures 11 and 12. Selected bond lengths and angles are given in Table 52. Only one enantiomorph of **11d** was found in the crystals that were studied. An enantiomorphic pair was found for the bis-phosphite complex.[8]

The manganese atom of **11d** is in a pseudo-octahedral environments with the cyclohexadienyl ligands occupying three facial coordination sites, Figure 11b. In **11d**, the two CO and the $P(OMe)_3$ ligands, the "legs" of a "three-legged piano stool", have bond angles of 87.67 (8)° (P-Mn-C13), 95.88 (8)° (P-Mn-C14), and 92.4 (1)° (C13-Mn-C14). These ligand positions affirm that the manganese atom in **11d** has an octahedral ligand environment. The bis-phosphite complex has similar structural features that establish its pseudo-octahedral configuration about the manganese atom.[8]

In **11d**, the cyclohexadienyl ring is positioned with the saturated carbon, C1, eclipsing one of the carbonyls. The remaining carbonyl and phosphite ligands of **11d** eclipse atoms C5 and C3, respectively. In the bis-phosphite complex, one of the phosphite ligands is found positioned eclipsing the saturated ring carbon atom.[8] In **11d**, a small amount of localization of π-bond electron density is observed in the cyclohexadienyl ligand; the C2-C3 and C5-C6 bond lengths are 1.394 (3) Å, while the C3-C4 and C4-C5 bond lengths are 1.431 (3) Å. In **11d**, the cyclohexadienyl ring is shifted off-center relative to the $Mn(CO)_2P(OMe)_3$ "piano stool" tripod, and away from the phosphite ligand.

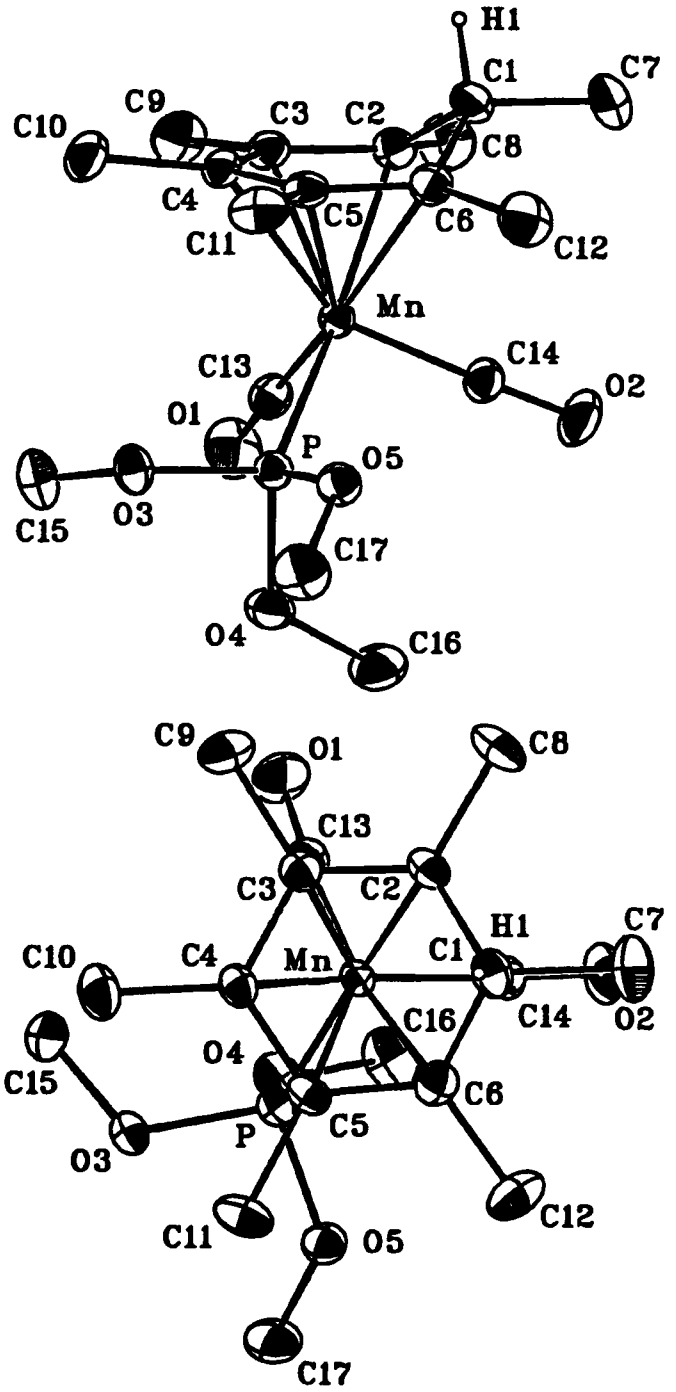

Figure 11. ORTEP drawings of **11d** with 25% probability ellipsoids: (a) side view and (b) top view

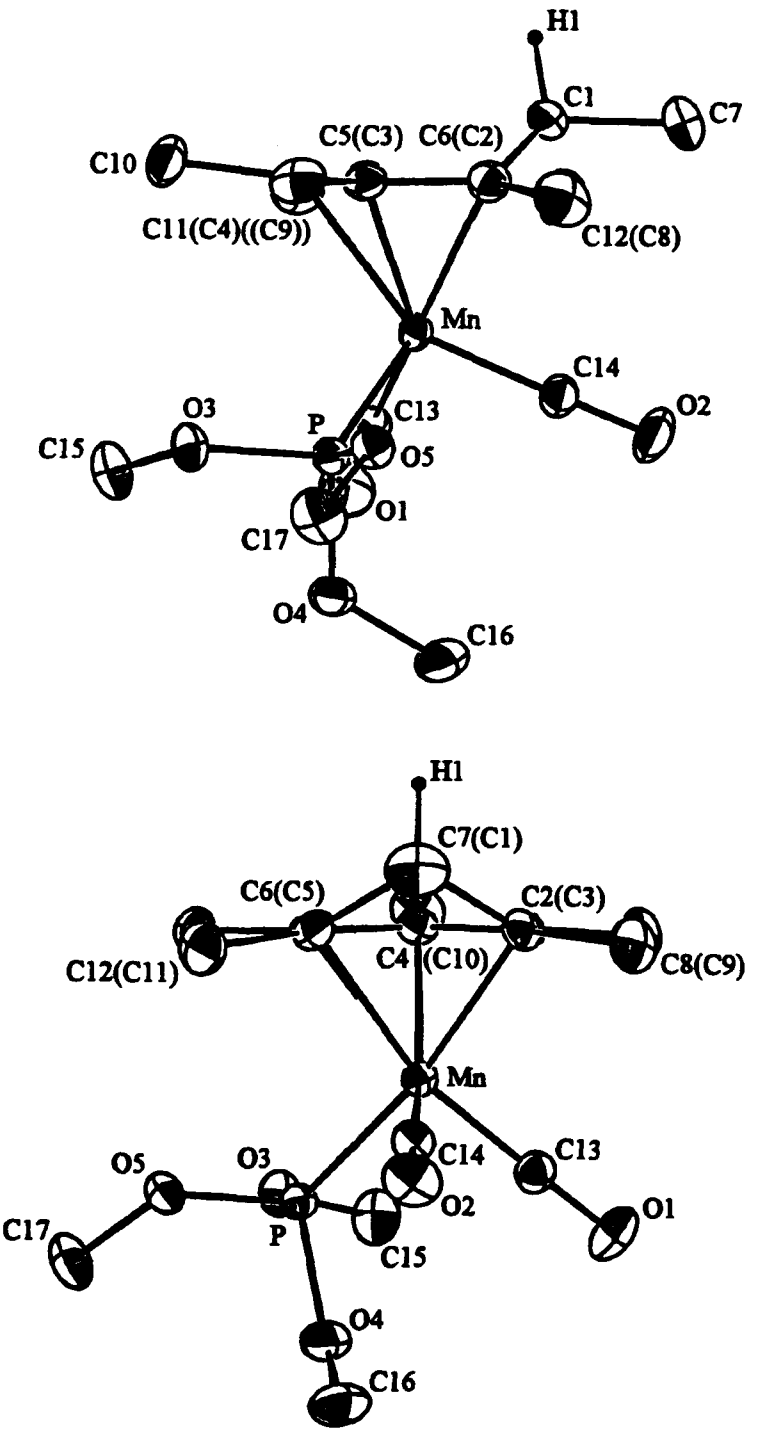

Figure 12. ORTEP drawing of **11d**: orthogonal side views

Table 52. Selected Bond Distances (Å) and Angles (°) for **11d**

		Distances	
Mn–C(2)	2.197 (2)	C(14)–O(2)	1.152 (3)
Mn–C(3)	2.148 (2)	Mn–P	2.1790 (7)
Mn–C(4)	2.165 (2)	C(1)–C(2)	1.516 (4)
Mn–C(5)	2.178 (2)	C(1)–C(6)	1.520 (4)
Mn–C(6)	2.231 (2)	C(2)–C(3)	1.394 (3)
Mn–C(13)	1.772 (3)	C(3)–C(4)	1.431 (3)
C(13)–O(1)	1.167 (3)	C(4)–C(5)	1.431 (3)
Mn–C(14)	1.772 (3)	C(5)–C(6)	1.394 (3)
		Angles	
P–Mn–C(13)	87.67 (8)	C(2)–C(3)–C(4)	119.0 (2)
P–Mn–C(14)	95.88 (8)	C(3)–C(4)–C(5)	118.6 (2)
C(13)–Mn–C(14)	92.4 (1)	C(4)–C(5)–C(6)	118.5 (2)
Mn–C(13)–O(1)	176.5 (2)	C(5)–C(6)–C(1)	117.4 (2)
Mn–C(14)–O(2)	177.5 (2)	C(6)–C(1)–C(7)	114.2 (2)
C(2)–C(1)–C(6)	102.6 (2)	C(2)–C(1)–C(7)	115.4 (2)
C(1)–C(2)–C(3)	116.7 (2)		

The Mn–C6 bond, 2.231 (2) Å, is longer than the Mn–C2, Mn–C5, and Mn–C4 bonds, 2.197 (2), 2.178 (2), and 2.165 (2) Å, respectively. The Mn–C3, eclipsed by the phosphite, is the shortest with a distance of 2.148 (2) Å.

For **11d**, the planes program [40] calculated the dihedral angle of 47.5° between the plane of the five unsaturated carbons, C2/C3/C4/C5/C6, and the plane formed from atoms C1/C2/C6, best seen in Figure 12a. The dihedral angle calculated for the bis-phosphite complex is 47.4°.[8] The saturated ring carbon atom, C1, is 0.694 Å above the plane of unsaturated carbon atoms of the cyclohexadienyl ring. As well, the methyl carbon atoms, C9 and C11 are below the plane by 0.087 Å and 0.017 Å, respectively.

Methyl carbon atom C10 is 0.172 Å above, while the methyl carbon atoms attached to the ring carbons adjacent to the saturated carbon are below the ring plane at distances of 0.162 Å and 0.177 Å, respectively.

Conclusions

The comparison of ground state structures mono- and bis-substituted phosphite complexes shows that steric requirements do not favor positioning the first phosphite ligand eclipsing the saturated ring carbon atom. Steric repulsions of the first phosphite shift the position the cyclohexadienyl ligand to allow the second phosphite to eclipse the saturated ring carbon atom. This structure may be used with other (η^5–cyclohexadienyl)manganese complexes to support molecular orbital calculations for the interaction of the $Mn(CO)_2P(OMe)_3$ moiety and the cyclohexadienyl ligand. These calculations could potentially lend support to arguments concerning the influence of the manganese d_{xy} orbital on the reactivity of both the exo-hydride and the exocyclic methylene in (η^5–cyclohexadienyl)manganese complexes.

Methyl carbon atom C10 is 0.172 Å above, while the methyl carbon atoms attached to the ring carbons adjacent to the saturated carbon are below the ring plane at distances of 0.162 Å and 0.177 Å, respectively.

Conclusions

The comparison of ground state structures mono- and bis-substituted phosphite complexes shows that steric requirements do not favor positioning the first phosphite ligand eclipsing the saturated ring carbon atom. Steric repulsions of the first phosphite shift the position the cyclohexadienyl ligand to allow the second phosphite to eclipse the saturated ring carbon atom. This structure may be used with other (η^5–cyclohexadienyl)manganese complexes to support molecular orbital calculations for the interaction of the $Mn(CO)_2P(OMe)_3$ moiety and the cyclohexadienyl ligand. These calculations could potentially lend support to arguments concerning the influence of the manganese d_{xy} orbital on the reactivity of both the exo-hydride and the exocyclic methylene in (η^5–cyclohexadienyl)manganese complexes.

The second compound has a μ-η^1-dithioformate bridging two (η^6-arene)manganese moieties. The metal-mediated conversion of an η^1-dithioformate into thio-C_1 ligands, including thioformamides and alkanethiolates, is reported here. An η^1-alkyl dithioformate ester intermediate is formed by the coordination of a Lewis acid to the uncoordinated sulfur of the η^1-dithioformate ligand. The *N*- and *N*,*N*-substituted thioformamides, resulting from the nucleophilic attack of amines on this η^1-alkyl dithioformate ester complex, retain the η^1-coordination through the sulfur to the metal. The reactions reported here have potentially useful synthetic applications in thioderivatization. In a similar vein, potassium dithioformate has been used to form thioformamide derivatives of proteins to better understand their chemical and physical properties.[70]

Fast atom bombardment mass spectrometry (FAB-MS) has been reported to be very useful for elucidating the composition and structure of organometallic complexes.[71] The energetic FAB process can lead to rearrangement or side reactions of the parent ion.[72] By using FAB tandem mass spectrometry (MS/MS) on these organometallic complexes, the parent ion is isolated and the spectra reveal information about its structural features in addition to its dissociation pathways.[73] The application of FAB-MS/MS to the analysis of several (arene)manganese dicarbonyl complexes with sulfur-coordinated dithioformate and thioformamide ligands is reported here. In each case, fast atom bombardment ionization followed by collision-induced dissociation (CID) of the molecular ion of each of these complexes, produces fragment ions consistent with the proposed structures for each complex reported here, including $[(\eta^6\text{-}C_6Me_6)Mn(CO)_2SCHNEt_2][BF_4]$ whose crystal structure is also reported. The spectral fragmentation patterns reveal simple bond cleavage within the thioformamide ligands and between the metal and the coordinated ligands. The bare metal ion is also observed.

Experimental

Syntheses

$[(\eta^6\text{-}C_6Me_6)Mn(CO)_2(\eta^1\text{-}SCHSCPh_3)][BF_4]$ (52).

$(\eta^6\text{-}C_6Me_6)Mn(CO)_2SC(S)H$ (**51**) (200 mg, 571 μmol) and $[Ph_3C][BF_4]$ (190 mg, 576 μmol) in THF (125 mL) were stirred for 30 min, during which the solution turned from orange to deep red. Compound **52** was not isolated from solution. IR spectral results for **52–55** are tabulated in Table 53. The ^1H NMR spectral results for **52–55** are listed in Table 54. The results of the HRFAB-MS analyses for **52–55** are recorded in Table 56. The FAB-MS/MS results for **52** are listed in Table 60.

Table 53. Infrared Stretching Bands for **52–55**

			solution IR, cm^{-1} [a] solid state IR, cm^{-1} [b]		
compd no.	R	R′	ν_{CO}	ν_{CN}	ν_{CS}
52			1982, 1940		
53	Et	Et	1975, 1932 1973, 1923	1551 1552	 1387, 1039, 596
54	H	Ph	1978, 1927 1969, 1919	1581 1556	 1385, 1038, 595
55	H	*t*-Bu	1973, 1925 1967, 1916	1581 1577	 1391, 1040, 598

[a] Solution spectra were obtained in THF.

[b] Solid state spectra were obtained from KBr mulls.

Table 54. ^{1}H NMR Data for **52–55**

compd no.	R	R′	^{1}H NMR [a] δ, ppm [b]	
52			2.39	(s, 18 H, $-CH_3$)
			7.34	(m, 15 H, $-C_6H_5$)
			10.75	(s, 1 H, S_2CH)
53	Et	Et	1.32	(t, 6 H, $-CH_3$)
			2.35	(s, 18 H, $-CH_3$)
			3.94	(d–q, 4 H, $-CH_2-$)
			8.89	(s, 1 H, SCHN)
54	H	Ph	2.35	(s, 18 H, $-CH_3$)
			7.40	(m, 5 H, $-CH_3$)
			9.36	(s, 1 H, NH)
			10.71	(s, 1 H, SCHN)
55	H	*t*-Bu	1.45	(s, 3 H, $NCCH_3$)
			1.51	(s, 6 H, $NCCH_3$)
			2.33	(s, 18 H, $-CH_3$)
			8.73, 8.75 8.84, 8.80	(d, 1 H, NH, 1:3)
			10.18 10.90	(s, 1 H, SCHN, 1:3)

[a] All spectra in $(CD_3)_2CO$ at 297 K.

[b] (multiplicity, no. of protons, assignment, ratio of isomers).

$[(\eta^6\text{-}C_6Me_6)Mn(CO)_2SCHNEt_2)][BF_4]$ (53). $HNEt_2$ (0.2 mL, 2.460 mmol) was added to 125 mL of 4.57 mM (THF) solution of **52**, resulting in an immediate color change of the solution from deep red to orange.

Table 55. $^{13}C\{^1H\}$ NMR Data for **52–55**

compd no.	R	'R	$^{13}C\{^1H\}$ NMR [a] δ, ppm [b]	
52			224.8	(s, CO)
			221.1 [c]	(d, SCHS, J_{C-H} = 188.3 Hz)
			132.2, 130.7, 129.7	(s, $-C_6H_5$)
			111.3	(ring–C)
			53.5, 48.2	(NCH_2)
			16.8 [c]	(q, ring–CH_3, J_{C-H} = 129.7 Hz)
53	Et	Et	227.6	(CO)
			188.3	(SCN)
			108.6	(ring–C)
			53.5, 48.2	(NCH_2)
			16.3	(ring–CH_3)
			14.2, 10.9	($NCH_2\underline{C}H_3$)
54	H	Ph	232.6	(SCN)
			227.1, 226.8	(CO)
			131.8	($-C_6H_5$)
			108.7	(ring–C)
			16.3	(ring–CH_3)
55	H	*t*–Bu	227.7	(CO)
			190.6, 188.4	(SCN)
			108.8, 108.5	(ring–C)
			62.8, 59.9, 57.7	($N\underline{C}(CH_3)_3$
			27.0, 26.9, 26.5	($NC(\underline{C}H_3)_3$
			16.3	(ring–CH_3)

[a] All spectra were obtained in d_6–acetone at 210 K.

[b] (mult., assignment, coupling).

[c] ^{13}C–^1H Coupling experiment to verify presence of SCHS moiety.

Table 56. HRFAB-MS Data for **52–55**

compd no.	chemical formula	MW_{calc}	M^+_{exp}, *m/z*	Δm, mmu
52	$MnS_2O_2C_{34}H_{34}$	593.1381	593.1377	+0.4
53	$MnSO_2NC_{19}H_{29}$	390.1299	390.1284	+1.5
54	$MnSO_2NC_{21}H_{25}$	410.0986	410.1006	−2.0
55	$MnSO_2NC_{21}H_{25}$	390.1299	390.1304	−0.5

Table 57. ^1H NMR and IR Spectral Characterization Data for **57**

	^1H NMR [a]	solution IR [b]	
compd no.	δ, ppm [c]	ν_{CO}, cm^{-1}	ν_{CN}, cm^{-1}
56	2.10 (s, 18 H, CH_3) 7.30 (m, 15 H, CH)	1998, 1956	2139

[a] Spectrum obtained in d_6-acetone at 297 K.

[b] Spectrum obtained in THF at 297 K.

[c] (multiplicity, no. of protons, assignment).

The solution was adsorbed onto silica gel and chromatographed using a hexane wash (250 mL), 5/95 acetone/hexane (200 mL), 20/80 acetone/hexane (200 mL), and 60/40 acetone/hexane (200 mL). Recrystallization of the final fraction product yielded 90 mg (40% yield) of **53** as clear orange diffractable crystals. The other fractions consisted mainly of starting material. The FAB-MS/MS results for **53** are listed in Table 61.

[(η^6-C_6Me_6)Mn(CO)$_2$SCHNHPh][BF_4] (54). Aniline (0.04 mL, 439 μmol) was added in 0.5 mL of THF to 125 mL of a 2.28 mM (THF) solution of **52**, resulting in a rapid color change of the solution from deep red to red-orange. The product was isolated as in **53**. The product, **54**, was obtained from the last fraction, and when dried, it yielded 33 mg (28% yield) of medium orange compound. The other fractions consisted mainly of starting material. The FAB-MS/MS results for **54** are listed in Table 62.

[(η^6-C_6Me_6)Mn(CO)$_2$SCHNH(*t*-Bu)][BF_4] (55). *tert*-Butylamine (0.5 mL, 4.760 mmol) was added in 0.5 mL of THF to 125 mL of a 3.63 mM (THF) solution of **52**, resulting in a rapid color change of the solution from deep red to orange. The product was isolated as in **53**. The product, **55**, was obtained from the second fraction, and when dried, it yielded 127 mg (72% yield) of bright orange compound. The other fractions consisted mainly of starting material. The FAB-MS/MS results for **55** are listed in Table 63.

[(η^6-C_6Me_6)Mn(CO)$_2$CN·CPh$_3$][BF_4] (57). (η^6-C_6Me_6)Mn(CO)$_2$CN (24 mg, 80 μmol) and [Ph_3C][BF_4] (26 mg, 79 μmol) in THF (125 mL) were stirred for 30 min, during which the solution turned from yellow to chartreuse. The yellow product, **57**, was obtained by reducing the solvent volume and adding hexane. The ^{1}H NMR and IR spectral results are listed in Table 57.

Solid State Structure of [(η^6-C_6Me_6)Mn(CO)$_2$SCHNEt$_2$][BF_4] (53)

Collection and Reduction of X-ray Data. Crystals of **3** were obtained as orange prisms from a THF solution, upon slow addition of hexane, under dinitrogen. A crystal, 0.69 × 0.13 × 0.19 mm, sealed in a glass capillary tube with a small amount of mother liquor to prevent solvent loss, was mounted on the diffractometer. A

summary of crystallographic parameters are listed in Table 58. A complete listing of data and refinement parameters is found in Appendix D. Graphite monochromated Mo Kα radiation, average wavelength = 0.710 73 Å, was used to collect data at 295 K on an Enraf–Nonius CAD4 diffractometer, using an ω-scan range, 0.80 + 0.35 tan θ, and background at 25% below and above range; the horizontal aperture was varied from 2.5 to 3.0 mm depending on the angle; the scan speed ranged from 0.71 to 3.3 deg/min for a hemisphere with θ ranging from 1 to 25°. Lorentz, polarization, and empirical absorption corrections were made (μ = 6.9 cm^{-1}; maximum and minimum corrections, 0.97–1.0 on F). Three standards were used to monitor crystal decay and indicated a maximum decline in F of 5.5%; intensity corrections for decay were made. A total of 5192 reflections were measured for the hemisphere ($\pm h, \pm k, \pm l$) in reciprocal space for 2θ ranging from 2 to 50°. Averaging 4451 independent reflections greater than 3σ above background gave 2475 reflections that were used in the least-squares refinement. The cell dimensions for the triclinic crystal, space group $P\bar{1}$, a = 8.312 (6) Å, b = 12.303 (4) Å, c = 13.325 (6) Å, α = 61.14 (3)°, β = 74.69 (5)°, and γ = 75.69 (4)°, were obtained by a least-squares fit to 21 orientation reflections.

The positions of the manganese and sulfur atoms were located by Patterson methods. Subsequent cycles of least-squares refinement and difference Fourier calculations were used to locate all other non-hydrogen atoms and half the hydrogen atoms. During the final stages of refinement, the remaining hydrogen atom positions were calculated by assigning C–H distances of 0.95 Å and normalizing their positions with respect to located hydrogen atoms. Final positions of the non-hydrogen atoms are listed in Appendix D. No solvent molecules were found. Anisotropic refinement on all non-hydrogen atoms (262 variables, including scale and extinction) gave R values of R_1 = 0.054 and R_2 = 0.088; the standard deviation of an observation of unit weight = 1.17; the maximum parameter shift/estimated error was less than 0.04; the maximum

Table 58. Crystallographic Data and Refinement Parameters for 53 [a]

fw	477.25	space group	$P\bar{1}$
a, Å	8.312 (6)	T, °C	22
b, Å	12.303 (4)	λ, Å	0.710 73
c, Å	13.325 (6)	ρ_{calc}, g cm^{-3}	1.39
α, deg	61.14 (3)	linear abs coeff, cm^{-1}	6.9
β, deg	74.69 (5)	transm coeff	1.00–0.97
γ, deg	75.69 (4)	reflections measured	5192
V, Å^3	1138. (2)	independent reflections	4451
Z	2	after averaging ($> 3\sigma$)	2475
R_1 [b]	0.054	parameters refined	262
R_2 [c]	0.088		

[a] Values for the esd are given in parentheses.

[b] $R_1 = \sum \| F_o | - | F_c \| / \sum | F_o |$.

[c] $R_2 = [\sum w(| F_o | - | F_c |)^2 / \sum w | F_o |^2]^{1/2}$, $w = 1/\sigma^2(F)$, where $\sigma^2(F) = \sigma^2(F) + [(\mathrm{PWT})F]^2$, PWT = 0.07.

peak height on the electron density difference map was 0.85 e^-/Å^3. Weights used in refinement are $1/\sigma^2(F)$, where $\sigma^2(F) = \sigma^2(F) + [(\mathrm{PWT})F]^2$, PWT = 0.07, is the estimate of the propagated error due to counting error plus the estimated error based on agreement of equivalent reflections (F = 0.013). The data were processed using scattering factor tables provided in the Enraf-Nonius SDP software on a MicroVax 2 computer.[40]

Results and Discussion

General Discussion

In compound **51**, the dithioformate ligand is assumed to be σ-bonded through the sulfur to the manganese. Since ^{1}H NMR and IR spectral data confirm the presence of η^6-hexamethylbenzene (HMB) and two terminal carbonyls, this leaves only one coordination site available for the dithioformate. Addition of triphenylcarbenium (trityl cation) to the uncoordinated sulfur of the dithioformate apparently results in significant delocalization of electrons from the metal center through the coordinated sulfur, eq 15.

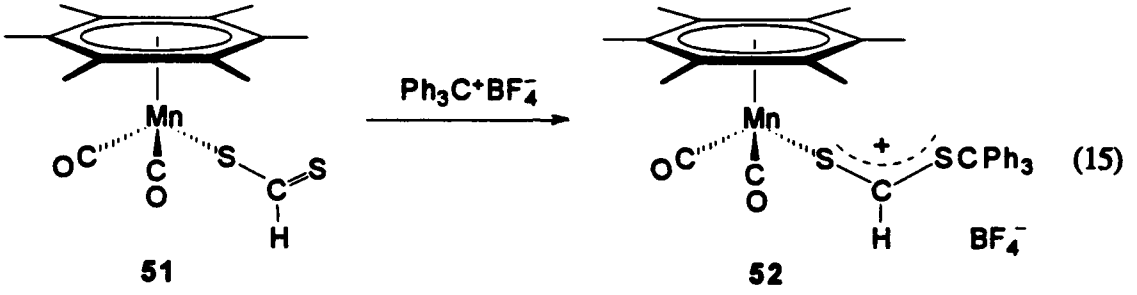

(15)

The resulting dithioformate ester ligand is probably η^1-coordinated through sulfur to the manganese as in *fac*-[Et_4N][$W(CO)_3$(dppe)(η^1-SCHS)] rather than η^2-coordinated to the C=S bond as found in *mer*-$W(CO)_3$(dppe)(η^2-SCHSR)] by Schenk et al.[68j] This argument is supported by the chemical shift of the dithioformate proton, which goes from 11.44 to 10.78 upon alkylation, as opposed to the much higher field shift (5.15-5.3) observed by Schenk for the η^2-coordinated ligand.[68j] This coordination mode has been observed in dithio esters with other metals, when the remaining coordination sphere is occupied by strong π-acceptor ligands.[74] In Figure 13, the ^{13}C-^{1}H coupling of doublet observed for the SCHS carbon in the ^{13}C NMR spectrum,

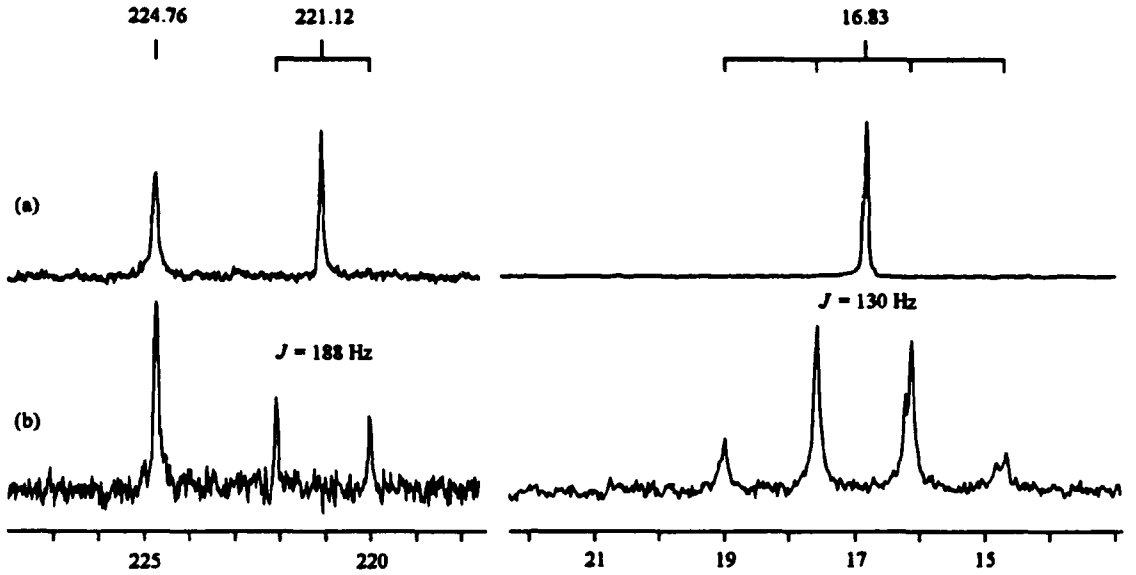

Figure 13. ^{1}H–^{13}C Coupling of SCHS (δ 221) and ring methyls (δ 16.8) in **52** in (a) $^{13}C\{^{1}H\}$ and (b) ^{13}C NMR Spectra

which in the $^{13}C\{^{1}H\}$ spectrum becomes a singlet, supports the η^{1}–coordination of the sulfur to the manganese in **52**.

Synthesis and Characterization of $[(\eta^{6}\text{–}C_6Me_6)Mn(CO)_2SCHSCPh_3][BF_4]$ (52)

The ^{1}H, ^{13}C, and $^{13}C\{^{1}H\}$ NMR and IR spectral data indicate that the red adduct **52** has formed. The ^{1}H NMR spectrum reveals a singlet for the six equivalent methyl groups on the arene ring and a singlet at δ 10.78 for the dithioformate proton. The shift for the dithioformate proton in the ester is nearly identical with shifts typically observed for the proton in bridging (μ^{2}–η^{2}) dithioformate ions.[68,20,75] Both ^{13}C and $^{13}C\{^{1}H\}$ decoupled NMR spectra were obtained to confirm the presence of the SCHS

$$J_{^{13}C\text{-}H}\,(Hz) = 500\,\rho_{C\text{-}H} \qquad (16)$$

moiety in the dithioformate ester. The dithioformate carbon resonance is observed at δ 221.1 with a coupling constant of 188.3 Hz, which is a reasonable value for a sp^2 carbon atom (175–220 Hz).[76] The fraction of *s* character, ρ, is calculated to be 0.38 using eq 16.[76] In the same experiment, the ring methyl groups are observed as a quartet at 16.8 with a ^{13}C–^{1}H coupling of 129.7 Hz, which is in the range typical of sp^3 carbon atoms (100–140 Hz).[76] The infrared spectrum of **52** shows two carbonyls, shifted to higher frequency, bound to the metal. The shift in carbonyl stretching frequencies is similar to that was previously reported for the dithioformate bridged binuclear manganese species, $[(HMB)_2Mn_2(CO)_4S_2CH][BF_4]$ (**56**).[20] A similar degree of shifting of the carbonyl bands to higher frequency was observed for $(\eta^6$–$C_6Me_6)Mn(CO)_2CN$ upon addition of the Lewis acids $[Ph_3C]^+$ and $AlMe_3$ to form the adducts $[(\eta^6$–$C_6Me_6)Mn(CO)_2CN \cdot CPh_3][BF_4]$ (**7**) and $(\eta^6$–$C_6Me_6)Mn(CO)_2CN \cdot AlMe_3$.[77]

Reactions of $[(\eta^6$–$C_6Me_6)Mn(CO)_2SCHSCPh_3][BF_4]$ (**52**) with Amines

The reaction of **22** with secondary and primary amines, $HNEt_2$, H_2NPh, and H_2N–*t*–Bu, produces **53–55**, respectively. The ^{1}H and $^{13}C\{^{1}H\}$ NMR, IR, FAB–MS, and FAB–MS/MS spectral data for compounds **53–55** are consistent with structures having *S*–coordinated thioformamide ligands, this structure was confirmed for **53** by a crystallographic structure determination. The ^{1}H NMR spectrum of each reveals a singlet for the six equivalent methyl groups on the arene ring suggesting the presence of HMB. The infrared spectra of **53–55** show two carbonyl stretches, consistent with two carbonyls attached to the metal, suggesting the thioformamide ligand is monodentate; which retains an 18-electron count on the manganese. In addition, a C–N stretching frequency of 1551 cm^{-1} for **53** and 1581 cm^{-1} for **54** and **55**, attributable to the thioformamide, is observed in solution and solid state IR spectra. A broad band at

$\sim 1009\ cm^{-1}$, characteristic of the B-F stretching mode, in the solid state IR spectra confirms the presence of BF_4^-.[78]

A proposed mechanism for the observed conversion of coordinated dithioformate to thioformamides is shown in Scheme VIII. Coordination of trityl cation to the uncoordinated sulfur is followed by nucleophilic attack of the amine on the dithioformate carbon. The formation of **53** apparently is made possible by the enhanced electrophilicity at the thioformyl carbon upon conversion of **51** to **52**, because we have observed that **51** does not react with excess $HNEt_2$ to give **53**. In the nucleophilic attack by an amine on the dithioformate ester cation complex, the thioformate carbon is apparently the most electrophilic site. Proton transfer from the nitrogen to the sulfur results in the formation of the coordinated thioformamide and triphenylmethanethiol, similar to the acid decomposition of methyl dithio esters producing methanethiol observed by Roper *et al.*[79] Proton transfer from nitrogen to sulfur also has been shown to occur in the acid induced decomposition of dithiocarbamates.[80] The decomposition of the intermediate in Scheme VIII, an analogue of a protonated dithiocarbamate, follows the proton transfer from the amine to the alkylated sulfur. This is the reverse reaction of that observed by Miller and Latimer in their kinetic studies of dithiocarbamate decomposition, where the nitrogen protonation produced the uncoordinated amine.[81] The proposed intermediate of Scheme VIII is analogous to the cycloaddition product of diphenylnitrilimine with η^1-coordinated CS_2, eq 17.[82]

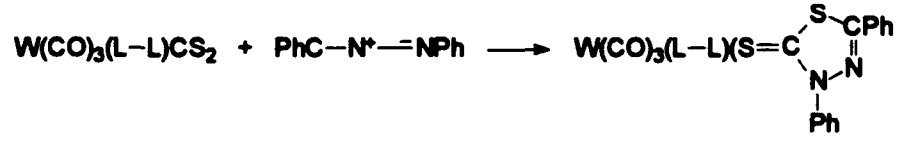

(17)

Scheme VIII. Synthesis of $[(\eta^6\text{-}C_6Me_6)Mn(CO)_2SCHNRR'][BF_4]$ compounds

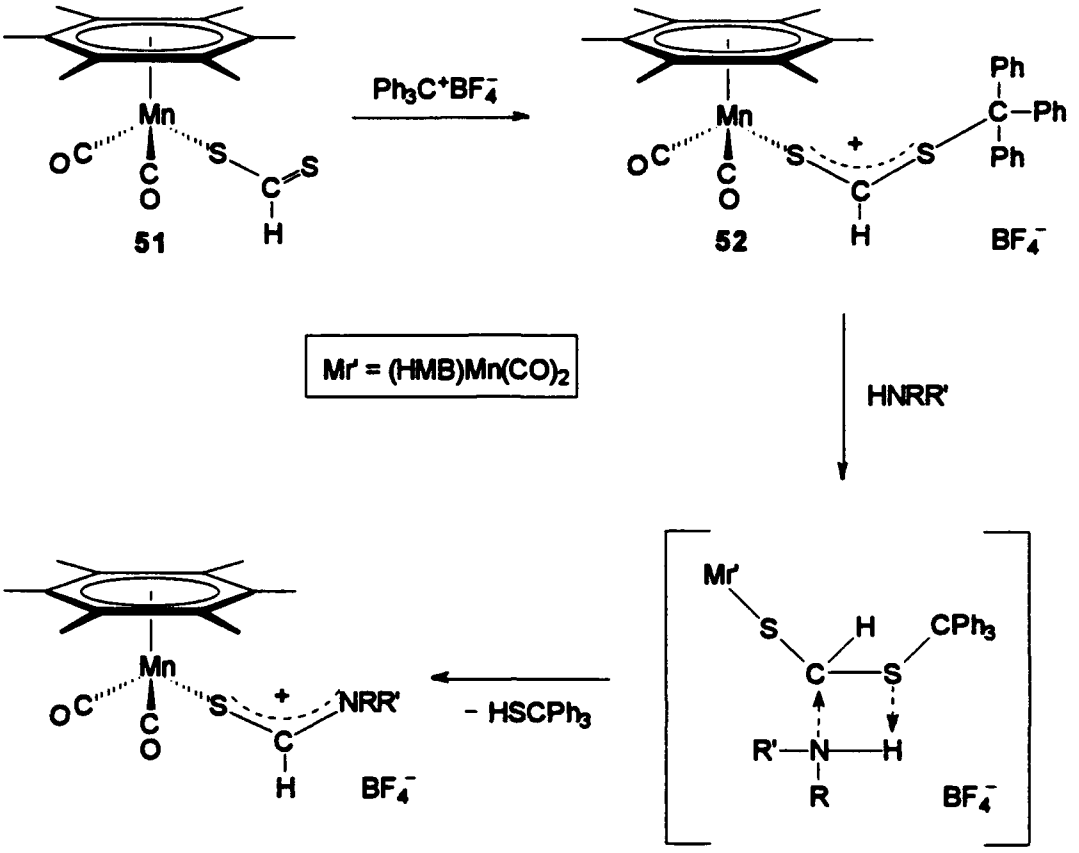

compd no.	R	R'
53	Et	Et
54	H	Ph
55	H	*t*-Bu

Synthesis and Characterization of $[(\eta^6\text{-}C_6Me_6)Mn(CO)_2SCHNEt_2][BF_4]$ (53)

The reaction of **52** with diethylamine to produce the orange complex, $[(\eta^6\text{-}C_6Me_6)Mn(CO)_2SCHNEt_2][BF_4]$ (**53**), is shown in eq 18. The ^1H NMR spectrum

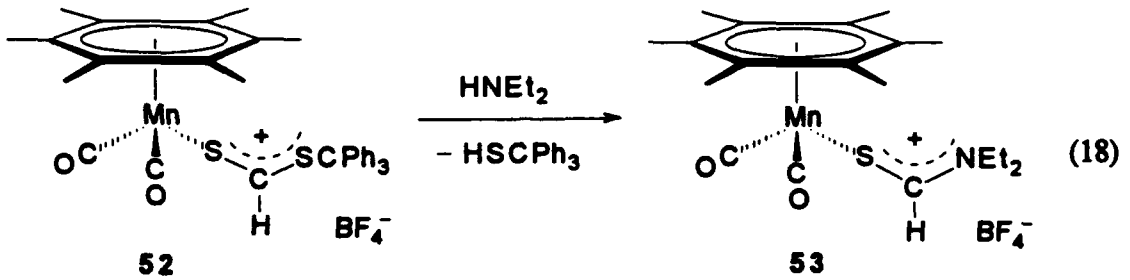

52 53 (18)

displayed a singlet at δ 8.89 for the thioformyl proton. Further, the appearance of a doublet of quartets for the methylene protons of the ethyl groups suggests restricted rotation around the C-N bond, making the methylene protons of the ethyl groups nonequivalent. The methyl protons on the ethyl groups appear as a broad singlet. The ^{1}H and $^{13}C\{^{1}H\}$ NMR spectral results are similar to those for uncoordinated *N,N*-diethylthioformamide, which show two quartets for the methylene protons and two triplets for the methyls.[83] The presence of two resonances for the methylene protons, implies either that rotation around the carbon-nitrogen bond is restricted due to significant C-N double bond character or that an anisotropic effect leads to methylene protons splitting each other resulting in a quartet of doublets.[84] The carbon-nitrogen bond length established by the crystal structure is 1.291 Å, shorter than the usual single, 1.472 Å, or partial double, 1.352 Å, bond lengths.[85] In fact, the carbon-nitrogen bond length is the same as that of a carbon-nitrogen double bond in a cyanodithiocarbamate ligand reported by Cotton and Harris.[86] It is therefore likely that there is sufficient double bond character to inhibit free rotation around the carbon-nitrogen bond.

Syntheses and Characterization of $[(\eta^6\text{-}C_6Me_6)Mn(CO)_2SCHNHPh][BF_4]$ (54) and $[(\eta^6\text{-}C_6Me_6)Mn(CO)_2SCHNH(t\text{-}Bu)][BF_4]$ (55)

The reactions of aniline and *tert*-butylamine with **52** result in the formation of $[(\eta^6\text{-}C_6Me_6)Mn(CO)_2SCHNHPh][BF_4]$ (**54**), a dark orange complex, and $[(\eta^6\text{-}C_6Me_6)Mn(CO)_2SCHNH(t\text{-}Bu)][BF_4]$ (**55**), a light orange complex, respectively, as shown in eq 19. The unsymmetrical mono-substituted thioformamide can form *cis*

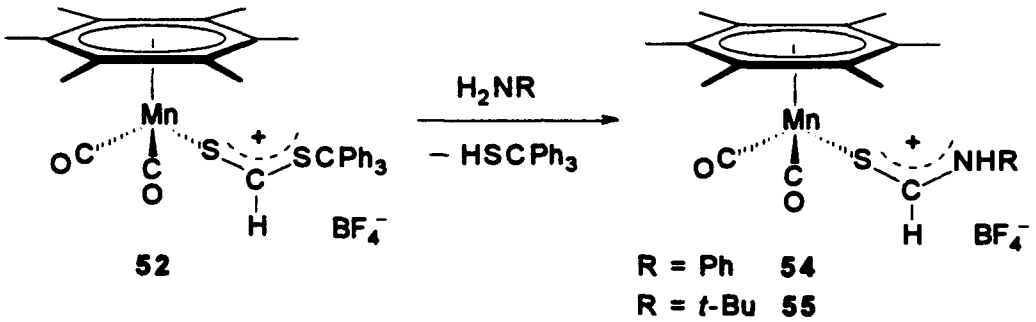

(19)

and *trans* isomers due to the restricted rotation around the carbon-nitrogen bond. The ^1H NMR spectrum of **54** indicates that apparently only one isomer is formed with singlets at δ 10.71 for the thioformyl proton and at δ 9.36 for the amide proton. The ^1H NMR spectral evidence for **55** indicates the formation of cis and trans isomers with singlets at δ 10.18 and 10.90 for the thioformyl proton and two doublets at δ 8.74 and 8.82 for the amide proton.

Reactions of $[(\eta^6\text{-}C_6Me_6)Mn(CO)_2SCHSCPh_3][BF_4]$ (52) with Alcohols

The reaction of methanol and ethanol with **52** produced similar color changes in solution to those observed in the reactions with amines and a shift to lower frequency of the carbonyl stretches in the IR spectra.[87] The ^1H NMR spectra of the products were also consistent with *O*-alkyl thioformates, but these were not isolated. This is to

be expected since coordinated *O*-alkyl thioformate ligands are reported to be unstable, dissociating even at low temperatures.[88] In our laboratories it has been observed that the product of an insertion reaction of carbonyl sulfide (COS) into a manganese hydrogen bond, presumably a thioformate, shows complete dissociation with liberation of COS at low pressure after its formation at high pressures.[89]

Reaction of $[(\eta^6\text{-}C_6Me_6)Mn(CO)_2SCHSCPh_3][BF_4]$ (52) with BH_4^-

The addition of excess BH_4^- to **52** results in a reaction which produces species that display carbonyl stretching frequencies slightly higher than those for **51**, 1972 and 1925 cm^{-1}, and broadened. Attempted purification by column chromatography did not effect isolation of the products. The ^1H NMR spectrum displays peaks for **1** and a species which we tentatively assign as an η^1-coordinated methanethiolate. The methanethiolate complex may result from hydride transfer from the product counterion, $H_3BSCPh_3^-$, to an intermediate coordinated thioformaldehyde, both possible products of BH_4^- reacting with **52**. In similar reactions, the reduction of coordinated thiocarbonyls by hydride transfer has been reported to produce (thioformaldehyde)- and (methanethiolato)osmium complexes.[90] The proposed product, $(\eta^6\text{-}C_6H_6)Mn(CO)_2SCH_3$, has carbonyl stretching frequencies similar to those reported for $(\eta^6\text{-}C_6H_6)Mn(CO)_2SPh$, ν_{CO} = 1973, 1923 cm^{-1}.[91]

Reaction of $[(\eta^6\text{-}C_6Me_6)Mn(CO)_2SCHSCPh_3][BF_4]$ (52) with BEt_3H^-

The addition of a stoichiometric amount of BEt_3H^- to **52** results in a reaction which produces species that have carbonyl frequencies at 1969 and 1920 cm^{-1}. The ^1H NMR spectrum suggests the formation of several products including **51**, **52**, and an η^1-coordinated methanethiolate complex as was observed with BH_4^-. No peaks were observed that could be assigned to the proposed thioformaldehyde intermediate; however, the intermediate may have undergone rapid decomposition involving loss of

thioformaldehyde.[68]

Synthesis and Characterization of $[Mn_2(\eta^6\text{-}C_6Me_6)_2(CO)_4S_2CH]^+$ (56)

As Schauer et al. previously reported, the decomposition of **51** to **56** is slow under ambient conditions and increases rapidly with increasing temperature.[20] The FAB tandem MS provides an unambiguous assignment of structural features of the bridged dithioformate dimanganese complex. Similar behavior was observed for $[W(CO)_3(dppe)(SC(S)H)]^-$ decomposing to the binuclear species, $[(W(CO)_3(dppe))_2(\mu\text{-}S_2CH)]^-$ by Schenk et al.[68]

FAB Tandem Mass Spectrometry

Compounds **51** and **56** have previously been examined by FAB-MS and were reanalyzed by FAB tandem mass spectrometry for comparison and validation of our results.[20] In all cases, the fragment ion resulting from the loss of two carbonyls was more abundant than the fragment ion from loss of one carbonyl. This suggests that the second carbonyl is more easily dissociated than the first carbonyl alone or in conjunction with loss of part or all of the thioformamide ligand. The structural components of compounds **52–55** are unambiguously identified using FAB-MS/MS. The bare metal ion (*m/z* 55) is observed in each case.

The chemical composition and relative abundance of the molecular and CID product ions of **51** (*m/z* 351) are shown in Table 59; the CID FAB tandem mass spectrum of **51** is shown in Figure 14. Loss of dithioformate (*m/z* 273) with subsequent sequential loss of the two carbonyls (*m/z* 245 and 217), as well as the loss of both carbonyls (*m/z* 295) followed by loss of the dithioformate, results in the appearance of the $[Mn(HMB)]^+$ (*m/z* 217) fragment ion. In addition, fragment ions showing initial loss of HMB (*m/z* 189) followed by loss of carbonyls (*m/z* 161 and 133) are observed.

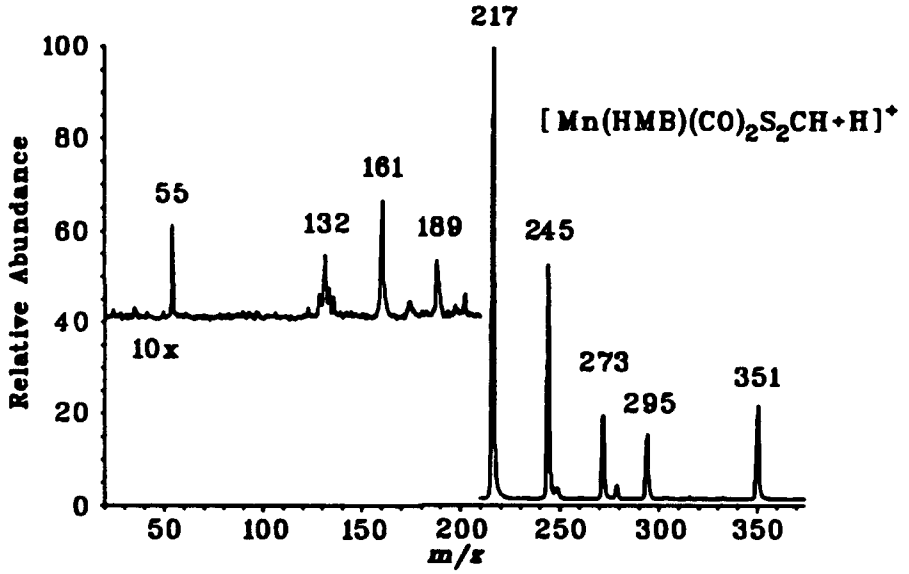

Figure 14. Low-energy collision spectrum of **51** (*m/z* 351)

Table 59. Abundant Ions in the FAB-MS/MS Spectrum of **51**

m/z	structural assignment	rel abund [a]
351	[M] [b]	21
295	[M] − 2 CO	14
273	[M] − $[SC(S)H]^-$ and H^+	19
245	[M] − $[SC(S)H]^-$, CO, and H^+	52
217	$[Mn(HMB)]^+$	100
189	[M] − HMB	1
161	[M] − HMB and CO	1
133	[M] − HMB and 2 CO	1
55	Mn^+	1

[a] Abundances are relative to 100 for the most abundant analyte ion listed.

[b] $[M] = [Mn(HMB)(CO)_2SC(S)H + H]^+$.

These fragment ions are much lower in relative abundance due to the bonding strength of HMB to the metal. These results unambiguously characterize the structure of **51**.

The chemical composition and relative abundance of the molecular and CID product ions of **52** (*m/z* 593) are shown in Table 60; the CID FAB tandem mass spectrum of **52** is shown in Figure 15. Compound **52**, formed in situ, was analyzed in a solution of tetramethylene sulfone. The major peak (*m/z* 243) is due to the metastable triphenylcarbenium ion. The loss of trityl cation produces $[Mn(HMB)(CO)_2(SCHS) + H]^+$ (*m/z* 351). The additional loss of carbonyls produces $[Mn(HMB)(SCHS) + H]^+$ (*m/z* 294). The loss of CO, trityl cation, and HMB results in $[Mn(CO)(SCHS) + H]^+$ (*m/z* 161) and $[Mn(SCS)]^+$ (*m/z* 131). $[Mn(SCHSCPh_3)]^+$ (*m/z* 375) results from the loss of HMB and CO. Loss of triphenylmethyl thioformate ester and CO gives the characteristic $[Mn(HMB)]^+$ (*m/z* 217) ion. The cleavage of a C–C bond results in loss of phenyl and the loss of CO gives $[Mn(HMB)(CO)(SCHSCPh_2]^+$ (*m/z* 490). The formation of $Ph_3CSSCPh_3$ (*m/z* 375) is also observed.

The chemical composition and relative abundance of the molecular and CID product ions of **53** (*m/z* 390), **54** (*m/z* 410), and **55** (*m/z* 390) are shown in Tables 61–63, respectively; the CID FAB tandem mass spectra of **53–55** are shown in Figures 3–5, respectively. The major product ion (*m/z* 334) for **53** and **55** is formed by the elimination of the two carbonyl ligands. In contrast with the dissociation of **51** and **54**, which show the $[Mn(HMB)]^+$ (*m/z* 217) fragment ion to be the most stable, the thioformamide ligands in **53** and **55** show stronger bonding to the metal. The HMB is more strongly bonded to Mn than are dithioformate or the thioformamides, which is indicated by the ratio of the intensities of their metal-bonded fragment ions (*m/z* 217 and 132/172/192, respectively).

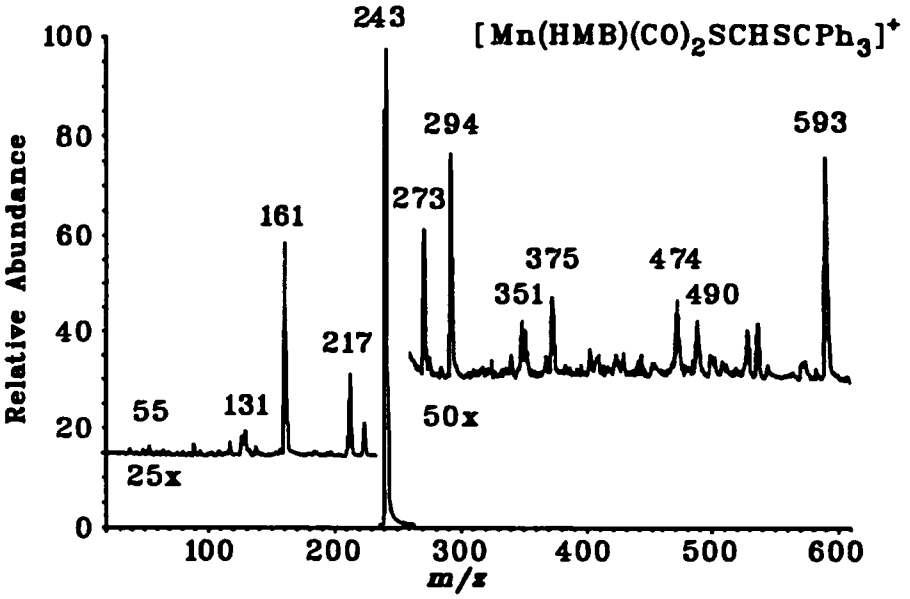

Figure 15. Low-energy collision spectrum of **52** (*m/z* 593)

Table 60. Abundant Ions in the FAB-MS/MS Spectrum of **52**

m/z	structural assignment	rel abund[a]
593	[M][b]	0.6
490	[M] − Ph and CO	0.2
474	$Ph_3CSSCPh_3$	0.3
375	[M] − HMB and 2 CO	0.3
351	[M] − Ph_3C^+ + H^+	0.2
350	[M] − Ph_3C^+	0.3
294	[M] − Ph_3C^+ and 2 CO	0.9
273	[M] − [(S)CHSCPh$_3$]	0.6
243	Ph_3C^+	100
217	[Mn(HMB)]$^+$	0.6
161	[M] − HMB, CO, Ph_3C^+ + H^+	0.2
131	[M] − HMB, 2CO, Ph_3C^+, H^-	0.2
55	Mn^+	<0.1

[a] Abundances are relative to 100 for the most abundant analyte ion listed.

[b] [M] = [Mn(HMB)$(CO)_2$(SCHSCPh$_3$)]$^+$.

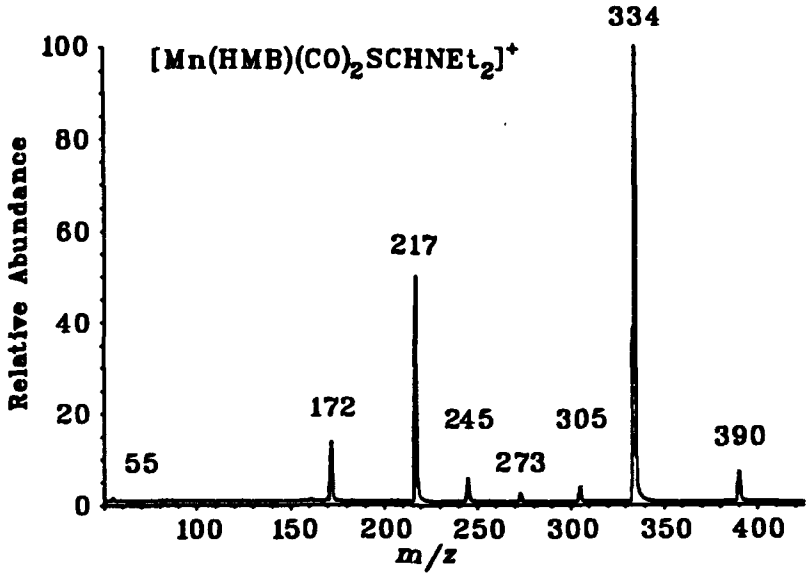

Figure 16. Low-energy collision spectrum of **53** (*m/z* 390)

Table 61. Abundant Ions in the FAB–MS/MS Spectrum of **53**

m/z	structural assignment	rel abund [a]
390	[M] [b]	6
334	$[M]^+ - 2$ CO	100
305	$[M]^+ - 2$ CO and Et	3
273	$[M]^+ - [(S)CHNEt_2]$	2
245	$[M]^+ - [(S)CHNEt_2]$ and CO	5
217	$[Mn(HMB)]^+$	49
172	$[M]^+ -$ HMB and 2 CO	13
55	Mn^+	1

[a] Abundances are relative to 100 for the most abundant analyte ion listed.

[b] [M] = $[Mn(HMB)(CO)_2SCHNEt_2]^+$.

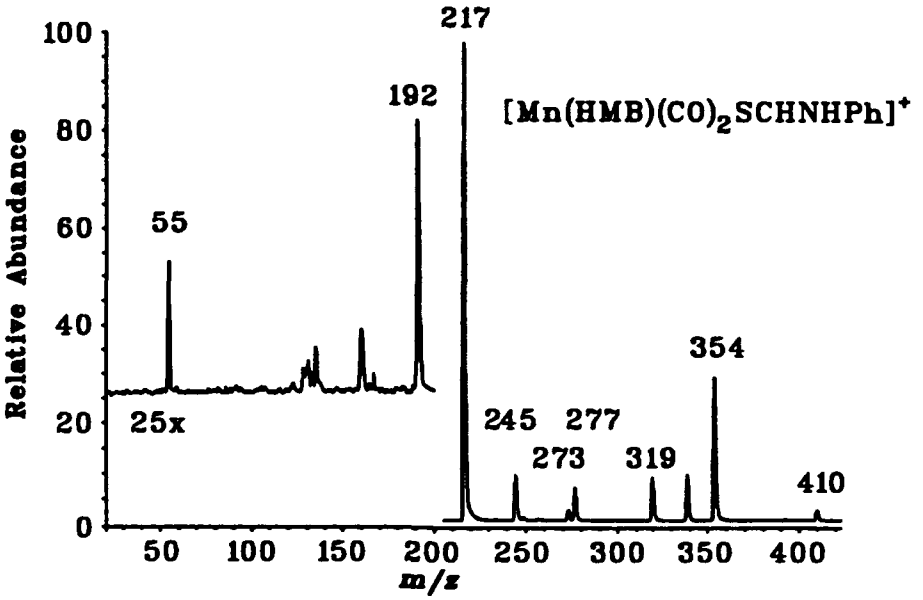

Figure 17. Low-energy collision spectrum of **54** (*m/z* 410)

Table 62. Abundant Ions in the FAB-MS/MS Spectrum of **54**

m/z	structural assignment	rel abund [a]
410	[M] [b]	2
354	[M] − 2 CO	29
319	[Mn(HMB)NHPh + H^+]$^+$	8
277	[M] − Ph and 2 CO	7
273	[M] − [(S)CHNHPh]	2
245	[M] − [(S)CHNHPh] and CO	9
217	[Mn(HMB)]$^+$	100
192	[M] − HMB and 2 CO	3
55	Mn^+	1

[a] Abundances are relative to 100 for the most abundant analyte ion listed.

[b] [M] = [Mn(HMB)$(CO)_2$SCHNHPh]$^+$.

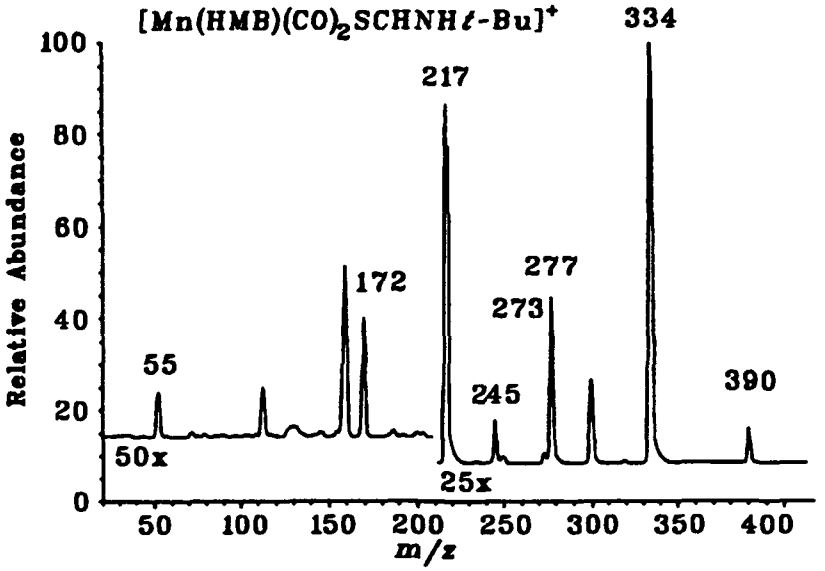

Figure 18. Low-energy collision spectrum of **55** (*m/z* 390)

Table 63. Abundant Ions in the FAB-MS/MS Spectrum of **55**

m/z	structural assignment	rel abund [a]
390	[M] [b]	7
334	[M] − 2 CO	100
277	[M] − *t*-Bu and 2 CO	36
273	[M] − [(S)CHNH-*t*-Bu]	2
245	[M] − [(S)CHNH-*t*-Bu] and CO	9
217	$[Mn(HMB)]^+$	84
172	[M] − HMB and 2 CO	1
55	Mn^+	<1

[a] Abundances are relative to 100 for the most abundant analyte ion listed.

[b] [M] = $[Mn(HMB)(CO)_2SCHNH\text{-}t\text{-}Bu]^+$.

Consideration of the relative intensities of product ions (*m/z* 334/354/334), resulting from the loss of two carbonyls from **53/54/55**, (*m/z* 217) from $[Mn(HMB)]^+$, and (*m/z* 172/192/172), from the manganese thioformamide fragments of **53/54/55** provides an ordering of the relative strengths of the thioformamide bonding to Mn: NEt_2 > NH-*t*-Bu > NHPh; with respect to one another. For the monosubstituted thioformamides **54** and **55**, the bonding of the thioformamide ligand to the metal is not as enhanced as in **53**. The *tert*-butylthioformamide is more strongly bonded than the phenyl derivative. A recurring dissociation pattern is observed after the loss of the thioformamide ligand (*m/z* 273) as the two carbonyls are lost (*m/z* 245 and 217) to form the $[Mn(HMB)]^+$ fragment ion; loss of the thioformamide from *m/z* 334 in **53** and **55** and from *m/z* 354 in **54** also contributes to the intensity of this ion. The third peak (*m/z* 305) for **53** shows the cleavage of a C-N bond of one of the ethyl groups. The fourth peak (*m/z* 320) for **54** shows the cleavage of the phenyl C-N bond within the thioformamide. The third peak (*m/z* 277) for **55** shows the cleavage of the butyl C-N bond within the thioformamide. The FAB tandem mass spectral interpretation gives an unambiguous structural connectivity for **53-55**.

The chemical compositions and relative abundances of the molecular and CID product ions of **56** (*m/z* 623) are shown in Table 64. Within 30 s of initial bombardment, the bridged binuclear species **56** is formed from **51** in the FAB ion source. The CID FAB tandem mass spectrum of **26** is shown in Figure 19. Carbonyls are removed in pairs from the bridged dithioformate dimanganese complex: loss of the first two carbonyls results in the fragment ion at *m/z* 567 and an additional loss of another pair results in the fragment ion at *m/z* 511. All but three of the fragment ions (*m/z* 294, 132, and 55, the bare metal ion) retain the bridging dithioformate indicating an enhanced strength of the M-S bonds.

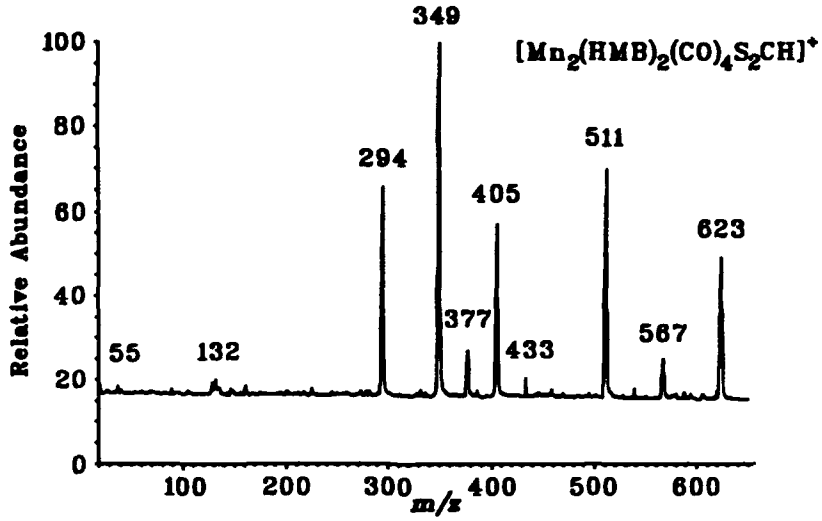

Figure 19. Low-energy collision spectrum of **56** (*m/z* 623)

Table 64. Abundant Ions in the FAB-MS/MS Spectrum of **56**

m/z	structural assignment	rel abund [a]
623	[M] [b]	40
567	[M] − 2 CO	12
539	[M] − 3 CO	4
511	[M] − 4 CO	65
433	[M] − HMB and CO	6
405	[M] − HMB and 2 CO	49
377	[M] − HMB and 3 CO	14
349	[M] − HMB and 4 CO	100
294	[M] − Mn, HMB, and 4 CO	59
132	[M] − Mn, 2 HMB, and 4 CO	5
55	Mn^+	<2

[a] Abundances are relative to 100 for the most abundant analyte ion listed.

[b] [M] = $[Mn_2(HMB)_2(CO)_4S_2CH]^+$.

The enhanced stability of the bridged species allows the scission of one HMB as evidenced by fragment ions that show loss of one carbonyl (*m/z* 433), two carbonyls (*m/z* 405), three carbonyls (*m/z* 377), and all four carbonyls (*m/z* 349), which gives the major fragment ion. The bare metal ion (*m/z* 55) is also observed. This dissociation pattern is more straightforward than the comparable FAB mass spectrum reported previously, since all observed fragments must result from the molecular ion.[20]

Crystallographic Study of $[(\eta^6\text{-}C_6Me_6)Mn(CO)_2SCHNEt_2][BF_4]$ (53)

The crystallographic study was performed to establish the molecular structure of **53**, which is illustrated in the ORTEP plots in Figures 20 and 21. Positional parameters are reported in Appendix D. Selected bond distances and angles are given in Table 65. As seen in Figure 21, the molecule has a "piano stool" arrangement with the three ligands underneath in a staggered configuration with respect to the ring carbons. The HMB ring is slightly tilted away from the sulfur as evidenced by the shorter Mn–C bonds to C(4) and C(5), which are greater than the bonds to C(1) and C(2).

The bonding in the manganese thioformamide fragment of **53** is of particular interest in understanding the results of spectroscopic methods used in the characterization of **53–55**. The Mn–S bond, 2.322 Å, is shorter than that in $(Ph_2P\text{-}CH_2\text{-}PPh_2)Mn(CO)_3(\eta^2\text{-}S_2CH)$ (Mn–S = 2.40 and 2.39 Å)[92] and $(\eta^6\text{-}C_6H_6)Mn(CO)_2SPh$ (Mn–S = 2.350 Å),[91] but is between the distances in $[Mn_2(CO)_6(\mu\text{-}S_2CPCy_3)]$ (Mn(I)–S = 2.282, 2.276, 2.335, and 2.332 Å).[93] The short length of our Mn–S bond suggests a very strong Mn–S interaction. The carbon–sulfur bond length, 1.686 Å, is equal to the shorter of the two C–S bonds in $Ni[\eta^2\text{-}S_2C\text{-}NH_2]_2$,[94] $[NH_4][S_2C\text{-}NH_2]$,[95] and the aforementioned cyanodithiocarbamate.[86] The C–N bond of the thioformamide is equal in length to the carbon–nitrogen double bond in the aforementioned cyanodithiocarbamate.[86]

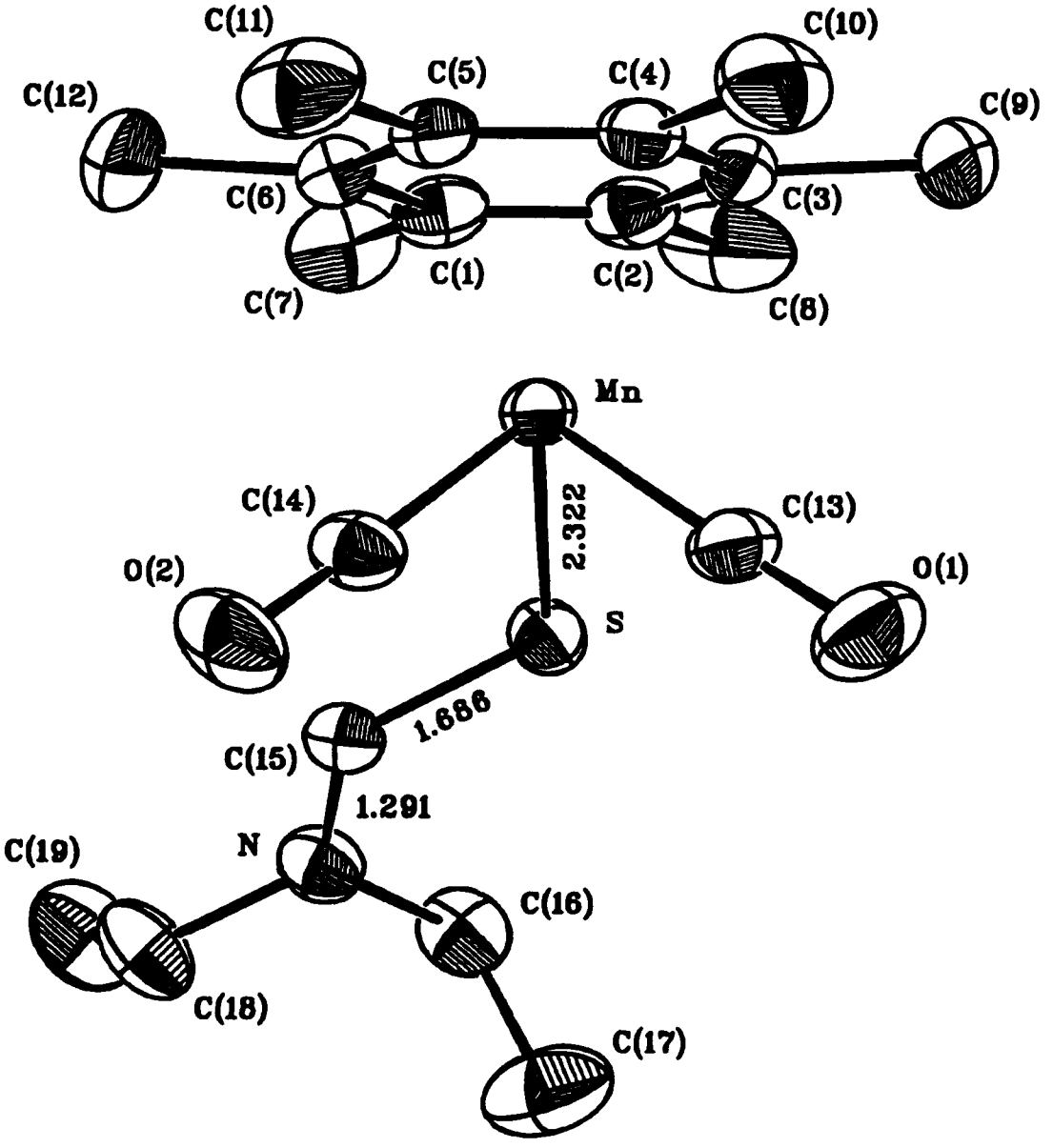

Figure 20. ORTEP drawing of 53 with 25% probability ellipsoids

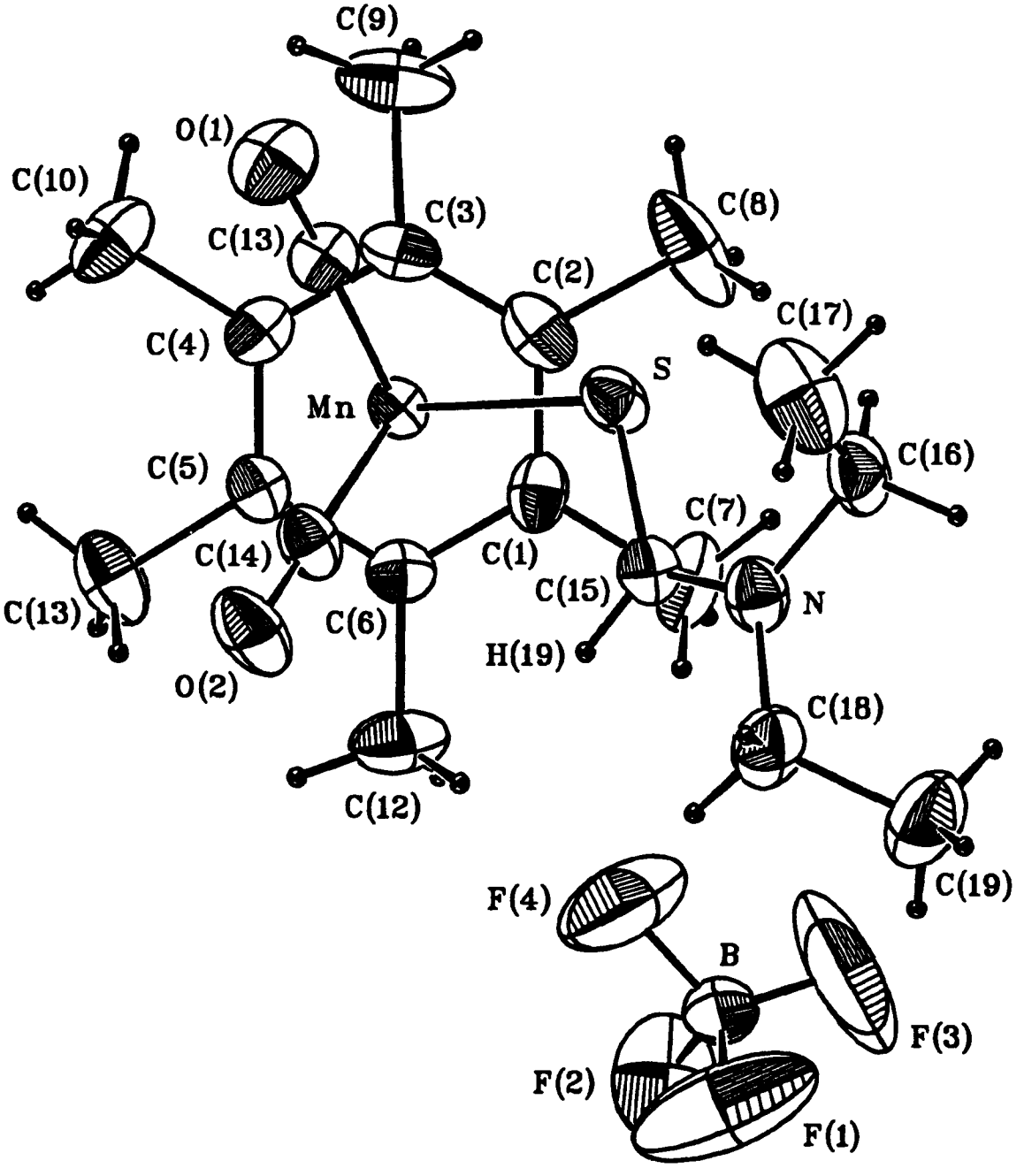

Figure 21. ORTEP drawing of 53 with 25% probability ellipsoids (bottom view)

Table 65. Selected Bond Distances (Å) and Angles (°) for **53**

		Distances	
Mn–C(1)	2.216 (5)	C(1)–C(2)	1.40 (1)
Mn–C(2)	2.197 (6)	C(1)–C(6)	1.394 (8)
Mn–C(3)	2.198 (6)	C(1)–C(7)	1.536 (9)
Mn–C(4)	2.164 (5)	C(2)–C(3)	1.41 (1)
Mn–C(5)	2.178 (5)	C(2)–C(8)	1.54 (1)
Mn–C(6)	2.221 (6)	C(3)–C(4)	1.426 (9)
Mn–C(13)	1.783 (7)	C(3)–C(9)	1.51 (1)
Mn–C(14)	1.776 (6)	C(4)–C(5)	1.379 (9)
Mn–S	2.322 (2)	C(4)–C(10)	1.512 (9)
S–C(15)	1.686 (6)	C(5)–C(6)	1.448 (8)
N–C(15)	1.291 (8)	C(5)–C(11)	1.504 (9)
N–C(16)	1.47 (1)	C(6)–C(12)	1.49 (1)
N–C(18)	1.482 (9)	C(16)–C(17)	1.46 (1)
O(1)–C(13)	1.142 (8)	C(18)–C(19)	1.51 (1)
O(2)–C(14)	1.150 (7)	C(15)–H(19)	0.947 (1)
		Angles	
S–Mn–C(13)	87.1 (2)	C(16)–N–C(18)	118.5 (6)
S–Mn–C(14)	91.8 (2)	N–C(16)–C(17)	112.7 (7)
C(13)–Mn–C(14)	89.5 (3)	N–C(18)–C(19)	113.3 (7)
Mn–C(13)–O(1)	178.3 (6)	C(1)–C(2)–C(3)	120.3 (6)
Mn–C(14)–O(2)	178.0 (6)	C(2)–C(3)–C(4)	119.3 (5)
Mn–S–C(15)	111.5 (2)	C(3)–C(4)–C(5)	120.6 (5)
S–C(15)–N	124.4 (5)	C(4)–C(5)–C(6)	119.7 (5)
C(15)–N–C(16)	122.0 (5)	C(5)–C(6)–C(1)	119.5 (6)
C(15)–N–C(18)	119.2 (6)	C(6)–C(1)–C(2)	120.6 (6)
S–C(15)–H(19)	117.2 (6)	N–C(15)–H(19)	118.5 (6)

[a] Values for the esd, in this and subsequent tables, are given in parentheses.

The atoms Mn, S, C(15), H(19) (the thioformyl hydrogen), N, C(16), and C(18) were all found to lie in the same plane by a least-squares plane analysis,[41] Appendix D.

Bond angles within the *N,N*-diethylthioformamide ligand are S-C(15)-N = 124.4°, S-C(15)-H(19) = 117.8°, N-C(15)-H(19) = 117.8°, C(15)-N-C(16) = 122.0°, C(15)-N-C(18) = 119.2°, and C(16)-N-C(18) = 118.5°, which indicate significant sp^2 character in the bonding of the amide nitrogen. The planar geometry about the nitrogen indicates that the lone pair electrons have been delocalized into the N-C-S π-bonding system. This results in decreased length of the C-N bond and inequivalence of the methylene protons in the ^{1}H NMR spectrum resulting from hindered rotation about that bond.

Conclusions

Triphenylcarbenium ion reacts with **51**, not with hydride abstraction, but by simple addition to the uncoordinated sulfur of the η^1-dithioformate. Addition of either secondary or primary amines to the η^1-coordinated alkyl dithioformate ester results in the nucleophilic displacement of the thiolate to form thioformamide complexes. Other nucleophiles, such as alcohols and hydrides, produce analogous displacement reactions forming thioformates, thioformaldehyde, and methanethiolate complexes, which are less stable than the thioformamides. Addition of other Lewis acids to the uncoordinated sulfur of **51** would probably produce similar reactivity at the thioformyl carbon. The η^1-dithioformate ester ligand donates more electron density than the *N*-alkylthioformamides; this is indicated by carbonyl stretching frequencies which decrease with increasing electron density on the metal. The FAB-MS/MS data suggest a strong Mn-S bond which may arise because of delocalization of electron density through the Mn-S-C-N bonds. The crystal structure of **53** reveals substantial delocalization of the nitrogen lone-pair electrons through the N-C-S moiety of the ligand, resulting in planarity of that moiety.

APPENDIX A

SUPPLEMENTAL TABLES

FOR

PHOSPHINE DERIVATIVES OF MANGANESE COMPLEXES

Table 66. ^{1}H and $^{13}C\{^{1}H\}$ NMR Spectral Data for **1a–e**

	^{1}H NMR	$^{13}C\{^{1}H\}$ NMR
R	δ, ppm [a]	δ, ppm [b]
n-Bu	2.32 (s, 18 H, Me)	226.8 (d, CO, J_{C-P} = 29.5)
(1a)	1.41 (m, 18 H, P(*n*-Bu)$_3$)	110.2 (s, ring-C)
	0.95 (t, 9 H, P(*n*-Bu)$_3$, $^{2}J_{H-H}$ = 6.3 Hz)	26.3-24.5 (m, P(*n*-Bu)$_3$)
		17.3 (s, ring-CH_3)
Me	2.35 (s, 18 H, Me)	225.7 (d, CO, J_{C-P} = 29.1 Hz)
(1b)	1.51 (d, 9 H, PMe_3, J_{P-H} = 9.76 Hz)	110.2 (s, ring-C)
		18.5 (d, PMe_3, J_{C-P} = 30.3 Hz)
		17.2 (s, ring-CH_3)
Ph	7.6-7.4 (m, 15 H, Ph)	233.8 (s, CO)
(1c)	2.05 (s, 18 H, Me)	134.2, 132.6, 130.1, 129.9 (PPh_3)
		109.4 (s, ring-C)
		17.8 (s, ring-CH_3)
OMe	3.85 (d, 9 H, P(OMe)$_3$, J_{P-H} = 11.25 Hz)	227.6 (d, CO, J_{C-P} = 47.6 Hz)
(1d)	2.44 (s, 18 H, Me)	109.5 (s, ring-C)
		55.1 (d, P(OMe)$_3$)
		17.5 (s, ring-CH_3)
OPh	7.3-7.0 (m, 15 H, Ph)	228.1 (s, CO)
(1e)	2.31 (s, 18 H, Me)	148.8, 129.5, 124.1, 120.4 (P(OPh)$_3$)
		109.7 (s, ring-C)
		17.1 (s, ring-CH_3)

[a] (mult, no. protons, assignment, coupling).

[b] (mult, assignment, coupling).

Table 67. Comparison of Infrared Carbonyl Stretching Bands for **1a–e**, **11a–e**, **2a–e**

	ν_{CO}, cm^{-1} [a]		
R	$Mr(6)PR_3^+$	$Mc(6)PR_3$ [b]	$Mz(5)PR_3$
n-Bu	1969, 1920 1977, 1930 [c]	1908, 1846	1920, 1859 1928, 1867 [d]
Me	1972, 1923 1981, 1933 [c]	1910, 1847	1924, 1858 1932, 1870 [d]
Ph	1978, 1926 1983, 1935 [c]	1913, 1865	1927, 1864 1934, 1878 [d]
OMe	1990, 1941	1924, 1865	1939, 1877 1948, 1886 [d]
OPh	1996, 1947 2003, 1956 [c]	1941, 1882	1955, 1893 1964, 1899 [d]

[a] Solution spectra obtained in THF unless otherwise noted. $Mr(6)PR_3^+ \equiv [(\eta^6\text{-}C_6Me_6)Mn(CO)_2PR_3]^+$. $Mc(6)PR_3 \equiv (\eta^5\text{-}C_6Me_6H)Mn(CO)_2PR_3$. $Mz(5)PR_3 \equiv (\eta^5\text{-}C_6Me_5CH_2)Mn(CO)_2PR_3$.

[b] Snyder, D. B.; Schauer, S. J.; Eyman, D. P.; Moler, J. L.; Weers, J. J., *J. Am. Chem. Soc.*, in press.

[c] Solution spectra obtained in dichloromethane.

[d] Solution spectra obtained in hexane.

Table 68. ^{31}P NMR Data for **1a–e** and **11a–e**

R	δ, ppm [a]		
	$Mr(6)PR_3^+$	$Mc(6)PR_3$ [b]	$Mz(5)PR_3$ [c]
n-Bu	55.5	54.2	57.2
Me	36.3	36.3	21.3
Ph	79.7	79.9	83.0
OMe	185.7	196.5	196.4
OPh	170.3	177.2	170.0

[a] Obtained in d_6-acetone at 298 K and externally referenced to H_3PO_4 (85%) unless otherwise noted.

[b] Snyder, D. B.; Schauer, S. J.; Eyman, D. P.; Moler, J. L.; Weers, J. J., *J. Am. Chem. Soc.*, in press.

[c] Obtained in d_6-benzene at 298 K.

APPENDIX B

SUPPLEMENTAL TABLES AND FIGURES

FOR

THE CRYSTAL STRUCTURE

AND

MOLECULAR MODELING

OF

$(\eta^5\text{-}C_6Me_5CH_2)Mn(CO)_2PMe_3$

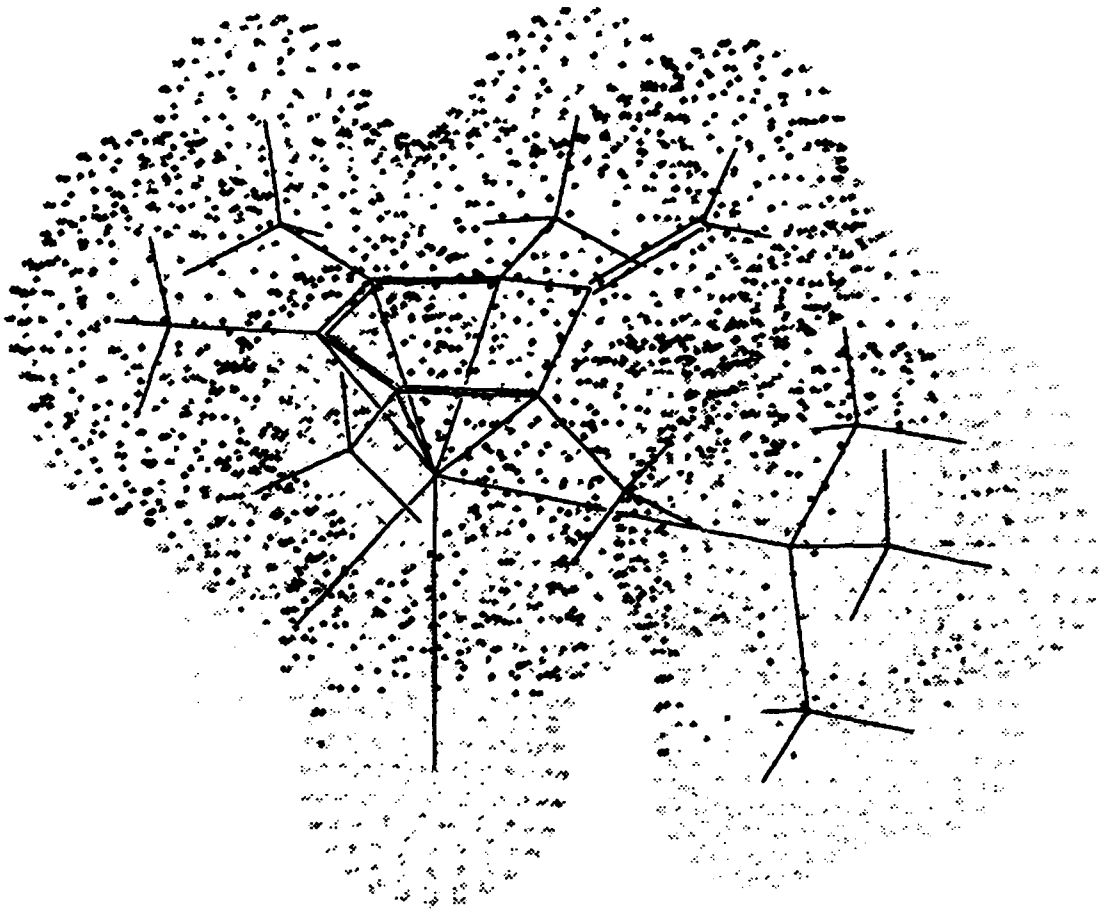

Figure 22. Molecular model of 2b based on crystallographic parameters

The molecular modeling illustration of **2b**, Figure , was obtained using the SYBYL 6.0 Molecular Modeling Software, TRIPOS Assoc. Inc., St. Louis, MO, Nov. 92. The structure geometry and energy minimized using the MAXMIN2 program and elevating the temperature to 500 K in 50 K increments and then cooling to 300 K.

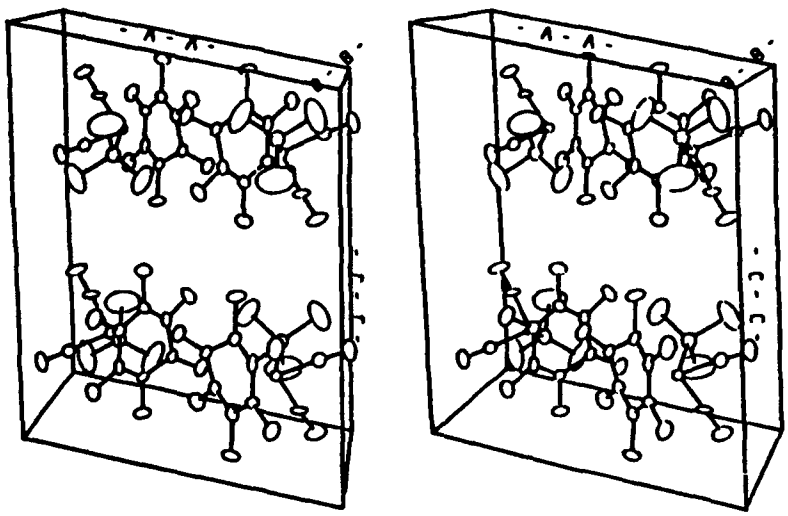

Figure 23. Stereoscopic view of the unit cell of **2b**

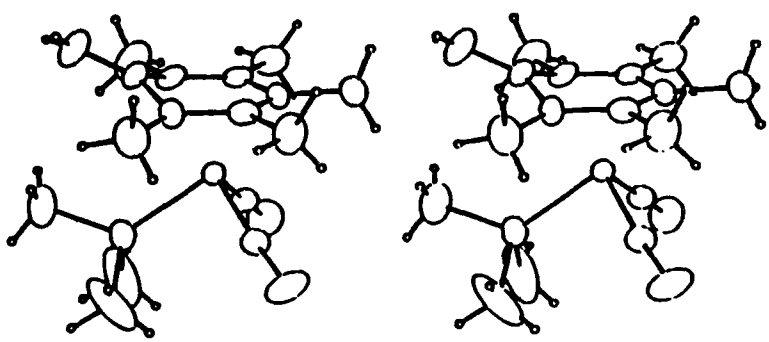

Figure 24. Stereoscopic view of **2b** (single molecule)

Table 69. Complete Crystallographic Data and Refinement Parameters for **2b**

empirical formula	$MnPO_2C_{17}H_{26}$
fw, amu	420.37
color of crystal	burnt orange
crystal dimensions, mm	0.39 × 0.15 × 0.12
space group	$P2_1/c$ (No. 14)
cell dimensions	
a, Å	11.967 (4)
b, Å	10.093 (6)
c, Å	15.232 (4)
β, deg	102.70 (5)
V, Å^3	1795 (1)
Z	4
ρ_{calc}, g/cm^3	1.556
wavelength (λ), Å (graphite)	0.710 73
μ, cm^{-1} (Mo Kα)	7.7
T (data collection), K	296 (2)
omega (ω) scan range	0.80 + 0.35 tan(θ)
omega (ω) scan speed, deg/min (θ from 1° to 25°)	3.3−0.71
horizontal aperture, mm	2.5-3.0
linear abs coeff, cm^{-1}	6.9
max and min corrections on F	1.00-0.97
crystal decay, %	10.7
reflections collected (1-25°)	4649
reflections > 3 σ	1163
after averaging	2047
parameters refined	185
R_1 [b]	0.059
R_2 [c]	0.078
residual electron density in final DF map, e^-/Å^3	0.56
std deviation, obs. of unit wt	1.28
largest shift/esd	0.03
systematic absences	none

[a] In this and subsequent tables esd's are given in parentheses.

[b] $R_1 = \Sigma \| F_o | - | F_c \| / \Sigma | F_o |$.

[c] $R_2 = [\Sigma w(| F_o | - | F_c |)^2 / \Sigma w | F_o |^2]^{1/2}$, $w = 1/\sigma^2(F)$, where $\sigma^2(F) = \sigma^2(F) + [(PWT)F]^2$, PWT = 0.07.

Table 70. Fractional Coordinates and Isotropic Thermal Parameters for Hydrogen Atoms of **2b**

atom	x	y	z	B_{iso}, Å^{2} [a]
H7c	0.484	0.220	0.808	8.8
H7a	0.530	0.109	0.877	8.8
H7b	0.417	0.182	0.882	8.8
H8c	0.375	−0.138	0.939	8.9
H8a	0.263	−0.056	0.926	8.9
H8b	0.381	0.015	0.946	8.9
H9c	0.143	−0.287	0.746	9.1
H9b	0.166	−0.221	0.840	9.1
H9b	0.253	−0.322	0.817	9.1
H10a	0.212	−0.319	0.617	9.7
H10b	0.193	−0.214	0.541	9.7
H10c	0.109	−0.222	0.604	9.7
H11a	0.254	−0.078	0.499	10.2
H11b	0.386	−0.061	0.518	10.2
H11c	0.308	0.062	0.513	10.2
H12a	0.576	0.101	0.714	9.6
H12b	0.510	0.095	0.607	9.6
H15a	0.016	0.304	0.614	10.0
H15b	0.090	0.398	0.569	10.0
H15c	0.068	0.253	0.535	10.0
H16a	0.266	0.369	0.797	12.0
H16b	0.200	0.465	0.724	12.0
H16c	0.133	0.367	0.772	12.0
H17a	0.324	0.283	0.571	9.5
H17b	0.293	0.420	0.605	9.5
H17c	0.382	0.330	0.667	9.5

[a] Starred atoms were refined isotropically.

Table 71. Additional Supplemental Bond Distances (Å) and Angles (°) for **2b** [a]

Distances

C10–H10a	0.955 (0)	C9–H9c	0.952 (0)
C10–H10b	0.937 (0)	C9–H9b	0.946 (0)
C10–H10c	0.950 (0)	C9–H9b	0.947 (0)
C11–H11a	0.951 (0)	C15–H15a	0.960 (0)
C11–H11b	0.948 (0)	C15–H15b	0.950 (0)
C11–H11c	0.943 (0)	C15–H15c	0.948 (0)
C12–H12a	0.961 (0)	C16–H16a	0.957 (0)
C12–H12b	0.952 (0)	C16–H16b	0.952 (0)
C7–H7c	0.951 (0)	C16–H16c	0.950 (0)
C7–H7a	0.949 (0)	C17–H17a	0.941 (0)
C7–H7b	0.948 (0)	C17–H17b	0.949 (0)
C8–H8c	0.952 (0)	C17–H17c	0.971 (0)
C8–H8a	0.943 (0)		
C8–H8b	0.949 (0)		

Angles

H10a–C10–H10b	110. (0)	H9c–C9–H9b	109. (0)
H10a–C10–H10c	108. (0)	H9c–C9–H9b	109. (0)
H10b–C10–H10c	110. (0)	H9b–C9–H9b	110. (0)
H11a–C11–H11b	109. (0)	H15a–C15–H15b	108. (0)
H11a–C11–H11c	109. (0)	H15a–C15–H15c	108. (0)
H11b–C11–H11c	110. (0)	H15b–C15–H15c	109. (0)
H12a–C12–H12b	118. (0)	H16a–C16–H16b	108. (0)
H7c–C7–H7a	109. (0)	H16a–C16–H16c	108. (0)
H7c–C7–H7b	109. (0)	H16b–C16–H16c	109. (0)
H7a–C7–H7b	109. (0)	H17a–C17–H17b	110. (0)
H8c–C8–H8a	109. (0)	H17a–C17–H17c	108. (0)
H8c–C8–H8b	109. (0)	H17b–C17–H17c	107. (0)
H8a–C8–H8b	110. (0)		

Table 72. General Displacement Parameter Expressions [a] — U's for **2b**

Name	U(1,1)	U(2,2)	U(3,3)	U(1,2)	U(1,3)	U(2,3)
Mn	0.0401 (8)	0.043 (1)	0.0413 (7)	0.001 (1)	0.0121 (6)	0.003 (1)
P	0.063 (2)	0.055 (2)	0.082 (2)	−0.001 (2)	0.017 (2)	0.016 (2)
O1	0.049 (5)	0.12 (1)	0.126 (8)	−0.011 (6)	−0.011 (6)	−0.003 (7)
O2	0.143 (7)	0.16 (1)	0.076 (5)	0.042 (7)	0.068 (4)	−0.004 (7)
C1	0.037 (6)	0.053 (8)	0.068 (7)	−0.005 (7)	0.006 (5)	0.012 (8)
C2	0.047 (7)	0.059 (8)	0.050 (6)	0.011 (8)	0.003 (5)	−0.010 (8)
C3	0.050 (7)	0.043 (8)	0.050 (6)	0.009 (6)	0.012 (5)	0.021 (6)
C4	0.027 (6)	0.047 (8)	0.094 (9)	0.000 (7)	0.011 (6)	−0.023 (7)
C5	0.041 (6)	0.075 (9)	0.051 (6)	0.004 (8)	0.017 (5)	−0.016 (7)
C6	0.037 (6)	0.066 (9)	0.059 (6)	0.004 (7)	0.016 (5)	0.009 (7)
C7	0.075 (9)	0.08 (1)	0.09 (1)	−0.02 (1)	−0.014 (8)	−0.00 (1)
C8	0.10 (1)	0.12 (1)	0.040 (6)	0.00 (1)	0.007 (7)	0.033 (8)
C9	0.074 (8)	0.06 (1)	0.14 (1)	0.007 (8)	0.044 (8)	0.027 (9)
C10	0.067 (9)	0.08 (1)	0.13 (1)	−0.011 (9)	0.015 (8)	−0.04 (1)
C11	0.11 (1)	0.15 (2)	0.042 (6)	−0.01 (1)	0.033 (6)	−0.011 (9)
C12	0.059 (8)	0.13 (2)	0.11 (1)	−0.002 (9)	0.039 (7)	0.03 (1)
C13	0.057 (7)	0.052 (9)	0.062 (7)	−0.000 (7)	0.017 (6)	−0.015 (6)
C14	0	0	0	0	0	0
C15	0.14 (2)	0.14 (2)	0.30 (2)	−0.03 (1)	−0.07 (2)	0.13 (2)
C16	0.50 (4)	0.05 (1)	0.24 (2)	−0.01 (2)	0.15 (2)	−0.00 (2)
C17	0.17 (1)	0.12 (1)	0.35 (2)	0.04 (1)	0.16 (1)	0.14 (1)

[a] The form of the anisotropic displacement parameter is : $\exp[-2\pi^2\{h^2b^2U(1,1) + k^2b^2U(2,2) + l^2c^2U(3,3) + 2hkabU(1,2) + 2hlacU(1,3) + 2klbcU(2,3)\}]$, where a, b, and c are reciprocal lattice constants.

Table 73. General Displacement Parameter Expressions [a] — B's for **2b**

Name	B(1,1)	B(2,2)	B(3,3)	B(1,2)	B(1,3)	B(2,3)	B_{iso}
Mn	3.17 (6)	3.41 (8)	3.26 (6)	0.09 (9)	0.95 (5)	0.25 (8)	3.24 (3)
P	5.0 (2)	4.3 (2)	6.5 (2)	-0.0 (2)	1.3 (1)	1.3 (2)	5.26 (9)
O1	3.9 (4)	9.6 (8)	10.0 (6)	-0.8 (5)	-0.9 (5)	-0.3 (6)	8.2 (3)
O2	11.3 (6)	12.5 (8)	6.0 (4)	3.3 (6)	5.4 (4)	-0.4 (5)	9.4 (3)
C1	2.9 (5)	4.2 (6)	5.4 (5)	-0.4 (6)	0.5 (4)	1.0 (6)	4.2 (3)
C2	3.7 (5)	4.6 (6)	4.0 (5)	0.8 (6)	0.2 (4)	-0.8 (6)	4.2 (3)
C3	3.9 (5)	3.4 (6)	3.9 (5)	0.7 (5)	1.0 (4)	1.7 (4)	3.7 (3)
C4	2.1 (5)	3.7 (6)	7.4 (7)	0.0 (5)	0.9 (5)	-1.8 (6)	4.5 (3)
C5	3.3 (5)	5.9 (7)	4.0 (5)	0.3 (6)	1.3 (4)	-1.3 (6)	4.3 (3)
C6	2.9 (5)	5.2 (7)	4.7 (5)	0.3 (6)	1.3 (4)	0.7 (6)	4.2 (3)
C7	6.0 (7)	6.5 (9)	7.0 (8)	-1.8 (8)	-1.1 (7)	-0.1 (8)	6.9 (4)
C8	8.0 (8)	9. (1)	3.1 (5)	0.2 (9)	0.6 (5)	2.6 (7)	6.9 (4)
C9	5.8 (7)	4.6 (8)	11.2 (9)	0.5 (7)	3.5 (6)	2.1 (7)	6.9 (4)
C10	5.3 (7)	6.2 (9)	10.2 (9)	-0.9 (7)	1.2 (7)	-3.4 (8)	7.3 (4)
C11	8.7 (8)	12. (1)	3.3 (5)	-1.1 (9)	2.6 (5)	-0.9 (7)	7.9 (5)
C12	4.6 (6)	10. (1)	8.5 (8)	-0.2 (7)	3.0 (5)	2.1 (8)	7.6 (5)
C13	4.5 (6)	4.1 (7)	4.9 (5)	-0.0 (6)	1.3 (5)	-1.1 (5)	4.4 (3)
C14	0	0	0	0	0	0	4
C15	11. (1)	11. (1)	23. (2)	-3. (1)	-5. (1)	10. (1)	16.5 (8)
C16	39. (3)	4. (1)	19. (2)	-1. (2)	12. (2)	-0. (1)	20. (1)
C17	13. (1)	10. (1)	28. (2)	3. (1)	12.3 (9)	11. (1)	15.6 (7)

[a] The form of the anisotropic displacement parameter is : $\exp[-0.25\{h^2b^2B(1,1) + k^2b^2B(2,2) + l^2c^2B(3,3) + 2hkabB(1,2) + 2hlacB(1,3) + 2klbcB(2,3)\}]$, where a, b, and c are reciprocal lattice constants.

Table 74. Deviations [a] from Least-Squares-Planes Analysis for 2b

	1	2	3	4	5	6
C1	−6	−4	−8	0	7	—
C2	9	4	—	—	—	0
C3	−7	−17	—	—	—	0
C4	2	−4	—	—	—	0
C5	2	4	−8	0	−6	—
C6	390	396	26	0	—	—
C7	−74	−68	392	−411	−3	—
C8	13	3	—	—	—	—
C9	84	66	—	—	—	—
C10	−13	−22	—	—	—	—
C11	−28	−22	−397	−418	3	—
C12	950	962	−10	−92	—	—
Mn	−1,705	−1,708	−1,140	−1,066	—	—

	A	B	C	D
1	−7,723	6,249	−1,147	−26,665
2	−7,756	6,211	−1,127	−26,499
3	−4,179	8,669	−2,716	−36,227
4	−3,799	8,807	−2,830	−36,609
5	−8,108	5,769	−990	−25,755
6	−7,608	6,381	−1,181	−27,089

1:3	26.41 ±1.07	2:3	26.72 ±1.17	2:6	1.33	
1:4	28.82 ±1.84	2:4	29.13 ±1.88	3:5	30.02	±1.66
1:5	3.64	2:5	3.34	4:5	32.43	±2.13

[a] Deviations are in Å × 10^3. Atoms used to define the planes are marked with an asterisk (*) following the deviation.

[b] Parameters A, B, C, and D (Å × 10^4) define a plane having the form: $Ax + By + Cz - D = 0$.

Table 75. Calculated FOFC's (× 10) for **2b**

H	K	L	F_{obs}	F_{calc}	SigF	H	K	L	F_{obs}	F_{calc}	SigF	H	K	L	F_{obs}	F_{calc}	SigF
4	2	−17	135	103	14	8	3	−14	159	191	12	4	0	−12	104	136	14
1	6	−17	139	83	14	9	3	−14	114	108	16	5	0	−12	201	172	9
2	1	−16	149	48	12	3	4	−14	111	80	16	6	0	−12	208	224	8
5	1	−16	121	62	16	5	4	−14	157	105	11	8	0	−12	278	274	7
2	4	−16	144	112	12	7	4	−14	112	28	16	1	2	−12	171	168	12
5	4	−16	106	78	17	1	5	−14	137	145	13	2	2	−12	186	188	17
3	5	−16	134	119	13	2	5	−14	102	124	16	3	2	−12	288	285	7
2	7	−16	148	26	13	2	5	−14	196	132	9	5	2	−12	285	300	7
1	8	−16	106	29	16	2	5	−14	115	117	16	7	2	−12	111	107	14
3	8	−16	113	26	17	4	5	−14	103	177	15	8	2	−12	265	267	7
1	1	−15	174	185	10	4	5	−14	169	173	10	1	3	−12	289	306	7
1	1	−15	170	180	11	6	5	−14	129	141	14	2	3	−12	241	263	8
3	1	−15	102	82	16	7	5	−14	120	134	15	4	3	−12	367	372	13
2	2	−15	105	65	14	9	5	−14	132	140	15	6	3	−12	247	241	21
6	2	−15	148	98	13	5	6	−14	124	29	15	8	3	−12	140	157	12
3	3	−15	109	134	14	1	7	−14	115	125	16	9	3	−12	154	149	11
1	4	−15	124	50	13	2	7	−14	209	23	9	11	3	−12	177	160	11
2	4	−15	125	100	12	3	7	−14	122	142	15	5	4	−12	104	72	15
3	4	−15	106	103	15	5	7	−14	133	98	14	2	5	−12	120	120	16
6	4	−15	108	27	17	3	8	−14	151	69	12	3	5	−12	141	146	12
4	5	−15	137	33	13	5	8	−14	111	118	16	4	5	−12	242	223	14
6	5	−15	142	20	13	3	9	−14	114	37	16	6	5	−12	128	143	14
1	6	−15	182	47	10	1	1	−13	172	169	10	7	5	−12	136	161	13
4	7	−15	155	74	12	2	1	−13	252	260	7	9	5	−12	106	120	17
1	8	−15	190	25	10	4	1	−13	289	285	11	1	7	−12	117	130	17
1	0	−14	168	166	10	6	1	−13	234	204	8	2	7	−12	124	95	15
3	0	−14	264	272	7	8	1	−13	167	181	11	4	7	−12	254	247	8
5	0	−14	189	151	9	9	1	−13	168	167	10	6	7	−12	212	226	10
1	1	−14	108	70	14	11	1	−13	159	164	15	7	7	−12	123	133	16
2	1	−14	143	123	11	1	2	−13	114	135	14	2	8	−12	132	129	16
3	1	−14	190	38	9	2	2	−13	165	163	10	1	1	−11	234	258	11
3	1	−14	156	37	11	3	2	−13	170	190	10	2	1	−11	396	393	16
5	1	−14	143	15	12	1	3	−13	112	116	15	3	1	−11	149	156	24
5	1	−14	128	14	14	4	3	−13	143	150	11	4	1	−11	365	378	7
2	2	−14	189	162	9	6	3	−13	167	177	10	5	1	−11	198	201	9
2	2	−14	140	152	12	3	4	−13	141	163	13	7	1	−11	340	338	7
4	2	−14	151	166	12	5	4	−13	180	165	10	9	1	−11	364	350	7
5	2	−14	111	175	14	8	4	−13	142	150	12	1	2	−11	124	137	12
7	2	−14	199	220	9	3	6	−13	182	169	10	3	2	−11	317	330	6
1	3	−14	179	224	10	5	6	−13	228	228	14	4	2	−11	125	150	13
2	3	−14	130	98	13	7	6	−13	131	145	17	5	2	−11	314	317	6
4	3	−14	101	89	15	8	6	−13	175	181	11	1	3	−11	202	201	8
5	3	−14	98	129	16	1	0	−12	175	198	9	2	3	−11	157	156	16
6	3	−14	111	111	15	3	0	−12	250	291	7	4	3	−11	169	173	10

Table 75 — continued

H	K	L	F_{obs}	F_{calc}	SigF	H	K	L	F_{obs}	F_{calc}	SigF	H	K	L	F_{obs}	F_{calc}	SigF
5	3	−11	107	125	15	4	2	−9	94	92	13	2	3	−8	570	572	9
7	3	−11	140	149	12	5	2	−9	348	327	7	3	3	−8	265	260	12
3	4	−11	293	299	7	6	2	−9	189	195	9	4	3	−8	355	362	16
4	4	−11	172	186	10	8	2	−9	145	150	11	5	3	−8	399	411	7
5	4	−11	324	325	7	2	3	−9	306	294	11	7	3	−8	321	334	10
6	4	−11	126	130	13	4	3	−9	361	374	7	8	3	−8	359	346	7
3	6	−11	254	242	8	9	3	−9	156	139	11	9	3	−8	199	220	9
4	6	−11	116	112	15	1	4	−9	240	242	7	10	3	−8	148	144	18
1	0	−10	316	296	6	3	4	−9	451	462	14	2	4	−8	163	210	9
2	0	−10	203	210	7	4	4	−9	218	219	13	3	4	−8	250	250	6
3	0	−10	337	345	6	5	4	−9	218	255	8	6	4	−8	131	170	12
5	0	−10	262	268	6	6	4	−9	253	257	7	7	4	−8	157	150	11
6	0	−10	267	284	6	8	4	−9	263	260	7	2	5	−8	339	348	6
7	0	−10	272	296	7	4	5	−9	108	107	15	4	5	−8	199	227	8
8	0	−10	353	345	7	1	6	−9	140	129	13	5	5	−8	209	207	8
7	1	−10	138	117	12	2	6	−9	178	185	10	7	5	−8	200	193	9
1	2	−10	502	512	9	3	6	−9	247	252	8	2	7	−8	284	271	9
3	2	−10	489	530	22	4	6	−9	249	260	8	3	7	−8	231	214	16
5	2	−10	281	286	8	6	6	−9	209	214	11	4	7	−8	177	178	11
6	2	−10	254	272	8	2	7	−9	247	234	8	5	7	−8	207	197	9
7	2	−10	156	145	10	5	7	−9	135	126	13	1	8	−8	277	281	19
8	2	−10	322	354	6	1	0	−8	159	146	7	2	8	−8	142	140	13
1	3	−10	143	156	10	2	0	−8	256	218	5	3	8	−8	209	200	9
2	3	−10	448	469	8	3	0	−8	372	391	7	2	1	−7	249	292	12
3	3	−10	105	88	13	4	0	−8	482	496	7	3	1	−7	801	775	9
4	3	−10	577	607	8	5	0	−8	390	403	8	4	1	−7	214	225	7
5	3	−10	327	347	7	6	0	−8	266	270	6	5	1	−7	553	550	7
6	3	−10	250	268	8	8	0	−8	341	328	7	7	1	−7	420	409	8
7	3	−10	238	254	11	9	0	−8	153	116	10	8	1	-7	327	317	6
9	3	−10	208	204	13	1	1	−8	134	145	8	9	1	−7	243	242	11
4	4	−10	179	208	10	3	1	−8	201	209	6	10	1	−7	167	188	11
3	5	−10	252	243	13	4	1	−8	195	200	6	1	2	−7	478	485	10
4	5	−10	203	223	11	5	1	−8	187	157	7	2	2	−7	133	121	9
5	5	−10	183	187	10	6	1	−8	162	163	9	3	2	−7	357	361	7
7	5	−10	161	153	11	1	2	−8	236	229	5	6	2	−7	195	184	8
2	7	−10	217	189	9	2	2	−8	356	343	8	7	2	−7	124	137	11
2	1	−9	335	341	7	3	2	−8	572	580	22	8	2	−7	247	222	8
4	1	−9	593	588	13	4	2	−8	779	779	6	9	2	−7	202	201	9
5	1	−9	497	506	8	5	2	−8	169	170	13	2	3	−7	271	261	8
7	1	−9	339	334	10	6	2	−8	438	458	8	3	3	−7	317	315	6
8	1	−9	198	213	9	7	2	−8	153	151	10	4	3	−7	233	224	7
9	1	−9	320	318	7	8	2	−8	284	304	7	5	3	−7	329	344	11
1	2	−9	267	269	10	9	2	−8	239	233	14	7	3	−7	117	116	13
3	2	−9	354	347	9	1	3	−8	157	145	11	9	3	−7	100	99	16

Table 75 — continued

H	K	L	F_{obs}	F_{calc}	SigF	H	K	L	F_{obs}	F_{calc}	SigF	H	K	L	F_{obs}	F_{calc}	SigF
1	4	−7	496	477	8	3	2	−6	198	240	5	8	1	−5	302	309	6
2	4	−7	195	175	7	4	2	−6	785	788	8	10	1	−5	302	300	7
3	4	−7	506	531	15	5	2	−6	268	277	6	11	1	−5	206	191	9
4	4	−7	286	270	9	6	2	−6	422	428	8	1	2	−5	268	286	6
5	4	−7	133	116	13	7	2	−6	392	395	8	2	2	−5	545	524	9
6	4	−7	342	340	7	8	2	−6	158	151	10	3	2	−5	387	404	14
7	4	−7	201	204	9	9	2	−6	385	392	8	4	2	−5	128	127	8
8	4	−7	249	249	8	11	2	−6	199	203	21	5	2	−5	225	221	5
9	4	−7	236	246	8	1	3	−6	389	384	7	6	2	−5	175	148	9
3	5	−7	189	184	8	2	3	−6	149	169	12	7	2	−5	171	147	8
4	5	−7	121	77	12	3	3	−6	529	546	21	9	2	−5	318	308	14
1	6	−7	245	243	7	4	3	−6	173	148	7	2	3	−5	245	267	5
2	6	−7	173	166	10	5	3	−6	221	253	6	3	3	−5	508	498	6
3	6	−7	219	219	8	6	3	−6	272	290	10	4	3	−5	173	167	7
4	6	−7	312	309	8	7	3	−6	169	154	9	5	3	−5	397	374	13
6	6	−7	200	203	19	8	3	−6	357	353	7	7	3	−5	195	213	10
7	6	−7	217	238	14	10	3	−6	179	194	10	8	3	−5	252	248	7
8	6	−7	164	195	11	2	4	−6	269	247	7	10	3	−5	158	151	11
1	7	−7	152	156	12	3	4	−6	210	224	6	1	4	−5	393	388	13
2	7	−7	146	128	12	5	4	−6	236	247	6	2	4	−5	413	420	8
3	7	−7	138	119	13	10	4	−6	147	125	17	3	4	−5	310	305	6
5	7	−7	214	228	9	2	5	−6	624	615	7	4	4	−5	431	450	8
1	8	−7	220	223	20	3	5	−6	217	183	8	6	4	−5	377	386	7
3	8	−7	142	145	15	4	5	−6	308	305	14	7	4	−5	211	216	8
2	0	−6	481	489	6	5	5	−6	381	359	8	8	4	−5	210	190	10
3	0	−6	480	467	6	7	5	−6	297	287	7	9	4	−5	347	338	7
4	0	−6	452	431	6	8	5	−6	280	285	7	4	5	−5	177	158	14
5	0	−6	104	113	10	9	5	−6	264	265	8	1	6	−5	377	368	17
6	0	−6	406	395	8	3	6	−6	146	130	11	2	6	−5	355	362	7
8	0	−6	336	356	7	4	6	−6	167	177	10	4	6	−5	290	303	6
9	0	−6	231	214	8	5	6	−6	128	124	13	5	6	−5	156	162	11
10	0	−6	165	157	10	6	6	−6	119	105	14	6	6	−5	154	154	12
11	0	−6	170	179	10	1	7	−6	224	214	18	7	6	−5	279	273	8
1	1	−6	228	244	5	2	7	−6	141	137	14	1	7	−5	176	162	10
2	1	−6	430	409	7	3	7	−6	293	291	15	5	7	−5	142	145	16
3	1	−6	217	223	5	5	7	−6	195	178	10	1	8	−5	218	233	9
4	1	−6	391	386	7	6	7	−6	197	220	10	2	8	−5	130	138	15
5	1	−6	172	163	6	1	8	−6	158	161	12	1	9	−5	200	210	11
6	1	−6	186	213	12	2	8	−6	274	275	8	2	9	−5	148	138	13
7	1	−6	280	288	6	4	8	−6	283	270	7	1	0	−4	663	658	4
9	1	−6	206	201	8	2	1	−5	847	836	9	2	0	−4	978	982	4
10	1	−6	122	105	13	3	1	−5	905	919	16	3	0	−4	231	247	5
1	2	−6	399	416	10	5	1	−5	303	286	5	4	0	−4	639	660	5
2	2	−6	643	645	5	7	1	−5	353	328	7	5	0	−4	258	240	6

Table 75 — continued

H	K	L	F_{obs}	F_{calc}	SigF	H	K	L	F_{obs}	F_{calc}	SigF	H	K	L	F_{obs}	F_{calc}	SigF
6	0	−4	891	922	6	8	5	−4	391	375	8	2	5	−3	132	108	18
8	0	−4	286	261	6	3	6	−4	288	266	7	3	5	−3	155	136	9
9	0	−4	360	335	8	4	6	−4	118	120	13	1	6	−3	305	324	8
11	0	−4	209	190	9	6	6	−4	137	140	13	2	6	−3	520	547	28
2	1	−4	626	630	7	1	7	−4	264	262	8	3	6	−3	136	141	11
3	1	−4	656	616	5	3	7	−4	183	200	15	4	6	−3	192	217	9
5	1	−4	450	484	6	4	7	−4	215	238	13	5	6	−3	173	179	10
6	1	−4	266	263	5	6	7	−4	215	213	9	7	6	−3	230	210	9
7	1	−4	321	344	8	2	8	−4	178	185	11	9	6	−3	164	151	12
8	1	−4	195	201	12	4	8	−4	186	187	11	6	7	−3	132	148	14
9	1	−4	176	153	9	5	8	−4	189	212	11	1	8	−3	199	206	10
10	1	−4	275	254	7	1	1	−3	597	591	4	2	8	−3	234	233	9
1	2	−4	536	506	5	2	1	−3	289	269	6	4	8	−3	159	170	21
2	2	−4	1067	1036	8	3	1	−3	625	595	5	5	8	−3	150	145	13
3	2	−4	583	589	5	5	1	−3	818	766	28	6	8	−3	132	132	14
4	2	−4	318	294	6	6	1	−3	401	417	7	1	9	−3	301	306	8
5	2	−4	312	316	6	7	1	−3	242	232	6	3	9	−3	303	303	8
6	2	−4	294	301	6	8	1	−3	171	168	14	1	0	−2	1089	1068	3
7	2	−4	330	334	6	10	1	−3	271	269	9	2	0	−2	1436	1442	3
9	2	−4	285	279	7	11	1	−3	208	200	9	3	0	−2	341	356	6
10	2	−4	201	191	12	1	2	−3	144	144	10	4	0	−2	826	823	5
1	3	−4	425	423	12	2	2	−3	214	204	5	5	0	−2	757	769	5
2	3	−4	139	176	10	3	2	−3	309	319	7	6	0	−2	631	585	6
3	3	−4	295	328	6	5	2	−3	407	381	7	7	0	−2	556	582	7
4	3	−4	316	320	7	6	2	−3	181	172	8	9	0	−2	589	583	9
5	3	−4	91	84	12	7	2	−3	278	279	5	10	0	−2	300	294	7
6	3	−4	415	394	8	9	2	−3	274	274	10	1	1	−2	440	473	4
8	3	−4	278	265	6	11	2	−3	123	113	14	2	1	−2	238	224	4
10	3	−4	190	189	10	1	3	−3	431	411	8	4	1	−2	259	296	5
1	4	−4	467	516	10	2	3	−3	489	461	16	5	1	−2	194	204	5
2	4	−4	175	185	16	3	3	−3	274	286	6	6	1	−2	420	426	8
3	4	−4	121	91	10	4	3	−3	582	530	7	7	1	−2	187	175	7
4	4	−4	201	188	6	5	3	−3	260	282	5	8	1	−2	336	320	7
5	4	−4	262	265	6	6	3	−3	399	384	11	10	1	−2	259	245	9
6	4	−4	295	282	6	8	3	−3	291	285	10	1	2	−2	307	299	8
7	4	−4	132	118	11	10	3	−3	208	214	9	2	2	−2	108	134	8
9	4	−4	154	147	12	1	4	−3	620	635	15	3	2	−2	379	377	6
1	5	−4	518	503	12	2	4	−3	547	542	8	5	2	−2	298	272	9
2	5	−4	590	574	7	4	4	−3	371	376	10	7	2	−2	107	124	12
3	5	−4	553	573	12	5	4	−3	292	302	6	9	2	−2	167	172	10
4	5	−4	222	216	7	6	4	−3	292	280	6	10	2	−2	163	166	13
5	5	−4	456	482	8	7	4	−3	336	343	6	1	3	−2	463	446	6
6	5	−4	130	132	12	9	4	−3	349	328	8	2	3	−2	467	453	6
7	5	−4	330	324	8	1	5	−3	213	204	6	4	3	−2	386	360	7

Table 75 — continued

H	K	L	F_{obs}	F_{calc}	SigF	H	K	L	F_{obs}	F_{calc}	SigF	H	K	L	F_{obs}	F_{calc}	SigF
6	3	−2	474	458	10	10	2	−1	165	176	11	2	1	0	559	540	6
8	3	−2	148	151	11	1	3	−1	918	925	15	3	1	0	441	436	7
9	3	−2	199	205	9	2	3	−1	144	151	12	4	1	0	280	262	6
1	4	−2	519	509	29	3	3	−1	102	95	10	6	1	0	308	272	6
2	4	−2	432	460	7	4	3	−1	177	201	6	7	1	0	123	90	11
3	4	−2	302	302	6	5	3	−1	236	212	6	8	1	0	243	248	7
4	4	−2	276	298	7	6	3	−1	463	466	8	9	1	0	245	231	8
5	4	−2	442	458	19	8	3	−1	372	356	8	11	1	0	178	187	11
6	4	−2	119	122	12	9	3	−1	302	293	7	0	2	0	969	995	3
7	4	−2	366	373	8	10	3	−1	173	186	11	1	2	0	383	372	5
9	4	−2	348	348	8	2	4	−1	439	459	7	2	2	0	316	277	7
10	4	−2	175	180	11	3	4	−1	586	565	6	3	2	0	797	753	11
1	5	−2	740	763	15	4	4	−1	318	316	6	7	2	0	102	117	16
2	5	−2	138	136	9	5	4	−1	514	521	8	1	3	0	374	364	8
3	5	−2	785	784	6	6	4	−1	279	265	16	2	3	0	826	808	5
4	5	−2	191	213	7	7	4	−1	397	384	11	3	3	0	181	168	6
5	5	−2	511	472	9	10	4	−1	257	267	8	4	3	0	631	667	8
6	5	−2	379	377	7	4	5	−1	130	127	11	6	3	0	333	346	11
7	5	−2	306	303	11	2	6	−1	415	420	18	9	3	0	185	189	11
8	5	−2	267	257	13	3	6	−1	285	278	6	0	4	0	623	613	6
9	5	−2	109	105	16	4	6	−1	277	278	7	1	4	0	299	300	6
2	6	−2	300	313	7	5	6	−1	343	360	7	2	4	0	306	307	11
4	6	−2	326	327	7	6	6	−1	224	241	8	3	4	0	140	124	9
5	6	−2	119	130	13	7	6	−1	154	138	12	5	4	0	752	732	10
7	6	−2	233	233	9	3	7	−1	157	164	11	6	4	0	226	220	7
1	7	−2	293	298	8	5	7	−1	116	104	16	7	4	0	338	341	7
4	7	−2	258	253	7	6	7	−1	184	199	11	8	4	0	352	371	9
6	7	−2	136	142	18	2	8	−1	190	189	18	9	4	0	155	161	13
1	9	−2	154	167	13	3	8	−1	197	200	11	10	4	0	256	268	8
1	1	−1	1854	1808	8	5	8	−1	285	277	11	1	5	0	568	555	7
2	1	−1	89	95	10	1	9	−1	325	326	9	2	5	0	412	419	8
3	1	−1	70	41	11	3	9	−1	247	233	11	3	5	0	474	465	9
5	1	−1	235	235	8	4	9	−1	191	199	11	4	5	0	724	692	7
6	1	−1	521	501	14	1	0	0	321	309	6	5	5	0	333	338	10
8	1	−1	358	372	8	2	0	0	1639	1583	24	6	5	0	576	564	9
9	1	−1	332	340	7	3	0	0	622	591	4	7	5	0	129	145	14
10	1	−1	172	169	11	4	0	0	534	503	6	9	5	0	237	237	9
1	2	−1	316	327	9	5	0	0	682	688	6	0	6	0	302	302	6
2	2	−1	848	771	35	6	0	0	170	178	7	2	6	0	389	392	8
3	2	−1	677	652	5	7	0	0	738	720	7	3	6	0	444	451	8
4	2	−1	103	81	9	8	0	0	498	476	9	5	6	0	297	288	7
5	2	−1	456	461	9	9	0	0	260	242	7	6	6	0	136	152	20
6	2	−1	170	161	9	10	0	0	418	415	9	7	6	0	258	252	12
7	2	−1	283	306	6	1	1	0	555	514	11	4	7	0	232	252	8

Table 75 — continued

H	K	L	F_{obs}	F_{calc}	SigF	H	K	L	F_{obs}	F_{calc}	SigF	H	K	L	F_{obs}	F_{calc}	SigF
6	7	0	196	187	10	4	6	1	181	175	10	2	4	2	237	201	5
4	9	0	196	198	12	5	6	1	447	463	9	3	4	2	211	201	6
0	1	1	455	434	3	6	6	1	141	146	22	4	4	2	356	335	7
1	1	1	1503	1479	15	7	6	1	175	165	15	5	4	2	392	400	17
3	1	1	183	179	5	1	7	1	180	173	10	6	4	2	168	148	10
4	1	1	785	782	8	0	8	1	196	212	11	7	4	2	117	110	14
5	1	1	169	139	6	3	8	1	221	209	10	8	4	2	349	372	8
6	1	1	303	312	8	5	8	1	292	278	8	9	4	2	110	126	16
8	1	1	217	210	8	1	9	1	276	280	8	0	5	2	716	708	6
9	1	1	329	328	14	0	0	2	2145	2219	8	1	5	2	588	587	10
0	2	1	324	302	9	1	0	2	1119	1129	3	2	5	2	428	445	8
1	2	1	305	305	7	2	0	2	492	513	5	4	5	2	651	650	10
2	2	1	499	496	5	3	0	2	1856	1874	4	5	5	2	143	122	11
3	2	1	1030	990	17	5	0	2	817	835	6	6	5	2	390	408	8
4	2	1	223	210	5	6	0	2	257	281	6	7	5	2	256	250	12
5	2	1	253	242	10	7	0	2	365	351	6	9	5	2	295	287	18
6	2	1	159	170	8	8	0	2	364	363	8	0	6	2	244	257	8
7	2	1	233	234	7	9	0	2	290	281	7	1	6	2	214	203	8
8	2	1	121	137	16	10	0	2	273	264	8	3	6	2	347	337	7
10	2	1	229	250	9	0	1	2	516	507	3	4	6	2	255	244	8
0	3	1	837	827	11	1	1	2	247	274	5	5	6	2	206	210	13
1	3	1	473	471	6	2	1	2	599	616	8	6	6	2	259	259	8
2	3	1	276	259	6	4	1	2	549	559	6	1	7	2	140	137	12
3	3	1	179	200	9	5	1	2	379	367	7	6	7	2	232	231	9
4	3	1	338	324	6	6	1	2	136	152	9	5	8	2	121	136	16
5	3	1	146	157	9	7	1	2	398	401	9	2	9	2	105	106	17
6	3	1	383	381	8	9	1	2	220	222	9	3	9	2	117	102	17
7	3	1	189	183	9	0	2	2	537	514	9	0	1	3	361	373	5
9	3	1	384	391	7	1	2	2	217	232	4	1	1	3	308	307	6
0	4	1	953	949	14	2	2	2	239	210	6	2	1	3	502	499	5
1	4	1	549	565	7	3	2	2	294	282	10	3	1	3	196	170	5
2	4	1	260	260	7	4	2	2	131	146	8	4	1	3	980	942	5
3	4	1	577	613	15	5	2	2	382	377	9	5	1	3	167	153	7
4	4	1	114	133	13	6	2	2	238	229	6	6	1	3	494	489	8
5	4	1	569	585	9	7	2	2	284	288	6	7	1	3	230	235	7
7	4	1	263	251	9	8	2	2	155	162	11	9	1	3	134	135	13
8	4	1	195	193	16	10	2	2	142	157	13	0	2	3	530	525	14
10	4	1	244	252	9	0	3	2	111	110	9	1	2	3	104	101	17
0	5	1	171	148	8	1	3	2	1014	964	39	2	2	3	208	219	5
1	5	1	219	221	7	2	3	2	180	175	8	3	2	3	355	370	14
2	5	1	216	224	7	4	3	2	365	371	7	4	2	3	328	291	6
0	6	1	470	491	8	6	3	2	199	184	11	5	2	3	145	158	12
2	6	1	306	316	9	9	3	2	159	154	11	6	2	3	371	376	7
3	6	1	289	281	10	1	4	2	470	478	6	8	2	3	196	193	9

Table 75 — continued

H	K	L	F_{obs}	F_{calc}	SigF	H	K	L	F_{obs}	F_{calc}	SigF	H	K	L	F_{obs}	F_{calc}	SigF
10	2	3	200	217	10	10	0	4	222	221	9	4	7	4	214	197	26
0	3	3	770	774	17	0	1	4	386	360	7	6	7	4	192	177	11
3	3	3	284	281	5	1	1	4	163	173	6	0	8	4	204	204	10
4	3	3	559	539	7	2	1	4	539	521	9	1	8	4	124	131	15
5	3	3	121	147	11	3	1	4	300	336	9	3	8	4	214	223	12
6	3	3	334	329	10	4	1	4	287	284	9	0	9	4	198	210	10
7	3	3	232	256	19	5	1	4	601	624	7	0	1	5	549	538	5
8	3	3	163	147	21	6	1	4	116	122	12	1	1	5	338	341	9
9	3	3	162	162	11	7	1	4	251	256	7	2	1	5	469	468	6
0	4	3	587	583	8	8	1	4	208	216	9	3	1	5	201	157	6
1	4	3	404	401	7	10	1	4	142	138	14	4	1	5	482	486	7
2	4	3	359	344	7	0	2	4	460	483	6	5	1	5	377	376	7
3	4	3	380	402	7	1	2	4	319	296	11	6	1	5	269	286	6
4	4	3	160	167	9	2	2	4	310	338	6	7	1	5	314	305	10
5	4	3	455	459	8	3	2	4	562	554	6	8	1	5	161	168	12
6	4	3	256	256	7	4	2	4	237	216	5	9	1	5	138	149	16
8	4	3	236	242	9	5	2	4	630	604	45	0	2	5	232	238	5
0	5	3	86	135	13	6	2	4	165	186	9	1	2	5	275	267	5
1	5	3	143	163	9	8	2	4	197	187	9	2	2	5	202	182	5
2	5	3	165	154	16	1	3	4	725	761	5	3	2	5	120	151	9
4	5	3	173	187	13	3	3	4	332	347	8	4	2	5	148	136	8
5	5	3	107	106	17	4	3	4	476	495	8	5	2	5	268	300	6
6	5	3	107	86	15	6	3	4	264	266	12	6	2	5	252	244	7
0	6	3	648	656	9	7	3	4	178	190	10	8	2	5	156	162	11
1	6	3	371	384	7	9	3	4	185	201	10	0	3	5	150	184	10
2	6	3	223	228	8	0	4	4	158	134	8	1	3	5	209	233	6
3	6	3	231	235	8	2	4	4	330	331	7	2	3	5	406	423	11
5	6	3	333	330	9	4	4	4	321	342	7	3	3	5	425	447	14
8	6	3	211	200	9	6	4	4	120	118	17	4	3	5	252	220	11
1	7	3	143	136	12	0	5	4	840	850	6	5	3	5	183	226	8
1	8	3	163	139	12	1	5	4	240	224	6	7	3	5	160	156	11
5	8	3	147	137	19	2	5	4	449	453	16	0	4	5	212	220	7
0	9	3	131	132	15	3	5	4	397	423	9	1	4	5	369	370	27
1	9	3	159	154	15	4	5	4	366	368	7	3	4	5	426	454	12
2	9	3	246	243	9	5	5	4	358	381	8	4	4	5	331	330	6
0	0	4	449	450	5	7	5	4	354	335	7	5	4	5	241	237	7
1	0	4	248	225	4	8	5	4	153	137	21	6	4	5	265	278	8
2	0	4	540	516	5	1	6	4	172	177	14	8	4	5	229	230	9
3	0	4	960	953	5	2	6	4	179	179	9	0	6	5	293	269	12
4	0	4	547	595	6	4	6	4	173	174	10	1	6	5	379	382	12
5	0	4	609	584	7	0	7	4	144	144	12	3	6	5	288	301	7
6	0	4	450	484	8	1	7	4	182	170	10	4	6	5	154	175	15
8	0	4	110	112	15	2	7	4	124	115	14	5	6	5	179	154	11
9	0	4	223	215	9	3	7	4	118	96	17	6	6	5	215	212	9

Table 75 — continued

H	K	L	F_{obs}	F_{calc}	SigF	H	K	L	F_{obs}	F_{calc}	SigF	H	K	L	F_{obs}	F_{calc}	SigF
0	7	5	106	94	16	0	6	6	124	124	13	0	0	8	229	231	5
2	7	5	108	133	15	0	7	6	214	224	25	2	0	8	405	433	7
4	7	5	206	229	13	1	7	6	142	149	13	4	0	8	312	317	6
1	8	5	197	201	11	2	7	6	296	295	7	6	0	8	107	77	15
4	8	5	137	145	14	4	7	6	168	143	17	7	0	8	178	185	10
0	9	5	236	240	11	5	7	6	186	204	11	8	0	8	150	143	12
0	0	6	375	353	6	0	8	6	172	184	11	1	2	8	492	471	12
1	0	6	408	411	6	1	8	6	241	263	9	2	2	8	386	369	10
2	0	6	277	243	6	3	8	6	253	275	9	3	2	8	392	388	7
4	0	6	448	468	8	0	1	7	172	196	6	4	2	8	431	433	8
5	0	6	311	303	6	1	1	7	425	407	9	6	2	8	275	284	11
6	0	6	339	345	6	2	1	7	297	273	10	0	3	8	610	621	10
7	0	6	198	213	9	3	1	7	403	388	8	1	3	8	151	154	10
9	0	6	187	172	10	4	1	7	315	327	7	2	3	8	480	470	12
0	1	6	388	355	6	5	1	7	478	485	15	3	3	8	296	278	6
1	1	6	387	352	9	7	1	7	129	142	13	4	3	8	137	131	11
3	1	6	243	228	5	0	2	7	183	212	6	5	3	8	312	313	7
4	1	6	136	136	9	1	2	7	455	445	7	7	3	8	250	253	8
5	1	6	174	156	8	3	2	7	161	142	8	0	4	8	154	146	9
8	1	6	143	147	12	4	2	7	164	152	9	2	4	8	94	101	15
0	2	6	184	195	6	5	2	7	147	175	11	1	5	8	163	149	10
1	2	6	595	610	13	6	2	7	129	130	13	2	5	8	123	146	13
3	2	6	545	552	7	8	2	7	140	159	13	6	5	8	147	150	12
4	2	6	307	313	13	1	3	7	199	209	8	0	6	8	141	147	20
5	2	6	457	467	9	2	3	7	314	334	7	0	7	8	297	302	7
6	2	6	398	414	8	3	3	7	241	265	8	2	7	8	243	253	9
0	3	6	374	371	7	4	3	7	194	186	8	3	7	8	242	232	9
1	3	6	366	336	12	5	3	7	254	273	8	0	1	9	373	364	7
2	3	6	422	463	8	1	4	7	424	454	18	1	1	9	362	341	8
3	3	6	137	119	10	2	4	7	167	131	10	2	1	9	241	236	6
4	3	6	526	529	8	3	4	7	210	224	8	3	1	9	251	233	11
5	3	6	234	240	9	4	4	7	235	236	11	5	1	9	165	165	10
6	3	6	169	164	10	6	4	7	248	248	8	6	1	9	232	244	22
7	3	6	281	278	7	7	4	7	154	149	12	7	1	9	158	159	11
2	4	6	267	283	6	1	5	7	99	50	15	0	2	9	118	126	11
4	4	6	94	85	14	2	5	7	157	164	13	1	2	9	255	258	8
8	4	6	107	118	16	1	6	7	277	279	8	2	2	9	291	282	9
0	5	6	480	471	8	3	6	7	248	231	8	4	2	9	211	223	8
1	5	6	184	170	11	4	6	7	217	224	10	0	3	9	229	221	7
2	5	6	295	291	6	2	7	7	199	218	10	1	3	9	248	250	6
3	5	6	319	303	6	3	7	7	113	120	16	2	3	9	230	233	7
5	5	6	283	291	7	4	7	7	135	158	14	5	3	9	162	159	11
6	5	6	190	205	15	1	8	7	195	202	10	0	4	9	206	211	8
7	5	6	197	201	10	2	8	7	105	92	16	1	4	9	146	142	11

Table 75 — continued

H	K	L	F_{obs}	F_{calc}	SigF	H	K	L	F_{obs}	F_{calc}	SigF	H	K	L	F_{obs}	F_{calc}	SigF
2	4	9	283	290	7	0	3	11	189	177	18	2	2	14	118	152	15
4	4	9	217	213	12	1	3	11	248	249	12	1	3	14	160	199	11
5	4	9	135	91	13	2	3	11	171	145	10	2	3	14	121	102	14
6	4	9	164	174	11	0	4	11	201	223	9	0	5	14	144	40	13
0	5	9	131	117	17	2	4	11	300	297	7	1	5	14	167	148	11
1	6	9	194	162	10	0	6	11	162	157	11	2	5	14	204	67	9
2	6	9	204	214	9	0	0	12	169	180	10	2	5	14	116	59	16
0	7	9	161	161	14	2	0	12	241	250	8	0	7	14	211	87	8
1	7	9	169	164	11	0	2	12	369	379	16	1	7	14	121	100	16
2	7	9	169	167	10	2	2	12	320	345	8	0	8	14	111	115	15
0	0	10	177	171	8	3	2	12	111	132	15	0	10	14	131	71	14
1	0	10	227	213	7	5	2	12	173	174	11	1	1	15	185	209	9
2	0	10	92	113	15	7	2	12	157	167	13	1	1	15	172	203	11
5	0	10	307	306	7	1	3	12	380	402	10	2	2	15	119	94	13
4	1	10	109	99	15	2	3	12	103	85	15	1	4	15	123	71	13
0	2	10	337	342	6	3	3	12	200	198	16	3	4	15	107	105	15
1	2	10	398	404	10	4	3	12	110	139	16	1	5	15	125	27	13
2	2	10	285	289	17	6	3	12	131	136	15	4	5	15	115	14	16
4	2	10	186	178	9	1	5	12	168	178	11	1	6	15	174	125	10
5	2	10	235	254	8	3	5	12	114	105	16	2	7	15	119	43	14
6	2	10	134	132	13	1	7	12	190	195	12	4	7	15	134	59	14
0	3	10	167	174	9	1	1	13	296	311	17	1	8	15	193	47	10
1	3	10	508	505	9	2	1	13	109	134	14	0	0	16	195	196	10
3	3	10	432	437	9	3	1	13	122	146	14	2	1	16	115	19	16
5	3	10	222	229	9	4	1	13	120	153	14	5	1	16	137	8	15
1	4	10	107	102	16	6	1	13	140	158	22	0	2	16	144	96	12
1	5	10	177	180	10	0	2	13	244	265	9	2	2	16	116	22	14
3	5	10	153	159	12	2	2	13	180	196	10	4	3	16	124	82	14
0	1	11	242	239	12	5	2	13	127	108	14	0	5	16	149	72	11
1	1	11	324	323	6	1	3	13	198	188	9	3	6	16	118	35	15
2	1	11	162	157	10	0	4	13	204	216	9	0	7	16	205	106	10
3	1	11	146	149	12	2	4	13	166	158	18	2	7	16	149	62	13
4	1	11	196	197	10	0	6	13	182	187	11	1	6	17	148	97	13
0	2	11	221	224	22	0	0	14	224	223	8	2	7	17	108	39	18
2	2	11	363	363	7	2	1	14	140	32	12	0	4	18	152	30	13
4	2	11	176	158	21	0	2	14	188	210	10						

APPENDIX C

SUPPLEMENTAL TABLES AND FIGURES

FOR

THE CRYSTAL STRUCTURE

OF

endo-(η^5-C_6Me_6H)$Mn(CO)_2P(OMe)_3$

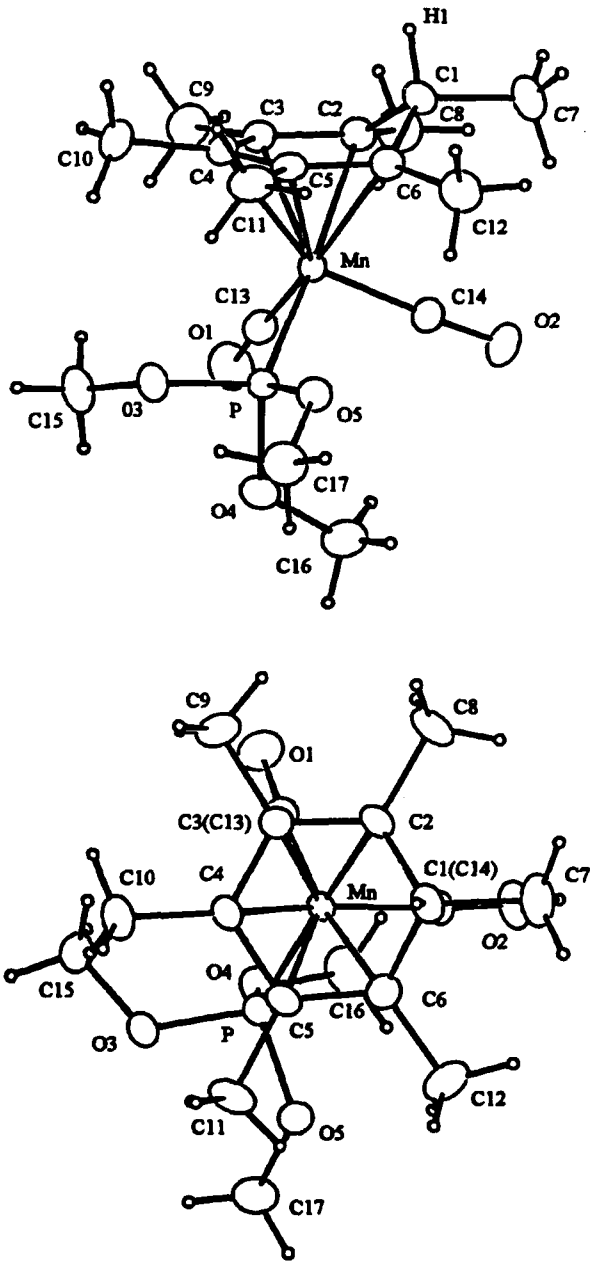

Figure 25. ORTEP drawing of **11d** with hydrogen atoms: (a) canted side view and (b) top view

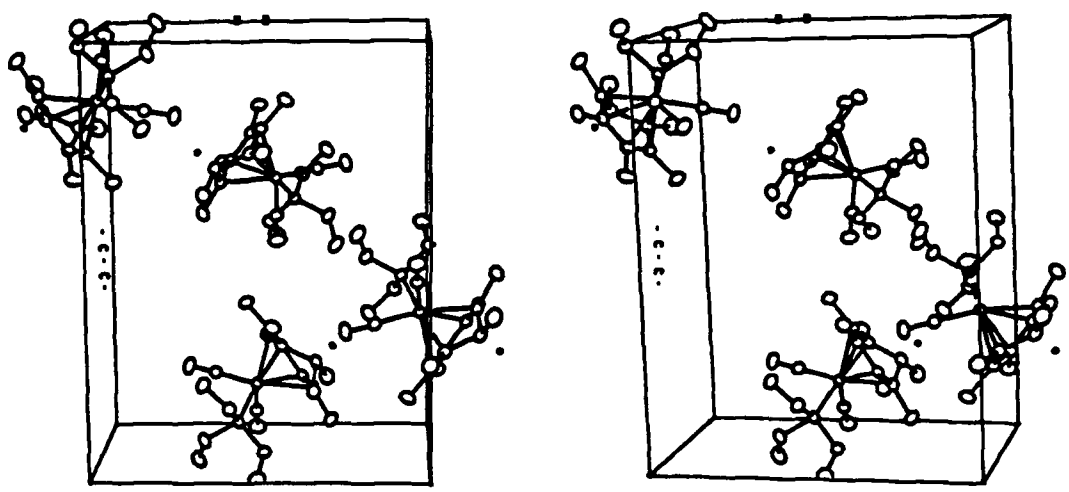

Figure 26. Stereoscopic view of the unit cell of **11d**

Table 76. Complete Crystallographic Data and Refinement Parameters for **11d** [a]

formula	$C_{17}H_{28}MnO_5P$
fw, amu	398.32
color	yellow
crystal size, mm	0.58 × 0.19 × 0.25
space group	$P2_12_12_1$
cell dimensions	
a, Å	8.945 (6)
b, Å	12.911 (4)
c, Å	16.528 (6)
V, Å^3	1909 (5)
Z	4
ρ_{calc}, kg·m^{-3}	1 386
λ, Å (graphite)	0.710 73
μ, cm^{-1} (Mo Kα)	7.7
T (data collection), K	296
omega (ω) scan range	0.80 + 0.35 tan(θ)
omega (ω) scan speed, deg/min (θ from 1° to 25°)	3.3–0.71
horizontal aperture, mm	2.5–3.0
systematic absences	$h00$, $h \neq 2n$ $0k0$, $k \neq 2n$ $00l$, $l \neq 2n$
reflections collected	7547
after averaging	3861
reflections > 3σ used in least squares refinement	3380
parameters refined	217
R_1 [b]	0.025
R_2 [c]	0.033
residual electron density in final DF map, e^-/Å^3	0.372
largest shift/esd	0.00

[a] In this and subsequent tables esd's are given in parentheses.

[b] $R_1 = \sum \| F_o | - | F_c \| / \sum | F_o |$.

[c] $R_2 = [\sum w(| F_o | - | F_c |)^2 / \sum w | F_o |^2]^{1/2}$, $w = 1/\sigma^2(F)$, where $\sigma^2(F) = \sigma^2(F) + [(PWT)F]^2$, PWT = 0.07.

Table 77. Fractional Coordinates and Isotropic Thermal Parameters for **11d** [a]

atom	x	y	z	B_{iso} [b]
Mn	0.21343 (3)	0.03177 (2)	0.13857 (2)	0.335 (5)
P	0.01625 (6)	0.08174 (4)	0.07171 (3)	0.69 (1)
O1	0.2722 (3)	0.2500 (2)	0.1779 (1)	0.50 (5)
O2	0.4231 (2)	0.0407 (2)	0.0031 (1)	0.27 (4)
O3	−0.1357 (2)	0.1025 (1)	0.1216 (1)	0.47 (3)
O4	0.0165 (2)	0.1907 (1)	0.0253 (1)	0.99 (4)
O5	−0.0459 (2)	0.0023 (1)	0.00614 (9)	0.39 (3)
C1	0.3753 (3)	−0.1478 (2)	0.1728 (2)	0.52 (5)
C2	0.3893 (2)	−0.0418 (2)	0.2115 (1)	0.15 (4)
C3	0.2711 (3)	−0.0099 (2)	0.2605 (1)	0.02 (4)
C4	0.1238 (2)	−0.0473 (2)	0.2435 (1)	0.89 (4)
C5	0.1019 (3)	−0.1112 (2)	0.1737 (1)	0.93 (4)
C6	0.2266 (3)	−0.1404 (2)	0.1286 (1)	0.33 (4)
C7	0.5062 (4)	−0.1802 (3)	0.1192 (2)	0.66 (7)
C8	0.5441 (3)	0.0038 (3)	0.2226 (2)	0.16 (7)
C9	0.2942 (4)	0.0655 (2)	0.3304 (2)	0.80 (6)
C10	−0.0048 (3)	−0.0249 (3)	0.3007 (2)	0.55 (6)
C11	−0.0533 (3)	−0.1495 (2)	0.1539 (2)	0.44 (6)
C12	0.2078 (4)	−0.1986 (2)	0.0492 (2)	0.35 (7)
C13	0.2445 (3)	0.1636 (2)	0.1632 (1)	0.29 (5)
C14	0.3378 (3)	0.0372 (2)	0.0553 (1)	0.26 (4)
C15	−0.1395 (3)	0.1839 (2)	0.1796 (2)	0.65 (6)
C16	0.1240 (4)	0.2141 (3)	−0.0364 (2)	0.51 (7)
C17	−0.1822 (3)	0.0194 (3)	−0.0384 (2)	0.25 (6)
H1	0.3769 (3)	−0.2023 (3)	0.2116 (2)	4.7 (1)

[a] Anisotropically refined atoms are given in the form of the isotropic equivalent displacement parameter defined as: $(4/3)[a^2B(1,1) + b^2B(2,2) + c^2B(3,3) + ab(\cos\gamma)B(1,2) + ac(\cos\beta)B(1,3) + bc(\cos\alpha)B(2,3)]$

[b] Hydrogen atoms were refined isotropically.

Table 78. Fractional Coordinates and Isotropic Thermal Parameters for Hydrogen Atoms of **11d**

atom	x	y	z	B_{iso} [a]
H1	0.3769	−0.2023	0.2116	4.7
H2	0.4895	−0.2470	0.0980	7.3
H3	0.5183	−0.1317	0.0767	7.3
H4	0.5960	−0.1810	0.1512	7.3
H5	0.6095	−0.0268	0.1840	6.7
H6	0.5400	0.0763	0.2141	6.7
H7	0.5781	−0.0107	0.2754	6.7
H8	0.3980	0.0826	0.3336	6.3
H9	0.2380	0.1263	0.3211	6.3
H10	0.2640	0.0337	0.3793	6.3
H11	0.0292	0.0187	0.3430	5.9
H12	−0.0826	0.0086	0.2717	5.9
H13	−0.0403	−0.0881	0.3224	5.9
H14	−0.0482	−0.1909	0.1061	5.9
H15	−0.0899	−0.1898	0.1972	5.9
H16	−0.1167	−0.0921	0.1445	5.9
H17	0.3035	−0.2123	0.0261	7.0
H18	0.1581	−0.2627	0.0589	7.0
H19	0.1506	−0.1584	0.0124	7.0
H20	−0.2361	0.1863	0.2042	6.2
H21	−0.0667	0.1711	0.2206	6.2
H22	−0.1192	0.2480	0.1543	6.2
H23	0.1065	0.2822	−0.0564	7.1
H24	0.2219	0.2107	−0.0141	7.1
H25	0.1149	0.1658	−0.0791	7.1
H26	−0.1983	−0.0368	−0.0742	6.8
H27	−0.2630	0.0249	−0.0017	6.8
H28	−0.1732	0.0818	−0.0686	6.8

[a] Atoms were refined isotropically.

Table 79. Additional Supplemental Bond Distances (Å) and Angles (°) for **11d**

		Distances	
Mn-P	2.1790 (7)	O(4)-C(16)	1.434 (4)
Mn-C(2)	2.197 (2)	O(5)-C(17)	1.441 (3)
Mn-C(3)	2.148 (2)	C(1)-C(2)	1.516 (4)
Mn-C(4)	2.165 (2)	C(1)-C(6)	1.520 (4)
Mn-C(5)	2.178 (2)	C(1)-C(7)	1.526 (4)
Mn-C(6)	2.231 (2)	C(2)-C(3)	1.394 (3)
Mn-C(13)	1.772 (3)	C(2)-C(8)	1.516 (4)
Mn-C(14)	1.772 (2)	C(3)-C(4)	1.431 (3)
P-O(3)	1.613 (2)	C(3)-C(9)	1.526 (3)
P-O(4)	1.602 (2)	C(4)-C(5)	1.431 (3)
P-O(5)	1.592 (2)	C(4)-C(10)	1.517 (3)
O(1)-C(13)	1.167 (3)	C(5)-C(6)	1.394 (3)
O(2)-C(14)	1.152 (3)	C(5)-C(11)	1.509 (3)
O(3)-C(15)	1.422 (3)	C(6)-C(12)	1.522 (4)
C(1)-H1	0.954 (3)	C(11)-H15	0.945 (3)
C(7)-H2	0.944 (3)	C(11)-H16	0.945 (3)
C(7)-H3	0.947 (3)	C(12)-H17	0.954 (4)
C(7)-H4	0.962 (3)	C(12)-H18	0.953 (3)
C(8)-H5	0.951 (3)	C(12)-H19	0.948 (3)
C(8)-H6	0.947 (3)	C(15)-H20	0.956 (3)
C(8)-H7	0.945 (3)	C(15)-H21	0.955 (3)
C(9)-H8	0.956 (3)	C(15)-H22	0.945 (3)
C(9)-H9	0.944 (3)	C(16)-H23	0.953 (3)
C(9)-H10	0.946 (3)	C(16)-H24	0.951 (3)
C(10)-H11	0.949 (3)	C(16)-H25	0.945 (3)
C(10)-H12	0.949 (3)	C(17)-H26	0.948 (3)
C(10)-H13	0.947 (3)	C(17)-H27	0.946 (3)
C(11)-H14	0.955 (3)	C(17)-H28	0.951 (3)
		Angles	
C(13)-Mn-C(14)	92.4 (1)	C(6)-C(1)-C(7)	114.2 (2)
P-Mn-C(13)	87.67 (8)	C(1)-C(2)-C(3)	116.7 (2)
P-Mn-C(14)	95.88 (8)	C(1)-C(2)-C(8)	118.5 (2)
Mn-P-O(3)	118.17 (7)	C(3)-C(2)-C(8)	120.5 (2)
Mn-P-O(4)	120.12 (8)	C(2)-C(3)-C(4)	119.0 (2)
Mn-P-O(5)	115.93 (7)	C(2)-C(3)-C(9)	121.7 (2)
Mn-C(13)-O(1)	176.5 (2)	C(4)-C(3)-C(9)	119.2 (2)
Mn-C(14)-O(2)	177.5 (2)	C(3)-C(4)-C(5)	118.6 (2)

Table 79 — Continued

Angles			
O(3)-P-O(4)	95.8 (1)	C(3)-C(4)-C(10)	120.8 (2)
O(3)-P-O(5)	99.25 (9)	C(5)-C(4)-C(10)	120.5 (2)
O(4)-P-O(5)	103.9 (1)	C(4)-C(5)-C(6)	118.5 (2)
P-O(3)-C(15)	119.2 (2)	C(4)-C(5)-C(11)	119.4 (2)
P-O(4)-C(16)	121.7 (2)	C(6)-C(5)-C(11)	122.1 (2)
P-O(5)-C(17)	123.0 (2)	C(1)-C(6)-C(5)	117.4 (2)
C(2)-C(1)-C(6)	102.6 (2)	C(1)-C(6)-C(12)	118.7 (2)
C(2)-C(1)-C(7)	115.4 (2)	C(5)-C(6)-C(12)	120.4 (3)
C(2)-C(1)-H1	112.4 (2)	C(5)-C(11)-H16	109.3 (2)
C(6)-C(1)-H1	112.6 (2)	H14-C(11)-H16	109.4 (3)
C(7)-C(1)-H1	100.2 (2)	H14-C(11)-H15	109.5 (3)
C(1)-C(7)-H3	109.8 (3)	H15-C(11)-H16	110.3 (3)
C(1)-C(7)-H2	110.2 (3)	C(6)-C(12)-H17	109.7 (3)
C(1)-C(7)-H4	108.9 (3)	C(6)-C(12)-H18	109.6 (3)
H2-C(7)-H3	110.3 (3)	C(6)-C(12)-H19	110.0 (3)
H2-C(7)-H4	109.0 (3)	H17-C(12)-H18	108.9 (3)
H3-C(7)-H4	108.7 (3)	H17-C(12)-H19	109.3 (3)
C(2)-C(8)-H5	108.6 (3)	H18-C(12)-H19	109.4 (4)
C(2)-C(8)-H6	109.4 (2)	O(3)-C(15)-H20	109.5 (3)
C(2)-C(8)-H7	109.2 (3)	O(3)-C(15)-H21	109.6 (3)
H5-C(8)-H6	109.6 (3)	O(3)-C(15)-H22	110.3 (3)
H5-C(8)-H7	109.8 (3)	H20-C(15)-H21	108.6 (3)
H6-C(8)-H7	110.2 (3)	H20-C(15)-H22	109.4 (3)
C(3)-C(9)-H8	108.7 (2)	H21-C(15)-H22	109.5 (3)
C(3)-C(9)-H9	109.6 (2)	O(4)-C(16)-H23	109.3 (3)
C(3)-C(9)-H10	109.4 (3)	O(4)-C(16)-H24	109.5 (3)
H8-C(9)-H9	109.5 (3)	O(4)-C(16)-H25	109.6 (3)
H8-C(9)-H10	109.3 (3)	H23-C(16)-H24	109.1 (3)
H9-C(9)-H10	110.3 (3)	H23-C(16)-H25	109.6 (3)
C(4)-C(10)-H11	109.2 (2)	H24-C(16)-H25	109.8 (3)
C(4)-C(10)-H12	109.2 (2)	O(5)-C(17)-H26	109.3 (3)
C(4)-C(10)-H13	109.1 (3)	O(5)-C(17)-H27	109.3 (2)
H11-C(10)-H12	109.7 (3)	O(5)-C(17)-H28	109.1 (3)
H11-C(10)-H13	109.8 (2)	H26-C(17)-H27	110.0 (3)
H12-C(10)-H13	109.8 (3)	H26-C(17)-H28	109.5 (3)
C(5)-C(11)-H14	108.7 (2)	H27-C(17)-H28	109.7 (3)
C(5)-C(11)-H15	109.6 (2)		

Table 80. General Displacement Parameter Expressions [a] — U's for **11d**

Name	U(1,1)	U(2,2)	U(3,3)	U(1,2)	U(1,3)	U(2,3)
Mn	0.0242 (1)	0.0320 (1)	0.0325 (1)	−0.0013 (1)	0.0021 (1)	0.0005 (1)
P	0.0297 (2)	0.0351 (3)	0.0377 (2)	0.0012 (2)	0.0000 (2)	0.0027 (2)
O(1)	0.082 (1)	0.0401 (9)	0.087 (1)	−0.014 (1)	0.006 (1)	−0.0129 (9)
O(2)	0.055 (1)	0.094 (1)	0.0520 (9)	0.001 (1)	0.0237 (7)	0.009 (1)
O(3)	0.0298 (7)	0.0500 (9)	0.0519 (9)	0.0024 (7)	0.0030 (6)	−0.0057 (8)
O(4)	0.0462 (9)	0.0449 (9)	0.061 (1)	0.0036 (9)	0.0005 (8)	0.0147 (8)
O(5)	0.0416 (8)	0.048 (1)	0.0389 (7)	0.0038 (7)	−0.0073 (6)	−0.0022 (7)
C(1)	0.038 (1)	0.043 (1)	0.053 (1)	0.009 (1)	0.004 (1)	0.008 (1)
C(2)	0.027 (1)	0.049 (1)	0.044 (1)	−0.000 (1)	−0.0052 (8)	0.005 (1)
C(3)	0.038 (1)	0.043 (1)	0.033 (1)	0.000 (1)	−0.0044 (8)	0.0032 (9)
C(4)	0.032 (1)	0.043 (1)	0.0354 (9)	−0.000 (1)	0.0034 (8)	0.0062 (9)
C(5)	0.032 (1)	0.037 (1)	0.042 (1)	−0.005 (1)	−0.0033 (8)	0.0112 (9)
C(6)	0.049 (1)	0.034 (1)	0.044 (1)	−0.002 (1)	0.003 (1)	−0.0001 (9)
C(7)	0.062 (2)	0.071 (2)	0.082 (2)	0.028 (1)	0.021 (1)	0.003 (2)
C(8)	0.030 (1)	0.084 (2)	0.082 (2)	−0.012 (1)	−0.008 (1)	0.007 (2)
C(9)	0.070 (2)	0.065 (2)	0.047 (1)	−0.004 (2)	−0.014 (1)	−0.012 (1)
C(10)	0.046 (1)	0.079 (2)	0.048 (1)	0.003 (2)	0.015 (1)	0.008 (1)
C(11)	0.047 (1)	0.054 (1)	0.068 (2)	−0.021 (1)	−0.012 (1)	0.014 (1)
C(12)	0.090 (2)	0.054 (1)	0.059 (1)	0.008 (2)	−0.010 (2)	−0.019 (1)
C(13)	0.040 (1)	0.043 (1)	0.042 (1)	−0.005 (1)	0.0022 (8)	0.001 (1)
C(14)	0.036 (1)	0.049 (1)	0.039 (1)	0.001 (1)	0.0035 (8)	0.001 (1)
C(15)	0.048 (1)	0.061 (2)	0.068 (2)	0.010 (1)	0.005 (1)	−0.020 (1)
C(16)	0.068 (2)	0.064 (2)	0.078 (2)	−0.003 (2)	0.012 (1)	0.030 (1)
C(17)	0.056 (2)	0.083 (2)	0.060 (1)	0.003 (2)	−0.024 (1)	−0.007 (2)

[a] The form of the anisotropic displacement parameter is : $\exp[-2\pi^2\{h^2a^2U(1,1) + k^2b^2U(2,2) + l^2c^2U(3,3) + 2hkabU(1,2) + 2hlacU(1,3) + 2klbcU(2,3)\}]$, where a, b, and c are reciprocal lattice constants.

Table 81. General Displacement Parameter Expressions [a] — B's for **11d**

Name	B(1,1)	B(2,2)	B(3,3)	B(1,2)	B(1,3)	B(2,3)	B_{iso}
Mn	1.912 (9)	2.52 (1)	2.568 (9)	−0.10 (1)	0.162 (9)	0.04 (1)	2.335 (5)
P	2.34 (2)	2.77 (2)	2.97 (2)	0.09 (2)	0.00 (2)	0.22 (2)	2.69 (1)
O(1)	6.5 (1)	3.17 (7)	6.9 (1)	−1.11 (8)	0.45 (9)	−1.02 (7)	5.50 (5)
O(2)	4.32 (8)	7.4 (1)	4.11 (7)	0.09 (9)	1.87 (6)	0.71 (8)	5.27 (4)
O(3)	2.36 (6)	3.95 (7)	4.10 (7)	0.19 (6)	0.23 (5)	−0.45 (6)	3.47 (3)
O(4)	3.65 (7)	3.54 (7)	4.79 (7)	0.28 (7)	0.04 (6)	1.16 (6)	3.99 (4)
O(5)	3.29 (6)	3.81 (7)	3.07 (6)	0.30 (6)	−0.58 (5)	−0.17 (5)	3.39 (3)
C(1)	3.0 (1)	3.4 (1)	4.2 (1)	0.71 (9)	0.28 (8)	0.66 (9)	3.52 (5)
C(2)	2.11 (8)	3.9 (1)	3.48 (8)	−0.00 (8)	−0.41 (6)	0.39 (8)	3.15 (4)
C(3)	3.01 (8)	3.43 (9)	2.61 (8)	0.02 (8)	−0.35 (6)	0.25 (7)	3.02 (4)
C(4)	2.50 (8)	3.4 (1)	2.79 (7)	−0.02 (8)	0.26 (6)	0.49 (7)	2.89 (4)
C(5)	2.54 (9)	2.93 (8)	3.33 (8)	−0.40 (8)	−0.26 (7)	0.88 (7)	2.93 (4)
C(6)	3.8 (1)	2.66 (8)	3.51 (9)	−0.12 (8)	0.20 (8)	−0.01 (7)	3.33 (4)
C(7)	4.9 (1)	5.6 (1)	6.4 (2)	2.2 (1)	1.6 (1)	0.3 (1)	5.66 (7)
C(8)	2.40 (9)	6.6 (2)	6.5 (1)	−1.0 (1)	−0.6 (1)	0.6 (1)	5.16 (7)
C(9)	5.5 (1)	5.2 (1)	3.7 (1)	−0.3 (1)	−1.1 (1)	−0.93 (9)	4.80 (6)
C(10)	3.6 (1)	6.2 (1)	3.79 (9)	0.3 (1)	1.19 (8)	0.7 (1)	4.55 (6)
C(11)	3.7 (1)	4.3 (1)	5.3 (1)	−1.64 (9)	−0.97 (9)	1.1 (1)	4.44 (6)
C(12)	7.1 (2)	4.3 (1)	4.7 (1)	0.6 (1)	−0.8 (1)	−1.5 (1)	5.35 (7)
C(13)	3.2 (1)	3.4 (1)	3.29 (9)	−0.39 (8)	0.18 (6)	0.04 (8)	3.29 (5)
C(14)	2.84 (8)	3.8 (1)	3.09 (8)	0.05 (9)	0.28 (6)	0.09 (9)	3.26 (4)
C(15)	3.8 (1)	4.8 (1)	5.4 (1)	0.8 (1)	0.4 (1)	−1.6 (1)	4.65 (6)
C(16)	5.3 (1)	5.0 (1)	6.2 (1)	−0.3 (1)	0.9 (1)	2.3 (1)	5.51 (7)
C(17)	4.4 (1)	6.6 (2)	4.8 (1)	0.3 (1)	−1.91 (9)	−0.5 (1)	5.25 (6)

[a] The form of the anisotropic displacement parameter is : $\exp[-0.25\{h^2a^2B(1,1) + k^2b^2B(2,2) + l^2c^2B(3,3) + 2hkabB(1,2) + 2hlacB(1,3) + 2klbcB(2,3)\}]$, where a, b, and c are reciprocal lattice constants.

Table 82. Deviations [a] from Least-Squares-Planes Analysis for **11d**

Atoms	1	2	3	4
C1	705.	690.	815.	0.*
C2	1.*	−4.*	78.	0.*
C3	−11.*	4.*	0.*	
C4	20.*	45.	0.*	
C5	−19.*	−4.*	0.*	
C6	9.*	4.*	94.	0.*
C7	694.	658.	877.	
C8	−162.	−179.	−51.	
C9	−87.	−61.	−117.	
C10	172.	219.	81.	
C11	−17.	9.	−29.	
C12	−177.	−194.	−49.	
Mn	−1689.	−1683.	−1644.	
Parameters for L.S. Planes [b]				
A	−1455.	−1343.	−1799	4715.
B	7999.	7959.	8138	3377.
C	−5822.	−5903.	−5526	−8147.
D	−29722.	−29646.	−29195	−13878.

[a] Deviations are in Å × 10^3. Atoms used to define the planes are marked with an asterisk (*) following the deviation. Dihedral angle between planes 1 and 4 is 47.5°, between planes 2 and 4 is 46.7°, and between planes 2 and 3 is 3.5°.

[b] Parameters A, B, C, and D (Å × 10^4) define a plane having the form: $Ax + By + Cz - D = 0$.

Table 83. Calculated FOFC's (× 10) for **11d**

H	K	L	F_{obs}	F_{calc}	SigF	H	K	L	F_{obs}	F_{calc}	SigF	H	K	L	F_{obs}	F_{calc}	SigF
0	2	0	1680	1841	19	0	13	3	236	231	4	0	8	7	108	101	3
0	4	0	1052	1060	3	0	14	3	111	111	5	0	9	7	408	416	6
0	6	0	565	566	3	0	0	4	381	384	2	0	10	7	193	203	7
0	8	0	100	98	3	0	1	4	82	75	2	0	11	7	331	330	5
0	10	0	69	62	7	0	2	4	261	260	3	0	0	8	290	268	3
0	14	0	180	168	3	0	3	4	269	269	5	0	1	8	332	335	12
0	1	1	601	610	3	0	4	4	792	789	9	0	2	8	703	689	3
0	3	1	713	728	4	0	5	4	369	345	7	0	3	8	108	105	3
0	4	1	531	541	3	0	6	4	234	213	4	0	4	8	402	412	4
0	5	1	1143	1138	6	0	7	4	489	490	3	0	5	8	387	372	3
0	6	1	395	399	12	0	10	4	248	243	5	0	6	8	520	514	10
0	7	1	398	412	4	0	11	4	221	234	4	0	7	8	285	296	4
0	9	1	74	75	4	0	12	4	97	100	5	0	8	8	165	174	3
0	11	1	178	181	3	0	13	4	128	130	4	0	9	8	85	89	5
0	12	1	170	175	3	0	14	4	168	162	5	0	10	8	67	69	10
0	13	1	216	227	8	0	15	4	109	107	9	0	11	8	83	76	5
0	14	1	107	110	7	0	1	5	274	290	3	0	12	8	182	193	4
0	15	1	76	74	7	0	3	5	881	873	12	0	13	8	148	148	4
0	0	2	109	113	2	0	4	5	457	433	3	0	14	8	119	120	5
0	1	2	1947	2174	10	0	5	5	153	149	3	0	1	9	78	90	7
0	2	2	335	332	2	0	6	5	794	783	5	0	3	9	172	157	3
0	3	2	592	592	2	0	7	5	198	196	4	0	4	9	249	259	5
0	4	2	68	65	3	0	8	5	464	459	4	0	5	9	140	139	3
0	5	2	167	167	4	0	9	5	79	74	4	0	6	9	326	351	5
0	6	2	82	106	9	0	10	5	399	387	7	0	7	9	56	62	6
0	7	2	112	101	3	0	12	5	232	228	8	0	8	9	377	390	10
0	8	2	249	249	7	0	0	6	1093	1106	2	0	9	9	63	67	6
0	9	2	153	161	4	0	1	6	535	524	2	0	10	9	328	323	5
0	10	2	292	294	4	0	2	6	113	95	10	0	11	9	116	118	4
0	13	2	139	143	4	0	3	6	338	350	7	0	12	9	203	211	4
0	14	2	110	107	5	0	4	6	241	242	3	0	0	10	498	508	3
0	15	2	183	179	4	0	5	6	90	121	5	0	1	10	268	291	4
0	1	3	363	364	2	0	6	6	455	459	8	0	2	10	196	199	5
0	2	3	606	606	9	0	7	6	333	325	4	0	3	10	277	289	14
0	3	3	472	462	5	0	8	6	179	180	4	0	4	10	109	119	3
0	4	3	1327	1338	7	0	10	6	203	201	4	0	5	10	312	307	4
0	5	3	472	450	7	0	11	6	197	185	6	0	6	10	75	85	5
0	6	3	504	470	5	0	12	6	103	102	5	0	7	10	118	112	4
0	7	3	142	131	5	0	13	6	108	114	5	0	8	10	108	104	4
0	8	3	117	126	3	0	14	6	148	137	5	0	9	10	71	71	6
0	9	3	293	309	4	0	4	7	153	160	3	0	10	10	119	113	4
0	10	3	79	71	6	0	5	7	505	505	9	0	11	10	142	145	7
0	11	3	174	169	3	0	6	7	209	189	4	0	12	10	138	136	4
0	12	3	137	142	4	0	7	7	514	539	6	0	13	10	209	201	4

Table 83 — continued

H	K	L	F_{obs}	F_{calc}	SigF	H	K	L	F_{obs}	F_{calc}	SigF	H	K	L	F_{obs}	F_{calc}	SigF
0	2	11	141	144	3	0	3	16	289	293	6	1	1	−13	184	194	4
0	3	11	327	310	4	0	5	16	72	71	6	1	2	−13	184	187	6
0	4	11	260	267	6	0	6	16	52	62	8	1	3	−13	217	224	4
0	5	11	278	279	7	0	2	17	163	165	5	1	4	−13	87	82	8
0	6	11	175	173	4	0	4	17	166	167	4	1	5	−13	251	253	5
0	7	11	244	229	9	0	6	17	135	132	4	1	6	−13	118	116	4
0	9	11	254	239	10	0	7	17	84	79	6	1	7	−13	279	274	6
0	10	11	85	93	5	0	0	18	107	108	5	1	8	−13	107	110	4
0	11	11	252	245	5	0	1	18	160	163	4	1	9	−13	211	209	4
0	0	12	48	24	6	0	2	18	155	146	4	1	10	−13	59	61	8
0	1	12	493	492	4	0	4	18	120	121	5	1	11	−13	190	184	5
0	3	12	375	369	8	0	5	18	98	89	5	1	2	−12	322	330	4
0	4	12	163	166	3	0	1	19	69	64	7	1	3	−12	198	190	4
0	6	12	148	141	4	1	1	−19	126	126	5	1	4	−12	168	173	3
0	7	12	81	85	5	1	3	−19	71	74	11	1	5	−12	257	247	5
0	9	12	100	103	5	1	1	−18	169	168	8	1	6	−12	124	125	4
0	11	12	127	129	7	1	2	−18	61	68	8	1	7	−12	104	113	4
0	12	12	204	195	4	1	3	−18	177	180	4	1	8	−12	120	125	4
0	2	13	143	144	3	1	5	−18	86	82	6	1	10	−12	132	133	4
0	3	13	207	210	4	1	2	−17	199	199	4	1	11	−12	91	95	6
0	4	13	422	413	6	1	5	−17	140	140	4	1	12	−12	139	137	4
0	5	13	115	115	4	1	7	−17	96	94	6	1	1	−11	144	153	3
0	6	13	167	162	12	1	1	−16	135	130	4	1	2	−11	178	180	4
0	7	13	71	64	7	1	2	−16	276	273	5	1	3	−11	124	131	3
0	8	13	162	159	6	1	3	−16	193	193	4	1	4	−11	263	274	12
0	10	13	210	207	7	1	4	−16	155	155	4	1	5	−11	64	59	6
0	0	14	322	336	4	1	5	−16	142	145	9	1	6	−11	366	364	7
0	1	14	115	113	6	1	6	−16	83	89	6	1	8	−11	273	270	6
0	2	14	497	516	4	1	1	−15	135	139	4	1	9	−11	70	70	6
0	3	14	111	107	4	1	2	−15	106	104	4	1	10	−11	189	185	4
0	4	14	171	175	4	1	3	−15	119	121	4	1	11	−11	127	125	8
0	10	14	64	63	8	1	4	−15	232	243	4	1	12	−11	141	138	5
0	1	15	84	84	5	1	5	−15	98	103	5	1	1	−10	529	533	3
0	2	15	140	145	4	1	6	−15	235	231	5	1	2	−10	357	364	4
0	3	15	410	422	5	1	7	−15	108	104	5	1	3	−10	283	292	4
0	4	15	72	78	6	1	8	−15	160	153	4	1	4	−10	204	211	12
0	5	15	301	311	5	1	1	−14	262	253	5	1	5	−10	277	286	4
0	6	15	125	127	4	1	2	−14	212	214	7	1	6	−10	187	199	5
0	7	15	135	132	5	1	3	−14	268	268	5	1	7	−10	129	122	3
0	8	15	60	59	8	1	4	−14	307	325	5	1	8	−10	133	137	4
0	9	15	84	82	13	1	5	−14	127	123	4	1	9	−10	147	141	3
0	0	16	260	259	5	1	6	−14	67	72	6	1	10	−10	104	110	5
0	1	16	332	339	5	1	8	−14	65	71	8	1	11	−10	167	167	7
0	2	16	191	202	8	1	9	−14	77	79	6	1	12	−10	155	157	7

Table 83 — continued

H	K	L	F_{obs}	F_{calc}	SigF	H	K	L	F_{obs}	F_{calc}	SigF	H	K	L	F_{obs}	F_{calc}	SigF
1	13	−10	121	112	13	1	5	−6	137	125	6	1	10	−3	248	254	5
1	1	−9	249	256	4	1	6	−6	357	351	10	1	11	−3	185	189	4
1	2	−9	65	53	4	1	8	−6	233	230	4	1	12	−3	234	229	4
1	3	−9	265	277	4	1	9	−6	160	159	6	1	13	−3	142	140	5
1	4	−9	106	108	3	1	10	−6	178	176	4	1	14	−3	120	116	5
1	5	−9	281	283	6	1	11	−6	162	162	3	1	15	−3	81	82	7
1	6	−9	234	236	11	1	12	−6	120	122	4	1	1	−2	773	768	4
1	7	−9	469	477	4	1	13	−6	71	68	7	1	2	−2	727	729	5
1	8	−9	63	65	8	1	1	−5	657	657	3	1	3	−2	770	775	6
1	9	−9	269	263	5	1	2	−5	275	273	4	1	4	−2	606	606	2
1	10	−9	98	99	5	1	3	−5	451	436	3	1	5	−2	276	274	3
1	11	−9	194	189	6	1	4	−5	256	276	4	1	6	−2	319	317	3
1	12	−9	129	134	4	1	5	−5	738	767	3	1	7	−2	273	273	4
1	13	−9	101	93	9	1	6	−5	324	345	4	1	8	−2	274	291	4
1	1	−8	387	391	3	1	7	−5	556	562	4	1	9	−2	184	185	5
1	2	−8	276	287	5	1	8	−5	323	326	6	1	10	−2	337	346	4
1	3	−8	512	514	4	1	9	−5	320	326	5	1	12	−2	185	183	4
1	4	−8	262	273	4	1	10	−5	73	74	5	1	13	−2	105	100	5
1	5	−8	356	353	6	1	11	−5	167	166	4	1	14	−2	185	185	4
1	6	−8	254	254	4	1	12	−5	167	168	6	1	1	−1	798	790	7
1	7	−8	204	209	6	1	13	−5	110	111	6	1	2	−1	221	225	2
1	8	−8	142	140	3	1	14	−5	91	91	9	1	3	−1	317	306	2
1	9	−8	92	97	5	1	1	−4	581	564	4	1	4	−1	478	466	3
1	10	−8	184	186	5	1	2	−4	368	360	2	1	5	−1	646	645	5
1	11	−8	151	153	3	1	3	−4	523	536	4	1	6	−1	546	544	6
1	12	−8	126	127	4	1	4	−4	508	506	3	1	7	−1	351	364	4
1	13	−8	101	106	7	1	5	−4	237	271	3	1	8	−1	360	368	4
1	1	−7	271	272	9	1	6	−4	170	175	3	1	9	−1	350	352	4
1	2	−7	251	255	4	1	7	−4	473	466	4	1	10	−1	200	202	4
1	3	−7	343	327	3	1	8	−4	224	221	10	1	11	−1	229	229	5
1	4	−7	284	291	3	1	9	−4	331	335	4	1	12	−1	82	89	5
1	5	−7	460	461	8	1	10	−4	183	183	4	1	13	−1	155	161	4
1	6	−7	599	596	3	1	11	−4	211	213	4	1	14	−1	80	82	8
1	7	−7	387	389	5	1	13	−4	111	110	6	1	1	0	1678	1762	24
1	8	−7	411	421	12	1	14	−4	97	98	6	1	2	0	692	685	5
1	9	−7	149	147	3	1	1	−3	234	225	2	1	3	0	450	436	4
1	10	−7	276	274	5	1	2	−3	469	473	5	1	4	0	302	289	3
1	11	−7	159	157	5	1	3	−3	582	575	4	1	5	0	523	518	6
1	12	−7	153	155	4	1	4	−3	255	243	3	1	6	0	207	209	4
1	13	−7	129	124	4	1	5	−3	745	731	6	1	8	0	244	244	6
1	1	−6	347	345	6	1	6	−3	514	524	12	1	9	0	272	265	4
1	2	−6	496	506	3	1	7	−3	524	526	7	1	10	0	231	222	4
1	3	−6	70	52	5	1	8	−3	433	449	4	1	11	0	342	346	5
1	4	−6	497	507	3	1	9	−3	294	303	4	1	12	0	105	106	4

Table 83 — continued

H	K	L	F_{obs}	F_{calc}	SigF	H	K	L	F_{obs}	F_{calc}	SigF	H	K	L	F_{obs}	F_{calc}	SigF
1	13	0	187	192	5	1	11	3	197	196	4	1	11	6	161	164	3
1	14	0	100	98	5	1	12	3	241	240	5	1	12	6	119	119	4
1	15	0	148	140	4	1	13	3	143	141	4	1	13	6	63	70	7
1	0	1	592	580	3	1	14	3	124	121	4	1	14	6	111	101	5
1	1	1	802	799	5	1	15	3	85	84	6	1	0	7	125	100	3
1	2	1	206	208	2	1	0	4	87	90	2	1	1	7	269	268	3
1	3	1	292	282	2	1	1	4	575	558	4	1	2	7	261	267	3
1	4	1	500	486	3	1	2	4	349	344	4	1	3	7	328	317	9
1	5	1	645	644	3	1	3	4	507	517	6	1	4	7	282	289	4
1	6	1	557	554	4	1	4	4	498	494	4	1	5	7	454	450	5
1	7	1	329	347	3	1	5	4	253	279	3	1	6	7	571	580	5
1	8	1	361	371	4	1	6	4	157	166	5	1	7	7	381	382	7
1	9	1	370	367	5	1	7	4	481	467	4	1	8	7	417	424	6
1	10	1	197	193	4	1	8	4	225	229	4	1	9	7	147	144	8
1	11	1	250	250	6	1	9	4	328	331	9	1	10	7	259	258	5
1	12	1	75	87	6	1	10	4	177	177	4	1	11	7	156	156	3
1	13	1	165	168	3	1	11	4	213	206	4	1	12	7	149	151	5
1	14	1	77	82	6	1	13	4	122	120	4	1	13	7	132	129	4
1	0	2	1318	1335	13	1	14	4	103	98	7	1	0	8	551	575	6
1	1	2	770	767	7	1	0	5	172	157	3	1	1	8	381	382	3
1	2	2	692	700	5	1	1	5	655	658	6	1	2	8	287	297	9
1	3	2	773	779	6	1	2	5	274	271	3	1	3	8	499	500	10
1	4	2	606	607	5	1	3	5	479	461	6	1	4	8	282	287	4
1	5	2	267	267	3	1	4	5	259	275	3	1	5	8	355	344	4
1	6	2	314	314	4	1	5	5	725	750	6	1	6	8	264	261	4
1	7	2	284	279	6	1	6	5	328	341	3	1	7	8	195	208	12
1	8	2	274	288	4	1	7	5	540	554	7	1	8	8	140	147	3
1	9	2	182	183	3	1	8	5	315	316	5	1	9	8	102	103	4
1	10	2	338	344	4	1	9	5	319	320	4	1	10	8	189	192	4
1	12	2	183	188	4	1	10	5	82	80	11	1	11	8	156	154	4
1	13	2	105	105	5	1	11	5	159	156	3	1	12	8	136	138	4
1	14	2	195	189	4	1	12	5	177	172	3	1	13	8	118	109	5
1	15	2	71	71	10	1	13	5	113	117	4	1	0	9	50	64	5
1	0	3	545	549	4	1	14	5	94	94	6	1	1	9	232	247	4
1	1	3	234	222	2	1	0	6	169	188	3	1	2	9	57	46	5
1	2	3	486	493	19	1	1	6	338	344	6	1	3	9	271	280	5
1	3	3	594	586	7	1	2	6	469	478	3	1	4	9	107	105	5
1	4	3	226	217	3	1	3	6	77	63	3	1	5	9	292	288	4
1	5	3	769	750	6	1	4	6	472	481	5	1	6	9	243	237	9
1	6	3	504	507	3	1	5	6	123	111	2	1	7	9	486	489	5
1	7	3	533	530	6	1	6	6	362	354	6	1	9	9	272	270	5
1	8	3	435	449	9	1	8	6	232	227	4	1	10	9	102	100	4
1	9	3	298	307	7	1	9	6	157	155	3	1	11	9	189	186	4
1	10	3	268	270	5	1	10	6	172	171	3	1	12	9	133	133	4

Table 83 — continued

H	K	L	F_{obs}	F_{calc}	SigF	H	K	L	F_{obs}	F_{calc}	SigF	H	K	L	F_{obs}	F_{calc}	SigF
1	13	9	102	94	5	1	9	13	214	212	5	2	2	−18	187	189	4
1	0	10	162	159	3	1	10	13	55	57	9	2	3	−18	75	75	7
1	1	10	523	532	6	1	11	13	181	179	6	2	4	−18	143	139	4
1	2	10	356	360	4	1	0	14	182	180	4	2	5	−18	100	96	6
1	3	10	300	306	4	1	1	14	258	252	8	2	5	−18	100	96	5
1	4	10	206	217	4	1	2	14	214	215	5	2	1	−17	110	101	5
1	5	10	286	294	4	1	3	14	256	260	5	2	2	−17	105	108	5
1	6	10	193	199	4	1	4	14	320	327	5	2	3	−17	127	121	4
1	7	10	127	122	5	1	5	14	120	119	4	2	5	−17	106	95	5
1	8	10	139	142	3	1	6	14	54	67	8	2	5	−17	102	95	5
1	9	10	151	143	3	1	8	14	71	70	6	2	6	−17	127	133	5
1	10	10	111	111	4	1	9	14	79	81	6	2	6	−17	141	133	4
1	11	10	178	176	5	1	0	15	99	98	4	2	7	−17	76	82	8
1	12	10	161	157	4	1	1	15	129	134	9	2	7	−17	84	81	6
1	13	10	110	113	8	1	2	15	110	107	6	2	1	−16	164	163	7
1	0	11	193	204	4	1	3	15	117	119	4	2	2	−16	115	116	4
1	1	11	138	145	4	1	4	15	232	245	5	2	3	−16	233	230	4
1	2	11	173	173	4	1	5	15	93	91	6	2	4	−16	103	106	6
1	3	11	118	123	4	1	6	15	220	228	5	2	5	−16	148	149	11
1	4	11	276	282	8	1	7	15	100	103	5	2	6	−16	132	129	4
1	6	11	390	381	7	1	8	15	160	156	4	2	6	−16	132	129	4
1	8	11	280	279	5	1	0	16	218	212	5	2	7	−16	107	112	6
1	10	11	190	189	4	1	1	16	135	131	4	2	7	−16	108	112	5
1	11	11	120	120	7	1	2	16	276	269	5	2	8	−16	60	66	9
1	12	11	132	133	4	1	3	16	192	193	4	2	8	−16	70	66	7
1	0	12	386	398	6	1	4	16	155	154	4	2	1	−15	74	77	6
1	2	12	315	324	4	1	5	16	143	146	4	2	5	−15	108	106	5
1	3	12	209	202	4	1	6	16	97	97	5	2	6	−15	77	81	6
1	4	12	169	172	4	1	8	16	62	52	8	2	6	−15	81	81	5
1	5	12	250	249	5	1	0	17	249	253	5	2	7	−15	180	178	4
1	6	12	120	120	6	1	2	17	194	201	4	2	7	−15	183	177	4
1	7	12	96	110	5	1	3	17	64	62	7	2	8	−15	140	141	5
1	8	12	123	121	4	1	5	17	135	135	4	2	8	−15	144	140	4
1	10	12	135	137	4	1	6	17	65	62	7	2	9	−15	134	121	5
1	11	12	97	100	11	1	7	17	88	92	9	2	9	−15	120	120	5
1	12	12	136	138	5	1	1	18	165	157	4	2	1	−14	289	294	5
1	1	13	176	187	4	1	3	18	182	174	4	2	2	−14	62	59	6
1	2	13	181	180	5	1	4	18	68	65	7	2	3	−14	234	230	5
1	3	13	219	220	4	1	5	18	90	86	7	2	4	−14	132	130	4
1	4	13	77	74	6	1	1	19	124	129	5	2	5	−14	183	190	4
1	5	13	262	260	5	1	3	19	85	75	13	2	6	−14	167	164	3
1	6	13	105	107	4	2	1	−19	100	103	6	2	6	−14	172	163	3
1	7	13	283	275	6	2	2	−19	147	146	5	2	7	−14	111	102	5
1	8	13	113	110	5	2	1	−18	130	137	4	2	7	−14	106	102	4

Table 83 — continued

H	K	L	F_{obs}	F_{calc}	SigF	H	K	L	F_{obs}	F_{calc}	SigF	H	K	L	F_{obs}	F_{calc}	SigF
2	9	−14	76	66	6	2	3	−10	176	180	3	2	11	−7	160	162	3
2	10	−14	87	93	7	2	4	−10	408	418	4	2	12	−7	171	169	7
2	10	−14	99	93	5	2	5	−10	313	322	6	2	13	−7	156	149	4
2	1	−13	77	88	8	2	6	−10	347	345	5	2	14	−7	127	122	5
2	2	−13	104	96	4	2	7	−10	147	154	5	2	1	−6	842	819	17
2	3	−13	121	119	4	2	8	−10	136	135	4	2	3	−6	471	481	7
2	4	−13	149	149	4	2	9	−10	59	60	7	2	4	−6	97	82	3
2	5	−13	141	147	3	2	10	−10	96	98	5	2	5	−6	140	131	3
2	6	−13	298	297	5	2	11	−10	82	77	8	2	6	−6	501	491	3
2	7	−13	158	162	4	2	12	−10	145	141	4	2	7	−6	153	159	3
2	7	−13	159	161	3	2	1	−9	269	253	4	2	8	−6	237	233	6
2	8	−13	268	257	5	2	2	−9	216	223	4	2	9	−6	165	169	4
2	8	−13	260	255	5	2	3	−9	204	213	5	2	10	−6	173	176	4
2	9	−13	153	161	4	2	4	−9	449	471	4	2	13	−6	67	67	7
2	9	−13	161	160	4	2	5	−9	244	243	5	2	2	−5	930	931	5
2	10	−13	195	198	4	2	6	−9	244	253	4	2	3	−5	341	348	3
2	10	−13	201	197	3	2	7	−9	90	83	4	2	4	−5	472	454	21
2	11	−13	88	85	7	2	8	−9	134	131	3	2	5	−5	226	239	8
2	11	−13	82	85	6	2	9	−9	284	290	9	2	6	−5	632	650	4
2	1	−12	179	179	4	2	10	−9	142	145	7	2	7	−5	451	439	16
2	2	−12	308	313	4	2	11	−9	111	122	4	2	8	−5	249	256	4
2	3	−12	136	137	6	2	12	−9	57	62	9	2	9	−5	122	123	4
2	4	−12	77	82	6	2	13	−9	113	112	5	2	10	−5	149	153	3
2	5	−12	353	351	6	2	1	−8	350	359	14	2	11	−5	222	225	5
2	7	−12	155	163	4	2	2	−8	593	602	5	2	12	−5	192	195	8
2	9	−12	69	76	7	2	3	−8	289	278	4	2	13	−5	111	111	5
2	9	−12	74	75	6	2	4	−8	90	88	6	2	14	−5	106	118	5
2	10	−12	60	52	7	2	5	−8	114	128	3	2	1	−4	615	605	4
2	11	−12	142	143	4	2	6	−8	111	108	15	2	2	−4	782	771	2
2	11	−12	148	142	4	2	7	−8	149	148	4	2	3	−4	274	282	3
2	1	−11	166	161	3	2	8	−8	183	182	4	2	4	−4	507	519	3
2	2	−11	84	84	4	2	9	−8	105	105	4	2	5	−4	300	309	7
2	3	−11	394	403	4	2	11	−8	96	92	5	2	6	−4	339	346	4
2	4	−11	299	304	8	2	13	−8	62	67	8	2	7	−4	461	461	3
2	5	−11	350	370	4	2	1	−7	346	348	10	2	8	−4	216	215	6
2	6	−11	179	183	5	2	2	−7	116	113	3	2	9	−4	269	265	8
2	7	−11	350	345	8	2	3	−7	430	480	3	2	10	−4	188	191	4
2	8	−11	198	199	4	2	4	−7	224	221	4	2	11	−4	105	109	4
2	9	−11	199	197	6	2	5	−7	455	460	5	2	12	−4	185	183	4
2	10	−11	93	95	7	2	6	−7	224	221	4	2	14	−4	142	138	4
2	11	−11	147	146	4	2	7	−7	249	253	5	2	1	−3	935	916	9
2	11	−11	150	145	4	2	8	−7	78	69	6	2	2	−3	1208	1182	6
2	1	−10	334	335	6	2	9	−7	200	196	7	2	4	−3	447	446	3
2	2	−10	506	526	8	2	10	−7	145	149	4	2	5	−3	371	360	3

Table 83 — continued

H	K	L	F_{obs}	F_{calc}	SigF	H	K	L	F_{obs}	F_{calc}	SigF	H	K	L	F_{obs}	F_{calc}	SigF
2	6	−3	225	211	6	2	7	0	222	229	6	2	8	3	429	438	7
2	7	−3	446	451	3	2	8	0	238	225	4	2	9	3	209	212	8
2	8	−3	433	442	4	2	9	0	141	140	3	2	10	3	286	286	6
2	9	−3	218	219	6	2	10	0	379	388	5	2	11	3	120	122	4
2	10	−3	289	291	6	2	12	0	278	283	5	2	12	3	136	139	4
2	11	−3	117	118	4	2	14	0	225	219	5	2	13	3	182	185	7
2	12	−3	137	140	4	2	15	0	113	114	5	2	14	3	81	79	8
2	13	−3	177	180	4	2	0	1	257	245	6	2	0	4	1028	1018	4
2	14	−3	79	76	6	2	1	1	169	165	3	2	1	4	621	613	2
2	1	−2	364	339	5	2	2	1	676	659	11	2	2	4	788	776	11
2	2	−2	66	70	4	2	3	1	571	556	5	2	3	4	276	276	9
2	3	−2	582	572	5	2	4	1	205	197	3	2	4	4	506	519	6
2	4	−2	307	293	4	2	5	1	134	139	3	2	5	4	302	306	7
2	5	−2	473	484	4	2	6	1	428	426	5	2	6	4	347	349	5
2	6	−2	293	295	5	2	7	1	259	274	5	2	7	4	468	457	7
2	7	−2	406	418	4	2	8	1	493	492	5	2	8	4	215	212	4
2	8	−2	364	356	4	2	9	1	532	530	7	2	9	4	263	263	4
2	9	−2	226	229	6	2	10	1	224	220	5	2	10	4	185	188	4
2	10	−2	83	80	5	2	11	1	162	162	3	2	11	4	113	121	4
2	11	−2	310	313	5	2	12	1	140	136	4	2	12	4	198	192	6
2	12	−2	159	160	3	2	13	1	122	124	4	2	14	4	145	140	4
2	13	−2	249	248	5	2	15	1	87	85	6	2	0	5	381	373	4
2	14	−2	57	59	9	2	0	2	744	714	2	2	2	5	920	926	3
2	1	−1	192	184	3	2	1	2	342	317	4	2	3	5	339	346	3
2	2	−1	685	678	19	2	2	2	83	84	7	2	4	5	478	470	6
2	3	−1	584	572	4	2	3	2	597	591	11	2	5	5	216	234	7
2	4	−1	213	210	3	2	4	2	314	295	3	2	6	5	640	660	13
2	5	−1	135	140	4	2	5	2	477	488	5	2	7	5	450	439	6
2	6	−1	434	437	3	2	6	2	287	289	4	2	8	5	244	251	4
2	7	−1	257	274	4	2	7	2	417	421	7	2	9	5	117	115	3
2	8	−1	499	499	4	2	8	2	362	354	6	2	10	5	126	130	3
2	9	−1	536	535	8	2	9	2	220	222	6	2	11	5	219	222	4
2	10	−1	223	213	7	2	10	2	94	89	4	2	12	5	196	198	9
2	11	−1	163	163	3	2	11	2	315	312	6	2	13	5	114	113	4
2	12	−1	140	137	4	2	12	2	166	168	4	2	14	5	122	122	5
2	13	−1	122	125	5	2	13	2	250	248	5	2	0	6	444	469	13
2	15	−1	83	78	7	2	0	3	153	146	5	2	1	6	826	815	3
2	0	0	251	233	2	2	1	3	922	903	7	2	2	6	50	40	4
2	1	0	180	170	4	2	2	3	1199	1174	13	2	3	6	467	476	5
2	2	0	73	76	12	2	3	3	73	73	4	2	4	6	87	75	5
2	3	0	327	324	5	2	4	3	438	435	5	2	5	6	127	119	2
2	4	0	536	541	8	2	5	3	383	370	6	2	6	6	487	476	3
2	5	0	74	68	3	2	6	3	215	207	5	2	7	6	158	158	5
2	6	0	170	166	3	2	7	3	449	453	7	2	8	6	217	224	11

Table 83 — continued

H	K	L	F_{obs}	F_{calc}	SigF	H	K	L	F_{obs}	F_{calc}	SigF	H	K	L	F_{obs}	F_{calc}	SigF
2	9	6	162	163	3	2	0	10	671	678	3	2	10	13	196	197	5
2	10	6	168	169	3	2	1	10	342	337	4	2	11	13	95	90	6
2	11	6	62	59	10	2	2	10	526	534	9	2	0	14	83	78	5
2	12	6	96	95	10	2	3	10	177	177	3	2	1	14	295	294	10
2	13	6	78	79	9	2	4	10	423	424	13	2	2	14	83	83	5
2	14	6	55	51	9	2	5	10	332	333	4	2	3	14	230	231	8
2	1	7	352	349	3	2	6	10	352	348	9	2	4	14	128	124	4
2	2	7	106	104	3	2	7	10	160	165	3	2	5	14	181	187	4
2	3	7	432	477	3	2	8	10	139	137	3	2	6	14	162	163	5
2	4	7	208	207	4	2	10	10	108	104	4	2	7	14	97	99	9
2	5	7	466	472	6	2	11	10	84	81	5	2	10	14	103	93	5
2	6	7	235	225	4	2	12	10	146	148	4	2	1	15	77	69	9
2	7	7	236	248	6	2	0	11	302	303	9	2	5	15	111	109	4
2	8	7	70	74	5	2	1	11	164	153	4	2	6	15	86	85	6
2	9	7	168	171	4	2	2	11	82	85	4	2	7	15	185	178	4
2	10	7	153	155	7	2	3	11	394	400	4	2	8	15	143	141	11
2	11	7	146	145	3	2	4	11	320	312	4	2	9	15	122	119	5
2	12	7	167	167	3	2	5	11	369	376	4	2	1	16	181	176	8
2	13	7	153	153	10	2	6	11	188	187	4	2	2	16	118	121	4
2	14	7	127	127	5	2	7	11	360	352	14	2	3	16	243	237	5
2	0	8	344	347	13	2	8	11	192	199	4	2	4	16	105	107	5
2	1	8	347	364	3	2	9	11	192	191	4	2	5	16	160	155	7
2	2	8	592	599	3	2	10	11	97	96	5	2	6	16	127	127	4
2	3	8	311	296	3	2	11	11	147	146	4	2	7	16	119	116	5
2	4	8	111	109	4	2	0	12	279	286	4	2	0	17	91	86	5
2	5	8	114	123	10	2	1	12	182	177	4	2	1	17	112	103	5
2	6	8	114	119	6	2	2	12	309	312	4	2	2	17	98	100	5
2	7	8	148	148	3	2	3	12	141	135	3	2	3	17	126	118	7
2	8	8	183	180	8	2	4	12	92	91	4	2	5	17	89	93	6
2	9	8	106	102	5	2	5	12	340	344	15	2	6	17	133	130	4
2	11	8	99	101	5	2	6	12	60	62	7	2	7	17	71	76	8
2	0	9	178	170	3	2	7	12	158	161	3	2	0	18	123	120	6
2	1	9	263	249	6	2	9	12	77	74	6	2	1	18	138	139	4
2	2	9	214	213	4	2	11	12	147	144	4	2	2	18	196	194	4
2	3	9	213	219	4	2	0	13	85	83	5	2	3	18	79	78	6
2	4	9	462	472	7	2	1	13	80	90	5	2	4	18	144	143	4
2	5	9	246	245	4	2	2	13	87	86	5	2	5	18	99	96	6
2	6	9	269	273	4	2	3	13	129	131	3	2	0	19	142	143	4
2	7	9	79	81	5	2	4	13	157	154	5	2	1	19	97	99	6
2	8	9	136	135	3	2	5	13	154	156	3	2	2	19	155	149	5
2	9	9	288	291	5	2	6	13	304	301	5	3	1	−18	111	117	5
2	10	9	121	123	4	2	7	13	158	163	3	3	3	−18	112	121	5
2	11	9	112	121	6	2	8	13	261	256	12	3	3	−18	124	120	4
2	13	9	120	114	5	2	9	13	166	163	5	3	4	−18	84	93	7

Table 83 — continued

H	K	L	F_{obs}	F_{calc}	SigF	H	K	L	F_{obs}	F_{calc}	SigF	H	K	L	F_{obs}	F_{calc}	SigF
3	4	−18	88	93	6	3	8	−14	199	195	4	3	6	−11	364	368	5
3	1	−17	82	86	6	3	8	−14	198	194	4	3	7	−11	113	111	4
3	2	−17	69	64	7	3	1	−13	198	199	4	3	7	−11	112	111	4
3	3	−17	142	141	4	3	3	−13	119	116	4	3	8	−11	209	216	4
3	3	−17	142	140	4	3	3	−13	120	115	4	3	8	−11	204	214	4
3	4	−17	133	134	5	3	4	−13	117	120	4	3	9	−11	75	68	7
3	4	−17	129	133	4	3	4	−13	112	119	4	3	9	−11	66	67	6
3	5	−17	101	104	6	3	5	−13	238	233	4	3	10	−11	138	137	4
3	5	−17	104	103	5	3	5	−13	232	232	5	3	10	−11	134	136	4
3	6	−17	148	143	4	3	6	−13	144	150	4	3	1	−10	337	333	5
3	6	−17	143	143	4	3	6	−13	148	149	3	3	2	−10	323	323	4
3	2	−16	223	225	5	3	7	−13	217	209	4	3	3	−10	417	424	4
3	2	−16	227	224	5	3	7	−13	213	208	4	3	3	−10	416	421	4
3	4	−16	123	120	5	3	8	−13	107	118	5	3	4	−10	64	65	6
3	4	−16	122	120	4	3	8	−13	118	118	4	3	4	−10	63	64	5
3	5	−16	117	118	5	3	9	−13	123	117	5	3	5	−10	349	358	4
3	5	−16	117	118	4	3	9	−13	115	117	5	3	5	−10	355	356	4
3	6	−16	94	91	6	3	1	−12	191	197	4	3	7	−10	103	106	5
3	6	−16	87	90	6	3	2	−12	211	217	5	3	7	−10	100	106	4
3	7	−16	156	158	4	3	2	−12	214	218	4	3	8	−10	144	141	4
3	7	−16	166	157	4	3	3	−12	133	125	3	3	8	−10	144	140	3
3	2	−15	109	108	5	3	3	−12	133	126	4	3	9	−10	106	108	5
3	2	−15	109	107	4	3	4	−12	364	369	4	3	9	−10	114	108	4
3	4	−15	158	162	4	3	4	−12	371	371	5	3	10	−10	77	91	7
3	4	−15	163	161	3	3	5	−12	76	82	6	3	10	−10	86	91	5
3	5	−15	123	133	5	3	5	−12	84	81	5	3	11	−10	86	95	7
3	5	−15	132	132	4	3	6	−12	164	162	3	3	11	−10	94	95	5
3	6	−15	167	165	4	3	6	−12	164	161	3	3	12	−10	77	73	8
3	6	−15	164	165	4	3	7	−12	168	174	4	3	12	−10	57	73	9
3	7	−15	156	158	4	3	7	−12	174	173	3	3	1	−9	182	185	8
3	7	−15	161	157	4	3	9	−12	185	184	4	3	2	−9	509	512	3
3	8	−15	84	97	7	3	9	−12	18?	183	4	3	3	−9	255	260	4
3	8	−15	86	97	6	3	10	−12	67	73	7	3	4	−9	116	113	3
3	1	−14	175	176	4	3	11	−12	130	131	5	3	5	−9	387	410	4
3	2	−14	90	98	5	3	11	−12	140	131	4	3	5	−9	404	407	4
3	2	−14	93	97	4	3	1	−11	381	374	10	3	6	−9	197	203	4
3	3	−14	123	127	4	3	2	−11	95	99	4	3	6	−9	206	202	4
3	3	−14	125	126	4	3	3	−11	220	217	4	3	7	−9	220	223	4
3	5	−14	130	125	4	3	3	−11	219	216	4	3	7	−9	209	224	5
3	5	−14	125	124	4	3	4	−11	467	467	4	3	8	−9	102	105	5
3	6	−14	149	155	4	3	4	−11	468	464	4	3	8	−9	116	105	4
3	6	−14	158	154	3	3	5	−11	138	136	4	3	9	−9	133	135	4
3	7	−14	100	106	5	3	5	−11	144	135	3	3	9	−9	136	135	3
3	7	−14	103	105	5	3	6	−11	373	366	4	3	10	−9	88	101	6

Table 83 — continued

H	K	L	F_{obs}	F_{calc}	SigF	H	K	L	F_{obs}	F_{calc}	SigF	H	K	L	F_{obs}	F_{calc}	SigF
3	10	−9	100	100	5	3	8	−5	115	122	8	3	12	−2	137	136	4
3	11	−9	133	133	4	3	9	−5	142	144	4	3	14	−2	137	143	8
3	1	−8	512	512	3	3	10	−5	136	139	4	3	1	−1	541	527	4
3	2	−8	353	334	4	3	11	−5	163	168	4	3	2	−1	144	145	10
3	3	−8	354	364	4	3	13	−5	193	190	4	3	3	−1	336	327	3
3	4	−8	587	583	6	3	14	−5	85	89	7	3	4	−1	197	199	4
3	5	−8	136	145	3	3	1	−4	979	950	4	3	5	−1	557	546	4
3	6	−8	191	198	4	3	2	−4	270	267	3	3	6	−1	183	197	7
3	7	−8	213	210	11	3	3	−4	383	397	3	3	7	−1	280	280	4
3	8	−8	96	98	5	3	4	−4	206	206	4	3	8	−1	210	209	4
3	9	−8	138	138	9	3	5	−4	217	217	4	3	9	−1	264	270	6
3	10	−8	102	104	5	3	6	−4	223	235	9	3	10	−1	175	171	3
3	1	−7	551	568	7	3	7	−4	267	269	4	3	11	−1	211	208	5
3	2	−7	196	205	4	3	8	−4	225	227	6	3	12	−1	200	204	4
3	3	−7	215	224	4	3	9	−4	293	303	5	3	13	−1	208	206	4
3	4	−7	220	223	9	3	10	−4	175	177	4	3	14	−1	149	145	4
3	5	−7	259	255	4	3	11	−4	255	258	5	3	1	0	795	756	6
3	6	−7	179	180	3	3	12	−4	152	152	4	3	2	0	97	104	3
3	7	−7	275	273	6	3	13	−4	180	180	4	3	3	0	268	262	4
3	8	−7	91	84	5	3	1	−3	1015	957	17	3	4	0	124	118	2
3	9	−7	109	108	4	3	2	−3	623	599	12	3	5	0	529	520	5
3	10	−7	116	121	4	3	3	−3	378	360	3	3	6	0	135	152	4
3	11	−7	91	94	5	3	4	−3	387	369	6	3	7	0	452	444	3
3	12	−7	161	156	4	3	5	−3	265	261	6	3	8	0	476	481	4
3	1	−6	451	456	3	3	6	−3	545	551	9	3	10	0	421	419	5
3	2	−6	653	653	3	3	7	−3	96	107	11	3	12	0	133	131	4
3	3	−6	365	363	5	3	8	−3	319	325	12	3	0	1	120	124	3
3	4	−6	260	265	5	3	9	−3	155	153	3	3	1	1	529	513	6
3	5	−6	457	457	6	3	10	−3	224	224	7	3	2	1	121	121	10
3	6	−6	206	206	4	3	11	−3	177	179	3	3	3	1	326	315	8
3	7	−6	225	223	4	3	12	−3	248	251	5	3	4	1	213	213	4
3	8	−6	69	68	6	3	13	−3	156	154	4	3	5	1	553	542	4
3	9	−6	181	181	4	3	14	−3	115	114	5	3	6	1	164	176	7
3	10	−6	146	138	3	3	1	−2	444	418	4	3	7	1	289	288	4
3	11	−6	183	180	3	3	2	−2	450	456	6	3	8	1	210	209	4
3	12	−6	123	118	4	3	3	−2	251	251	3	3	9	1	271	277	6
3	13	−6	82	90	7	3	4	−2	365	358	6	3	10	1	166	161	3
3	1	−5	341	338	3	3	5	−2	188	178	5	3	11	1	197	200	4
3	2	−5	508	504	4	3	6	−2	382	372	6	3	12	1	197	204	4
3	3	−5	337	318	6	3	7	−2	281	288	6	3	13	1	205	204	7
3	4	−5	235	235	4	3	8	−2	131	123	5	3	14	1	150	146	4
3	5	−5	413	413	6	3	9	−2	337	332	4	3	0	2	1069	1004	4
3	6	−5	200	203	4	3	10	−2	185	182	4	3	1	2	449	425	3
3	7	−5	275	276	5	3	11	−2	151	152	3	3	2	2	488	491	3

Table 83 — continued

H	K	L	F_{obs}	F_{calc}	SigF	H	K	L	F_{obs}	F_{calc}	SigF	H	K	L	F_{obs}	F_{calc}	SigF
3	3	2	259	253	3	3	4	5	234	240	8	3	6	8	192	206	4
3	4	2	354	351	8	3	5	5	425	419	8	3	7	8	196	199	4
3	5	2	216	199	4	3	6	5	201	209	4	3	8	8	93	96	9
3	6	2	382	375	5	3	7	5	289	290	4	3	9	8	124	125	4
3	7	2	278	287	7	3	8	5	129	131	3	3	10	8	100	96	4
3	8	2	127	121	3	3	9	5	150	148	4	3	12	8	70	72	7
3	9	2	331	331	8	3	10	5	124	127	4	3	0	9	522	528	4
3	10	2	191	188	4	3	11	5	162	164	3	3	1	9	186	193	4
3	11	2	162	158	5	3	12	5	70	67	6	3	2	9	503	510	10
3	12	2	121	125	4	3	13	5	193	190	4	3	3	9	258	257	4
3	14	2	143	139	7	3	14	5	99	92	6	3	4	9	136	127	3
3	0	3	139	149	3	3	0	6	680	654	3	3	5	9	386	398	4
3	1	3	996	949	10	3	1	6	434	444	3	3	6	9	203	205	4
3	2	3	615	584	11	3	2	6	659	661	9	3	7	9	218	221	11
3	3	3	369	349	3	3	3	6	352	351	10	3	8	9	109	107	4
3	4	3	375	361	8	3	4	6	287	287	7	3	9	9	125	129	4
3	5	3	254	255	5	3	5	6	458	452	3	3	10	9	94	100	5
3	6	3	546	554	8	3	6	6	212	210	4	3	11	9	134	132	4
3	7	3	104	114	7	3	7	6	231	219	4	3	0	10	334	350	4
3	8	3	331	338	7	3	8	6	66	68	5	3	1	10	342	339	4
3	9	3	150	150	3	3	9	6	165	167	3	3	2	10	312	314	5
3	10	3	218	223	7	3	10	6	150	146	3	3	3	10	406	410	5
3	11	3	163	165	3	3	11	6	187	185	4	3	4	10	68	71	6
3	12	3	253	251	5	3	12	6	123	124	7	3	5	10	349	352	6
3	13	3	148	152	4	3	13	6	100	98	7	3	7	10	114	116	4
3	14	3	118	112	5	3	0	7	719	694	3	3	8	10	134	132	4
3	0	4	176	185	3	3	1	7	533	553	10	3	9	10	99	99	4
3	1	4	1003	970	7	3	2	7	210	216	4	3	10	10	80	82	12
3	2	4	253	251	6	3	3	7	218	231	5	3	11	10	90	92	5
3	3	4	419	424	7	3	4	7	232	235	6	3	0	11	146	154	4
3	4	4	221	214	6	3	5	7	267	263	4	3	1	11	370	370	4
3	5	4	237	232	6	3	6	7	178	185	5	3	2	11	112	110	3
3	6	4	225	232	4	3	7	7	284	277	4	3	3	11	217	221	5
3	7	4	272	276	10	3	8	7	84	81	11	3	4	11	459	459	8
3	8	4	217	228	5	3	9	7	122	115	5	3	5	11	144	143	3
3	9	4	300	308	6	3	10	7	110	111	4	3	6	11	381	358	6
3	10	4	164	168	3	3	11	7	95	89	5	3	7	11	108	112	4
3	11	4	267	262	5	3	12	7	154	155	4	3	8	11	210	212	4
3	12	4	162	163	6	3	0	8	551	547	3	3	9	11	77	74	6
3	13	4	184	181	4	3	1	8	505	507	4	3	10	11	140	137	4
3	0	5	937	961	7	3	2	8	350	326	8	3	0	12	183	188	7
3	1	5	335	330	3	3	3	8	366	374	4	3	1	12	188	194	4
3	2	5	491	494	4	3	4	8	593	578	8	3	2	12	200	204	4
3	3	5	318	300	5	3	5	8	148	153	3	3	3	12	119	111	6

Table 83 — continued

H	K	L	F_{obs}	F_{calc}	SigF	H	K	L	F_{obs}	F_{calc}	SigF	H	K	L	F_{obs}	F_{calc}	SigF
3	4	12	350	354	5	4	2	−18	125	122	5	4	1	−13	269	267	5
3	5	12	96	98	13	4	1	−17	121	110	5	4	2	−13	153	150	3
3	6	12	167	162	10	4	1	−17	112	109	5	4	2	−13	147	151	4
3	7	12	178	176	3	4	2	−17	75	63	6	4	3	−13	217	218	5
3	9	12	187	183	4	4	3	−17	143	137	4	4	3	−13	228	219	4
3	11	12	138	132	4	4	3	−17	138	136	4	4	4	−13	214	217	5
3	0	13	170	171	3	4	4	−17	143	138	5	4	4	−13	219	216	4
3	1	13	200	202	5	4	4	−17	144	138	4	4	5	−13	119	118	5
3	3	13	113	112	4	4	5	−17	100	99	6	4	5	−13	118	117	4
3	4	13	131	131	4	4	5	−17	98	98	5	4	6	−13	197	201	4
3	5	13	230	229	11	4	1	−16	247	255	5	4	6	−13	201	200	4
3	6	13	148	151	3	4	1	−16	250	253	5	4	8	−13	77	79	7
3	7	13	200	205	4	4	2	−16	57	50	8	4	8	−13	65	78	7
3	8	13	118	122	4	4	3	−16	83	86	7	4	9	−13	62	63	9
3	9	13	118	120	5	4	3	−16	94	85	5	4	9	−13	67	62	7
3	0	14	167	160	4	4	4	−16	82	77	7	4	1	−12	267	265	5
3	1	14	179	179	4	4	4	−16	62	77	8	4	1	−12	256	263	5
3	2	14	89	90	5	4	6	−16	147	148	5	4	3	−12	94	92	5
3	3	14	125	127	7	4	6	−16	138	147	4	4	3	−12	93	92	4
3	5	14	133	129	6	4	1	−15	152	150	4	4	4	−12	56	61	7
3	6	14	164	159	5	4	1	−15	154	149	3	4	4	−12	61	61	8
3	7	14	111	114	5	4	2	−15	209	218	4	4	5	−12	108	106	4
3	8	14	195	195	4	4	2	−15	212	216	4	4	5	−12	106	107	5
3	0	15	64	57	7	4	3	−15	158	159	4	4	6	−12	222	217	4
3	2	15	95	98	5	4	3	−15	151	158	3	4	6	−12	220	216	4
3	4	15	160	155	4	4	4	−15	183	180	4	4	8	−12	151	146	4
3	5	15	132	135	5	4	4	−15	178	179	3	4	8	−12	147	146	3
3	6	15	164	163	5	4	5	−15	205	203	4	4	10	−12	124	128	5
3	7	15	164	161	4	4	5	−15	206	202	4	4	10	−12	127	127	4
3	8	15	86	87	6	4	6	−15	144	147	5	4	1	−11	181	178	4
3	0	16	187	182	14	4	6	−15	148	146	4	4	1	−11	175	177	4
3	2	16	234	231	5	4	7	−15	63	71	8	4	2	−11	307	308	4
3	4	16	125	129	4	4	2	−14	210	210	4	4	2	−11	317	310	5
3	5	16	118	114	5	4	2	−14	217	208	4	4	3	−11	135	129	3
3	6	16	100	96	5	4	3	−14	62	61	6	4	3	−11	131	130	4
3	7	16	158	155	5	4	5	−14	162	164	4	4	4	−11	213	215	4
3	1	17	73	79	7	4	5	−14	165	163	3	4	4	−11	214	214	5
3	3	17	139	134	6	4	7	−14	193	190	4	4	5	−11	216	216	5
3	4	17	133	132	8	4	7	−14	187	189	4	4	5	−11	222	214	5
3	5	17	101	103	5	4	8	−14	65	56	9	4	6	−11	59	65	8
3	6	17	153	145	10	4	8	−14	64	56	7	4	6	−11	57	64	7
3	1	18	124	122	4	4	9	−14	145	142	5	4	7	−11	250	250	5
3	3	18	129	128	4	4	9	−14	146	141	4	4	7	−11	255	249	5
3	4	18	86	91	6	4	1	−13	264	265	5	4	9	−11	116	112	5

Table 83 — continued

H	K	L	F_{obs}	F_{calc}	SigF	H	K	L	F_{obs}	F_{calc}	SigF	H	K	L	F_{obs}	F_{calc}	SigF
4	9	−11	110	111	4	4	10	−9	189	186	4	4	8	−6	207	210	8
4	10	−11	117	114	5	4	11	−9	122	123	5	4	9	−6	154	155	7
4	10	−11	110	114	5	4	11	−9	116	123	5	4	10	−6	224	219	4
4	11	−11	89	96	7	4	12	−9	89	89	7	4	11	−6	215	214	4
4	11	−11	109	96	5	4	12	−9	81	88	7	4	12	−6	166	162	8
4	1	−10	66	50	5	4	1	−8	288	293	4	4	13	−6	123	119	5
4	2	−10	149	155	4	4	2	−8	130	128	3	4	1	−5	593	574	5
4	2	−10	154	154	3	4	2	−8	127	127	3	4	2	−5	263	237	5
4	3	−10	77	75	6	4	3	−8	281	291	4	4	3	−5	274	301	4
4	3	−10	70	74	5	4	3	−8	291	290	4	4	4	−5	93	105	4
4	4	−10	197	197	4	4	4	−8	373	378	4	4	5	−5	223	213	4
4	4	−10	192	198	4	4	4	−8	368	380	4	4	6	−5	104	101	4
4	5	−10	335	333	4	4	5	−8	530	542	4	4	7	−5	89	102	5
4	5	−10	332	335	5	4	5	−8	537	539	4	4	8	−5	373	384	4
4	6	−10	189	193	4	4	6	−8	503	512	4	4	9	−5	146	148	4
4	6	−10	199	192	4	4	6	−8	501	509	4	4	10	−5	246	252	5
4	7	−10	188	193	4	4	7	−8	297	302	5	4	11	−5	108	112	5
4	7	−10	197	192	4	4	7	−8	299	304	5	4	12	−5	120	112	12
4	8	−10	134	136	4	4	8	−8	152	152	4	4	1	−4	502	466	4
4	8	−10	140	135	3	4	8	−8	153	152	3	4	2	−4	321	330	4
4	9	−10	115	109	5	4	9	−8	173	166	3	4	3	−4	214	222	4
4	9	−10	111	108	4	4	9	−8	166	167	3	4	4	−4	295	302	8
4	10	−10	71	82	8	4	10	−8	115	113	5	4	5	−4	275	283	6
4	10	−10	79	82	6	4	10	−8	108	112	4	4	6	−4	182	178	4
4	11	−10	143	137	5	4	11	−8	123	122	5	4	7	−4	400	407	4
4	11	−10	140	136	4	4	11	−8	129	121	4	4	8	−4	150	143	3
4	1	−9	520	524	4	4	12	−8	156	154	10	4	9	−4	190	190	4
4	1	−9	515	521	4	4	1	−7	95	88	3	4	10	−4	265	271	5
4	2	−9	214	199	4	4	2	−7	775	766	8	4	11	−4	233	224	10
4	2	−9	198	197	4	4	3	−7	238	237	9	4	12	−4	134	133	4
4	3	−9	333	314	4	4	4	−7	379	374	4	4	13	−4	111	109	5
4	3	−9	321	317	4	4	6	−7	209	218	6	4	1	−3	340	322	3
4	4	−9	124	122	4	4	7	−7	297	297	7	4	2	−3	292	302	3
4	4	−9	124	120	3	4	8	−7	79	84	6	4	3	−3	291	294	5
4	5	−9	148	146	4	4	9	−7	262	265	5	4	4	−3	169	190	9
4	5	−9	147	145	3	4	10	−7	101	98	5	4	5	−3	507	509	5
4	6	−9	343	348	4	4	11	−7	163	167	4	4	6	−3	198	198	5
4	6	−9	346	350	5	4	1	−6	332	309	3	4	7	−3	281	286	4
4	7	−9	210	209	4	4	2	−6	161	164	3	4	8	−3	146	139	4
4	7	−9	204	207	4	4	3	−6	428	427	3	4	9	−3	406	416	6
4	8	−9	279	279	5	4	4	−6	376	377	4	4	10	−3	184	183	5
4	8	−9	278	278	5	4	5	−6	365	360	8	4	11	−3	128	128	4
4	9	−9	63	66	7	4	6	−6	431	446	4	4	12	−3	161	161	6
4	10	−9	185	187	4	4	7	−6	272	284	10	4	13	−3	85	80	6

Table 83 — continued

H	K	L	F_{obs}	F_{calc}	SigF	H	K	L	F_{obs}	F_{calc}	SigF	H	K	L	F_{obs}	F_{calc}	SigF
4	14	−3	135	137	5	4	7	1	149	147	3	4	9	4	190	186	3
4	1	−2	314	319	3	4	8	1	192	197	4	4	10	4	276	277	5
4	2	−2	53	46	6	4	9	1	113	118	4	4	11	4	218	218	4
4	3	−2	92	98	4	4	10	1	117	118	4	4	12	4	119	132	7
4	4	−2	492	484	3	4	11	1	195	194	5	4	13	4	111	108	6
4	5	−2	246	242	5	4	12	1	119	120	4	4	1	5	570	552	3
4	6	−2	370	366	5	4	13	1	156	156	4	4	2	5	260	240	5
4	8	−2	380	386	9	4	0	2	253	202	3	4	3	5	276	297	10
4	9	−2	161	156	7	4	1	2	320	325	3	4	5	5	228	219	4
4	10	−2	247	236	5	4	2	2	63	59	4	4	6	5	115	110	3
4	11	−2	92	91	5	4	3	2	98	103	3	4	7	5	91	94	4
4	12	−2	142	139	4	4	4	2	504	497	7	4	8	5	379	386	4
4	1	−1	186	201	6	4	5	2	241	236	9	4	9	5	151	156	4
4	2	−1	506	487	4	4	6	2	373	370	6	4	10	5	251	252	6
4	3	−1	304	300	4	4	7	2	80	86	7	4	11	5	118	120	4
4	4	−1	520	510	6	4	8	2	402	404	5	4	12	5	110	109	5
4	5	−1	306	311	5	4	9	2	164	162	3	4	13	5	60	67	8
4	6	−1	389	380	4	4	10	2	234	231	7	4	0	6	62	58	5
4	7	−1	159	155	3	4	11	2	91	82	5	4	1	6	327	307	4
4	8	−1	184	192	4	4	12	2	137	141	6	4	2	6	155	157	3
4	9	−1	103	107	4	4	0	3	305	298	3	4	3	6	431	431	6
4	10	−1	126	124	6	4	1	3	336	319	3	4	4	6	396	390	6
4	11	−1	183	183	3	4	2	3	277	297	8	4	5	6	368	360	6
4	12	−1	129	130	6	4	3	3	295	298	5	4	6	6	445	450	4
4	13	−1	159	160	4	4	4	3	191	208	4	4	7	6	266	273	15
4	0	0	798	788	3	4	5	3	512	513	9	4	8	6	212	210	6
4	1	0	385	361	3	4	6	3	195	200	4	4	9	6	170	165	8
4	2	0	281	302	3	4	7	3	294	297	5	4	10	6	211	206	4
4	3	0	179	170	4	4	8	3	152	148	5	4	11	6	211	216	10
4	4	0	426	408	7	4	9	3	414	421	7	4	12	6	161	159	6
4	5	0	254	272	5	4	10	3	194	193	5	4	13	6	119	119	9
4	6	0	188	192	4	4	11	3	130	126	4	4	0	7	829	837	4
4	7	0	311	334	10	4	12	3	159	162	3	4	1	7	96	95	3
4	9	0	315	317	5	4	13	3	81	81	11	4	2	7	758	751	5
4	11	0	218	222	4	4	14	3	130	126	4	4	3	7	248	240	5
4	12	0	184	189	5	4	0	4	395	399	3	4	4	7	385	382	4
4	13	0	92	88	6	4	1	4	494	459	5	4	6	7	216	222	8
4	0	1	370	364	3	4	2	4	338	343	5	4	7	7	297	288	5
4	1	1	197	210	4	4	3	4	236	238	5	4	8	7	77	81	5
4	2	1	497	480	8	4	4	4	306	308	6	4	9	7	261	260	5
4	3	1	324	316	5	4	5	4	285	285	4	4	10	7	94	100	5
4	4	1	523	507	10	4	6	4	184	185	5	4	11	7	165	164	5
4	5	1	309	313	4	4	7	4	425	421	4	4	0	8	116	124	4
4	6	1	394	388	4	4	8	4	157	151	5	4	1	8	288	287	9

Table 83 — continued

H	K	L	F_{obs}	F_{calc}	SigF	H	K	L	F_{obs}	F_{calc}	SigF	H	K	L	F_{obs}	F_{calc}	SigF
4	2	8	142	138	4	4	9	11	112	112	4	4	0	18	155	160	4
4	3	8	277	286	4	4	10	11	111	107	5	4	0	18	158	159	4
4	4	8	380	385	6	4	11	11	101	98	5	4	2	18	127	123	4
4	5	8	544	546	4	4	1	12	271	268	5	5	1	−17	87	86	7
4	6	8	502	498	4	4	3	12	92	92	5	5	2	−17	162	160	4
4	7	8	302	304	5	4	4	12	60	55	7	5	2	−17	168	160	4
4	8	8	142	143	4	4	5	12	89	92	7	5	1	−16	76	81	8
4	9	8	160	162	3	4	6	12	208	206	4	5	1	−16	88	80	6
4	10	8	107	112	4	4	8	12	143	146	4	5	2	−16	168	166	4
4	11	8	117	118	5	4	10	12	137	133	4	5	2	−16	171	165	4
4	12	8	157	157	4	4	0	13	164	173	3	5	3	−16	124	117	5
4	0	9	232	232	4	4	0	13	165	172	4	5	3	−16	111	117	5
4	1	9	509	512	4	4	1	13	247	253	7	5	4	−16	134	134	5
4	2	9	211	206	4	4	2	13	141	140	3	5	4	−16	137	133	4
4	3	9	312	306	4	4	3	13	203	203	4	5	5	−16	152	152	5
4	4	9	139	136	4	4	4	13	211	212	7	5	5	−16	152	151	4
4	5	9	155	159	3	4	5	13	119	118	4	5	1	−15	235	243	5
4	6	9	352	350	5	4	6	13	191	194	4	5	1	−15	233	241	5
4	7	9	211	211	4	4	0	14	342	324	5	5	2	−15	153	152	4
4	8	9	292	282	5	4	0	14	335	323	5	5	2	−15	149	151	4
4	9	9	64	63	7	4	2	14	215	215	4	5	3	−15	147	147	4
4	10	9	195	187	5	4	5	14	166	164	3	5	3	−15	146	146	4
4	11	9	113	114	5	4	7	14	194	189	5	5	4	−15	128	125	5
4	12	9	82	89	7	4	9	14	145	141	4	5	4	−15	124	124	4
4	0	10	198	203	4	4	0	15	188	193	4	5	5	−15	80	77	7
4	2	10	153	155	4	4	0	15	190	192	4	5	6	−15	64	64	9
4	3	10	92	93	4	4	1	15	144	144	3	5	6	−15	58	64	8
4	4	10	185	187	3	4	1	15	154	145	4	5	1	−14	79	87	7
4	5	10	317	321	5	4	2	15	203	209	11	5	1	−14	90	86	5
4	6	10	188	190	9	4	3	15	157	157	8	5	2	−14	166	165	4
4	7	10	181	178	5	4	4	15	176	182	5	5	2	−14	163	164	3
4	8	10	130	133	7	4	5	15	211	205	6	5	4	−14	195	195	4
4	9	10	108	107	5	4	6	15	146	148	5	5	4	−14	194	193	3
4	10	10	81	81	6	4	1	16	260	254	5	5	5	−14	95	103	6
4	11	10	155	143	4	4	1	16	252	256	5	5	5	−14	94	103	5
4	0	11	174	176	4	4	3	16	81	86	6	5	6	−14	142	142	5
4	0	11	180	176	4	4	6	16	146	150	5	5	6	−14	141	141	4
4	1	11	181	180	4	4	0	17	70	62	8	5	7	−14	113	104	6
4	2	11	283	282	5	4	0	17	67	62	7	5	7	−14	110	103	5
4	3	11	140	142	4	4	1	17	106	108	5	5	8	−14	90	88	6
4	4	11	194	196	4	4	1	17	109	108	5	5	1	−13	239	244	5
4	5	11	215	215	9	4	3	17	141	137	5	5	1	−13	239	242	5
4	6	11	69	74	6	4	4	17	152	146	9	5	2	−13	330	339	5
4	7	11	249	248	5	4	5	17	98	99	6	5	2	−13	328	337	5

Table 83 — continued

H	K	L	F_{obs}	F_{calc}	SigF	H	K	L	F_{obs}	F_{calc}	SigF	H	K	L	F_{obs}	F_{calc}	SigF
5	3	−13	124	115	5	5	3	−10	273	265	5	5	5	−8	140	137	4
5	3	−13	118	114	4	5	4	−10	260	260	5	5	6	−8	441	450	4
5	4	−13	173	176	4	5	4	−10	259	258	5	5	6	−8	449	453	5
5	4	−13	178	177	4	5	5	−10	125	125	4	5	7	−8	210	201	4
5	5	−13	78	89	7	5	5	−10	123	123	4	5	7	−8	204	202	4
5	5	−13	81	88	5	5	6	−10	182	188	3	5	8	−8	373	387	5
5	6	−13	69	59	8	5	6	−10	190	187	4	5	8	−8	386	385	5
5	7	−13	64	66	9	5	7	−10	268	259	5	5	9	−8	148	146	3
5	7	−13	60	66	8	5	7	−10	248	261	5	5	9	−8	142	147	4
5	1	−12	63	68	8	5	8	−10	192	186	4	5	10	−8	207	219	4
5	1	−12	67	68	6	5	8	−10	185	187	4	5	10	−8	210	218	4
5	2	−12	149	145	3	5	9	−10	193	191	4	5	11	−8	179	177	4
5	2	−12	144	146	4	5	9	−10	188	190	4	5	11	−8	180	177	4
5	3	−12	211	214	5	5	10	−10	147	142	5	5	12	−8	101	106	6
5	3	−12	214	212	4	5	10	−10	150	141	4	5	12	−8	107	106	5
5	5	−12	205	207	5	5	11	−10	103	98	6	5	1	−7	372	370	4
5	5	−12	205	209	4	5	11	−10	108	98	5	5	2	−7	163	167	3
5	6	−12	79	79	5	5	1	−9	46	51	7	5	2	−7	161	166	4
5	7	−12	136	137	4	5	2	−9	86	82	5	5	3	−7	371	366	4
5	7	−12	140	136	4	5	2	−9	87	82	4	5	3	−7	379	368	4
5	8	−12	108	114	6	5	3	−9	85	88	4	5	5	−7	392	402	4
5	8	−12	110	113	5	5	3	−9	84	89	6	5	5	−7	397	400	4
5	9	−12	103	107	6	5	4	−9	213	211	4	5	6	−7	175	178	4
5	9	−12	109	106	5	5	4	−9	220	212	4	5	6	−7	178	177	4
5	1	−11	264	259	5	5	5	−9	113	122	4	5	7	−7	227	218	4
5	1	−11	257	258	5	5	5	−9	113	123	5	5	7	−7	220	217	4
5	3	−11	200	207	5	5	6	−9	189	184	3	5	8	−7	238	235	4
5	3	−11	207	206	4	5	6	−9	188	183	4	5	8	−7	239	236	5
5	4	−11	139	145	4	5	7	−9	178	189	4	5	9	−7	83	88	5
5	4	−11	144	144	3	5	7	−9	186	188	4	5	9	−7	75	89	7
5	5	−11	183	188	4	5	9	−9	86	99	7	5	10	−7	116	124	5
5	5	−11	186	187	4	5	9	−9	95	99	5	5	11	−7	209	203	4
5	6	−11	125	124	5	5	10	−9	108	103	6	5	12	−7	79	76	9
5	6	−11	121	123	4	5	10	−9	108	103	5	5	2	−6	396	399	5
5	7	−11	86	89	5	5	11	−9	111	110	6	5	3	−6	98	96	6
5	7	−11	86	90	6	5	11	−9	113	110	5	5	4	−6	148	142	3
5	8	−11	70	69	6	5	1	−8	120	118	3	5	5	−6	307	316	5
5	10	−11	95	94	7	5	1	−8	122	119	4	5	6	−6	156	160	6
5	10	−11	92	93	6	5	2	−8	47	61	6	5	7	−6	383	383	5
5	1	−10	151	147	3	5	3	−8	99	98	4	5	8	−6	239	247	5
5	1	−10	150	149	3	5	3	−8	101	99	5	5	9	−6	334	338	8
5	2	−10	111	114	4	5	4	−8	188	195	4	5	10	−6	209	215	4
5	2	−10	107	115	5	5	4	−8	194	193	4	5	11	−6	168	177	7
5	3	−10	261	264	5	5	5	−8	133	136	3	5	12	−6	145	148	5

Table 83 — continued

H	K	L	F_{obs}	F_{calc}	SigF	H	K	L	F_{obs}	F_{calc}	SigF	H	K	L	F_{obs}	F_{calc}	SigF
5	12	−6	147	148	4	5	10	−2	126	133	4	5	7	2	348	348	4
5	1	−5	220	220	4	5	11	−2	137	140	6	5	9	2	110	107	4
5	2	−5	569	554	3	5	13	−2	110	113	5	5	10	2	129	127	5
5	3	−5	136	150	8	5	1	−1	823	814	7	5	11	2	147	146	4
5	4	−5	424	427	4	5	2	−1	540	530	8	5	13	2	114	116	5
5	5	−5	113	116	4	5	3	−1	379	364	14	5	0	3	533	534	4
5	6	−5	371	386	4	5	4	−1	234	231	5	5	1	3	231	234	4
5	7	−5	209	206	9	5	5	−1	162	163	3	5	2	3	344	328	5
5	8	−5	183	188	4	5	6	−1	163	165	3	5	3	3	383	382	7
5	9	−5	230	234	9	5	7	−1	161	160	3	5	4	3	101	94	5
5	10	−5	209	213	4	5	8	−1	96	93	4	5	5	3	142	131	3
5	11	−5	65	66	10	5	9	−1	145	147	5	5	6	3	126	122	3
5	12	−5	164	172	4	5	10	−1	120	118	4	5	7	3	119	116	4
5	1	−4	502	498	4	5	12	−1	123	116	5	5	8	3	226	224	4
5	2	−4	72	92	6	5	1	0	272	279	5	5	9	3	172	173	4
5	3	−4	262	261	4	5	2	0	403	386	5	5	10	3	75	79	6
5	4	−4	307	306	4	5	3	0	73	78	5	5	11	3	218	221	7
5	6	−4	294	297	4	5	4	0	486	485	8	5	12	3	66	65	7
5	7	−4	174	171	4	5	5	0	136	135	4	5	13	3	80	91	8
5	8	−4	199	204	4	5	6	0	376	379	4	5	1	4	496	490	3
5	9	−4	216	220	5	5	7	0	150	157	4	5	2	4	59	84	8
5	10	−4	185	190	3	5	8	0	178	178	3	5	3	4	267	261	4
5	11	−4	175	174	5	5	10	0	66	62	6	5	4	4	315	319	4
5	12	−4	126	127	5	5	12	0	202	200	7	5	5	4	65	61	8
5	1	−3	211	215	5	5	0	1	357	348	5	5	6	4	301	303	4
5	2	−3	363	342	5	5	1	1	804	800	10	5	7	4	171	170	3
5	3	−3	375	377	8	5	2	1	563	547	8	5	8	4	206	209	8
5	4	−3	84	79	4	5	3	1	371	359	6	5	9	4	217	214	4
5	5	−3	143	133	3	5	4	1	240	236	4	5	10	4	181	181	9
5	6	−3	138	135	4	5	5	1	167	167	4	5	11	4	167	170	3
5	7	−3	126	124	6	5	6	1	157	159	4	5	12	4	128	126	6
5	8	−3	224	228	4	5	7	1	155	152	3	5	0	5	173	150	7
5	9	−3	167	165	6	5	8	1	104	100	4	5	1	5	212	208	4
5	10	−3	62	71	8	5	9	1	141	141	4	5	2	5	569	551	10
5	11	−3	219	219	7	5	10	1	135	128	4	5	3	5	143	149	4
5	13	−3	106	102	5	5	12	1	118	113	4	5	4	5	434	433	6
5	1	−2	201	201	4	5	13	1	81	73	8	5	5	5	102	102	4
5	2	−2	238	225	6	5	0	2	462	460	3	5	6	5	387	379	6
5	3	−2	476	474	6	5	1	2	192	195	4	5	7	5	200	202	9
5	4	−2	111	120	5	5	2	2	220	207	5	5	8	5	186	185	5
5	5	−2	456	450	9	5	3	2	475	475	5	5	9	5	236	240	5
5	6	−2	161	157	3	5	4	2	104	108	3	5	10	5	214	215	5
5	7	−2	335	337	4	5	5	2	468	459	7	5	11	5	78	69	6
5	9	−2	89	85	5	5	6	2	162	159	3	5	12	5	169	170	11

Table 83 — continued

H	K	L	F_{obs}	F_{calc}	SigF	H	K	L	F_{obs}	F_{calc}	SigF	H	K	L	F_{obs}	F_{calc}	SigF
5	0	6	304	297	9	5	10	9	94	97	6	5	0	14	73	80	7
5	2	6	402	393	4	5	11	9	109	105	10	5	0	14	72	79	6
5	3	6	91	96	4	5	1	10	152	151	3	5	1	14	105	96	5
5	4	6	133	128	3	5	1	10	155	150	3	5	1	14	85	95	5
5	5	6	319	320	4	5	2	10	126	122	3	5	2	14	167	163	4
5	6	6	161	153	3	5	3	10	281	279	5	5	2	14	165	162	3
5	7	6	380	376	7		4	10	268	270	9	5	4	14	194	198	7
5	8	6	234	238	13		5	10	136	136	4	5	5	14	88	93	6
5	9	6	329	328	5	5	6	10	190	190	5	5	6	14	145	140	10
5	10	6	204	212	7	5	7	10	269	264	5	5	7	14	98	96	5
5	11	6	171	171	9	5	8	10	188	185	4	5	0	15	232	234	5
5	12	6	155	146	4	5	9	10	190	197	5	5	0	15	222	235	5
5	1	7	354	351	7	5	10	10	147	144	4	5	1	15	240	240	4
5	2	7	164	166	3	5	11	10	104	107	6	5	1	15	238	241	5
5	3	7	389	380	4	5	0	11	59	43	8	5	2	15	145	149	4
5	5	7	403	407	4	5	1	11	251	251	5	5	2	15	150	148	4
5	6	7	168	167	4	5	1	11	251	250	5	5	3	15	141	142	4
5	7	7	222	214	4	5	3	11	199	201	6	5	3	15	146	141	4
5	8	7	245	241	5	5	4	11	153	152	3	5	4	15	126	128	5
5	9	7	87	91	5	5	5	11	188	194	4	5	5	15	63	66	8
5	10	7	115	121	4	5	6	11	132	132	4	5	6	15	66	70	8
5	11	7	205	199	4	5	7	11	86	91	5	5	0	16	158	152	4
5	12	7	83	79	6	5	8	11	74	76	6	5	0	16	149	152	4
5	0	8	191	182	3	5	10	11	81	88	7	5	1	16	86	79	7
5	0	8	188	180	3	5	1	12	61	68	8	5	1	16	67	79	7
5	1	8	121	121	4	5	1	12	57	68	7	5	2	16	168	165	4
5	3	8	96	100	4	5	2	12	155	158	3	5	2	16	166	166	4
5	4	8	200	207	4	5	2	12	158	158	3	5	3	16	118	121	5
5	5	8	140	144	4	5	3	12	223	217	4	5	3	16	125	120	4
5	6	8	451	452	9	5	4	12	63	67	7	5	4	16	138	129	4
5	7	8	199	199	4	5	5	12	212	212	4	5	5	16	159	158	4
5	8	8	389	384	5	5	7	12	131	125	4	5	0	17	205	200	4
5	9	8	138	143	8	5	8	12	118	114	5	5	0	17	204	199	4
5	10	8	213	221	9	5	9	12	105	99	5	5	1	17	87	86	7
5	11	8	189	181	4	5	0	13	409	417	5	5	1	17	91	85	6
5	0	9	154	152	3	5	0	13	404	415	5	5	2	17	177	164	4
5	0	9	151	153	3	5	1	13	227	236	5	5	2	17	171	164	4
5	2	9	56	50	7	5	1	13	229	238	5	6	2	−16	54	65	9
5	3	9	91	94	5	5	2	13	328	333	5	6	1	−15	109	112	6
5	4	9	232	227	5	5	2	13	326	334	5	6	1	−15	109	111	5
5	5	9	123	128	4	5	3	13	116	113	5	6	2	−15	168	160	4
5	6	9	190	190	4	5	4	13	171	176	4	6	2	−15	158	159	4
5	7	9	191	195	9	5	5	13	86	93	5	6	3	−15	150	149	5
5	9	9	107	106	4	5	7	13	75	76	7	6	3	−15	156	148	4

Table 83 — continued

H	K	L	F_{obs}	F_{calc}	SigF	H	K	L	F_{obs}	F_{calc}	SigF	H	K	L	F_{obs}	F_{calc}	SigF
6	1	−14	73	70	6	6	8	−11	110	110	5	6	7	−8	238	228	5
6	3	−14	142	139	5	6	1	−10	125	123	4	6	8	−8	183	183	4
6	3	−14	143	138	4	6	1	−10	124	123	3	6	8	−8	184	182	4
6	4	−14	114	117	6	6	2	−10	52	53	7	6	9	−8	219	217	4
6	4	−14	118	116	5	6	2	−10	55	53	9	6	9	−8	223	216	4
6	5	−14	153	150	5	6	3	−10	222	228	4	6	10	−8	148	147	5
6	5	−14	153	149	4	6	3	−10	229	230	4	6	10	−8	152	147	4
6	6	−14	126	124	5	6	5	−10	233	233	4	6	11	−8	121	133	6
6	6	−14	128	123	4	6	5	−10	228	235	4	6	11	−8	131	132	5
6	1	−13	377	381	5	6	6	−10	152	149	3	6	1	−7	122	122	4
6	1	−13	377	379	5	6	6	−10	145	150	4	6	1	−7	119	122	3
6	2	−13	97	97	6	6	7	−10	212	209	4	6	2	−7	117	114	5
6	2	−13	99	97	5	6	7	−10	204	211	4	6	2	−7	118	113	3
6	3	−13	252	262	5	6	8	−10	139	144	5	6	3	−7	285	279	5
6	3	−13	270	263	5	6	8	−10	142	143	4	6	3	−7	283	278	5
6	4	−13	91	87	7	6	9	−10	184	190	4	6	4	−7	129	125	4
6	4	−13	96	86	5	6	9	−10	190	189	4	6	4	−7	121	125	4
6	5	−13	70	68	8	6	1	−9	197	198	4	6	5	−7	302	302	5
6	5	−13	67	67	7	6	1	−9	201	199	3	6	5	−7	300	304	5
6	7	−13	94	99	7	6	2	−9	109	100	4	6	6	−7	99	95	4
6	7	−13	95	98	5	6	2	−9	99	100	5	6	6	−7	99	96	6
6	1	−12	101	96	5	6	3	−9	195	196	4	6	7	−7	132	124	3
6	1	−12	100	96	4	6	3	−9	199	194	4	6	7	−7	124	125	5
6	2	−12	121	120	5	6	4	−9	164	160	3	6	10	−7	126	132	5
6	2	−12	121	119	4	6	4	−9	162	161	4	6	10	−7	130	131	4
6	3	−12	83	83	5	6	5	−9	180	189	4	6	2	−6	187	189	4
6	3	−12	87	84	6	6	5	−9	177	188	4	6	3	−6	80	82	6
6	4	−12	231	230	4	6	8	−9	102	105	5	6	4	−6	288	292	7
6	4	−12	228	228	4	6	8	−9	116	106	5	6	6	−6	291	293	8
6	5	−12	101	103	5	6	10	−9	68	47	9	6	7	−6	156	157	4
6	5	−12	98	104	6	6	10	−9	59	47	8	6	8	−6	247	248	6
6	6	−12	164	167	4	6	1	−8	169	168	3	6	9	−6	102	96	6
6	6	−12	169	166	3	6	1	−8	174	169	4	6	10	−6	204	208	4
6	7	−12	68	77	9	6	2	−8	331	328	4	6	11	−6	139	134	5
6	7	−12	82	76	6	6	2	−8	333	330	5	6	11	−6	135	133	4
6	8	−12	161	158	4	6	3	−8	100	99	4	6	1	−5	354	340	4
6	8	−12	161	157	4	6	3	−8	103	100	5	6	2	−5	253	260	5
6	2	−11	331	332	5	6	4	−8	130	139	3	6	3	−5	355	356	6
6	2	−11	329	329	5	6	4	−8	136	140	4	6	4	−5	137	136	4
6	4	−11	287	286	6	6	5	−8	256	245	5	6	5	−5	205	206	5
6	4	−11	287	283	5	6	5	−8	253	246	5	6	6	−5	213	212	6
6	6	−11	115	122	4	6	6	−8	231	229	4	6	7	−5	214	216	4
6	6	−11	128	123	5	6	6	−8	232	228	4	6	8	−5	98	105	5
6	8	−11	107	111	6	6	7	−8	230	229	5	6	9	−5	91	87	6

Table 83 — continued

H	K	L	F_{obs}	F_{calc}	SigF	H	K	L	F_{obs}	F_{calc}	SigF	H	K	L	F_{obs}	F_{calc}	SigF
6	10	−5	77	75	7	6	3	0	511	508	4	6	6	4	112	104	4
6	11	−5	178	176	4	6	4	0	111	105	3	6	7	4	230	219	4
6	1	−4	390	386	4	6	5	0	332	333	4	6	8	4	141	139	4
6	2	−4	96	99	4	6	6	0	158	159	5	6	9	4	172	172	5
6	3	−4	267	276	7	6	7	0	271	273	5	6	10	4	109	104	4
6	5	−4	319	322	5	6	8	0	226	228	4	6	11	4	186	191	4
6	6	−4	114	110	4	6	12	0	87	86	6	6	12	4	74	81	9
6	7	−4	230	233	5	6	0	1	490	482	4	6	0	5	297	288	4
6	8	−4	139	141	5	6	1	1	493	490	6	6	1	5	343	340	12
6	9	−4	182	178	3	6	2	1	289	287	6	6	2	5	252	256	5
6	10	−4	96	99	6	6	3	1	270	274	6	6	3	5	348	346	6
6	11	−4	186	189	4	6	4	1	128	126	3	6	4	5	133	131	4
6	12	−4	75	80	8	6	5	1	153	162	4	6	5	5	203	197	4
6	1	−3	481	467	8	6	6	1	82	85	11	6	6	5	209	206	4
6	2	−3	614	610	4	6	7	1	88	92	5	6	7	5	219	217	4
6	3	−3	150	155	3	6	8	1	195	196	4	6	8	5	102	109	5
6	4	−3	345	346	4	6	9	1	134	139	4	6	9	5	93	86	5
6	5	−3	55	52	9	6	0	2	356	350	5	6	11	5	173	170	4
6	6	−3	247	244	7	6	2	2	392	390	6	6	0	6	368	371	4
6	7	−3	152	150	4	6	3	2	86	78	5	6	1	6	62	51	6
6	8	−3	146	148	4	6	4	2	419	420	4	6	2	6	195	195	4
6	10	−3	126	124	4	6	5	2	128	123	6	6	3	6	79	80	5
6	12	−3	116	110	5	6	6	2	336	336	4	6	4	6	283	283	8
6	2	−2	393	391	4	6	7	2	257	264	5	6	6	6	279	277	5
6	3	−2	87	81	4	6	8	2	141	138	4	6	7	6	159	160	7
6	4	−2	418	422	5	6	9	2	101	102	4	6	8	6	251	247	5
6	5	−2	131	124	3	6	10	2	147	141	3	6	9	6	99	100	7
6	6	−2	348	339	4	6	11	2	165	166	7	6	10	6	201	205	4
6	7	−2	268	268	5	6	12	2	188	184	3	6	11	6	132	134	4
6	8	−2	150	144	3	6	0	3	686	677	5	6	0	7	132	136	4
6	9	−2	101	103	9	6	1	3	475	465	5	6	1	7	121	118	7
6	10	−2	135	134	5	6	2	3	609	602	5	6	2	7	132	127	3
6	11	−2	168	166	4	6	3	3	168	171	4	6	3	7	280	276	5
6	12	−2	180	181	4	6	4	3	337	336	4	6	4	7	121	111	4
6	1	−1	508	499	4	6	5	3	53	42	7	6	5	7	288	296	5
6	2	−1	276	273	5	6	6	3	248	243	5	6	6	7	103	100	4
6	3	−1	292	296	4	6	7	3	147	145	7	6	7	7	124	125	10
6	4	−1	110	112	8	6	8	3	143	147	4	6	10	7	128	133	4
6	5	−1	155	167	3	6	10	3	122	118	4	6	0	8	268	271	5
6	6	−1	90	93	8	6	12	3	108	106	5	6	0	8	273	272	5
6	7	−1	93	92	5	6	1	4	398	392	5	6	1	8	177	170	4
6	8	−1	197	200	5	6	2	4	106	100	4	6	1	8	173	169	4
6	9	−1	141	143	4	6	3	4	268	272	4	6	2	8	332	324	7
6	1	0	170	168	5	6	5	4	316	312	4	6	3	8	105	97	5

Table 83 — continued

H	K	L	F_{obs}	F_{calc}	SigF	H	K	L	F_{obs}	F_{calc}	SigF	H	K	L	F_{obs}	F_{calc}	SigF
6	4	8	118	130	14	6	7	12	77	86	12	7	5	−12	125	127	4
6	5	8	242	238	4	6	8	12	161	163	5	7	6	−12	124	126	6
6	6	8	234	230	5	6	0	13	75	76	6	7	6	−12	124	125	4
6	7	8	236	234	5	6	0	13	66	76	8	7	1	−11	260	268	5
6	8	8	188	186	4	6	1	13	379	381	5	7	1	−11	266	266	5
6	9	8	217	219	4	6	1	13	381	379	5	7	3	−11	197	198	4
6	10	8	155	148	6	6	2	13	89	94	6	7	3	−11	206	200	4
6	11	8	134	137	4	6	2	13	96	94	5	7	4	−11	57	28	7
6	1	9	204	205	4	6	3	13	259	264	5	7	5	−11	140	141	4
6	1	9	209	206	4	6	3	13	260	265	6	7	5	−11	141	142	5
6	2	9	105	100	4	6	4	13	88	82	6	7	6	−11	110	108	6
6	2	9	94	100	5	6	4	13	84	82	6	7	6	−11	111	107	5
6	3	9	219	216	4	6	5	13	66	69	7	7	7	−11	75	68	9
6	4	9	160	160	3	6	7	13	93	95	6	7	7	−11	64	68	8
6	5	9	198	196	3	6	1	14	68	70	7	7	1	−10	78	71	5
6	8	9	111	110	4	6	1	14	69	71	8	7	2	−10	116	119	5
6	9	9	64	56	8	6	3	14	143	134	4	7	2	−10	115	118	4
6	1	10	126	121	4	6	3	14	137	135	4	7	3	−10	155	157	4
6	1	10	117	120	4	6	4	14	129	119	5	7	3	−10	157	156	3
6	3	10	224	225	5	6	4	14	121	119	5	7	4	−10	166	168	4
6	5	10	237	241	5	6	5	14	152	147	4	7	4	−10	165	167	3
6	6	10	156	157	3	6	6	14	127	131	5	7	5	−10	169	168	3
6	7	10	212	217	4	6	0	15	224	225	5	7	5	−10	166	170	4
6	8	10	144	149	10	6	0	15	235	224	5	7	6	−10	189	190	4
6	9	10	192	193	7	6	1	15	99	108	6	7	6	−10	186	189	4
6	0	11	359	370	5	6	1	15	104	108	5	7	7	−10	85	76	8
6	0	11	376	368	4	6	2	15	161	160	4	7	7	−10	67	75	7
6	2	11	333	337	5	6	2	15	157	159	4	7	8	−10	180	182	4
6	2	11	330	335	5	6	3	15	143	144	5	7	8	−10	174	181	4
6	4	11	296	295	5	6	3	15	145	144	4	7	2	−9	257	253	5
6	6	11	132	126	4	6	0	16	61	60	9	7	2	−9	255	251	5
6	8	11	113	114	5	6	2	16	59	68	8	7	3	−9	89	82	5
6	0	12	83	80	5	7	2	−13	176	172	4	7	3	−9	88	82	6
6	0	12	67	81	8	7	2	−13	172	171	4	7	4	−9	156	155	4
6	1	12	104	95	5	7	4	−13	180	184	4	7	4	−9	155	154	3
6	1	12	101	95	5	7	4	−13	184	183	4	7	6	−9	66	55	6
6	2	12	126	123	4	7	5	−13	97	82	5	7	7	−9	82	79	8
6	2	12	125	123	4	7	1	−12	57	59	8	7	7	−9	88	79	5
6	3	12	76	75	6	7	2	−12	95	94	6	7	8	−9	69	55	9
6	3	12	55	74	8	7	2	−12	91	94	5	7	9	−9	77	73	8
6	4	12	240	235	5	7	3	−12	70	66	7	7	9	−9	66	73	7
6	4	12	234	233	5	7	4	−12	162	158	4	7	1	−8	146	150	4
6	5	12	112	110	5	7	4	−12	161	157	4	7	1	−8	144	149	3
6	6	12	181	177	3	7	5	−12	128	127	5	7	2	−8	151	145	3

Table 83 — continued

H	K	L	F_{obs}	F_{calc}	SigF	H	K	L	F_{obs}	F_{calc}	SigF	H	K	L	F_{obs}	F_{calc}	SigF
7	2	−8	147	146	4	7	7	−5	86	86	6	7	3	0	80	84	5
7	3	−8	205	217	4	7	9	−5	82	84	7	7	4	0	285	281	5
7	3	−8	209	218	4	7	10	−5	95	98	6	7	5	0	202	198	5
7	4	−8	246	250	5	7	1	−4	209	203	4	7	6	0	321	323	5
7	4	−8	254	249	5	7	2	−4	99	101	5	7	7	0	290	297	6
7	5	−8	223	220	4	7	3	−4	344	353	13	7	0	1	106	103	4
7	5	−8	224	221	4	7	4	−4	166	163	3	7	1	1	207	209	7
7	6	−8	210	202	4	7	5	−4	154	162	6	7	2	1	219	220	4
7	6	−8	210	203	4	7	6	−4	324	334	14	7	3	1	334	334	4
7	7	−8	118	118	5	7	8	−4	236	236	4	7	4	1	119	115	4
7	7	−8	113	117	4	7	9	−4	118	125	5	7	5	1	264	266	7
7	8	−8	87	90	8	7	10	−4	169	164	4	7	6	1	205	204	4
7	8	−8	89	89	6	7	1	−3	480	473	8	7	7	1	222	224	5
7	9	−8	79	80	8	7	2	−3	183	178	4	7	8	1	61	54	7
7	9	−8	74	80	7	7	3	−3	232	226	5	7	10	1	141	140	4
7	1	−7	377	381	5	7	4	−3	298	302	5	7	11	1	156	152	4
7	1	−7	378	380	4	7	5	−3	165	157	6	7	1	2	305	297	5
7	2	−7	78	79	7	7	6	−3	287	285	5	7	2	2	182	180	4
7	2	−7	83	79	5	7	9	−3	133	141	7	7	4	2	160	158	4
7	3	−7	198	193	4	7	10	−3	141	137	4	7	5	2	328	322	5
7	3	−7	198	194	4	7	11	−3	144	137	8	7	6	2	222	230	4
7	4	−7	182	181	3	7	1	−2	289	291	5	7	7	2	341	344	8
7	4	−7	178	182	4	7	2	−2	180	179	6	7	8	2	87	87	5
7	5	−7	61	47	6	7	3	−2	76	70	7	7	9	2	292	286	5
7	6	−7	71	72	8	7	4	−2	154	155	3	7	10	2	102	99	5
7	6	−7	69	72	6	7	5	−2	331	326	5	7	11	2	171	170	4
7	8	−7	76	68	8	7	6	−2	222	233	4	7	0	3	198	192	6
7	8	−7	61	68	8	7	7	−2	346	347	6	7	1	3	471	467	7
7	10	−7	69	65	9	7	8	−2	92	91	6	7	2	3	190	187	4
7	10	−7	79	65	6	7	9	−2	296	293	5	7	3	3	222	216	5
7	1	−6	165	169	4	7	10	−2	96	96	6	7	4	3	301	302	9
7	3	−6	166	167	3	7	11	−2	173	171	11	7	5	3	166	157	5
7	4	−6	171	179	3	7	1	−1	192	194	4	7	6	3	288	283	9
7	4	−6	175	180	4	7	2	−1	250	244	5	7	7	3	69	70	6
7	5	−6	313	304	5	7	3	−1	319	319	7	7	8	3	60	64	7
7	6	−6	78	74	6	7	4	−1	140	130	3	7	9	3	142	138	4
7	7	−6	251	259	7	7	5	−1	264	263	5	7	10	3	140	133	4
7	9	−6	130	132	5	7	6	−1	202	201	9	7	11	3	136	134	4
7	1	−5	71	73	6	7	7	−1	226	224	4	7	0	4	480	473	8
7	2	−5	377	384	5	7	8	−1	54	55	9	7	1	4	208	207	4
7	3	−5	80	75	6	7	10	−1	142	143	4	7	2	4	112	115	7
7	4	−5	147	157	4	7	11	−1	152	154	5	7	3	4	360	361	4
7	5	−5	262	278	8	7	1	0	205	208	4	7	4	4	170	157	5
7	6	−5	114	116	5	7	2	0	276	278	5	7	5	4	172	167	3

Table 83 — continued

H	K	L	F_{obs}	F_{calc}	SigF	H	K	L	F_{obs}	F_{calc}	SigF	H	K	L	F_{obs}	F_{calc}	SigF
7	6	4	333	331	10	7	2	9	254	256	5	7	4	13	187	188	4
7	8	4	228	231	5	7	2	9	267	258	5	7	5	13	78	81	7
7	9	4	128	128	4	7	3	9	88	82	6	7	5	13	91	81	6
7	10	4	161	161	5	7	3	9	99	81	4	7	0	14	54	74	8
7	0	5	478	485	11	7	4	9	168	164	3	8	3	−12	153	152	5
7	1	5	71	61	6	7	7	9	69	79	7	8	3	−12	153	151	4
7	2	5	384	382	4	7	8	9	59	56	8	8	2	−11	195	197	4
7	3	5	69	65	6	7	9	9	70	72	7	8	2	−11	199	196	4
7	4	5	142	146	4	7	1	10	71	68	6	8	4	−11	123	131	6
7	5	5	265	272	7	7	1	10	69	69	8	8	4	−11	129	130	4
7	6	5	122	117	6	7	2	10	109	111	4	8	5	−11	129	122	6
7	7	5	83	82	5	7	2	10	121	112	4	8	5	−11	124	121	5
7	9	5	92	85	7	7	3	10	141	147	4	8	1	−10	120	120	4
7	10	5	90	94	6	7	3	10	145	147	3	8	1	−10	123	120	5
7	0	6	78	88	6	7	4	10	162	165	3	8	2	−10	117	120	6
7	1	6	174	175	4	7	4	10	159	166	4	8	2	−10	124	119	4
7	2	6	71	71	9	7	5	10	172	169	3	8	3	−10	91	87	5
7	3	6	158	157	3	7	6	10	186	194	4	8	3	−10	94	88	7
7	4	6	182	180	4	7	7	10	85	82	8	8	4	−10	201	204	4
7	5	6	297	296	5	7	8	10	182	187	7	8	4	−10	209	205	4
7	6	6	73	67	6	7	1	11	263	267	6	8	5	−10	156	154	4
7	7	6	264	262	5	7	1	11	262	265	5	8	5	−10	149	155	5
7	9	6	129	133	4	7	3	11	202	209	4	8	6	−10	87	84	8
7	1	7	382	386	5	7	3	11	209	210	4	8	6	−10	87	83	6
7	2	7	76	73	6	7	5	11	146	145	4	8	1	−9	307	308	5
7	3	7	205	198	4	7	5	11	147	144	4	8	1	−9	312	310	6
7	4	7	177	178	7	7	6	11	105	108	5	8	3	−9	181	181	3
7	5	7	50	50	8	7	7	11	59	65	9	8	3	−9	185	183	4
7	6	7	68	69	6	7	0	12	62	46	8	8	4	−9	104	105	7
7	8	7	72	70	7	7	0	12	57	46	7	8	4	−9	111	104	5
7	9	7	70	65	7	7	2	12	93	91	6	8	5	−9	75	70	6
7	1	8	135	144	4	7	2	12	100	90	5	8	6	−9	104	102	5
7	1	8	138	144	3	7	3	12	53	61	8	8	6	−9	83	103	8
7	2	8	141	140	4	7	3	12	65	61	8	8	1	−8	90	93	7
7	2	8	136	140	4	7	4	12	164	159	4	8	1	−8	93	93	5
7	3	8	201	210	5	7	4	12	159	158	4	8	2	−8	115	111	4
7	4	8	240	238	5	7	5	12	136	130	4	8	2	−8	111	112	6
7	5	8	217	217	4	7	5	12	137	130	4	8	3	−8	171	185	4
7	6	8	205	202	4	7	6	12	130	132	5	8	3	−8	177	184	4
7	7	8	117	123	4	7	0	13	239	237	4	8	4	−8	159	165	4
7	8	8	99	97	5	7	0	13	245	239	4	8	4	−8	175	166	4
7	9	8	86	83	6	7	2	13	173	175	4	8	5	−8	177	179	4
7	0	9	368	373	5	7	2	13	173	175	4	8	5	−8	184	180	4
7	0	9	370	372	5	7	4	13	180	187	4	8	6	−8	142	134	5

Table 83 — continued

H	K	L	F_{obs}	F_{calc}	SigF	H	K	L	F_{obs}	F_{calc}	SigF	H	K	L	F_{obs}	F_{calc}	SigF
8	6	−8	129	133	4	8	1	−2	118	118	4	8	0	3	361	366	9
8	7	−8	71	70	9	8	2	−2	126	125	4	8	1	3	172	173	5
8	7	−8	72	69	7	8	3	−2	189	194	6	8	2	3	257	258	9
8	2	−7	322	321	5	8	4	−2	203	206	4	8	3	3	187	186	8
8	2	−7	319	323	6	8	5	−2	142	152	4	8	4	3	163	167	5
8	3	−7	116	107	5	8	6	−2	293	291	5	8	5	3	195	198	4
8	3	−7	102	106	5	8	7	−2	100	100	5	8	7	3	143	143	4
8	4	−7	113	107	4	8	8	−2	275	281	6	8	8	3	97	93	7
8	4	−7	98	108	7	8	10	−2	193	194	4	8	1	4	104	102	5
8	5	−7	109	106	4	8	1	−1	202	199	7	8	2	4	149	146	9
8	5	−7	112	106	6	8	2	−1	195	195	9	8	3	4	152	149	3
8	6	−7	80	83	8	8	3	−1	56	50	8	8	4	4	143	148	4
8	2	−6	254	260	5	8	4	−1	195	184	6	8	5	4	204	206	5
8	3	−6	121	126	5	8	5	−1	84	83	6	8	6	4	132	132	6
8	4	−6	166	167	4	8	6	−1	218	226	4	8	7	4	234	235	9
8	4	−6	164	166	3	8	7	−1	124	126	5	8	9	4	134	130	4
8	5	−6	100	102	6	8	8	−1	151	158	6	8	0	5	95	104	5
8	5	−6	98	102	5	8	9	−1	160	160	4	8	1	5	411	414	5
8	6	−6	187	188	3	8	10	−1	120	121	5	8	2	5	77	78	6
8	6	−6	181	189	4	8	0	0	281	268	5	8	3	5	229	227	8
8	7	−6	88	87	7	8	1	0	72	78	7	8	4	5	137	139	7
8	7	−6	90	87	5	8	2	0	124	130	5	8	5	5	100	93	5
8	8	−6	80	73	8	8	3	0	84	84	5	8	6	5	70	72	7
8	1	−5	407	414	12	8	4	0	195	200	5	8	7	5	90	95	6
8	2	−5	79	76	6	8	0	1	198	192	4	8	0	6	133	137	4
8	3	−5	207	208	6	8	1	1	218	215	5	8	2	6	251	252	8
8	4	−5	141	142	4	8	2	1	196	194	4	8	3	6	122	125	4
8	5	−5	92	85	6	8	3	1	63	61	8	8	4	6	158	162	4
8	6	−5	70	77	7	8	4	1	202	190	4	8	5	6	99	98	5
8	7	−5	104	97	5	8	5	1	87	83	5	8	6	6	196	199	4
8	1	−4	101	104	5	8	6	1	226	227	11	8	7	6	80	81	7
8	2	−4	149	153	6	8	7	1	122	125	4	8	8	6	74	84	7
8	3	−4	158	159	7	8	8	1	151	155	5	8	0	7	425	429	5
8	4	−4	141	146	4	8	9	1	158	162	4	8	0	7	432	427	5
8	5	−4	198	200	4	8	10	1	119	117	5	8	2	7	315	323	5
8	6	−4	133	135	4	8	0	2	113	113	5	8	3	7	117	112	4
8	7	−4	219	231	5	8	1	2	116	112	4	8	4	7	120	118	4
8	9	−4	136	137	10	8	2	2	143	137	6	8	5	7	111	111	5
8	1	−3	174	173	3	8	3	2	191	196	4	8	6	7	77	75	6
8	2	−3	243	241	5	8	4	2	218	218	6	8	0	8	146	145	4
8	3	−3	190	191	4	8	5	2	159	155	3	8	0	8	139	146	4
8	4	−3	140	146	4	8	6	2	300	301	5	8	1	8	97	94	5
8	5	−3	199	203	4	8	7	2	95	102	5	8	1	8	89	95	6
8	7	−3	145	149	6	8	8	2	286	285	5	8	2	8	121	114	4

Table 83 — continued

H	K	L	F_{obs}	F_{calc}	SigF	H	K	L	F_{obs}	F_{calc}	SigF	H	K	L	F_{obs}	F_{calc}	SigF
8	2	8	120	114	5	9	3	−9	164	168	5	9	6	−3	88	95	9
8	3	8	177	184	4	9	4	−9	151	159	5	9	7	−3	72	72	8
8	4	8	163	165	4	9	4	−9	152	158	4	9	1	−2	126	125	4
8	5	8	185	186	6	9	1	−8	190	191	4	9	2	−2	93	101	10
8	6	8	136	133	4	9	1	−8	195	190	4	9	3	−2	218	228	6
8	7	8	95	88	6	9	2	−8	83	87	6	9	4	−2	97	103	6
8	1	9	310	303	6	9	2	−8	76	87	9	9	5	−2	213	216	4
8	1	9	296	301	5	9	3	−8	85	89	6	9	7	−2	247	246	7
8	2	9	61	57	7	9	3	−8	83	90	8	9	1	−1	227	230	4
8	2	9	63	58	8	9	5	−8	72	70	7	9	2	−1	233	237	5
8	3	9	182	180	4	9	1	−7	122	128	6	9	3	−1	96	96	9
8	3	9	186	179	3	9	1	−7	122	128	4	9	4	−1	97	97	6
8	4	9	106	107	6	9	2	−7	128	129	4	9	7	−1	123	125	5
8	4	9	111	106	5	9	2	−7	122	130	6	9	8	−1	99	113	12
8	6	9	109	106	5	9	3	−7	135	138	4	9	0	1	229	232	5
8	6	9	113	106	5	9	3	−7	132	138	5	9	1	1	233	230	5
8	7	9	64	63	8	9	4	−7	192	192	4	9	2	1	247	244	9
8	1	10	130	123	5	9	4	−7	187	191	4	9	3	1	96	101	5
8	1	10	124	123	4	9	5	−7	112	107	5	9	4	1	99	98	10
8	2	10	113	123	6	9	5	−7	105	107	7	9	5	1	79	81	12
8	2	10	126	123	4	9	6	−7	81	79	9	9	7	1	136	133	8
8	3	10	93	89	6	9	6	−7	80	79	6	9	8	1	113	113	13
8	3	10	96	88	5	9	1	−6	192	187	7	9	0	2	72	73	7
8	4	10	210	207	4	9	2	−6	93	104	8	9	1	2	131	125	5
8	4	10	203	208	4	9	3	−6	100	124	7	9	2	2	109	109	5
8	5	10	148	152	4	9	3	−6	120	123	4	9	3	2	229	232	5
8	5	10	153	152	4	9	5	−6	92	75	5	9	4	2	112	109	5
8	6	10	85	82	6	9	5	−6	77	75	9	9	5	2	220	219	4
8	0	11	238	237	5	9	6	−6	93	91	6	9	6	2	83	80	6
8	0	11	234	235	5	9	6	−6	97	92	7	9	7	2	251	252	7
8	2	11	188	191	4	9	1	−5	169	178	4	9	0	3	241	242	4
8	2	11	197	190	4	9	2	−5	132	138	6	9	1	3	191	194	4
8	4	11	126	128	5	9	3	−5	171	176	5	9	2	3	205	203	4
8	4	11	125	127	4	9	4	−5	132	130	5	9	3	3	209	213	4
8	5	11	127	123	5	9	6	−5	95	98	6	9	5	3	79	77	6
8	5	11	131	124	5	9	1	−4	113	113	5	9	6	3	96	101	6
8	3	12	161	157	4	9	2	−4	130	130	8	9	7	3	82	79	6
8	3	12	161	158	4	9	4	−4	129	134	5	9	0	4	126	130	5
9	2	−10	154	144	5	9	6	−4	161	167	4	9	1	4	120	117	11
9	2	−10	144	143	4	9	7	−4	112	117	6	9	2	4	125	126	6
9	1	−9	74	72	9	9	1	−3	180	187	7	9	4	4	137	137	6
9	2	−9	167	167	4	9	2	−3	200	201	4	9	6	4	176	177	4
9	2	−9	160	168	5	9	3	−3	203	206	4	9	7	4	112	114	5
9	3	−9	169	167	4	9	4	−3	59	62	9	9	0	5	81	81	6

Table 83 — continued

H	K	L	F_{obs}	F_{calc}	SigF	H	K	L	F_{obs}	F_{calc}	SigF	H	K	L	F_{obs}	F_{calc}	SigF
9	1	5	168	179	4	9	1	9	80	75	8	10	4	−1	86	96	10
9	2	5	136	142	5	9	2	9	148	154	4	10	0	1	264	266	5
9	3	5	176	176	4	9	3	9	175	168	4	10	1	1	143	140	7
9	4	5	141	136	7	9	4	9	152	147	4	10	2	1	154	152	4
9	5	5	107	105	5	9	0	10	205	206	4	10	3	1	119	119	6
9	6	5	100	103	10	9	2	10	143	146	4	10	4	1	89	96	12
9	0	6	164	169	4	10	1	−6	105	107	6	10	5	1	84	86	7
9	1	6	183	184	4	10	2	−6	86	88	7	10	1	2	152	150	4
9	2	6	102	109	5	10	1	−5	79	71	7	10	2	2	120	118	5
9	3	6	107	112	5	10	3	−5	144	145	5	10	3	2	124	125	5
9	5	6	84	85	6	10	2	−4	168	169	6	10	4	2	169	172	4
9	6	6	77	84	7	10	3	−4	95	102	6	10	1	3	171	175	4
9	1	7	124	121	4	10	4	−4	138	135	5	10	2	3	150	145	7
9	2	7	135	135	4	10	1	−3	180	181	6	10	4	3	130	124	5
9	3	7	133	132	4	10	2	−3	150	149	4	10	0	4	129	131	5
9	4	7	200	195	4	10	4	−3	130	129	5	10	2	4	175	175	5
9	5	7	110	105	5	10	1	−2	137	141	5	10	3	4	96	95	7
9	6	7	79	84	7	10	2	−2	116	122	5	10	4	4	140	141	8
9	0	8	67	69	7	10	3	−2	112	119	5	10	0	5	79	86	11
9	1	8	187	192	4	10	4	−2	172	174	4	10	1	5	69	63	8
9	2	8	75	80	6	10	1	−1	143	139	5	10	3	5	140	140	5
9	3	8	90	92	7	10	2	−1	157	160	4	10	1	6	106	109	6
9	0	9	151	148	4	10	3	−1	117	120	5	10	2	6	74	79	8

APPENDIX D

SUPPLEMENTAL TABLES AND FIGURES

FOR

THE CRYSTAL STRUCTURE

OF

$[(\eta^6\text{-}C_6Me_6)Mn(CO)_2SCHNEt_2][BF_4]$

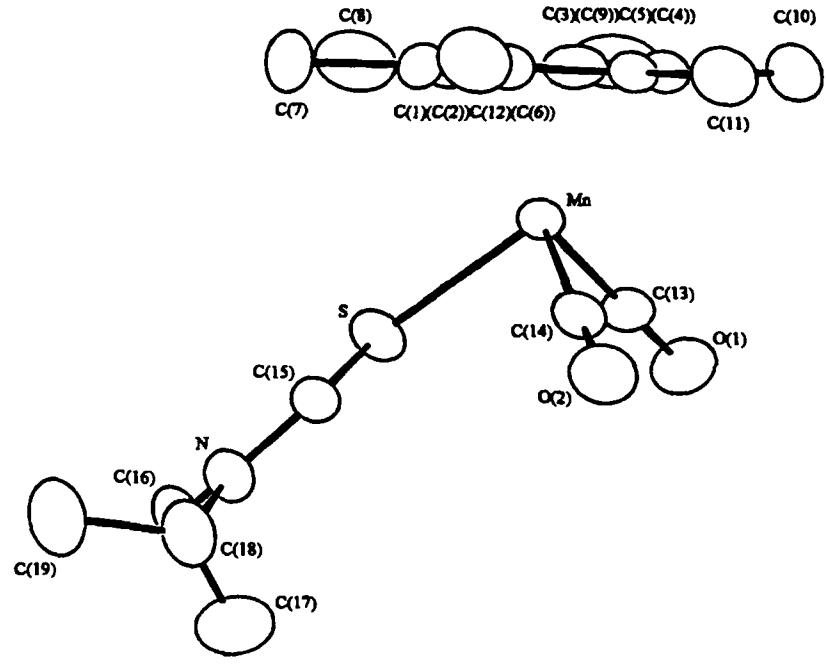

Figure 27. ORTEP drawing of **53** showing planarity of arene ring and $SCHNEt_2$ moiety

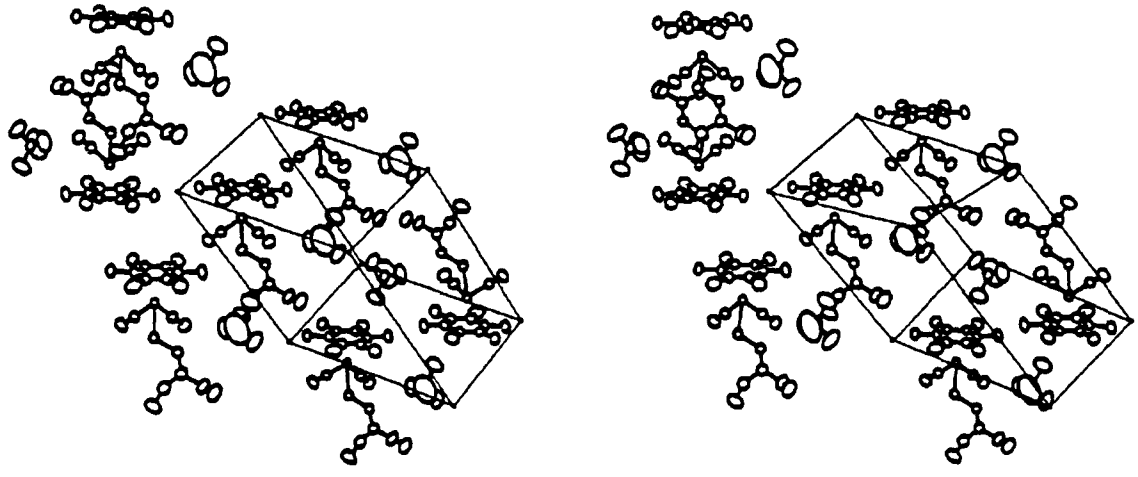

Figure 28. Stereoscopic View of the unit cell of **53**

Table 84. Complete Crystallographic Data and Refinement Parameters for **53** [a]

empirical formula	$MnSO_2NC_{19}H_{29}BF_4$
color of crystal	bright orange
fw, amu	477.25
crystal dimensions, mm	0.69 × 0.13 × 0.19
space group	$P\bar{1}$ (No. 2)
cell dimensions	
a, Å	8.312 (6)
b, Å	12.303 (4)
c, Å	13.325 (6)
α, deg	61.14 (3)
β, deg	74.69 (5)
γ, deg	75.69 (4)
V, Å^3	1138 (2)
Z	2
ρ_{calc}, g/cm^3	1.39
λ, Å (graphite)	0.710 73
μ, cm^{-1} (Mo Kα)	7.7
T (data collection), K	295
omega (ω) scan range	0.80 + 0.35 tan(θ)
horizontal aperture, mm	2.5–3.0
omega (ω) scan speed, deg/min (θ from 1° to 25°)	3.3–0.71
linear abs coeff, cm^{-1}	6.9
max and min corrections on F	1.00–0.97
crystal decay, %	5.5
reflections collected (1–25°)	5192
reflections > 3 σ	4451
after averaging	2475
Parameters refined	262
R_1 [b]	0.054
R_2 [c]	0.088
std deviation, observed of unit wt	1.17
residual electron density, e^-/Å^3	0.85
largest shift/esd	0.00

[a] In this and subsequent tables esd's are given in parentheses.

[b] $R_1 = \Sigma \| F_o | - | F_c \| / \Sigma | F_o |$.

[c] $R_2 = [\Sigma w(| F_o | - | F_c |)^2 / \Sigma w | F_o |^2]^{1/2}$, $w = 1/\sigma^2(F)$, where $\sigma^2(F) = \sigma^2(F) + [(\text{PWT})F]^2$, PWT = 0.07.

Table 85. Fractional Coordinates and Isotropic Thermal Parameters [a] for 53

atom	x	y	z	B_{iso}, Å^2
Mn	0.22583 (8)	0.10341 (6)	0.24722 (5)	3.76 (1)
S	−0.0341 (2)	0.2206 (1)	0.2716 (1)	5.15 (3)
C(1)	0.3004 (7)	0.2632 (5)	0.0780 (4)	5.2 (1)
C(2)	0.2169 (7)	0.1893 (5)	0.0606 (4)	5.7 (1)
C(3)	0.2738 (6)	0.0596 (4)	0.0995 (4)	5.1 (1)
C(4)	0.4119 (7)	0.0038 (4)	0.1614 (4)	4.7 (1)
C(5)	0.4938 (6)	0.0761 (4)	0.1793 (3)	4.3 (1)
C(6)	0.4390 (6)	0.2098 (4)	0.1350 (4)	4.7 (1)
C(7)	0.243 (1)	0.4052 (6)	0.0316 (6)	8.1 (2)
C(8)	0.0680 (9)	0.2515 (9)	−0.0061 (5)	10.7 (3)
C(9)	0.1922 (9)	−0.0226 (6)	0.0778 (5)	8.8 (2)
C(10)	0.468 (1)	−0.1355 (5)	0.2028 (5)	7.8 (2)
C(11)	0.6412 (8)	0.0222 (7)	0.2428 (5)	7.9 (2)
C(12)	0.5342 (9)	0.2888 (5)	0.1487 (6)	8.2 (2)
C(13)	0.1229 (7)	−0.0325 (4)	0.3344 (4)	5.1 (1)
O(1)	0.0590 (6)	−0.1207 (4)	0.3883 (4)	8.0 (1)
C(14)	0.2762 (6)	0.0903 (5)	0.3745 (4)	5.2 (1)
O(2)	0.3132 (5)	0.0828 (4)	0.4550 (3)	7.7 (1)
C(15)	−0.0260 (6)	0.3111 (4)	0.3325 (4)	4.6 (1)
N	−0.1552 (6)	0.3786 (4)	0.3634 (3)	5.5 (1)
C(16)	−0.3263 (8)	0.3807 (5)	0.3501 (5)	6.7 (2)
C(17)	−0.417 (1)	0.287 (1)	0.4534 (7)	10.8 (3)
C(18)	−0.134 (1)	0.4464 (5)	0.4245 (5)	7.5 (2)
C(19)	−0.195 (1)	0.5852 (6)	0.3659 (7)	10.0 (3)
B	0.2858 (9)	0.5915 (6)	0.2242 (5)	6.1 (2)
F(1)	−0.265 (1)	0.3752 (5)	0.6999 (5)	21.4 (3)
F(2)	0.5519 (8)	0.3953 (6)	−0.1653 (6)	14.1 (3)
F(3)	0.1917 (8)	0.658 (1)	0.1623 (7)	27.8 (5)
F(4)	0.2669 (9)	0.4700 (5)	0.2782 (7)	16.9 (3)

[a] Anisotropically refined atoms are given in the form of the isotropic equivalent displacement parameter defined as: $(4/3)[a^2B(1,1) + b^2B(2,2) + c^2B(3,3) + ab(\cos\gamma)B(1,2) + ac(\cos\beta)B(1,3) + bc(\cos\alpha)B(2,3)]$.

Table 86. Fractional Coordinates and Isotropic Thermal Parameters for Hydrogen Atoms of **53**

Atom	x	y	z	B_{iso} [a]
H(1)	0.2490	0.4308	0.0873	8
H(2)	0.1310	0.4244	0.0180	8
H(3)	0.3159	0.4481	−0.0390	8
H(4)	−0.0061	0.3065	0.0224	11
H(5)	0.0087	0.1884	0.0047	11
H(6)	0.1090	0.2972	−0.0864	11
H(7)	0.2315	−0.0114	0.0003	9
H(8)	0.0731	0.0001	0.0893	9
H(9)	0.2200	−0.1079	0.1305	9
H(10)	0.4334	−0.1626	0.1570	8
H(11)	0.4183	−0.1793	0.2821	8
H(12)	0.5872	−0.1525	0.1958	8
H(13)	0.6227	0.0498	0.3007	8
H(14)	0.7411	0.0497	0.1890	8
H(15)	0.6530	−0.0666	0.2781	8
H(16)	0.5862	0.3445	0.0744	9
H(17)	0.6181	0.2364	0.1949	9
H(18)	0.4585	0.3358	0.1857	9
H(19)	0.0807	0.3108	0.3456	4
H(20)	−0.3183	0.3642	0.2861	7
H(21)	−0.3877	0.4616	0.3349	7
H(22)	−0.4185	0.2994	0.5189	11
H(23)	−0.5297	0.2978	0.4429	11
H(24)	−0.3626	0.2060	0.4651	11
H(25)	−0.0174	0.4352	0.4270	8
H(26)	−0.1954	0.4118	0.5013	8
H(27)	−0.2744	0.6085	0.4207	11
H(28)	−0.2466	0.6038	0.3030	11
H(29)	−0.1018	0.6302	0.3380	11

[a] Atoms were refined isotropically.

Table 87. Additional Supplemental Bond Distances (Å) and Angles (°) for **53**

Distances [a]

C(7)-H(1)	0.950 (0)	C(10)-H(11)	0.951 (0)	C(16)-H(21)	0.949 (0)
C(7)-H(2)	0.948 (0)	C(10)-H(12)	0.951 (0)	C(17)-H(22)	0.950 (0)
C(7)-H(3)	0.950 (0)	C(11)-H(13)	0.949 (0)	C(17)-H(23)	0.948 (0)
C(8)-H(4)	0.949 (0)	C(11)-H(14)	0.951 (0)	C(17)-H(24)	0.946 (0)
C(8)-H(5)	0.952 (0)	C(11)-H(15)	0.948 (0)	C(18)-H(25)	0.950 (0)
C(8)-H(6)	0.948 (0)	C(12)-H(16)	0.948 (0)	C(18)-H(26)	0.949 (0)
C(9)-H(7)	0.948 (0)	C(12)-H(17)	0.950 (0)	C(19)-H(27)	0.951 (0)
C(9)-H(8)	0.950 (0)	C(12)-H(18)	0.952 (0)	C(19)-H(28)	0.948 (0)
C(9)-H(9)	0.950 (0)	C(15)-H(19)	0.947 (0)	C(19)-H(29)	0.948 (0)
C(10)-H(10)	0.948 (0)	C(16)-H(20)	0.950 (0)		
B-F(1)	1.222 (9)	B-F(2)	1.37 (1)	B-F(3)	1.6 (1)
B-F(4)	1.34 (1)				

Angles [a]

H(1)-C(7)-H(2)	109. (0)	H(13)-C(11)-H(15)	109. (0)
H(1)-C(7)-H(3)	109. (0)	H(14)-C(11)-H(15)	109. (0)
H(2)-C(7)-H(3)	109. (0)	H(16)-C(12)-H(17)	109. (0)
H(4)-C(8)-H(5)	109. (0)	H(16)-C(12)-H(18)	109. (0)
H(4)-C(8)-H(6)	109. (0)	H(17)-C(12)-H(18)	109. (0)
H(5)-C(8)-H(6)	109. (0)	H(20)-C(16)-H(21)	109. (0)
H(7)-C(9)-H(8)	109. (0)	H(22)-C(17)-H(23)	109. (0)
H(7)-C(9)-H(9)	109. (0)	H(22)-C(17)-H(24)	109. (0)
H(8)-C(9)-H(9)	109. (0)	H(23)-C(17)-H(24)	109. (0)
H(10)-C(10)-H(11)	109. (0)	H(25)-C(18)-H(26)	109. (0)
H(10)-C(10)-H(12)	109. (0)	H(27)-C(19)-H(28)	109. (0)
H(11)-C(10)-H(12)	109. (0)	H(27)-C(19)-H(29)	109. (0)
H(13)-C(11)-H(14)	109. (0)	H(28)-C(19)-H(29)	109. (0)
F(1)-B-F(2)	107.6 (8)	F(1)-B-F(3)	107. (1)
F(1)-B-F(4)	106.8 (8)	F(2)-B-F(3)	110. (1)
F(2)-B-F(4)	109.3 (7)	F(3)-B-F(4)	116. (1)

[a] Numbers in parentheses after bond distances and angles are estimated standard deviations in the least significant digits.

Table 88. General Displacement Parameter Expressions [a] — U's for **53**

Name	U(1,1)	U(2,2)	U(3,3)	U(1,2)	U(1,3)	U(2,3)
Mn	0.0428 (3)	0.0565 (3)	0.0432 (2)	−0.0077 (2)	−0.0036 (3)	−0.0235 (2)
S	0.0459 (6)	0.0868 (6)	0.0765 (5)	−0.0006 (5)	−0.0117 (4)	−0.0504 (3)
F(1)	0.465 (9)	0.236 (3)	0.169 (3)	−0.209 (4)	0.131 (4)	−0.152 (2)
F(2)	0.131 (4)	0.176 (5)	0.155 (4)	−0.023 (4)	0.024 (4)	−0.039 (4)
F(3)	0.215 (4)	0.37 (1)	0.390 (7)	0.028 (6)	−0.231 (3)	−0.052 (8)
F(4)	0.207 (5)	0.134 (2)	0.321 (6)	−0.068 (3)	0.013 (4)	−0.125 (2)
O(1)	0.099 (3)	0.086 (2)	0.092 (2)	−0.037 (2)	0.015 (2)	−0.025 (2)
O(2)	0.091 (2)	0.145 (2)	0.074 (1)	0.007 (2)	−0.036 (1)	−0.062 (1)
N	0.065 (2)	0.077 (2)	0.066 (2)	0.007 (2)	−0.014 (2)	−0.036 (1)
C(1)	0.063 (3)	0.057 (2)	0.051 (2)	−0.003 (2)	−0.001 (2)	−0.010 (2)
C(2)	0.063 (3)	0.106 (3)	0.042 (2)	−0.013 (2)	−0.007 (2)	−0.029 (2)
C(3)	0.062 (3)	0.094 (2)	0.053 (2)	−0.031 (2)	0.003 (2)	−0.040 (1)
C(4)	0.062 (3)	0.055 (2)	0.055 (2)	−0.011 (2)	0.008 (2)	−0.028 (1)
C(5)	0.043 (2)	0.068 (2)	0.048 (2)	−0.005 (2)	−0.000 (2)	−0.027 (1)
C(6)	0.054 (2)	0.067 (2)	0.058 (2)	−0.016 (2)	0.001 (2)	−0.029 (1)
C(7)	0.102 (5)	0.061 (3)	0.098 (4)	0.007 (3)	−0.007 (4)	−0.015 (3)
C(8)	0.085 (4)	0.238 (7)	0.080 (3)	0.030 (5)	−0.043 (2)	−0.078 (3)
C(9)	0.113 (4)	0.174 (3)	0.096 (2)	−0.078 (2)	0.021 (2)	−0.092 (2)
C(10)	0.112 (5)	0.063 (2)	0.107 (3)	−0.010 (3)	0.014 (3)	−0.046 (2)
C(11)	0.055 (3)	0.139 (5)	0.092 (3)	0.006 (3)	−0.019 (3)	−0.047 (3)
C(12)	0.096 (4)	0.108 (3)	0.133 (4)	−0.051 (2)	0.007 (3)	−0.070 (2)
C(13)	0.060 (3)	0.068 (2)	0.056 (2)	−0.014 (2)	0.005 (2)	−0.026 (2)
C(14)	0.050 (3)	0.087 (2)	0.060 (2)	0.004 (2)	−0.010 (2)	−0.038 (2)
C(15)	0.056 (3)	0.064 (2)	0.052 (2)	−0.003 (2)	−0.005 (2)	−0.027 (1)
C(16)	0.062 (3)	0.093 (3)	0.100 (3)	0.023 (3)	−0.026 (2)	−0.053 (2)
C(17)	0.077 (4)	0.189 (8)	0.098 (4)	−0.019 (5)	−0.000 (4)	−0.036 (5)
C(18)	0.123 (5)	0.084 (2)	0.095 (2)	0.018 (3)	−0.036 (3)	−0.059 (2)
C(19)	0.165 (7)	0.088 (3)	0.133 (4)	0.021 (4)	−0.039 (4)	−0.064 (2)
B	0.086 (4)	0.077 (3)	0.082 (3)	−0.011 (3)	−0.017 (3)	−0.045 (2)

[a] The form of the anisotropic displacement parameter is : $\exp[-2\pi^2\{h^2a^2U(1,1) + k^2b^2U(2,2) + l^2c^2U(3,3) + 2hkabU(1,2) + 2hlacU(1,3) + 2klbcU(2,3)\}]$, where a, b, and c are reciprocal lattice constants.

Table 89. General Displacement Parameter Expressions [a] — B's for 53

Name	B(1,1)	B(2,2)	B(3,3)	B(1,2)	B(1,3)	B(2,3)	B_{iso}
Mn	3.45 (3)	4.45 (2)	3.42 (2)	−0.59 (2)	−0.29 (2)	−1.88 (2)	3.78 (2)
S	3.58 (5)	7.09 (5)	6.11 (5)	−0.06 (4)	−0.87 (4)	−4.12 (3)	5.22 (4)
F (1)	39.1 (8)	17.7 (2)	12.1 (2)	**.* (3)	10.6 (4)	**.* (1)	21.6 (3)
F (2)	10.7 (4)	13.8 (4)	12.9 (4)	−2.7 (3)	1.7 (3)	−2.8 (3)	14.4 (3)
F (3)	16.2 (3)	31 (1)	28.7 (5)	2.9 (5)	**.* (2)	−3.4 (6)	27.9 (5)
F (4)	16.5 (4)	11.3 (2)	24.9 (5)	−6.6 (2)	2.2 (4)	10.0 (2)	17.0 (3)
O (1)	8.1 (3)	6.5 (2)	7.2 (2)	−2.9 (2)	1.6 (2)	−2.1 (2)	8.0 (2)
O (2)	7.3 (2)	11.9 (2)	5.9 (1)	0.6 (2)	−2.8 (1)	−5.3 (1)	7.9 (1)
N	5.1 (2)	5.7 (2)	5.7 (2)	0.8 (2)	−1.4 (2)	−2.8 (1)	5.6 (1)
C (1)	5.1 (3)	4.5 (2)	4.1 (2)	−0.5 (2)	0.2 (2)	−0.9 (2)	5.3 (2)
C (2)	4.5 (2)	8.1 (3)	3.4 (2)	−0.8 (2)	−0.5 (2)	−1.9 (2)	5.7 (2)
C (3)	4.9 (2)	7.4 (2)	4.5 (2)	−2.2 (2)	0.3 (2)	−3.3 (1)	5.3 (1)
C (4)	5.3 (3)	4.4 (2)	4.4 (2)	−1.0 (2)	0.9 (2)	−2.4 (1)	4.8 (1)
C (5)	3.2 (2)	5.3 (2)	3.9 (2)	−0.2 (2)	−0.1 (1)	−2.0 (1)	4.4 (1)
C (6)	4.0 (2)	5.3 (2)	4.5 (2)	−1.5 (2)	0.5 (2)	−2.3 (1)	4.6 (1)
C (7)	8.9 (5)	4.9 (3)	6.9 (3)	0.9 (3)	−0.4 (3)	−1.4 (2)	8.0 (2)
C (8)	5.9 (3)	17.4 (6)	6.7 (3)	2.2 (4)	−2.8 (2)	−5.6 (3)	10.3 (3)
C (9)	9.6 (4)	13.7 (3)	7.1 (2)	−6.3 (2)	1.8 (2)	−7.0 (2)	8.9 (2)
C (10)	10.1 (5)	4.7 (2)	8.3 (3)	−1.0 (3)	0.8 (3)	−3.4 (2)	8.0 (2)
C (11)	4.8 (3)	10.6 (4)	7.4 (3)	1.2 (3)	−1.7 (2)	−3.7 (3)	8.0 (3)
C (12)	7.2 (3)	8.8 (2)	10.5 (3)	−3.4 (2)	0.3 (3)	−6.0 (2)	8.0 (2)
C (13)	4.4 (2)	5.5 (2)	4.7 (2)	−0.9 (2)	0.6 (2)	−2.2 (1)	5.1 (2)
C (14)	3.8 (2)	6.7 (2)	4.7 (2)	0.4 (2)	−0.7 (2)	−2.8 (1)	5.2 (2)
C (15)	4.7 (2)	5.4 (2)	4.0 (2)	−0.3 (2)	−0.3 (2)	−2.3 (1)	4.8 (1)
C (16)	5.3 (3)	7.2 (3)	8.2 (3)	2.0 (2)	−2.2 (2)	−4.1 (2)	6.9 (2)
C (17)	5.5 (4)	16.2 (7)	7.3 (4)	−1.3 (4)	−0.5 (3)	−2.9 (4)	10.9 (4)
C (18)	9.6 (4)	6.2 (2)	7.5 (2)	1.4 (3)	−2.7 (2)	−4.6 (1)	7.4 (2)
C (19)	14.1 (7)	6.7 (3)	9.9 (4)	2.0 (4)	−2.4 (4)	−5.2 (2)	10.3 (3)
B	7.0 (4)	8.3 (3)	10.1 (3)	−1.6 (3)	−0.3 (3)	−6.2 (2)	7.7 (2)

[a] The form of the anisotropic displacement parameter is : $\exp[-0.25\{h^2a^2B(1,1) + k^2b^2B(2,2) + l^2c^2B(3,3) + 2hkabB(1,2) + 2hlacB(1,3) + 2klbcB(2,3)\}]$, where a, b, and c are reciprocal lattice constants.

Table 90. Deviations [a] from Least-Squares-Planes Analysis for **53**

Atoms	1	2
Mn	−241. (1)	
S	−23. (1)	
N	39. (4)	
C(1)		−5. (5)
C(2)		−12. (5)
C(3)		19. (4)
C(4)		−8. (4)
C(5)		−9. (4)
C(6)		15. (5)
C(7)		19. (8)
C(8)		13. (7)
C(9)		73. (6)
C(10)		9. (7)
C(11)		−20. (6)
C(12)		93. (7)
C(15)	20. (4)	
C(16)	−5. (6)	
C(17)	−1366. (9)	
C(18)	−30. (6)	
C(19)	1106. (8)	
H19	18. (0)	
Parameters for Least-Squares Planes [b]		
A	1090	4308
B	4276	−2458
C	−8974	−8683
D	-8407	−1176

[a] Deviations are in Å × 10^3. Atoms used to define the planes are marked with an asterisk (*) following the deviation.

[b] The equation of the plane is of the form: $Ax + By + Cz - D = 0$, where *A*, *B*, *C*, and *D* are constants (Å × 10^4) and x, y, and z are orthogonalized coordinates.

Table 91. Calculated FOFC's (× 10) for **53**

H	K	L	F_{obs}	F_{calc}	SigF	H	K	L	F_{obs}	F_{calc}	SigF	H	K	L	F_{obs}	F_{calc}	SigF
0	1	−12	77	79	4	0	7	−3	95	98	2	0	4	2	262	269	4
0	1	−11	77	80	3	0	8	−3	140	140	4	0	7	2	127	132	3
0	2	−11	84	84	3	0	1	−2	334	331	3	0	8	2	191	197	5
0	1	−10	135	133	5	0	2	−2	194	205	3	0	9	2	171	167	4
0	1	−9	131	119	3	0	4	−2	240	250	3	0	10	2	154	140	4
0	2	−9	158	151	6	0	5	−2	208	206	4	0	0	3	153	168	2
0	3	−9	152	147	8	0	6	−2	107	107	2	0	1	3	359	393	4
0	5	−9	57	56	5	0	7	−2	75	87	2	0	2	3	546	575	11
0	1	−8	133	116	3	0	9	−2	124	122	3	0	3	3	108	123	5
0	3	−8	108	106	2	0	1	−1	868	893	13	0	5	3	227	230	5
0	4	−8	165	171	3	0	2	−1	422	411	5	0	6	3	172	173	3
0	1	−7	169	163	3	0	3	−1	59	65	3	0	7	3	247	227	5
0	2	−7	247	247	3	0	4	−1	414	414	5	0	8	3	224	233	6
0	3	−7	150	140	2	0	5	−1	382	376	7	0	10	3	101	102	2
0	4	−7	36	37	3	0	6	−1	41	40	4	0	11	3	52	60	4
0	7	−7	39	43	7	0	7	−1	116	111	2	0	12	3	39	25	6
0	1	−6	373	377	6	0	8	−1	239	237	2	0	0	4	143	149	3
0	2	−6	98	105	3	0	9	−1	100	106	3	0	3	4	225	216	2
0	3	−6	262	264	6	0	11	−1	57	59	5	0	4	4	346	336	6
0	4	−6	121	108	2	0	1	0	343	349	4	0	5	4	59	63	2
0	5	−6	83	90	2	0	2	0	233	215	2	0	6	4	171	182	4
0	6	−6	108	109	6	0	3	0	215	221	3	0	7	4	81	66	2
0	1	−5	362	335	6	0	4	0	377	377	5	0	8	4	82	79	2
0	2	−5	428	434	7	0	5	0	43	42	4	0	9	4	172	169	2
0	3	−5	159	161	3	0	6	0	368	369	3	0	10	4	73	71	2
0	4	−5	147	151	4	0	7	0	48	55	5	0	12	4	55	54	9
0	6	−5	83	89	2	0	8	0	103	98	2	0	1	5	369	394	3
0	7	−5	63	61	3	0	9	0	132	134	3	0	2	5	267	287	2
0	1	−4	438	426	4	0	10	0	149	142	3	0	3	5	488	470	3
0	2	−4	170	163	3	0	0	1	155	136	2	0	4	5	250	264	4
0	3	−4	303	310	5	0	1	1	476	499	5	0	5	5	353	316	5
0	4	−4	193	197	3	0	2	1	890	871	11	0	6	5	48	41	4
0	5	−4	171	188	3	0	3	1	140	109	3	0	7	5	375	382	6
0	6	−4	106	95	2	0	4	1	54	52	2	0	8	5	246	256	3
0	7	−4	58	69	7	0	5	1	147	148	3	0	9	5	39	46	3
0	8	−4	48	48	4	0	6	1	106	128	2	0	10	5	65	70	2
0	9	−4	70	69	4	0	7	1	175	160	3	0	12	5	51	48	5
0	10	−4	63	49	5	0	8	1	298	310	3	0	0	6	220	225	6
0	1	−3	289	283	6	0	9	1	52	57	2	0	1	6	236	209	3
0	2	−3	505	507	7	0	11	1	73	74	4	0	2	6	189	144	3
0	3	−3	144	138	3	0	0	2	927	953	16	0	3	6	203	217	3
0	4	−3	110	109	2	0	1	2	171	183	3	0	5	6	474	468	8
0	5	−3	89	82	2	0	2	2	650	648	11	0	6	6	105	126	3
0	6	−3	88	88	2	0	3	2	289	287	6	0	7	6	163	156	3

Table 91 — continued

H	K	L	F_{obs}	F_{calc}	SigF	H	K	L	F_{obs}	F_{calc}	SigF	H	K	L	F_{obs}	F_{calc}	SigF
0	8	6	103	105	2	0	11	10	71	67	4	1	−5	−12	122	122	2
0	9	6	212	209	2	0	12	10	39	38	6	1	−4	−12	110	104	3
0	10	6	40	45	3	0	0	11	47	60	4	1	−3	−12	107	114	3
0	11	6	41	37	6	0	1	11	151	153	6	1	−2	−12	65	62	4
0	1	7	71	87	2	0	2	11	81	82	2	1	−11	−11	126	122	3
0	2	7	85	81	2	0	3	11	98	108	2	1	−10	−11	61	66	4
0	3	7	97	82	2	0	4	11	86	81	2	1	−9	−11	81	91	3
0	4	7	221	241	5	0	5	11	35	29	3	1	−8	−11	50	43	5
0	5	7	153	113	2	0	6	11	226	211	2	1	−7	−11	59	65	3
0	7	7	278	289	3	0	7	11	238	244	3	1	−5	−11	236	238	11
0	8	7	226	227	3	0	8	11	78	84	2	1	−4	−11	149	139	8
0	9	7	138	135	2	0	11	11	52	50	5	1	−3	−11	58	42	6
0	10	7	50	45	2	0	12	11	71	60	4	1	−2	−11	76	71	3
0	11	7	93	85	2	0	0	12	100	103	3	1	−1	−11	112	108	2
0	13	7	56	52	5	0	1	12	65	70	4	1	0	−11	82	89	3
0	0	8	189	187	4	0	2	12	74	68	3	1	1	−11	103	105	3
0	1	8	160	172	4	0	5	12	141	142	7	1	−12	−10	93	89	3
0	2	8	44	30	4	0	6	12	128	119	4	1	−10	−10	56	53	5
0	3	8	44	11	3	0	7	12	72	68	4	1	−9	−10	70	76	4
0	5	8	255	283	5	0	8	12	73	66	3	1	−8	−10	107	97	3
0	6	8	254	280	3	0	9	12	81	82	3	1	−7	−10	114	125	2
0	7	8	185	164	4	0	10	12	41	43	6	1	−6	−10	230	206	2
0	8	8	141	124	3	0	11	12	46	53	6	1	−5	−10	146	134	3
0	9	8	157	155	3	0	12	12	60	60	5	1	−4	−10	145	142	3
0	10	8	57	52	3	0	2	13	52	43	5	1	−3	−10	215	223	2
0	1	9	195	189	2	0	3	13	78	86	3	1	−2	−10	162	157	3
0	2	9	99	98	2	0	4	13	113	109	3	1	−1	−10	96	86	2
0	3	9	113	126	4	0	5	13	46	43	5	1	2	−10	109	111	3
0	4	9	141	156	3	0	6	13	81	84	3	1	3	−10	103	106	3
0	5	9	67	50	3	0	7	13	120	124	3	1	4	−10	42	39	6
0	7	9	286	288	2	0	8	13	86	85	3	1	−11	−9	105	103	3
0	8	9	100	94	2	0	5	14	125	126	3	1	−10	−9	117	110	5
0	9	9	47	38	3	0	6	14	106	102	3	1	−9	−9	111	106	2
0	10	9	55	58	4	0	9	14	52	52	5	1	−8	−9	35	37	3
0	11	9	159	144	3	1	−4	−14	57	53	5	1	−7	−9	48	59	2
0	13	9	49	58	6	1	−6	−13	55	51	5	1	−6	−9	113	122	2
0	0	10	200	200	4	1	−5	−13	90	83	3	1	−5	−9	307	312	2
0	1	10	41	47	3	1	−4	−13	106	98	3	1	−4	−9	127	127	2
0	4	10	92	88	2	1	−2	−13	93	95	3	1	−2	−9	189	177	2
0	5	10	148	171	3	1	−1	−13	67	75	4	1	−1	−9	128	135	3
0	6	10	226	217	2	1	−10	−12	89	80	3	1	0	−9	85	85	2
0	8	10	99	93	2	1	−8	−12	81	79	3	1	1	−9	127	115	3
0	9	10	119	117	2	1	−7	−12	108	106	3	1	2	−9	72	82	3
0	10	10	182	172	4	1	−6	−12	943	100	3	1	4	−9	80	76	3

Table 91 — continued

H	K	L	F_{obs}	F_{calc}	SigF	H	K	L	F_{obs}	F_{calc}	SigF	H	K	L	F_{obs}	F_{calc}	SigF
1	5	−9	70	70	4	1	3	−6	186	185	3	1	−1	−3	1052	1067	21
1	−13	−8	75	76	4	1	4	−6	141	138	3	1	0	−3	751	755	8
1	−12	−8	73	80	4	1	5	−6	64	62	2	1	2	−3	390	391	3
1	−11	−8	51	50	5	1	6	−6	54	52	5	1	3	−3	331	318	7
1	−10	−8	38	40	5	1	−11	−5	65	70	3	1	4	−3	401	402	5
1	−9	−8	73	70	2	1	−10	−5	82	87	5	1	5	−3	164	168	5
1	−8	−8	39	41	3	1	−8	−5	179	186	3	1	6	−3	134	138	6
1	−7	−8	156	160	2	1	−6	−5	253	274	5	1	7	−3	68	76	5
1	−6	−8	307	285	5	1	−5	−5	484	478	4	1	−12	−2	67	59	4
1	−5	−8	36	47	4	1	−4	−5	259	275	3	1	−9	−2	123	107	3
1	−4	−8	68	79	3	1	−3	−5	106	104	2	1	−8	−2	162	166	5
1	−3	−8	254	260	3	1	−2	−5	222	195	4	1	−7	−2	337	329	5
1	−2	−8	132	110	2	1	−1	−5	129	134	3	1	−6	−2	378	399	7
1	0	−8	55	60	3	1	0	−5	335	323	2	1	−5	−2	492	450	6
1	1	−8	81	91	2	1	1	−5	141	139	6	1	−4	−2	226	206	2
1	2	−8	167	158	3	1	2	−5	227	237	3	1	−3	−2	276	303	3
1	3	−8	167	166	8	1	3	−5	138	145	3	1	−2	−2	301	284	5
1	4	−8	144	140	5	1	4	−5	323	315	7	1	−1	−2	69	64	2
1	6	−8	72	70	4	1	5	−5	86	91	2	1	0	−2	640	629	8
1	−11	−7	51	58	5	1	6	−5	109	99	2	1	1	−2	548	518	5
1	−10	−7	140	138	3	1	−12	−4	63	70	4	1	2	−2	789	759	14
1	−8	−7	65	66	2	1	−11	−4	78	83	3	1	3	−2	575	581	6
1	−6	−7	205	221	4	1	−9	−4	124	115	2	1	5	−2	74	74	2
1	−5	−7	453	468	5	1	−8	−4	89	96	2	1	6	−2	266	260	3
1	−4	−7	257	272	7	1	−7	−4	304	294	2	1	7	−2	63	56	2
1	−2	−7	80	89	2	1	−6	−4	284	307	2	1	8	−2	82	89	2
1	−1	−7	237	237	3	1	−4	−4	374	383	2	1	11	−2	54	52	7
1	0	−7	160	172	4	1	−3	−4	509	502	2	1	−11	−1	51	49	5
1	1	−7	143	147	4	1	−2	−4	186	162	2	1	−9	−1	110	107	2
1	2	−7	59	68	2	1	0	−4	336	331	4	1	−8	−1	147	164	5
1	4	−7	119	110	2	1	1	−4	42	55	3	1	−6	−1	128	127	2
1	5	−7	118	124	5	1	2	−4	275	282	2	1	−5	−1	321	320	2
1	−12	−6	57	55	5	1	3	−4	428	450	6	1	−4	−1	78	81	2
1	−11	−6	93	97	3	1	4	−4	172	167	3	1	−3	−1	135	132	2
1	−10	−6	62	58	10	1	5	−4	184	181	5	1	−2	−1	88	68	2
1	−7	−6	298	283	3	1	6	−4	71	69	2	1	−1	−1	551	573	6
1	−6	−6	232	238	3	1	7	−4	73	75	2	1	0	−1	677	660	9
1	−4	−6	148	186	5	1	−9	−3	142	141	4	1	1	−1	263	289	4
1	−3	−6	330	287	5	1	−8	−3	113	133	2	1	2	−1	291	283	4
1	−2	−6	296	299	8	1	−7	−3	129	126	3	1	3	−1	138	128	4
1	−1	−6	200	217	5	1	−5	−3	410	405	6	1	4	−1	267	304	2
1	0	−6	210	199	5	1	−4	−3	271	281	6	1	5	−1	454	425	3
1	1	−6	179	181	4	1	−3	−3	151	125	3	1	6	−1	164	165	3
1	2	−6	80	93	5	1	−2	−3	162	132	4	1	7	−1	85	84	3

Table 91 — continued

H	K	L	F_{obs}	F_{calc}	SigF	H	K	L	F_{obs}	F_{calc}	SigF	H	K	L	F_{obs}	F_{calc}	SigF
1	9	−1	49	48	4	1	−5	2	175	183	3	1	0	4	58	65	2
1	10	−1	104	111	3	1	−4	2	228	211	2	1	1	4	447	431	9
1	−8	0	162	152	2	1	−3	2	88	75	3	1	2	4	669	699	18
1	−7	0	241	241	3	1	−2	2	42	51	3	1	3	4	322	300	2
1	−6	0	240	268	3	1	−1	2	331	309	4	1	4	4	314	297	2
1	−5	0	152	170	3	1	0	2	594	580	8	1	5	4	105	116	2
1	−4	0	172	164	5	1	1	2	323	285	2	1	6	4	52	42	2
1	−3	0	158	150	2	1	2	2	738	764	6	1	8	4	278	298	5
1	−2	0	669	610	8	1	3	2	338	328	5	1	9	4	205	199	2
1	−1	0	46	53	2	1	4	2	118	106	3	1	10	4	119	113	2
1	1	0	248	226	4	1	5	2	105	120	3	1	11	4	129	126	3
1	2	0	1145	1113	25	1	6	2	203	223	4	1	−9	5	43	43	6
1	3	0	472	469	7	1	7	2	71	92	2	1	−8	5	75	71	4
1	4	0	55	56	2	1	8	2	240	275	5	1	−6	5	161	149	3
1	5	0	175	168	3	1	9	2	115	115	3	1	−5	5	123	126	2
1	6	0	228	257	4	1	10	2	44	47	3	1	−4	5	162	150	3
1	7	0	121	113	2	1	11	2	85	87	2	1	−3	5	68	69	3
1	8	0	163	178	6	1	12	2	73	68	4	1	−2	5	120	112	4
1	9	0	171	180	3	1	−10	3	43	47	6	1	−1	5	92	71	4
1	11	0	60	59	5	1	−9	3	65	66	4	1	0	5	462	497	5
1	12	0	69	73	7	1	−8	3	94	101	4	1	1	5	428	368	6
1	−10	1	58	56	4	1	−7	3	70	56	2	1	2	5	271	309	2
1	−9	1	100	100	4	1	−6	3	168	145	2	1	3	5	140	127	2
1	−8	1	63	79	2	1	−5	3	142	150	4	1	4	5	499	494	4
1	−7	1	77	63	3	1	−4	3	292	307	4	1	5	5	109	122	4
1	−6	1	227	211	4	1	−2	3	397	383	5	1	6	5	65	63	2
1	−5	1	265	258	4	1	−1	3	408	431	5	1	7	5	237	223	2
1	−4	1	50	37	2	1	0	3	1011	1049	17	1	10	5	250	247	2
1	−2	1	580	578	8	1	1	3	217	213	4	1	11	5	72	74	3
1	−1	1	93	68	2	1	2	3	405	400	6	1	−7	6	90	93	3
1	0	1	1290	1298	11	1	3	3	182	171	3	1	−6	6	92	97	4
1	1	1	927	967	18	1	4	3	215	207	4	1	−4	6	64	71	2
1	2	1	206	181	3	1	5	3	320	329	11	1	−2	6	176	200	5
1	3	1	430	432	6	1	6	3	68	45	2	1	−1	6	350	331	6
1	4	1	911	892	10	1	7	3	140	111	5	1	0	6	162	176	4
1	5	1	431	396	2	1	9	3	196	202	5	1	1	6	134	147	3
1	7	1	114	96	4	1	10	3	214	219	6	1	2	6	683	391	3
1	8	1	72	70	2	1	11	3	88	92	3	1	3	6	612	567	5
1	9	1	156	150	10	1	−8	4	74	77	4	1	4	6	106	136	2
1	10	1	150	152	3	1	−7	4	178	178	5	1	7	6	284	304	5
1	11	1	66	65	8	1	−6	4	127	127	2	1	8	6	245	244	3
1	−8	2	161	154	3	1	−4	4	157	154	3	1	9	6	200	198	2
1	−7	2	118	115	7	1	−3	4	135	119	4	1	10	6	90	83	2
1	−6	2	239	246	3	1	−1	4	450	419	5	1	11	6	70	68	3

Table 91 — continued

H	K	L	F_{obs}	F_{calc}	SigF	H	K	L	F_{obs}	F_{calc}	SigF	H	K	L	F_{obs}	F_{calc}	SigF
1	12	6	60	56	4	1	4	9	71	72	2	1	7	13	66	70	4
1	13	6	45	46	6	1	5	9	189	204	3	1	10	13	73	70	4
1	−6	7	87	83	3	1	6	9	152	167	3	1	2	14	56	49	5
1	−5	7	199	195	5	1	7	9	249	222	2	1	3	14	75	75	4
1	−4	7	105	105	2	1	8	9	77	81	2	1	4	14	86	84	3
1	−3	7	99	101	2	1	9	9	226	229	2	1	5	14	77	76	3
1	−2	7	153	141	3	1	10	9	111	114	4	1	7	14	86	89	3
1	−1	7	72	56	2	1	−4	10	46	53	6	1	8	14	117	117	3
1	0	7	143	171	3	1	−2	10	125	128	8	1	9	14	61	62	5
1	1	7	322	308	5	1	−1	10	75	75	7	1	6	15	84	83	4
1	2	7	49	68	7	1	1	10	165	153	2	1	7	15	47	56	6
1	3	7	345	377	2	1	2	10	212	199	2	2	−8	−13	52	48	5
1	4	7	125	120	3	1	3	10	77	90	2	2	−3	−13	61	54	5
1	5	7	200	193	2	1	4	10	79	68	2	2	−2	−13	83	80	4
1	6	7	249	239	2	1	5	10	36	39	3	2	−9	−12	80	82	4
1	7	7	200	185	3	1	6	10	63	72	2	2	−6	−12	41	46	6
1	8	7	60	67	3	1	7	10	100	126	2	2	−5	−12	38	37	6
1	9	7	109	119	2	1	8	10	209	215	2	2	−4	−12	79	74	4
1	10	7	48	42	3	1	9	10	64	61	3	2	−3	−12	121	118	3
1	−6	8	72	74	4	1	11	10	189	177	4	2	−1	−12	90	93	3
1	−3	8	73	76	2	1	12	10	67	70	4	2	0	−12	77	73	4
1	−2	8	143	135	3	1	−1	11	44	39	5	2	−9	−11	83	81	3
1	−1	8	226	231	2	1	0	11	123	121	4	2	−8	−11	102	100	3
1	0	8	170	182	4	1	1	11	123	132	3	2	−7	−11	109	117	3
1	1	8	57	39	3	1	2	11	59	67	5	2	−5	−11	73	74	3
1	2	8	221	207	5	1	3	11	114	125	2	2	−3	−11	143	135	4
1	3	8	296	301	4	1	4	11	50	39	2	2	−2	−11	127	132	3
1	4	8	39	56	4	1	5	11	59	65	2	2	−1	−11	103	97	3
1	5	8	333	299	5	1	6	11	85	85	2	2	2	−11	45	45	6
1	6	8	202	226	4	1	7	11	81	74	2	2	−11	−10	49	40	6
1	7	8	91	107	5	1	9	11	145	145	3	2	−10	−10	132	126	3
1	8	8	230	218	2	1	10	11	148	145	3	2	−9	−10	85	93	3
1	9	8	78	89	2	1	−1	12	64	69	4	2	−8	−10	53	56	5
1	10	8	83	85	2	1	0	12	84	78	3	2	−5	−10	59	54	5
1	11	8	90	88	3	1	1	12	88	87	3	2	−4	−10	181	172	3
1	12	8	66	58	4	1	2	12	122	125	4	2	−3	−10	119	109	2
1	−5	9	57	53	5	1	7	12	131	140	7	2	−2	−10	61	60	3
1	−4	9	114	117	3	1	8	12	138	136	3	2	−1	−10	123	114	5
1	−3	9	131	136	4	1	11	12	83	83	3	2	0	−10	141	132	3
1	−1	9	126	112	3	1	12	12	57	55	5	2	1	−10	121	119	3
1	0	9	125	126	2	1	0	13	97	92	3	2	4	−10	43	48	6
1	1	9	187	175	2	1	1	13	89	93	3	2	−12	−9	52	52	6
1	2	9	77	79	3	1	2	13	55	53	5	2	−11	−9	102	95	3
1	3	9	219	230	4	1	6	13	138	135	2	2	−9	−9	58	66	4

Table 91 — continued

H	K	L	F_{obs}	F_{calc}	SigF	H	K	L	F_{obs}	F_{calc}	SigF	H	K	L	F_{obs}	F_{calc}	SigF
2	−8	−9	135	134	4	2	7	−7	86	75	4	2	−1	−4	69	67	2
2	−7	−9	84	89	3	2	−11	−6	85	84	3	2	0	−4	161	168	4
2	−5	−9	168	160	2	2	−10	−6	126	124	3	2	1	−4	171	144	2
2	−4	−9	68	71	2	2	−9	−6	132	128	3	2	2	−4	93	91	2
2	−3	−9	214	224	2	2	−8	−6	64	56	2	2	4	−4	151	140	5
2	−2	−9	113	107	2	2	−7	−6	107	109	2	2	5	−4	179	184	4
2	−1	−9	61	50	2	2	−6	−6	61	69	3	2	6	−4	100	105	4
2	0	−9	50	43	2	2	−5	−6	287	270	3	2	8	−4	52	50	5
2	1	−9	103	98	5	2	−4	−6	277	291	3	2	9	−4	40	43	6
2	2	−9	103	106	3	2	−3	−6	206	210	4	2	−12	−3	76	74	4
2	3	−9	119	116	3	2	−2	−6	70	74	3	2	−11	−3	118	123	3
2	−11	−8	76	70	4	2	−1	−6	614	620	9	2	−6	−3	376	412	4
2	−10	−8	94	91	3	2	0	−6	455	451	8	2	−5	−3	137	112	3
2	−9	−8	125	129	3	2	1	−6	72	67	2	2	−3	−3	377	378	5
2	−7	−8	37	40	3	2	2	−6	114	117	2	2	−2	−3	466	515	4
2	−6	−8	53	57	2	2	3	−6	59	42	2	2	−1	−3	148	152	4
2	−5	−8	144	151	3	2	5	−6	108	118	3	2	0	−3	425	405	7
2	−4	−8	188	191	2	2	6	−6	71	68	6	2	2	−3	88	71	4
2	−3	−8	73	81	2	2	−12	−5	76	73	4	2	3	−3	147	143	3
2	−2	−8	249	239	2	2	−11	−5	94	96	3	2	4	−3	284	294	6
2	−1	−8	263	262	2	2	−9	−5	114	114	2	2	5	−3	82	84	2
2	0	−8	176	181	2	2	−6	−5	90	110	3	2	6	−3	115	106	6
2	1	−8	80	72	2	2	−4	−5	81	79	4	2	7	−3	63	62	4
2	2	−8	70	73	2	2	−3	−5	287	275	4	2	8	−3	67	65	3
2	3	−8	65	65	3	2	−2	−5	473	491	10	2	−11	−2	56	57	5
2	4	−8	58	49	4	2	−1	−5	387	369	6	2	−10	−2	104	103	3
2	5	−8	78	80	4	2	0	−5	237	253	3	2	−9	−2	70	66	2
2	6	−8	77	68	4	2	1	−5	102	102	2	2	−8	−2	71	83	2
2	−12	−7	84	79	4	2	2	−5	117	119	2	2	−7	−2	130	101	3
2	−11	−7	73	74	4	2	3	−5	71	71	2	2	−5	−2	328	326	3
2	−9	−7	68	69	3	2	4	−5	197	204	2	2	−4	−2	496	526	6
2	−8	−7	130	131	3	2	5	−5	81	78	2	2	−3	−2	565	540	4
2	−6	−7	94	89	2	2	6	−5	79	85	3	2	−2	−2	49	18	2
2	−5	−7	218	233	3	2	7	−5	68	73	4	2	−1	−2	133	128	4
2	−3	−7	300	293	6	2	8	−5	61	61	4	2	1	−2	291	271	5
2	−2	−7	445	447	5	2	9	−5	49	39	6	2	2	−2	510	508	8
2	−1	−7	163	164	3	2	−10	−4	177	171	4	2	3	−2	329	311	4
2	0	−7	155	142	5	2	−9	−4	62	65	2	2	4	−2	162	169	3
2	1	−7	72	77	2	2	−7	−4	78	63	2	2	5	−2	323	312	5
2	2	−7	99	92	2	2	−6	−4	62	53	3	2	6	−2	180	191	5
2	3	−7	153	145	3	2	−5	−4	492	470	5	2	7	−2	91	93	2
2	4	−7	179	187	3	2	−4	−4	349	383	2	2	9	−2	41	44	5
2	5	−7	64	68	4	2	−3	−4	233	204	2	2	11	−2	60	62	5
2	6	−7	96	96	3	2	−2	−4	170	163	2	2	−11	−1	74	72	4

Table 91 — continued

H	K	L	F_{obs}	F_{calc}	SigF	H	K	L	F_{obs}	F_{calc}	SigF	H	K	L	F_{obs}	F_{calc}	SigF
2	−8	−1	64	59	2	2	5	1	146	137	5	2	−7	4	59	55	3
2	−7	−1	195	200	5	2	6	1	367	361	3	2	−5	4	89	92	2
2	−6	−1	224	267	2	2	7	1	286	242	5	2	−4	4	283	285	5
2	−5	−1	331	282	3	2	8	1	71	97	3	2	−3	4	166	161	5
2	−3	−1	846	878	5	2	12	1	76	75	4	2	−2	4	203	210	5
2	−2	−1	803	769	6	2	2	−9	2	53	55	2	−1	4	153	123	3
2	−1	−1	350	336	2	2	−7	2	88	76	2	2	0	4	288	327	11
2	0	−1	73	70	2	2	−5	2	241	256	9	2	1	4	558	499	9
2	1	−1	192	171	3	2	−4	2	114	137	2	2	2	4	931	956	13
2	2	−1	429	398	8	2	−3	2	189	190	3	2	3	4	151	151	3
2	3	−1	717	683	15	2	−2	2	241	223	3	2	4	4	222	204	6
2	4	−1	217	221	3	2	−1	2	258	235	7	2	5	4	368	397	9
2	5	−1	76	77	2	2	0	2	40	35	2	2	6	4	36	16	4
2	6	−1	277	283	3	2	1	2	135	147	4	2	9	4	183	171	2
2	7	−1	183	158	7	2	2	2	228	208	5	2	10	4	247	246	2
2	8	−1	95	104	2	2	3	2	274	283	6	2	11	4	148	152	4
2	−10	0	74	71	4	2	4	2	367	358	6	2	−7	5	67	66	4
2	−7	0	85	63	2	2	5	2	391	396	7	2	−6	5	123	124	4
2	−6	0	148	139	3	2	7	2	63	51	2	2	−4	5	83	83	3
2	−5	0	88	93	2	2	8	2	241	232	3	2	−3	5	276	263	3
2	−4	0	361	380	3	2	9	2	84	70	5	2	−2	5	144	177	4
2	−2	0	842	790	3	2	10	2	89	99	2	2	−1	5	159	113	4
2	−1	0	33	61	5	2	11	2	57	59	5	2	1	5	177	180	3
2	0	0	544	510	8	2	−8	3	64	68	3	2	2	5	265	314	4
2	2	0	584	573	9	2	−7	3	71	65	2	2	3	5	383	358	8
2	4	0	444	450	9	2	−6	3	166	178	5	2	4	5	246	273	6
2	5	0	312	299	3	2	−5	3	211	211	3	2	5	5	332	322	8
2	6	0	252	295	4	2	−4	3	132	128	5	2	6	5	464	419	6
2	7	0	128	120	3	2	−3	3	281	237	7	2	7	5	92	114	3
2	8	0	93	92	4	2	−2	3	103	127	3	2	8	5	143	135	4
2	10	0	39	47	5	2	−1	3	87	68	2	2	9	5	249	232	2
2	11	0	75	71	4	2	0	3	54	60	2	2	10	5	213	213	2
2	12	0	48	36	6	2	1	3	362	372	8	2	11	5	60	60	3
2	−7	1	99	110	2	2	2	3	104	111	2	2	12	5	58	66	5
2	−6	1	126	147	3	2	3	3	265	263	3	2	−6	6	85	77	2
2	−5	1	266	239	3	2	5	3	189	179	3	2	−5	6	123	125	3
2	−4	1	160	152	4	2	6	3	272	259	7	2	−4	6	143	134	3
2	−3	1	503	496	5	2	8	3	60	78	3	2	−2	6	57	44	3
2	−2	1	412	397	7	2	9	3	140	118	3	2	0	6	275	311	6
2	−1	1	201	188	4	2	11	3	44	39	5	2	1	6	443	382	7
2	1	1	554	529	4	2	12	3	64	71	4	2	2	6	261	314	5
2	2	1	469	431	15	2	13	3	67	61	7	2	3	6	99	90	3
2	3	1	336	341	11	2	−9	4	48	44	6	2	4	6	168	155	3
2	4	1	92	102	2	2	−8	4	54	53	5	2	5	6	628	609	12

Table 91 — continued

H	K	L	F_{obs}	F_{calc}	SigF	H	K	L	F_{obs}	F_{calc}	SigF	H	K	L	F_{obs}	F_{calc}	SigF
2	6	6	32	40	5	2	0	9	130	104	2	2	3	12	38	38	5
2	10	6	178	176	3	2	1	9	75	79	2	2	4	12	71	76	3
2	11	6	208	195	7	2	2	9	86	89	2	2	5	12	82	91	3
2	12	6	73	74	4	2	3	9	388	398	6	2	7	12	75	76	3
2	14	6	44	30	6	2	4	9	248	251	4	2	8	12	83	86	2
2	−7	7	53	60	6	2	6	9	62	68	4	2	10	12	82	71	3
2	−6	7	115	121	3	2	7	9	73	83	2	2	11	12	73	64	4
2	−4	7	174	175	3	2	8	9	139	124	3	2	0	13	83	81	4
2	−3	7	117	115	2	2	9	9	129	135	3	2	2	13	69	66	4
2	−2	7	133	140	3	2	10	9	81	77	8	2	3	13	103	112	3
2	−1	7	222	211	5	2	11	9	56	52	3	2	4	13	93	88	3
2	0	7	322	314	8	2	12	9	105	107	3	2	8	13	66	69	4
2	1	7	106	95	2	2	13	9	79	75	4	2	9	13	88	90	3
2	2	7	219	239	5	2	−4	10	78	82	4	2	10	13	45	48	5
2	3	7	326	306	6	2	−3	10	91	91	3	2	11	13	52	57	5
2	4	7	464	474	4	2	−1	10	46	43	4	2	12	13	67	68	4
2	5	7	104	120	2	2	0	10	87	91	2	2	2	14	71	70	4
2	6	7	113	106	3	2	1	10	90	103	2	2	6	14	78	73	3
2	7	7	171	153	3	2	2	10	137	114	2	2	7	14	76	78	4
2	8	7	110	101	2	2	3	10	117	105	3	2	8	14	75	63	4
2	9	7	118	117	2	2	4	10	236	218	2	2	10	14	85	90	4
2	10	7	231	215	2	2	5	10	146	155	3	2	11	14	74	71	4
2	12	7	62	74	4	2	6	10	95	89	2	2	8	15	67	71	4
2	13	7	77	74	4	2	8	10	38	37	3	3	−7	−12	102	100	3
2	−5	8	165	171	4	2	9	10	102	108	2	3	−6	−12	64	58	5
2	−4	8	202	197	3	2	10	10	140	136	5	3	−2	−12	103	102	3
2	0	8	79	89	3	2	11	10	81	89	3	3	−1	−12	111	115	3
2	1	8	238	227	6	2	12	10	48	33	5	3	−9	−11	130	130	3
2	2	8	342	362	4	2	13	10	49	50	6	3	−8	−11	87	92	4
2	3	8	58	62	3	2	−2	11	45	51	6	3	−6	−11	77	81	4
2	4	8	299	298	5	2	−1	11	70	72	4	3	−5	−11	105	102	3
2	5	8	261	276	5	2	0	11	75	71	3	3	−3	−11	124	128	3
2	6	8	199	194	3	2	2	11	95	100	5	3	−2	−11	112	112	3
2	7	8	64	53	3	2	3	11	112	116	2	3	0	−11	94	91	3
2	8	8	85	89	3	2	5	11	85	77	2	3	1	−11	80	81	4
2	10	8	115	110	2	2	8	11	118	118	5	3	−10	−10	62	60	5
2	11	8	72	69	3	2	9	11	89	87	2	3	−8	−10	113	99	3
2	12	8	90	91	3	2	10	11	56	57	3	3	−7	−10	182	187	3
2	13	8	48	49	6	2	11	11	66	71	4	3	−6	−10	75	72	3
2	−5	9	42	41	6	2	12	11	99	104	3	3	−1	−10	155	153	3
2	−4	9	57	47	5	2	13	11	61	55	5	3	0	−10	57	59	4
2	−3	9	140	135	7	2	−2	12	50	48	5	3	1	−10	54	48	5
2	−2	9	149	144	3	2	1	12	112	119	3	3	2	−10	77	77	4
2	−1	9	87	93	2	2	2	12	126	121	4	3	3	−10	53	49	5

Table 91 — continued

H	K	L	F_{obs}	F_{calc}	SigF	H	K	L	F_{obs}	F_{calc}	SigF	H	K	L	F_{obs}	F_{calc}	SigF
3	−10	−9	57	52	5	3	−2	−6	344	331	6	3	−6	−3	78	72	2
3	−9	−9	120	126	3	3	−1	−6	265	275	3	3	−5	−3	208	199	3
3	−8	−9	119	117	3	3	1	−6	233	217	4	3	−4	−3	274	304	3
3	−6	−9	87	86	6	3	2	−6	240	234	2	3	−3	−3	471	464	5
3	−5	−9	79	79	3	3	3	−6	122	114	2	3	−2	−3	274	285	5
3	−3	−9	89	77	2	3	4	−6	96	99	2	3	−1	−3	139	141	5
3	−2	−9	40	39	4	3	5	−6	99	103	4	3	0	−3	472	478	11
3	−1	−9	33	29	5	3	6	−6	53	45	5	3	1	−3	92	107	11
3	0	−9	94	95	5	3	7	−6	83	92	4	3	2	−3	113	99	3
3	1	−9	169	155	8	3	−10	−5	79	78	4	3	4	−3	73	70	2
3	3	−9	59	55	5	3	−9	−5	160	161	3	3	5	−3	127	111	4
3	4	−9	80	80	4	3	−8	−5	55	46	2	3	6	−3	140	137	3
3	−10	−8	65	61	4	3	−7	−5	85	83	2	3	7	−3	852	88	4
3	−8	−8	147	137	3	3	−6	−5	156	147	2	3	9	−3	90	83	3
3	−7	−8	187	183	3	3	−5	−5	47	36	4	3	10	−3	70	73	5
3	−6	−8	58	62	2	3	−4	−5	85	106	7	3	−11	−2	103	106	3
3	−5	−8	69	68	2	3	−3	−5	139	138	3	3	−10	−2	86	80	8
3	−4	−8	44	45	3	3	−1	5	204	187	6	3	−8	−2	140	132	3
3	−3	−8	98	90	2	3	0	−5	642	629	12	3	−7	−2	113	109	6
3	−2	−8	73	77	2	3	1	−5	145	148	8	3	−6	−2	88	96	2
3	0	−8	38	41	3	3	3	−5	36	38	3	3	−5	−2	158	131	4
3	1	−8	105	99	5	3	4	−5	42	31	3	3	−4	−2	64	79	3
3	2	−8	148	143	4	3	6	−5	121	120	6	3	−3	−2	72	81	3
3	3	−8	106	116	3	3	−11	−4	80	89	4	3	−2	−2	474	504	4
3	−10	−7	59	53	4	3	−10	−4	85	87	3	3	−1	−2	392	378	8
3	−9	−7	131	133	2	3	−8	−4	129	112	2	3	0	−2	116	104	3
3	−8	−7	105	102	2	3	−7	−4	78	65	2	3	1	−2	182	174	4
3	−7	−7	63	65	2	3	−5	−4	45	35	3	3	2	−2	280	297	4
3	−4	−7	73	76	2	3	−4	−4	112	122	4	3	3	−2	104	100	2
3	−3	−7	160	156	2	3	−3	−4	68	60	2	3	4	−2	262	270	7
3	−2	−7	142	136	3	3	−2	−4	216	257	4	3	5	−2	217	209	4
3	−1	−7	273	259	2	3	−1	−4	354	338	7	3	7	−2	38	39	3
3	0	−7	243	240	2	3	0	−4	153	129	2	3	8	−2	168	169	3
3	1	−7	211	202	2	3	1	−4	132	119	3	3	9	−2	95	89	3
3	2	−7	66	67	2	3	2	−4	146	168	3	3	−10	−1	108	108	3
3	5	−7	59	59	5	3	3	−4	53	62	3	3	−9	−1	124	120	3
3	6	−7	74	75	4	3	4	−4	179	191	3	3	−8	−1	63	74	3
3	−11	−6	69	62	4	3	5	−4	167	166	3	3	−6	−1	38	26	5
3	−8	−6	215	204	3	3	7	−4	84	82	2	3	−5	−1	245	240	2
3	−7	−6	113	118	2	3	8	−4	118	118	3	3	−4	−1	263	296	2
3	−6	−6	39	34	3	3	9	−4	57	57	5	3	−3	−1	336	299	4
3	−5	−6	64	71	2	3	−10	−3	104	107	4	3	−2	−1	234	248	2
3	−4	−6	48	44	3	3	−9	−3	217	212	3	3	−1	−1	319	306	7
3	−3	−6	91	88	2	3	−8	−3	71	75	2	3	0	−1	722	730	13

Table 91 — continued

H	K	L	F_{obs}	F_{calc}	SigF	H	K	L	F_{obs}	F_{calc}	SigF	H	K	L	F_{obs}	F_{calc}	SigF
3	1	−1	246	223	3	3	−5	2	247	245	4	3	4	4	182	195	3
3	2	−1	227	216	4	3	−4	2	170	168	3	3	5	4	287	284	9
3	4	−1	62	62	5	3	−3	2	126	121	4	3	7	4	256	271	7
3	5	−1	324	318	4	3	−2	2	230	282	5	3	8	4	206	218	3
3	6	−1	299	319	3	3	−1	2	389	366	6	3	9	4	52	51	2
3	7	−1	195	189	6	3	1	2	133	108	3	3	13	4	74	73	6
3	8	−1	66	68	2	3	2	2	256	224	6	3	−5	5	63	65	2
3	9	−1	50	45	4	3	3	2	164	160	3	3	−4	5	80	74	2
3	10	−1	77	82	9	3	4	2	391	371	11	3	−3	5	290	293	7
3	−8	0	85	85	4	3	5	2	485	426	12	3	−2	5	88	119	3
3	−7	0	101	97	2	3	6	2	33	33	4	3	−1	5	347	293	7
3	−6	0	112	121	2	3	7	2	254	243	7	3	0	5	330	374	6
3	−4	0	127	130	2	3	8	2	169	186	3	3	1	5	312	258	4
3	−3	0	388	403	6	3	9	2	123	127	4	3	2	5	72	79	2
3	−2	0	500	519	5	3	11	2	47	36	6	3	3	5	286	286	8
3	−1	0	547	532	7	3	12	2	47	46	6	3	4	5	71	63	4
3	0	0	69	67	3	3	−9	3	72	63	4	3	5	5	264	290	5
3	1	0	602	615	13	3	−8	3	59	56	5	3	6	5	292	299	7
3	2	0	228	227	6	3	−7	3	59	54	4	3	7	5	124	129	3
3	3	0	412	401	10	3	−6	3	47	54	3	3	8	5	145	128	4
3	4	0	364	331	9	3	−4	3	289	287	5	3	9	5	132	128	2
3	5	0	176	180	3	3	−3	3	273	286	3	3	10	5	175	177	3
3	6	0	211	207	3	3	−2	3	91	109	3	3	11	5	75	79	6
3	7	0	219	204	4	3	−1	3	362	344	10	3	12	5	79	81	4
3	8	0	121	126	2	3	0	3	81	46	4	3	−6	6	76	69	3
3	−10	1	71	71	5	3	1	3	194	162	6	3	−4	6	58	53	2
3	−9	1	853	82	3	3	2	3	348	347	11	3	−3	6	29	27	4
3	−7	1	51	39	7	3	4	3	251	245	7	3	−2	6	216	224	3
3	−6	1	97	85	3	3	6	3	221	245	6	3	−1	6	133	130	3
3	−5	1	58	65	3	3	7	3	251	242	9	3	0	6	102	97	2
3	−4	1	39	44	4	3	8	3	224	213	7	3	1	6	164	156	4
3	−3	1	280	264	3	3	9	3	135	124	2	3	2	6	162	164	3
3	−2	1	72	72	2	3	12	3	45	48	6	3	3	6	167	162	7
3	−1	1	264	269	6	3	−8	4	49	53	5	3	4	6	219	229	5
3	0	1	334	326	12	3	−7	4	46	44	4	3	5	6	73	70	2
3	1	1	420	402	9	3	−6	4	46	49	4	3	6	6	270	249	7
3	3	1	59	52	2	3	−5	4	270	269	8	3	7	6	198	237	7
3	5	1	391	376	10	3	−4	4	139	130	3	3	8	6	149	137	3
3	6	1	279	305	6	3	−3	4	113	85	2	3	9	6	89	81	2
3	7	1	214	221	4	3	−2	4	282	317	6	3	10	6	84	87	2
3	8	1	51	49	2	3	−1	4	160	164	5	3	13	6	56	55	5
3	−8	2	50	56	6	3	0	4	399	357	7	3	−5	7	52	54	5
3	−7	2	74	69	3	3	2	4	166	184	5	3	−4	7	120	115	9
3	−6	2	148	166	4	3	3	4	193	192	10	3	−3	7	75	85	2

Table 91 — continued

H	K	L	F_{obs}	F_{calc}	SigF	H	K	L	F_{obs}	F_{calc}	SigF	H	K	L	F_{obs}	F_{calc}	SigF
3	−1	7	45	33	4	3	12	9	105	109	3	4	−6	−11	97	95	3
3	0	7	149	157	6	3	−3	10	70	70	4	4	−4	−11	48	56	6
3	1	7	280	258	8	3	−2	10	102	97	3	4	−3	−11	71	65	4
3	2	7	277	293	4	3	1	10	72	67	2	4	−2	−11	114	109	3
3	3	7	239	228	5	3	3	10	123	135	2	4	−1	−11	146	153	3
3	4	7	54	58	3	3	4	10	285	265	2	4	−8	−10	92	86	3
3	5	7	408	407	9	3	6	10	75	80	2	4	−6	−10	86	81	3
3	6	7	276	281	8	3	7	10	200	198	2	4	−5	−10	181	184	3
3	7	7	90	96	5	3	8	10	77	77	2	4	−4	−10	78	82	4
3	9	7	62	66	2	3	9	10	48	52	3	4	−3	−10	61	64	4
3	10	7	86	80	2	3	10	10	107	107	3	4	−2	−10	99	113	3
3	11	7	135	129	5	3	12	10	52	50	5	4	0	−10	41	48	7
3	12	7	96	101	3	3	13	10	103	94	3	4	1	−10	70	75	4
3	−6	8	64	62	5	3	2	11	119	109	3	4	−7	−9	145	149	3
3	−5	8	60	64	5	3	3	11	50	60	3	4	−6	−9	174	180	4
3	−3	8	180	178	7	3	4	11	126	127	2	4	−4	−9	65	72	4
3	−2	8	186	169	3	3	5	11	182	181	3	4	−3	−9	60	52	3
3	−1	8	86	92	2	3	6	11	169	152	3	4	−1	−9	78	79	4
3	0	8	74	61	2	3	7	11	48	41	3	4	0	−9	108	103	3
3	2	8	151	157	6	3	10	11	39	41	5	4	2	−9	50	50	5
3	3	8	269	295	5	3	11	11	57	55	4	4	3	−9	91	90	3
3	4	8	499	501	7	3	12	11	85	89	3	4	−9	−8	69	74	4
3	5	8	189	198	4	3	1	12	59	60	4	4	−8	−8	96	97	3
3	6	8	80	89	2	3	3	12	129	134	8	4	−7	−8	131	129	3
3	7	8	178	187	4	3	4	12	193	181	3	4	−6	−8	53	51	4
3	8	8	121	103	2	3	5	12	81	80	2	4	−5	−8	184	181	6
3	10	8	109	111	2	3	7	12	50	56	6	4	−4	−8	64	70	3
3	13	8	74	77	4	3	8	12	50	36	3	4	−3	−8	60	67	8
3	14	8	56	53	5	3	10	12	68	74	4	4	1	−8	165	160	8
3	−5	9	52	54	5	3	11	12	48	46	5	4	2	−8	93	99	3
3	−4	9	146	148	3	3	1	13	58	52	5	4	4	−8	90	91	4
3	−3	9	49	43	5	3	2	13	123	125	3	4	5	−8	81	79	4
3	−1	9	105	94	2	3	3	13	79	73	3	4	−7	−7	202	209	4
3	0	9	165	155	3	3	5	13	153	156	3	4	−6	−7	177	175	3
3	1	9	66	73	2	3	6	13	174	185	3	4	−4	−7	79	72	2
3	2	9	139	123	2	3	7	13	86	89	3	4	−3	−7	115	93	2
3	3	9	136	141	5	3	8	13	57	65	4	4	−2	−7	45	45	3
3	4	9	63	53	4	3	11	13	43	45	6	4	−1	−7	84	82	2
3	5	9	300	313	8	3	12	13	69	71	4	4	0	−7	41	41	3
3	6	9	244	247	6	3	3	14	90	92	3	4	2	−7	113	112	5
3	8	9	65	66	2	3	4	14	120	115	3	4	3	−7	118	113	4
3	9	9	61	57	2	3	5	14	91	90	3	4	4	−7	42	35	6
3	10	9	107	115	2	3	5	15	47	45	6	4	−8	−6	132	143	3
3	11	9	104	101	2	4	−7	−11	97	95	3	4	−7	−6	64	70	7

Table 91 — continued

H	K	L	F_{obs}	F_{calc}	SigF	H	K	L	F_{obs}	F_{calc}	SigF	H	K	L	F_{obs}	F_{calc}	SigF
4	−6	−6	87	73	2	4	−5	−3	97	82	2	4	6	−1	59	58	2
4	−5	−6	113	110	2	4	−3	−3	48	55	3	4	8	−1	190	196	4
4	−3	−6	56	41	2	4	−2	−3	75	79	2	4	9	−1	192	198	4
4	−1	−6	49	43	2	4	−1	−3	179	192	3	4	10	−1	53	52	6
4	0	−6	144	141	3	4	0	−3	322	314	10	4	−9	0	104	99	3
4	1	−6	253	239	2	4	1	−3	74	105	3	4	−8	0	70	74	3
4	2	−6	153	139	3	4	2	−3	271	292	7	4	−6	0	201	199	2
4	4	−6	77	76	3	4	3	−3	124	138	5	4	−5	0	159	153	2
4	5	−6	82	81	3	4	4	−3	64	68	3	4	−3	0	244	215	5
4	6	−6	43	46	6	4	5	−3	144	139	3	4	−2	0	310	289	3
4	7	−6	41	39	7	4	6	−3	35	31	3	4	−1	0	89	86	2
4	−9	−5	58	65	5	4	7	−3	61	70	3	4	0	0	452	490	8
4	−8	−5	47	40	4	4	8	−3	154	154	4	4	1	0	314	267	13
4	−7	−5	208	212	3	4	9	−3	78	79	4	4	2	0	172	176	6
4	−6	−5	96	106	2	4	−9	−2	137	140	3	4	3	0	199	182	2
4	−5	−5	44	36	3	4	−8	−2	110	114	3	4	4	0	348	341	9
4	−4	−5	55	44	2	4	−7	−2	31	20	4	4	5	0	333	295	6
4	−3	−5	57	66	6	4	−6	−2	139	125	3	4	6	0	177	185	4
4	−2	−5	68	70	3	4	−5	−2	234	237	5	4	7	0	189	188	6
4	−1	−5	144	159	3	4	−4	−2	267	289	3	4	8	0	108	115	2
4	0	−5	130	125	3	4	−3	−2	196	180	5	4	10	0	148	147	3
4	2	−5	190	180	2	4	−2	−2	163	168	3	4	11	0	63	65	5
4	3	−5	203	199	2	4	0	−2	530	531	8	4	−8	1	53	53	5
4	4	−5	42	43	3	4	1	−2	371	369	6	4	−7	1	139	138	5
4	6	−5	42	35	6	4	2	−2	267	247	6	4	−6	1	116	109	8
4	7	−5	69	65	4	4	3	−2	200	172	5	4	−5	1	112	112	5
4	−9	−4	72	78	4	4	4	−2	145	147	4	4	−4	1	71	67	3
4	−8	−4	157	165	4	4	5	−2	57	52	2	4	−3	1	40	24	3
4	−6	−4	106	94	2	4	6	−2	122	113	2	4	−2	1	158	189	3
4	−5	−4	104	104	2	4	7	−2	99	99	2	4	−1	1	490	447	12
4	−4	−4	114	113	2	4	9	−2	102	97	3	4	0	1	536	535	11
4	−3	−4	128	129	3	4	10	−2	106	115	3	4	1	1	224	202	4
4	−1	−4	148	159	6	4	−10	−1	71	67	4	4	2	1	326	355	9
4	0	−4	181	176	4	4	−8	−1	111	104	2	4	3	1	125	118	3
4	1	−4	212	227	3	4	−7	−1	128	124	3	4	4	1	251	236	9
4	2	−4	157	135	3	4	−4	−1	149	130	3	4	5	1	55	56	5
4	4	−4	103	99	2	4	−3	−1	74	55	3	4	6	1	82	81	2
4	6	−4	60	60	4	4	−2	−1	269	283	2	4	8	1	133	132	5
4	8	−4	43	56	6	4	−1	−1	411	378	4	4	9	1	109	109	5
4	−10	−3	60	62	5	4	0	−1	140	148	6	4	−9	2	75	68	4
4	−9	−3	88	87	3	4	2	−1	443	463	11	4	−8	2	69	68	4
4	−8	−3	108	107	3	4	3	−1	186	181	6	4	−7	2	51	48	4
4	−7	−3	125	118	2	4	4	−1	107	115	3	4	−6	2	102	100	5
4	−6	−3	167	171	3	4	5	−1	65	79	4	4	−5	2	241	244	7

Table 91 — continued

H	K	L	F_{obs}	F_{calc}	SigF	H	K	L	F_{obs}	F_{calc}	SigF	H	K	L	F_{obs}	F_{calc}	SigF
4	−4	2	71	65	2	4	−7	5	90	85	3	4	−3	8	103	104	5
4	−3	2	207	218	6	4	−5	5	86	89	2	4	−2	8	87	90	2
4	−2	2	299	264	5	4	−4	5	164	149	3	4	−1	8	67	55	2
4	−1	2	262	271	5	4	−3	5	81	90	2	4	0	8	222	232	2
4	1	2	400	360	10	4	−2	5	134	148	4	4	1	8	166	171	2
4	3	2	55	48	2	4	−1	5	406	394	7	4	2	8	134	134	6
4	4	2	95	81	4	4	1	5	74	55	2	4	3	8	71	71	4
4	5	2	188	182	6	4	2	5	51	56	3	4	4	8	99	101	5
4	6	2	156	147	6	4	3	5	103	113	4	4	6	8	333	326	12
4	7	2	265	265	80	4	5	5	39	56	6	4	7	8	178	186	2
4	8	2	80	79	3	4	6	5	165	162	8	4	8	8	41	39	3
4	−7	3	106	106	3	4	7	5	217	237	4	4	9	8	161	162	3
4	−6	3	154	152	4	4	8	5	320	299	2	4	10	8	161	158	9
4	−5	3	113	131	4	4	9	5	130	117	2	4	11	8	43	45	4
4	−4	3	84	70	3	4	10	5	54	47	3	4	12	8	80	86	3
4	−3	3	130	110	3	4	11	5	74	65	3	4	−2	9	128	120	2
4	−2	3	92	104	6	4	−4	6	66	59	3	4	−1	9	116	124	4
4	−1	3	530	540	15	4	−3	6	154	159	3	4	0	9	52	36	2
4	0	3	417	407	6	4	−2	6	184	158	2	4	1	9	100	93	2
4	1	3	74	73	10	4	0	6	216	246	7	4	2	9	224	207	2
4	3	3	213	219	5	4	1	6	288	274	6	4	4	9	852	70	2
4	4	3	281	265	11	4	2	6	101	97	2	4	5	9	152	166	2
4	5	3	279	261	13	4	4	6	38	47	4	4	7	9	150	148	3
4	6	3	94	97	2	4	6	6	295	274	12	4	8	9	252	243	2
4	7	3	101	104	6	4	7	6	304	309	6	4	9	9	103	104	2
4	8	3	233	235	50	4	9	6	94	93	2	4	−3	10	76	74	4
4	9	3	75	73	5	4	10	6	133	125	3	4	0	10	62	53	4
4	11	3	64	59	6	4	12	6	52	53	5	4	1	10	74	82	4
4	−8	4	71	70	4	4	−6	7	58	52	5	4	3	10	64	58	2
4	−6	4	48	51	4	4	−5	7	59	56	5	4	5	10	63	70	2
4	−4	4	176	171	3	4	−3	7	53	62	4	4	6	10	109	91	2
4	−3	4	219	230	8	4	−2	7	197	190	3	4	7	10	74	72	2
4	−2	4	163	127	5	4	−1	7	210	206	2	4	9	10	134	144	4
4	−1	4	121	90	7	4	0	7	74	69	3	4	10	10	131	132	4
4	0	4	283	309	7	4	1	7	56	61	4	4	11	10	57	67	4
4	1	4	136	136	4	4	2	7	198	199	9	4	12	10	58	55	5
4	2	4	45	58	4	4	3	7	120	125	5	4	−2	11	68	61	4
4	3	4	56	62	4	4	4	7	81	73	4	4	−1	11	41	44	6
4	4	4	76	69	2	4	5	7	209	230	4	4	0	11	68	63	4
4	5	4	49	65	5	4	6	7	166	147	6	4	4	11	136	121	5
4	6	4	140	120	6	4	7	7	159	160	4	4	6	11	40	49	4
4	7	4	286	289	6	4	8	7	237	215	2	4	7	11	120	118	4
4	10	4	66	75	9	4	9	7	80	86	2	4	8	11	150	148	5
4	9	4	92	97	2	4	−4	8	53	57	5	4	9	11	67	61	5

Table 91 — continued

H	K	L	F_{obs}	F_{calc}	SigF	H	K	L	F_{obs}	F_{calc}	SigF	H	K	L	F_{obs}	F_{calc}	SigF
4	0	12	45	48	6	5	−6	−6	154	158	3	5	8	−3	42	54	7
4	3	12	841	84	3	5	−5	−6	125	121	5	5	−7	−2	78	84	4
4	5	12	163	165	7	5	−4	−6	60	54	3	5	−6	−2	166	170	3
4	6	12	210	202	7	5	−3	−6	126	128	4	5	−5	−2	195	192	6
4	7	12	115	113	5	5	−2	−6	131	130	9	5	−3	−2	216	201	2
4	4	13	166	167	3	5	−1	−6	98	98	2	5	−2	−2	146	139	5
4	5	13	153	154	2	5	1	−6	60	62	3	5	0	−2	129	111	3
4	6	13	58	56	5	5	3	−6	146	138	2	5	1	−2	135	161	3
4	7	13	117	123	3	5	4	−6	86	83	3	5	2	−2	129	131	3
4	8	13	110	109	3	5	−7	−5	163	161	3	5	3	−2	274	260	7
4	9	13	39	45	6	5	−6	−5	41	45	6	5	4	−2	166	160	5
4	3	14	39	32	6	5	−5	−5	104	104	4	5	5	−2	79	85	3
4	5	14	75	75	4	5	−4	−5	86	83	2	5	7	−2	62	65	3
4	6	14	181	181	4	5	−3	−5	108	105	2	5	8	−2	126	131	3
4	7	14	134	132	3	5	1	−5	144	142	3	5	9	−2	70	70	5
4	8	14	46	30	6	5	2	−5	215	208	9	5	−8	−1	87	92	3
4	9	14	47	49	6	5	3	−5	133	128	3	5	−4	−1	244	249	2
4	7	15	48	43	6	5	5	−5	116	116	3	5	−3	−1	112	113	3
5	−5	−10	87	79	4	5	6	−5	58	65	5	5	−2	−1	209	209	4
5	−3	−10	110	118	3	5	−8	−4	62	59	5	5	−1	−1	111	106	2
5	−2	−10	101	102	3	5	−7	−4	112	125	5	5	0	−1	253	269	7
5	−1	−10	104	102	3	5	−6	−4	247	256	9	5	1	−1	239	256	6
5	−5	−9	101	101	3	5	−5	−4	185	170	3	5	2	−1	366	339	10
5	−4	−9	154	163	3	5	−3	−4	95	87	2	5	4	−1	270	262	4
5	−3	−9	59	62	5	5	−2	−4	65	64	2	5	5	−1	101	100	7
5	0	−9	50	45	6	5	−1	−4	61	71	2	5	6	−1	69	70	2
5	−6	−8	117	118	3	5	0	−4	100	93	4	5	7	−1	70	73	3
5	−5	−8	121	123	3	5	1	−4	94	99	2	5	9	−1	66	59	5
5	−3	−8	110	112	3	5	2	−4	52	49	3	5	10	−1	88	88	6
5	−2	−8	102	99	3	5	3	−4	149	149	3	5	−7	0	62	62	4
5	−1	−8	83	88	4	5	4	−4	156	154	5	5	−4	0	66	61	2
5	3	−8	72	76	4	5	5	−4	66	64	4	5	−3	0	202	192	4
5	−7	−7	71	69	4	5	6	−4	71	59	4	5	−1	0	127	104	4
5	−6	−7	60	61	5	5	7	−4	56	47	5	5	0	0	121	133	2
5	−5	−7	134	139	2	5	−8	−3	83	84	4	5	2	0	179	185	5
5	−4	−7	127	126	3	5	−7	−3	201	199	3	5	3	0	317	317	10
5	−3	−7	89	80	4	5	−5	−3	157	166	6	5	4	0	106	107	3
5	−1	−7	101	98	3	5	−4	−3	148	150	3	5	8	0	97	95	2
5	0	−7	59	68	3	5	−3	−3	150	153	4	5	9	0	120	125	3
5	1	−7	86	84	3	5	−2	−3	106	90	2	5	10	0	89	96	5
5	2	−7	114	121	3	5	1	−3	234	248	8	5	−8	1	88	83	4
5	4	−7	68	68	5	5	2	−3	211	196	3	5	−7	1	60	62	5
5	5	−7	102	100	3	5	3	−3	222	226	3	5	−6	1	54	49	4
5	−7	−6	47	51	5	5	5	−3	58	60	4	5	−5	1	109	120	2

Table 91 — continued

H	K	L	F_{obs}	F_{calc}	SigF	H	K	L	F_{obs}	F_{calc}	SigF	H	K	L	F_{obs}	F_{calc}	SigF
5	−4	1	162	156	3	5	−6	4	125	125	3	5	8	6	160	144	3
5	−2	1	109	100	2	5	−5	4	71	79	4	5	9	6	155	153	3
5	−1	1	140	140	4	5	−4	4	63	73	3	5	10	6	113	114	8
5	0	1	195	204	3	5	−3	4	46	41	6	5	12	6	75	73	4
5	1	1	257	243	4	5	−2	4	119	115	4	5	13	6	60	46	5
5	2	1	405	397	14	5	−1	4	217	231	8	5	−5	7	54	52	5
5	4	1	249	250	9	5	0	4	249	231	8	5	−4	7	62	63	4
5	5	1	222	208	8	5	1	4	153	160	4	5	−3	7	56	63	3
5	6	1	155	146	4	5	2	4	196	191	6	5	−2	7	78	68	3
5	7	1	90	84	3	5	3	4	282	301	8	5	0	7	187	190	2
5	10	1	107	114	3	5	4	4	225	216	7	5	1	7	298	295	2
5	11	1	99	94	4	5	6	4	87	95	5	5	2	7	241	228	2
5	−7	2	46	47	6	5	8	4	132	117	2	5	3	7	199	189	7
5	−6	2	128	119	5	5	9	4	203	205	3	5	5	7	151	163	8
5	−5	2	67	71	7	5	10	4	74	76	4	5	6	7	89	77	2
5	−4	2	228	230	5	5	−7	5	68	71	5	5	7	7	202	222	2
5	−3	2	89	81	5	5	−5	5	94	88	3	5	8	7	118	111	2
5	−2	2	49	61	4	5	−4	5	74	62	3	5	10	7	88	74	3
5	−1	2	233	212	6	5	−3	5	76	88	2	5	11	7	91	84	3
5	0	2	234	260	6	5	−2	5	36	14	3	5	−2	8	72	73	3
5	1	2	253	228	7	5	−1	5	92	124	2	5	−1	8	141	152	3
5	2	2	205	199	5	5	0	5	73	83	3	5	0	8	165	152	3
5	3	2	288	290	9	5	1	5	394	376	14	5	2	8	160	149	3
5	4	2	275	283	8	5	2	5	156	153	7	5	3	8	175	182	2
5	5	2	63	65	5	5	4	5	96	106	5	5	4	8	187	170	2
5	7	2	61	50	2	5	5	5	204	207	11	5	5	8	78	89	2
5	9	2	97	103	3	5	6	5	71	53	3	5	6	8	219	201	2
5	10	2	89	79	3	5	7	5	106	110	2	5	8	8	175	160	3
5	−8	3	60	56	5	5	8	5	184	175	3	5	9	8	103	108	6
5	−7	3	55	61	5	5	9	5	56	56	3	5	10	8	79	69	4
5	−5	3	185	190	7	5	10	5	93	86	5	5	12	8	59	55	5
5	−4	3	161	143	5	5	11	5	59	68	5	5	−2	9	51	50	5
5	−3	3	51	63	3	5	12	5	47	39	6	5	−1	9	48	41	5
5	−2	3	103	91	4	5	−6	6	105	103	3	5	0	9	144	145	6
5	1	3	319	297	19	5	−2	6	67	70	2	5	1	9	189	192	7
5	2	3	428	432	15	5	−1	6	146	152	3	5	2	9	182	170	3
5	3	3	62	60	9	5	0	6	290	261	2	5	4	9	70	74	2
5	4	3	61	60	7	5	1	6	156	174	7	5	5	9	177	156	3
5	5	3	170	178	15	5	2	6	108	110	7	5	6	9	37	30	3
5	6	3	100	90	6	5	3	6	222	223	10	5	7	9	142	144	3
5	7	3	77	81	2	5	4	6	281	260	10	5	8	9	51	42	3
5	8	3	139	146	5	5	5	6	61	72	4	5	9	9	85	83	3
5	10	3	117	118	3	5	6	6	36	27	5	5	10	9	167	166	8
5	11	3	69	68	5	5	7	6	53	42	2	5	11	9	932	86	3

Table 91 — continued

H	K	L	F_{obs}	F_{calc}	SigF	H	K	L	F_{obs}	F_{calc}	SigF	H	K	L	F_{obs}	F_{calc}	SigF
5	−1	10	58	61	5	6	−2	−7	144	147	4	6	1	−2	75	76	2
5	0	10	123	120	3	6	−1	−7	116	109	3	6	2	−2	158	156	3
5	1	10	48	49	4	6	0	−7	76	76	4	6	3	−2	152	159	3
5	2	10	93	95	6	6	2	−7	46	45	6	6	4	−2	103	99	4
5	3	10	120	122	4	6	−4	−6	121	123	3	6	5	−2	73	78	3
5	4	10	75	73	2	6	−3	−6	142	144	3	6	6	−2	112	111	3
5	5	10	88	76	2	6	−2	−6	65	64	4	6	7	−2	72	66	4
5	6	10	82	76	2	6	0	−6	119	113	3	6	−6	−1	79	85	4
5	8	10	120	120	12	6	1	−6	70	73	4	6	−5	−1	210	203	6
5	9	10	132	131	7	6	−5	−5	106	110	3	6	−4	−1	110	100	3
5	10	10	42	45	6	6	−4	−5	97	97	3	6	−3	−1	39	23	4
5	11	10	51	61	5	6	−2	−5	107	106	6	6	−2	−1	211	216	2
5	12	10	60	53	5	6	−1	−5	207	200	7	6	−1	−1	119	110	2
5	1	11	65	63	4	6	1	−5	44	39	5	6	0	−1	107	106	2
5	2	11	134	135	3	6	3	−5	75	75	4	6	2	−1	79	76	2
5	5	11	67	61	3	6	4	−5	109	110	3	6	3	−1	117	109	3
5	8	11	87	83	3	6	5	−5	53	62	6	6	4	−1	168	158	3
5	10	11	121	120	3	6	−8	−4	57	54	5	6	5	−1	164	167	6
5	11	11	70	72	4	6	−4	−4	122	127	5	6	6	−1	65	65	5
5	0	12	73	72	4	6	−3	−4	172	170	6	6	7	−1	104	99	3
5	1	12	58	54	5	6	−2	−4	159	171	4	6	8	−1	105	99	3
5	2	12	40	52	6	6	0	−4	106	98	3	6	9	−1	57	61	6
5	3	12	63	59	4	6	2	−4	121	123	3	6	−7	0	61	64	5
5	5	12	80	83	3	6	3	−4	169	176	3	6	−4	0	51	54	5
5	8	12	88	89	3	6	5	−4	89	92	4	6	−3	0	239	231	5
5	9	12	117	112	3	6	6	−4	108	103	3	6	−1	0	142	121	3
5	10	12	58	60	5	6	7	−4	48	53	7	6	0	0	64	84	2
5	2	13	59	59	5	6	−6	−3	169	177	3	6	1	0	82	73	2
5	5	13	66	58	4	6	−5	−3	244	247	6	6	2	0	52	50	2
5	6	13	115	121	3	6	−4	−3	86	81	3	6	3	0	122	120	2
5	7	13	110	112	3	6	−2	−3	143	145	3	6	5	0	160	163	3
5	8	13	78	77	4	6	−1	−3	186	183	4	6	6	0	135	135	3
5	10	13	875	92	4	6	1	−3	43	41	3	6	7	0	66	60	3
5	11	13	64	58	5	6	3	−3	105	107	3	6	8	0	46	44	6
5	4	14	56	59	5	6	4	−3	146	146	5	6	−6	1	75	72	4
5	5	14	59	64	5	6	5	−3	118	117	3	6	−5	1	67	62	3
5	8	14	98	98	3	6	7	−3	65	59	6	6	−4	1	128	123	3
5	9	14	108	97	3	6	−7	−2	62	61	5	6	−3	1	53	49	3
6	−4	−8	92	86	4	6	−6	−2	113	113	4	6	−2	1	153	153	3
6	−3	−8	127	122	3	6	−5	−2	68	66	3	6	1	1	68	67	5
6	0	−8	63	60	5	6	−4	−2	167	167	5	6	3	1	113	95	2
6	−5	−7	60	65	5	6	−3	−2	192	195	4	6	4	1	251	243	5
6	−4	−7	76	75	4	6	−1	−2	151	148	4	6	5	1	156	170	3
6	−3	−7	76	88	4	6	0	−2	48	47	3	6	8	1	78	77	3

Table 91 — continued

H	K	L	F_{obs}	F_{calc}	SigF	H	K	L	F_{obs}	F_{calc}	SigF	H	K	L	F_{obs}	F_{calc}	SigF
6	−7	2	69	70	4	6	8	5	62	46	4	6	12	9	49	45	6
6	−4	2	161	147	3	6	9	5	93	109	9	6	1	10	76	71	4
6	−3	2	236	250	9	6	10	5	109	117	3	6	2	10	127	128	3
6	1	2	109	101	6	6	−4	6	122	118	3	6	3	10	106	108	4
6	2	2	193	186	5	6	−3	6	61	72	4	6	5	10	53	53	4
6	3	2	196	196	2	6	2	6	217	202	2	6	8	10	56	54	4
6	5	2	163	161	7	6	3	6	210	201	2	6	11	10	69	74	4
6	6	2	157	145	5	6	4	6	171	157	3	6	12	10	62	60	5
6	7	2	117	116	2	6	5	6	303	296	2	6	0	11	79	84	4
6	8	2	62	66	3	6	6	6	255	234	2	6	1	11	71	75	4
6	11	2	71	77	5	6	7	6	43	43	3	6	3	11	90	77	3
6	−5	3	110	109	3	6	8	6	111	106	8	6	4	11	127	126	3
6	−3	3	134	131	4	6	9	6	136	130	7	6	9	11	56	55	5
6	−2	3	123	104	6	6	10	6	44	38	6	6	10	11	89	89	3
6	−1	3	69	77	2	6	11	6	47	57	6	6	12	11	44	55	3
6	0	3	36	33	3	6	12	6	79	74	4	6	1	12	60	59	5
6	1	3	77	67	6	6	−2	7	105	112	3	6	2	12	118	125	3
6	3	3	116	122	2	6	−1	7	56	69	8	6	3	12	89	85	3
6	7	3	63	67	3	6	0	7	45	30	4	6	6	12	43	38	6
6	8	3	90	88	3	6	1	7	128	133	3	6	7	12	60	54	4
6	10	3	61	68	5	6	2	7	28	15	5	6	8	12	76	73	4
6	−4	4	198	191	4	6	3	7	213	214	2	6	9	12	45	40	6
6	−3	4	69	76	4	6	4	7	385	354	2	6	11	12	92	93	4
6	−1	4	84	92	5	6	5	7	259	252	2	6	3	13	111	111	3
6	1	4	65	67	3	6	6	7	63	67	2	6	4	13	81	93	4
6	2	4	152	148	8	6	7	7	49	47	3	6	9	13	71	69	4
6	3	4	98	96	2	6	9	7	106	106	6	6	10	13	92	97	4
6	4	4	106	90	2	6	10	7	109	113	3	7	−2	−6	89	93	4
6	5	4	163	171	3	6	0	8	83	93	6	7	−1	−6	132	131	3
6	6	4	198	180	3	6	1	8	107	109	5	7	0	−6	95	93	4
6	7	4	115	106	2	6	2	8	180	174	3	7	2	−6	69	66	5
6	10	4	54	66	7	6	3	8	126	111	2	7	−3	−5	112	110	3
6	11	4	78	77	4	6	5	8	205	204	3	7	−2	−5	108	115	3
6	−6	5	54	46	6	6	6	8	199	203	3	7	0	−5	74	72	4
6	−5	5	119	120	3	6	8	8	79	73	4	7	1	−5	123	121	3
6	−3	5	61	65	3	6	11	8	57	63	5	7	2	−5	53	51	6
6	−2	5	88	67	6	6	12	8	68	73	5	7	−2	−4	79	81	4
6	−1	5	54	59	3	6	0	9	59	59	4	7	−1	−4	155	159	3
6	0	5	83	61	2	6	2	9	61	71	7	7	0	−4	191	194	4
6	1	5	160	144	3	6	3	9	86	92	6	7	2	−4	49	48	6
6	3	5	239	235	2	6	4	9	161	157	10	7	4	−4	51	58	6
6	4	5	274	242	2	6	5	9	87	89	3	7	5	−4	69	66	5
6	6	5	83	88	2	6	9	9	82	80	3	7	−5	−3	61	60	9
6	7	5	106	109	2	6	10	9	85	85	3	7	−4	−3	57	61	5

Table 91 — continued

H	K	L	F_{obs}	F_{calc}	SigF	H	K	L	F_{obs}	F_{calc}	SigF	H	K	L	F_{obs}	F_{calc}	SigF
7	−3	−3	128	138	3	7	−5	2	70	71	5	7	4	6	155	148	8
7	−2	−3	110	112	3	7	−3	2	86	82	4	7	5	6	121	116	5
7	0	−3	104	107	3	7	−2	2	143	146	4	7	7	6	87	82	4
7	1	−3	191	200	4	7	−1	2	240	232	8	7	8	6	128	122	6
7	2	−3	74	78	4	7	0	2	41	46	5	7	−3	7	76	76	4
7	3	−3	62	65	5	7	4	2	100	95	2	7	0	7	85	86	3
7	6	−3	85	76	4	7	5	2	243	240	11	7	1	7	46	48	4
7	−6	−2	68	66	5	7	6	2	101	105	6	7	3	7	131	124	7
7	−5	−2	56	64	5	7	8	2	91	83	4	7	5	7	133	139	5
7	−4	−2	74	67	6	7	−3	3	166	168	4	7	6	7	229	228	15
7	−2	−2	82	87	4	7	−2	3	160	168	3	7	7	7	149	149	11
7	−1	−2	225	228	7	7	0	3	129	131	7	7	−1	8	68	60	4
7	0	−2	148	150	4	7	1	3	121	119	11	7	0	8	58	47	5
7	1	−2	52	51	4	7	3	3	97	86	2	7	4	8	165	165	12
7	3	−2	51	51	4	7	4	3	164	170	3	7	5	8	178	175	7
7	4	−2	72	69	4	7	5	3	59	54	5	7	7	8	123	117	8
7	5	−2	69	63	5	7	6	3	133	134	8	7	8	8	98	99	3
7	−4	−1	53	52	6	7	7	3	117	117	7	7	9	8	43	53	6
7	−3	−1	97	89	3	7	9	3	75	76	4	7	10	8	52	52	5
7	−2	−1	137	123	7	7	10	3	56	53	6	7	0	9	64	69	4
7	0	−1	185	187	6	7	−4	4	73	74	4	7	3	9	87	95	3
7	1	−1	103	109	3	7	−2	4	136	123	2	7	6	9	155	163	3
7	2	−1	58	62	4	7	−1	4	161	161	6	7	7	9	60	59	5
7	3	−1	77	85	4	7	0	4	65	62	4	7	2	10	55	58	5
7	6	−1	77	75	4	7	1	4	69	61	3	7	4	10	80	84	4
7	7	−1	98	104	4	7	3	4	40	42	4	7	5	10	114	110	3
7	−5	0	69	79	5	7	4	4	38	33	4	7	7	10	52	50	5
7	−4	0	91	85	4	7	5	4	105	117	2	7	8	10	45	50	6
7	−2	0	60	67	4	7	6	4	66	63	4	7	2	11	56	75	6
7	−1	0	246	242	7	7	8	4	132	135	3	7	3	11	100	95	3
7	3	0	103	103	4	7	9	4	54	54	6	7	4	11	81	77	4
7	4	0	112	109	7	7	−4	5	49	50	6	7	6	11	100	102	3
7	5	0	108	109	3	7	−3	5	152	158	3	7	7	11	41	50	6
7	8	0	76	74	5	7	−2	5	83	83	4	7	4	12	113	113	3
7	9	0	67	68	5	7	1	5	62	58	3	7	5	12	104	98	3
7	−3	1	129	140	3	7	2	5	63	59	2	7	8	12	56	51	5
7	−2	1	146	141	4	7	3	5	61	59	3	8	−2	−4	55	51	6
7	0	1	120	126	4	7	6	5	138	132	9	8	−1	−4	52	54	6
7	1	1	94	82	2	7	7	5	166	167	12	8	1	−4	86	83	4
7	2	1	73	77	3	7	−4	6	76	69	4	8	2	−4	94	88	4
7	3	1	140	133	3	7	−2	6	144	141	3	8	−1	−3	76	75	5
7	4	1	102	95	7	7	−1	6	77	85	4	8	0	−3	116	121	3
7	6	1	96	97	4	7	0	6	79	72	7	8	1	−3	78	81	5
7	7	1	77	88	6	7	1	6	77	78	9	8	1	−2	144	149	3

Table 91 — continued

H	K	L	F_{obs}	F_{calc}	SigF	H	K	L	F_{obs}	F_{calc}	SigF	H	K	L	F_{obs}	F_{calc}	SigF
8	2	−2	120	118	3	8	2	4	87	98	4	8	7	8	129	130	3
8	0	−1	127	129	6	8	5	4	76	80	4	8	8	8	57	64	5
8	1	−1	58	61	6	8	7	4	98	101	4	8	5	9	50	57	6
8	2	−1	107	111	3	8	8	4	66	62	5	8	6	9	84	77	4
8	3	−1	133	133	4	8	−1	5	107	108	3	8	8	9	76	78	4
8	1	0	165	164	3	8	0	5	133	129	3	8	9	9	60	59	5
8	2	0	139	139	3	8	1	5	67	65	5	8	6	10	57	57	5
8	4	0	45	45	7	8	2	5	50	54	6	8	7	10	97	90	3
8	5	0	57	55	6	8	3	5	55	61	5	8	5	11	78	79	4
8	7	0	64	78	6	8	5	5	68	53	4	8	6	11	69	74	5
8	−1	1	83	82	7	8	6	5	106	106	3	9	1	0	81	85	5
8	0	1	131	129	3	8	8	5	58	64	5	9	3	0	79	79	10
8	3	1	129	136	3	8	9	5	91	86	4	9	2	1	114	111	4
8	4	1	146	149	3	8	−2	6	92	97	4	9	3	1	89	90	6
8	5	1	83	84	4	8	0	6	54	63	6	9	5	1	67	75	6
8	−2	2	92	80	6	8	1	6	102	106	3	9	1	2	90	90	9
8		2	87	87	4	8	2	6	78	87	4	9	3	2	84	88	5
8	1	2	154	155	3	8	6	6	60	64	5	9	4	2	118	122	8
8	2	2	102	106	5	8	7	6	132	135	3	9	1	3	56	56	6
8	3	2	131	128	3	8	8	6	83	84	4	9	2	3	109	111	7
8	4	2	83	75	6	8	10	6	59	64	6	9	3	3	102	103	4
8	7	2	63	65	5	8	−1	7	77	79	4	9	0	4	70	75	5
8	8	2	60	60	6	8	0	7	81	83	4	9	1	4	86	94	4
8	−3	3	64	59	10	8	2	7	85	89	4	9	3	4	68	65	5
8	−1	3	139	139	4	8	3	7	61	67	5	9	4	4	98	94	4
8	0	3	126	127	3	8	4	7	50	44	5	9	5	4	60	61	6
8	5	3	103	106	8	8	5	7	84	85	4	9	2	5	104	101	4
8	6	3	98	103	4	8	6	7	89	84	3	9	3	5	95	97	4
8	9	3	78	82	6	8	8	7	85	92	4	9	1	6	90	88	4
8	−2	4	109	100	3	8	9	7	80	77	4	9	3	6	84	85	4
8	−1	4	97	96	3	8	1	8	69	56	4	9	4	6	98	96	4
8	0	4	62	65	5	8	2	8	55	56	5	9	2	7	92	105	4
8	1	4	156	147	3	8	6	8	57	67	5	9	3	7	71	59	5

REFERENCES

1. (a) Winkhaus, G.; Pratt, L.; Wilkinson, G. *J. Chem. Soc.* **1961**, 3807. (b) Winkhaus, G.; Wilkinson, G. *Proc. Chem. Soc.* **1960**, 311.

2. Coffield, T. H.; Closson, R. D. (to Ethyl Corp.) U. S. Patent 3 042 693, 1962; *Chem. Abstr.* **1963**, *59*, 11558.

3. Munro, G. A. M.; Pauson, P. L. *Isr. J. Chem.*. **1976/77**, *15*, 258–261.

4. Angelici, R. J.; Blacik, L. *J. Inorg. Chem.* **1972**, *11*, 1754.

5. Walker, P. J. C.; Mawby, R. J.; *Inorg. Chim. Acta* **1973**, *7*, 621.

6. (a) Bernhardt, R. J.; Wilmoth, M. A.; Weers, J. J.; LaBrush, D. M.; Eyman, D. P. *Organometallics* **1986**, *5*, 883. (b) Bernhardt, R. J.; Eyman, D. P. *Organometallics* **1984**, *3*, 1445–1446.

7. (a) Kane–Maguire, L.A.P.; Honig, E.D.; Sweigart, D.A. *Chem. Rev.* **1984**, *84*, 525. (b) Kane-Maguire, L. A. P.; Sweigart, D. A. *Inorg. Chem.* **1979**, *18*, 700.

8. Snyder, D. B.; Schauer, S. J.; Eyman, D. P.; Moler, J. L.; Weers, J. J., *J. Am. Chem. Soc.* in press.

9. (a) Pauson, P. L.; Segal, J. A. *J. Chem. Soc., Dalton Trans.* **1975**, 1677. (b) Walker, J. C.; Mawby, R. *J. Chem. Soc., Dalton Trans.* **1973**, 622. (c) Winkhaus, G. *Z. Anorg. Allg. Chem.* **1963**, *405*, 319.

10. LaBrush, D. M.; Eyman, D. P.; Baenziger, N. C.; Mallis, L. M. *Organometallics* **1991**, *10*, 1026–1033.

11. (a) Jaouen, G.; Top, S.; McGlinchey, M. J. *J. Organomet. Chem.* **1980**, *195*, C5–C8. (b) Simonneaux, G.; Jaouen, G. *Tetrahedron* **1979**, *35*, 2249–2254. (c) Jaouen, G.; Meyer, A.; Simonneaux, G. *J. Chem. Soc., Chem. Commun.* **1975**, 813–814.

12. Johnson, J. W.; Treichel, P. M. *J. Am. Chem. Soc.* **1977**, *99*, 1427–1436; *J. Chem. Soc., Chem. Commun.* **1976**, 688–689.

13. (a) Helling, J. F.; Hendrickson, W. A. *J. Organomet. Chem.* **1979**, *168*, 87-95. (b) Nesmeyanov, A. N.; Ustynyuk, N. A.; Makarova, L. G.; Andre, S.; Ustynyuk, Y. A.; Novikova, L. N.; Lusikov, Yu. N. *J. Organomet. Chem.* **1978**, *154*, 45-63. (c) Helling, J. F.; Hendrickson, W. A. *J. Organomet. Chem.* **1977**, *141*. 99-105. (d) Pauson, P. L.; Segal, J. A. *J. Chem. Soc., Dalton Trans.* **1975**, 1677-1682. (e) Helling, J. F.; Cash, G. G. *J. Organomet. Chem.* **1974**, *73*, C10-C12.

14. (a) Astruc, D.; Hamon, J.-R.; Román, E.; Michaud, P. *J. Am. Chem. Soc.* **1981**, *103*, 7502-7514. (b) Hamon, J.-R.; Astruc, D.; Román, E.; Batail, P.; Mayerle, J. J. *J. Am. Chem. Soc.* **1981**, *103*, 2431-2433.

15. Yaouanc, J.-J.; Clement, J.-C.; des Abbayes, H. *Chem. Commun.* **1983**, 1379.

16. Moler, J. L.; Eyman, D. P.; Nielsen, J. M.; Morken, A. M.; Snyder, D. B.; Schauer, S. J. *Organometallics*, in press.

17. Ueda, R.; Senba, Y.; Ota, K.; Morita, K.; Hayashi, H.; Kitada, K. Jpn. Patent 62 238 379 A2 190, 1987; *Chem. Abstr.*, **1987**, *108*, 116836e.

18. Spruegel, R. A.; Angerer, W. Ger. Patent 3 924 596 C1, 1990.

19. Kuliev, A B.; Adullaeva, M. I.; Akhadov, N. O. *Zh. Prikl. Khim.* (Leningrad) **1984**, *57*, 1835-8; *Chem. Abstr.*, **1984**, *102*, 78509s.

20. Schauer, S. J.; Eyman, D. P.; Bernhardt, R. J.; Wolff, M. A.; Mallis, L. M. *Inorg. Chem.* **1991**, *30*, 570.

21. Moler, J. L.; Eyman, D. P.; Mallis, L. M. *Inorg. Chem.* **1992**, *31*, 1816.

22. Micheel, F.; Istel, E.; Schnacke, E. *Chem. Ber.* **1949**, *82*, 131.

23. (a) Shriver, D. F.; Drezdon, M. A. *The Manipulation of Air Sensitive Compounds*; Wiley: New York, 1986. (b) *Experimental Organometallic Chemistry* Wayda, A.L.; Darensborg, M.Y., Eds.; ACS Symposium Series 357; American Chemical Society: Washington, D.C., 1987.

24. Perrin, D. D.; Armarego, W. L. F. *Purification of Laboratory Chemicals*, 3rd ed.; Pergamon Press: Oxford, 1988.

25. The VG Trio-3 mass spectrometer (VG Masslabs Ltd., Altrincham, Cheshire, U.K.) has QHQ geometry (Quadrupole mass analyzer, Hexapole collision cell, Quadrupole mass analyzer).

26. Winhaus, G. Singer, H. *Z. Naturforsch., B: Anorg. Chem., Org. Chem.* **1963**, *18B*, 418.

27. (a) Quick, M. H.; Angelici, R. J. *Inorg. Chem.* **1979**, *19*, 160. (b) Reimer, K.J.; Shaver, A. *Inorg. Syn.* **1979**, *19*, 159.

28. Brown, H. C.; Nazer, B.; Sikorski, J. A. *Organometallics*, **1983**, *2*, 634.

29. (a) Gottlieb, H. B. *J. Am. Chem. Soc.* **1932**, *54*, 748. (b) Characterization of $P(OC_6D_5)_3$: ^1H NMR (CD_3COCD_3) δ 6.89–6.24 (m, 15 D, $P(OC_6D_5)$); ^{31}P NMR (CD_3COCD_3) δ 132.0 (s, d_{15}-$P(OPh)_3$; $^{13}C\{^1H\}$ NMR (CD_3COCD_3) δ 132.0 ($-C_6D_5$).

30. (a) Jaehne, O. *Annalen. der Chemie* **1889**, *255*, 269–285. (b) Kopp, H. *Annalen. der Chemie* **1854**, *15*, 348–351. (c) Characterization of $P(OCD_3)_3$: ^2H NMR (THF) δ 3.54 (br s, 9 D, $P(OCD_3)$); ^{31}P NMR (CD_3COCD_3) δ 154.0 (s, d_9-$P(OMe)_3$; $^{13}C\{^1H\}$ NMR (CD_3COCD_3) δ 50.0 ($-CD_3$).

31. (a) Davies, A. G. *J. Organomet. Chem.* **1980**, *200*, 87–99. (b) Mayo, F. R. *Acc. Chem. Res.* **1968**, *1*, 193–201.

32. (a) Kochi, J. K. *Organometallic Mechanism and Catalysis*; Academic Press: New York, 1978; pp 517–522. (b) Stille, J. K.; Lau, K. S. Y. *Acc. Chem. Res.* **1977**, *10*, 434–442. (c) Osborn, J. A. *Organotransition Metal Chemistry*; Ishii, I.; Tsutsui, M., Eds; Plenum Press: New York, 1975; pp 65–80. (d) Halpern, J. *Acc. Chem. Res.* **1970**, *3*, 386–392. (e) Collman, J. P. *Acc. Chem. Res.* **1968**, 1, 136–143. (f) Collman, J. P.; Roper, W. R. *Adv. Organomet. Chem.* **1968**, 7, 53–94.

33. Thomson, M. E.; Baxter, S. M.; Bulls, A. R.; Burger, B. J.; Nolan, M. C.; Santarsiero, B. D.; Schaefer, W. P.; Bercaw, J. E. *J. Am. Chem. Soc.* **1987**, *109*, 203–219.

34. (a) Astruc, D. In *The Chemistry of the Metal-Carbon Bond*; Hartley, F. R., Patai, S.; Ed., Wiley: New York, 1987; Vol. 4, pp 625–731. (b) Hamon, J.-R.; Astruc, D. *Organometallics* **1988**, *7*, 1036–1046. (c) Madonik, A. M.: Astruc, D. *J. Am. Chem. Soc.* **1984**, *106*, 2437–2439. (c) Astruc, D.; Román, E.; Hamon, J.-R.; Batail, P. *J. Am. Chem. Soc.* **1979**, *101*, 2240–2242.

35. Hull, J. W., Jr.; Roesselet, K. J.; Gladfelter, W. L. *Organometallics* **1992**, *11*, 3630–3635.

36. (a) Astruc, D.; Mandon, D.; Madonik, A.; Michaud, P.; Ardoin, N.; Varret, F. *Organometallics* **1990**, *9*, 2155–2164. (b) Mandon, D.; Astruc, D. *Organometallics* **1990**, *9*, 341–346. (c) Astruc, D.; Hamon, J.-R.; Lacoste, M.; Desbois, M. -H.; Madonik, A. M.; Román, E. *Organomet. Synth.* **1988**, *4*, 172. (d) Mandon, D.; Astruc, D. *J. Organomet. Chem.* **1986**, *307*, C27–C30. (e) Astruc, D. *Acc. Chem. Res.* **1986**, *19*, 377–383. (f) Madonik, A. M.; Mandon, D.; Michaud, P.; Lapinte, C.; Astruc, D. *J. Am. Chem. Soc.* **1984**, *106*, 3381–3382. (g) Catheline, D.; Astruc, D. *Organometallics* **1984**, *3*, 1094–1100. (h) Madonik, A. M.; Astruc, D. *J. Am. Chem. Soc.* **1984**, *106*, 2437–2439. (i) Hamon, J.-R.; Astruc, D. *J. Am. Chem. Soc.* **1983**, *105*, 5951–5952.

37. (a) Moriarty, R. M.; Gill, U. S. *Organometallics* **1986**, *5*, 253–256. (b) Gill, U. S.; Moriarty, R. M. *Synth. React. Inorg. Met. Org. Chem.* **1986**, *16*, 485–490. (c) Lee, C. C.; Abd-El Aziz, A. S.; Chowdhurry, R. L.; Gill, U. S.; Piorko, A.; Sutherland, R. G. *J. Organomet. Chem.* **1986**, *315*, 79–92. (d) Khand, I. U.; Paulson, P. L.; Watts, W. E. *J. Chem. Soc. (C)* **1969**, 2024–2033.

38. Tolman, C. A. *Chem. Rev.* **1977**, *77*, 313–348.

39. Morken, A. M.; Eyman, D. P., The University of Iowa, unpublished results.

40. Frenz, B. A. *Enraf-Nonius Structure Determination Package*; Enraf-Nonius: College Station, TX, 1981.

41. Planes were calculated using the CAD4 Planes programs, Enraf-Nonius, a Table summarizing this data is provided in the Supplemental Materials.

42. Wilmoth, M. A.; Bernhardt, R. J.; Eyman, D. P.; Huffman, J. C. *Organometallics* **1986**, *5*, 2559–2561.

43. (a) Hoffmann, R.; Hofmann, P. *J. Am. Chem. Soc.* **1976**, *98*, 598–604. (b) Elian, M.; Hoffmann, R. *Inorg. Chem.* **1975**, *14*, 1058–1076.

44. Connelly, N. G.; Freeman, M. J.; Orpen, G.; Sheehan, A. R.; Sheridan, J. B.; Sweigart, D. A. *J. Chem. Soc., Dalton Trans.* **1985**, 1019–1026.

45. (a) Astruc, D. *Synlett.* **1991**, 369–380. (b) Green, J. C.; Kelly, M. R.; Payne, M. P.; Seddon, E. A.; Astruc, D.; Hamon, J. -R.; Michaud, P. *Organometallics* **1983**, *2*, 211–218.

46. Haddon, R. C. *J. Am. Chem. Soc.* **1987**, *109*, 1676–1685.

47. (a) Astruc, D. In *Transition Metal Coordination Chemistry*; Dewar, M. J. S., Ed.; Topics in Current Chemistry; Springer-Verlag: Berlin, 1991; Vol. 160, 63–72. (b) Moulines, F.; Gloaguen, B.; Astruc, D. *Angew. Chem. Int. Ed. Engl.* **1992**, *31*, 458–460. (c) Gloaguen, B.; Astruc, D. *J. Am. Chem. Soc.* **1990**, *112*, 4607–4609. (d) Astruc, D.; Desbois, M.-H.; Lacoste, M.; Moulines, F.; Hamon, J.-R.; Varret, F. *Polyhedron* **1990**, *9*, 2727–2732. (e) Moulines, F.; Astruc, D. *J. Chem. Soc., Chem. Commun.* **1989**, 614–615. (f) Moulines, F.; Astruc, D. *Angew. Chem.* **1988**, *100*, 1394–1396. (g) Hamon, J.-R.; Saillard, J.-Y.; Beuze, A. L.; McGlinchey, M. J.; Astruc, D. *J. Am. Chem. Soc.* **1982**, *104*, 7549–7555.

48. (a) Laube, T.; Wiedenhaupt, A.; Hunziker, R. *J. Am. Chem. Soc.* **1991**, *113*, 2561–2567. (b) Brown, M.; Waters, J. M. *J. Am. Chem. Soc.* **1991**, *113*, 2442–2443. (c) Colsman, M. R.; Newbound, T. D.; Marshall, L. J.; Noirot, M. D.; Miller, M. M.; Wulfsberg, G. P.; Frye, J. S.; Anderson, O. P.; Strauss, S. H. *J. Am. Chem. Soc.* **1990**, *112*, 2349–2362. (d) Newbound, T. D.; Colsman, M. R.; Miller, M. M.; Wulfsberg, G. P.; Anderson, O. P.; Strauss, S. H. *J. Am. Chem. Soc.* **1989**, *111*, 3762–3764. (e) Winter, C. H.; Veal, W. R.; Garner, C. M.; Arif, A. M.; Gladysz, J. A. *J. Am. Chem. Soc.* **1989**, *111*, 4766–4776. (f) Fernandez, J. M.; Gladysz, J. A. *Organometallics* **1989**, *8*, 207–219. (g) Winter, C. H.; Arif, A. M.; Gladysz, J. A. *Organometallics* **1989**, *8*, 219–225. (h) Barceló, F.; Lahuerta, P.; Ubeda, M. A.; Foces-Foces, C.; Cano, F. H.; Martínez-Ripoll, M. *Organometallics* **1988**, *7*, 584–590. (i) Colsman, M. R.; Noirot, M. D.; Miller, M. M.; Andersen, O. P.; Strauss, S. H. *J. Am. Chem. Soc.* **1988**, *110*, 6886–6888. (j) Winter, C. H.; Gladysz, J. A. *J. Organomet. Chem.* **1988**, *354*, C33–C36. (k) Karipedes, A.; Peiffer, K. *Inorg. Chem.* **1988**, *27*, 3255–56. (l) Kulawiec, R. J.; Crabtree, R. H. *Organometallics* **1988**, *7*, 1891–1893.

49. Worska, D. C.; Wilson, M.; Bartholomew, J.; Eriks, K.; Prock, A.; Giering, W. P. *Organometallics*, **1992**, *11*, 3343–3352.

50. (a) Pike, R. D.; Rieger, A. L.; Rieger, P. H. *J. Chem. Soc., Faraday Trans. 1* **1989**, *85*, 3913–3925. (b) Antanaitis, B. C.; Brown, R. D., III; Chasteen, D.; Freedman, J. H.; Koenig, S. H.; Lilienthal, H. R.; Peisach, J.; Brewer, C. F. *Biochemistry*, **1987**, *26*, 7932–7937. (c) Sakurai, H.; Nishida, M.; Yoshimura, T. *Inorg. Chim. Acta* **1982**, *66*, L17–L20. (d) Reed, G. H.; Leyh, T. S. *Biochemistry* **1980**, *19*, 5472–5480. (e) Reed, G. H.; Cohn, M. *J. Biol. Chem.* **1972**, *247*, 3072–3080. (f) Reed, G. H.; Leigh, J. S.; Pearson, J. E. *J. Chem. Phys.* **1971**, *55*, 3311–3316.

51. (a) Rattinger, G. B.; Belford, R. L.; Walker, H.; Brown, T. L. *Inorg. Chem.* **1989**, *28*, 1059–1066. (b) Wang, S. R.; Cheng, C. P.; Ho, T.-I. *J. Chem. Soc., Dalton Trans.* **1988**, 2695–2699. (c) Ho, T.-I.; Chang, C.-M.; Wang, S. R.; Cheng, C. P. *J. Chem. Soc., Dalton Trans.* **1988**, 123–127.

52. Snyder, D. B.; Eyman, D. P.; Narske, R. N.; Mundt, D., The University of Iowa, unpublished results.

53. Casey, C. P. In *Transition Metal Organometallics in Organic Synthesis*; Alper, H., Ed.; Academic: New York, 1976; Vol. 1, Chapter 3, pp 214–224.

54. (a) Nickon, A. *Acc. Chem. Res.* **1993**, *26*, 84–89. (b) Baron, W. J.; DeCamp, M. R. Hendrick, M. E.; Jones, M., Jr.; Levin, R. H.; Sohn, M. B. In *Reactive Intermediates in Organic Chemistry: Carbenes*; Jones, M., Jr.; Moss, R. A., Eds.; Wiley: New York, 1973; Vol. 1, 2–62. (c) Herzberg, G.; Johns, J. W. C. *Proc. Roy. Soc.* (London) **1967**, *107*, A295.

55. (a) Nazran, A. S.; Griller, D. *J. Chem. Soc., Chem. Commun.* **1983**, 850. (b) Rondan, N. G.; Houk, K. N.; Moss, R. A. *J. Am. Chem. Soc.* **1980**, *102*, 1770. (c) Wentrup, C. *Reactive Molecules: The Neutral Reactive Intermediates in Organic Chemistry*; Wiley: New York, 1984; Chapter 4.

56. (a) Gallop, M. A.; Roper, W. R. *Adv. Organomet. Chem.* **1986**, *25*, 121–198. (b) Casey, C. P. In *Reactive Intermediates*; Jones, M., Jr.; Moss, R. A., Eds.; Wiley: (i) New York, 1981; Vol. 2, p 135. (ii) New York, 1985; Vol. 2, p 150. (c) Fischer, E. O. *Adv. Organomet. Chem.* **1974**, *14*, 1.

57. *^{1}H Nuclear Magnetic Resonance Spectra*; Sadtler Standard Spectra

58. Lof, P. *Elservier's Periodic Table of Elements*; Elservier Science: Amsterdam, 1987.

59. (a) Brill, T. B.; Landon, S. J. *Chem. Rev.* **1984**, *84*, 577–585. (b) Bhattacharya, A. K.; Thyagarjan, G. *Chem. Rev.* **1981**, *81*, 415. (c) Kirby, A. J.; Warren, S. G. *The Organic Chemistry of Phosphorus*; Elsevier: New York, 1967; p 67. (d) Hudson, R. F. *Structure and Mechanism in Organo-phosphorus Chemistry*; Academic: New York, 1965; p 135. (e) Harvey, R. G.; DeSombre, E. R. *Top. Phosphorus Chem.* **1964**, *1*, 57. (f) Arbuzov, A. E. *Pure Appl. Chem.* **1964**, *9*, 307. (g) Michaelis, A.; Kaehne, R. *Chem. Ber.* **1898**, *31*, 1048.

60. (a) Crabtree, R. H. *The Organometallic Chemistry of the Transition Metals*; Wiley-Interscience: New York, 1988; pp 357–361. (b) Jaouen, G. *Pure Appl. Chem.* **1986**, *58*, 597. (c) Semmelhack, M. F. *Ann. N. Y. Acad. Sci.* **1977**, *333*, 36.

61. For reviews see: (a) Davies, S. G.; Green, M. L. H.; Mingos, D. M. P. *Tetrahedron* **1978**, *34*, 3047. (b) Kane-Maguire, L. A. P.; Honig, E. D.; Sweigart, D. A. *Chem. Rev.* **1984**, 525.

62. Tam, W.; Volhardt, K. P. C. *J. Organomet. Chem.* **1981**, *216*, 97.

63. (a) Chung, Y. K.; Sweigart, D. A.; Connelly, N. G.; Sheridan, J. B. *J. Am. Chem. Soc.* **1985**, *107*, 2388. (b) Chung, Y. K.; Choi, H. S.; Sweigart, D. A.; Connelly, N. G. *J. Am. Chem. Soc.* **1982**, *104*, 4245. (c) Brookhardt, M.; Lukacs, A.; *J. Am. Chem. Soc.* **1984**, *106*, 4161. (d) Brookhardt, M.; Lamanna, W.; Pinhas, A. R. *Organometallics* **1983**, *2*, 638. (e) Lamanna, W.; Brookhardt, M. *J. Am. Chem. Soc.* **1981**, *103*, 989.

64. (a) Abd El-Aziz, A. S.; Lee, C. C.; Piorko, A.; Sutherland, R. G. *J. Organomet. Chem.* **1988**, *348*, 95. (b) Astruc, D. Tetrahedron Report No. 157, *Tetrahedron* **1983**, *39*, 4027.

65. Cotton, F. A.; Wilkinson, G. *Advanced Inorganic Chemistry*, 5th ed.; Wiley–Interscience: New York, 1988; p 293.

66. (a) Pauson, P. L. *J. Organomet. Chem.* **1980**, *200*, 207. (b) Khand, I. U.; Pauson, P. L.; Watts, W. E. *J. Chem. Soc. (C)* **1968**, 2267. (c) Jones, D.; Pratt, L.; Wilkinson, G. *J. Am. Chem. Soc.* **1962**, 4458. (d) Winkhaus, G.; Singer, H. *Z. Naturforsch.* B **1963**, *18*, 418.

67. Mandon, D.; Astruc, D. *Organometallics* **1990**, *9*, 341.

68. (a) Yagupsky, M.; Wilkinson, G. *J. Chem. Soc. A* **1968**, 2813. (b) Palazzi, A.; Busetto, L.; Graziani, M. *J. Organomet. Chem.* **1971**, *30*, 273. (c) Albano, V. G.; Bellon, P. L.; Ciani, G. *J. Organomet. Chem.* **1971**, *31*, 75. (d) Einstein, F. W.; Enwall, E.; Flitcroft, N.; Leach, J. M. *J. Inorg. Nucl. Chem.* **1972**, *34*, 885. (e) Butler, I. S.; Fenster, A. E. *J. Organomet. Chem.* **1974**, *66*, 161. (f) Restivo, R. J.; Costin, A.; Ferguson, G.; Carty, A. J. *Can. J. Chem.* **1975**, *53*, 1949. (g) Albinati, A.; Musco, A.; Carturan, G.; Strukul, G. *Inorg. Chem. Acta* **1976**, *18*, 219. (h) Gattow, G.; Behrendt, W. In *Topics in Sulfur Chemistry*; Senning, A., Ed., Thieme: Stuttgart, Germany, 1977; Vol. 2. (i) Yaneff, P. V. *Coord. Chem. Rev.* **1977**, *23*, 183. (j) Schenk, W. A.; Schwietzke, T. *Organometallics* **1983**, *2*, 1905. (k) Bianchini, C.; Ghilardi, C. A.; Meli, A. Midollini, S.; Orlandini, A. *Inorg. Chem.* **1985**, *24*, 932. (l) Schenk, W. A.; Kümmerle, D.; Schwietzke, T. *J. Organomet. Chem.* **1988**, *349*, 163.

69. (a) De Filippo, D.; Lai, A.; Trogu, E. F.; Verani, G.; Preti, C. *J. Inorg. Nucl. Chem.* **1974**, *36*, 73. (b) Siedle, A. R. *Inorg. Nucl. Chem. Lett.* **1975**, *11*, 345. (c) Gingerich, R. G. W.; Angelici, R. J. *J. Organomet. Chem.* **1977**, *132*, 377. (d) Lindner, E.; Nagel, W. *Z. Naturforsch., B: Anorg. Chem., Org. Chem.* **1977**, *32B*, 1116. (e) Raubenheimer, H. G.; Kruger, G. J.; Lonbard, A. *Z. Naturforsch., B: Anorg. Chem., Org. Chem.* **1982**, *240*, C11.

70. Micheel, F.; Istel, E.; Schnacke, E. *Chem. Ber.* **1949**, *82*, 131.

71. (a) Miller, J. M. *Mass Spectrom. Rev.* **1989**, *9*, 319. (b) Bruce, M. I.; Liddell, M. J. *J. Organomet. Chem.* **1987**, *1*, 191. (c) Liang, X.; Suwanrupha, S.; Freas, R. B. *Inorg. Chem.* **1991**, *30*, 652. (d) Bojesen, G. *Org. Mass Spectrom.* **1985**, *20*, 413.

72. Kurlansik, L.; Williams, T. J.; Campana, J. E.; Green, B. N.; Anderson, L. W.; Strong, J. M. *Biochem. Biophys. Res. Commun.* **1983**, *111*, 478.

73. (a) *Collision Spectroscopy*; Cooks, R. G., Ed.; Plenum: New York, 1978. (b) *Tandem Mass Spectrometry*; McLafferty, F. W., Ed.; John Wiley and Sons: New York, 1983.

74. (a) Schenk, W. A.; Rüb, D.; Burschka, C. *J. Organomet. Chem.* **1987**, *328*, 287. (b) *J. Organomet. Chem.* **1987**, *328*, 305.

75. Francis, J. N.; Hawthorne, M. F. *Inorg. Chem.* **1971**, *10*, 594.

76. Drago, R. S. *Physical Methods for Chemists*; Saunders College: Ft. Worth, 1992; Chapters 7 and 8.

77. Mr(6)CN, ν_{CO} = 1975, 1926 cm^{-1}, and Mr(6)CN·$AlMe_3$, ν_{CO} = 1991, 1945 cm^{-1}: Weers, J. J. Ph.D. Thesis, University of Iowa, 1984.

78. (a) Nakamoto, K. *Infrared Spectra of Inorganic and Coordination Compounds*, Wiley: New York, 1963. (b) Green, M. L. H.; Pratt, L.; Wilkinson, G. *J. Chem. Soc.* **1959**, *989*, 3753. (c) Cotton, F. A.; Reynolds, L. T. *J. Am. Chem. Soc.* **1958**, *80*, 269.

79. (a) Collins, T. J.; Roper, W. R.; Town, K. G. *J. Organomet. Chem.* **1976**, *121*, C41. (b) Grundy, K. R.; Harris, R. O.; Roper, W. R. *J. Organomet. Chem.* **1975**, *90*, C34.

80. (a) Joris, S. J.; Aspila, K. I.; Chakrabarti, C. L. *J. Phys. Chem.* **1970**, *74*, 860. (b) Joris, S. J.; Aspila, K. I.; Chakrabarti, C. L. *Anal. Chem.* **1969**, *41*, 1441.

81. Miller, D. M.; Latimer, R. A. *Can. J. Chem.* **1962**, *40*, 246.

82. Schenk, W. A.; Kümmerle, D. *J. Organomet. Chem.* **1986**, *303*, C25.

83. Kalinowski, H.-O.; Lubosch, W.; Seebach, D. *Chem. Ber.* **1977**, *110*, 3733.

84. (a) LaPlanche, L. A.; Rogers, M. T. *J. Am. Chem. Soc.* **1963**, *85*, 3728. (b) Siddall, T. H. (III); Stewart, W. E.; Knight, F. D. *J. Phys. Chem.* **1970**, *74*, 3580.

85. *International Tables for X-ray Crystallography*; Kynoch Press: Birmingham, England, 1975; Vol. III, Physical and Chemical Tables.

86. $[(C_6H_5)_4As]_2[Ni(\eta^2\text{-}S_2C{=}N\text{-}CN)_2]$; Cotton, F. A.; Harris, C. B. *Inorg. Chem.* **1968**, *7*, 2140.

87. IR (THF): $[(\eta^6\text{-}C_6Me_6)Mn(CO)_2SCHOEt][BF_4]$, ν_{CO} = 1979, 1931 cm^{-1} and $[(\eta^6\text{-}C_6Me_6)Mn(CO)_2SCHOMe][BF_4]$, ν_{CO} = 1970, 1930 cm^{-1}.

88. Engler, V. R.; Gattow, G. *Z. Anorg. Allg. Chem.* **1972**, *388*, 78.

89. Schlom, P. Ph.D. Thesis, University of Iowa, 1989.

90. (a) Roper, W. R.; Town, K. G. *J. Chem. Soc., Chem. Commun.* **1977**, 781. (b) Collins, T. J.; Roper, W. R. *J. Organomet. Chem.* **1978**, *159*, 73. (c) Collins, T. J.; Roper, W. R. *J. Chem. Soc., Chem. Commun.* **1977**, 901.

91. Schindehutte, M.; van Rooyen, P. H.; Lotz, S. *Organometallics* **1990**, *2*, 293.

92. Einstein, F. W.; Enwall, E.; Flitcroft, N.; Leach, J. M. *J. Inorg. Nucl. Chem.* **1972**, *404*, 71.

93. Miguel, D.; Riera, V. *Organometallics* **1991**, *10*, 1683.

94. (a) Engler, R.; Kiel, G.; Gattow, G. Z. *Anorg. Allg. Chem.* **1974**, *404*, 71. (b) Gasparri, G. F.; Nardelli, M.; Villa, A. C. *Acta Crystallogr.* **1967**, *23*, 384.

95. Capacchi, L.; Villa, A. C.; Ferrari, M.; Nardelli, M. *Ric. Sci., Parte II, Sez. A* **1967**, *37*, 993.